Universidad Miguel Hernández de Elche

Departamento de Ciencia de Materiales, Óptica y Tecnología Electrónica

Mobile Relaying and Opportunistic Networking in Multi-Hop Cellular Networks

Baldomero Coll-Perales

Director: Prof. Javier Gozálvez Sempere

Thesis for the degree of PhD

July 2015

UNIVERSITAS
Miguel
Hernández

Departamento de Ciencia de Materiales, Óptica y Tecnología Electrónica
Universidad Miguel Hernández de Elche
Campus de Elche – Edificio Torrevaillo
Avda. Universidad, s/n- 03202, Elche (Alicante), ESPAÑA
Tel.: +34 96 665 8498 Fax: +34 96 665 8497
E-mail: cytmat@umh.es

Dª PIEDAD NIEVES DE AZA MOYA, Directora del Departamento de Ciencia de Materiales, Óptica y Tecnología Electrónica de la Universidad Miguel Hernández de Elche,

INFORMA

que la Tesis Doctoral titulada “Mobile Relaying and Opportunistic Networking in Multi-Hop Cellular Networks”, ha sido realizada por Don Baldomero Coll-Perales, Ingeniero de Telecomunicación, bajo la inmediata dirección y supervisión del Dr. Javier Gozálvez Sempere, y da su conformidad para que sea presentada ante la Comisión de Doctorado.

Para que conste y surta los efectos oportunos, firma el presente informe en Elche, a de de 2015.

Fdo. Dª Piedad Nieves de Aza Moya
Directora del Departamento de Ciencia de Materiales, Óptica y Tecnología Electrónica

UNIVERSITAS
Miguel
Hernández

JAVIER GOZÁLVEZ SEMPERE, Doctor Ingeniero, y Profesor Titular de Universidad por el Área de Teoría de la Señal y Comunicaciones de la Universidad Miguel Hernández de Elche,

HACE CONSTAR

que el presente trabajo, titulado “Mobile Relaying and Opportunistic Networking in Multi-Hop Cellular Networks”, ha sido realizado bajo mi dirección y recoge fielmente la labor realizada por Don Baldomero Coll-Perales, Ingeniero de Telecomunicación, para optar al grado de Doctor. Las investigaciones reflejadas en la Tesis se han desarrollado en el Laboratorio UWICORE del Departamento de Ingeniería de Comunicaciones de la Universidad Miguel Hernández de Elche.

El que suscribe considera que el trabajo reúne las condiciones de originalidad y rigor metodológico necesario para memoria de Tesis Doctoral, y de este modo puede ser presentado a la lectura y discusión ante tribunal en la Universidad Miguel Hernández de Elche. Y para que así conste, firma el presente certificado.

Elche, a de de 2015.

Fdo. Javier Gozálvez Sempere

UNIVERSITAS
Miguel
Hernández

This work was supported in part by the Spanish Ministry of Economy and Competitiveness and FEDER funds under the project TEC2011-26109, the Spanish Ministry of Science and Innovation under the project TEC2008-06728, and the Generalitat Valenciana under research grants ACIF/2010/161 and BEFPI/2012/065.

UNIVERSITAS Miguel Hernández

UNIVERSITAS
Miguel
Hernández

Abstract

Cellular systems have significantly evolved over the past decades through the introduction of novel radio access technologies designed to increase capacity and support higher data rates. The evolution has mainly focused around the traditional cell-centric approach where each mobile station directly communicates with the base station. Traditional cellular communications experience difficulties in providing high and homogeneous Quality of Service (QoS) levels throughout the cell (in particular at cell edges) due to the signal attenuation produced by obstacles and distance. In this context, a paradigm-shift is sought for the design of future mobile communications systems (5G networks) that will be required to efficiently support varying QoS and Quality of Experience (QoE) requirements of the exponentially increasing mobile data traffic. This thesis advocates for the need to explore and evolve from current cell-centric architectures to device-centric architectures which exploit the intelligence, communications and computing resources of smart mobile devices. One approach to do so is by exploiting Device-to-Device (D2D) communications and Multi-hop Cellular Networks (MCNs). In device-centric MCNs, smart mobile devices become *prosumers* of wireless connectivity and act as a bridge between the cellular infrastructure and other devices. Previous studies have demonstrated that MCNs can significantly improve the capacity and energy consumption, and provide higher and more homogeneous QoS and QoE levels. However, to date, most of these studies have remained analytical or simulation-based and hence there is the need to experimentally demonstrate the benefits of MCN technologies. In this context, one first and significant contribution of this thesis is the experimental evaluation of the performance of MCN through field tests using commercial live cellular networks. The conducted field tests are aimed at validating and quantifying the benefits that MCNs using mobile relays can provide over traditional cellular systems. To this aim, a unique hardware testbed has been designed and implemented together with the necessary software tools to monitor the operation, QoS and benefits of MCNs, and investigate the conditions under which such benefits can

be obtained. Using the data obtained from the field test measurements, the thesis then proposes a unique set of empirical models that characterize the communications performance of MCNs, and that can help design, test and optimize communications and networking protocols tailored for MCNs in analytical and simulation-based studies. Complementary to these studies, this thesis proposes to improve the transmission efficiency of delay-tolerant data traffic by integrating opportunistic networking principles into MCNs. Opportunistic networking can exploit the delay tolerance characteristic of relevant data traffic services in order to search for the most efficient transmission conditions in MCNs. In this context, this thesis first derives an analytical framework for opportunistic MCNs designed to identify their optimum configuration in terms of energy efficiency. Using this reference configuration, this thesis then proposes a set of opportunistic forwarding policies that exploit context information provided by the cellular network, and that demonstrate their potential to significantly contribute towards achieving the capacity and energy-efficiency gains sought for 5G networks.

Resumen

Los sistemas de comunicaciones móviles han experimentado una notable evolución en las últimas décadas con la aparición de nuevas tecnologías de acceso radio diseñadas para incrementar la capacidad del sistema y soportar mayores tasas de transmisión. Esta evolución se ha centrado principalmente en el marco del concepto tradicional de arquitectura celular centrada en infraestructura en la que cada estación móvil comunica directamente con la estación base. Las comunicaciones celulares tradicionales experimentan dificultades para proveer niveles de calidad de servicio (*Quality of Service*, QoS) elevados y homogéneos en toda la celda (en particular en los límites de la celda) debido a la atenuación que sufre la señal con la distancia y la presencia de obstáculos. En este contexto, un cambio en el paradigma es perseguido en el diseño de los futuros sistemas de comunicaciones móviles (los sistemas 5G) que deberán soportar de una manera eficiente los diversos requisitos de QoS y calidad de experiencia (*Quality of Experience*, QoE) del tráfico de datos de las redes móviles que crece a tasas exponenciales. Esta tesis defiende la necesidad de explorar y evolucionar desde las actuales arquitecturas celulares centradas en la infraestructura a tecnologías inalámbricas centradas en los dispositivos que sacan provecho de la inteligencia, y los recursos de comunicación y computación de los dispositivos móviles inteligentes. Una forma de conseguir estos objetivos es explotando las comunicaciones dispositivo a dispositivo (*Device-to-Device*, D2D) y las redes celulares multi-salto (*Multi-hop Cellular Networks*, MCNs). En las redes MCNs, los dispositivos móviles pasan a ser productores/consumidores de conectividad inalámbrica actuando como pasarela entre la infraestructura celular y otros dispositivos. Estudios anteriores han demostrado el potencial de las redes MCNs para conseguir importantes beneficios de capacidad y eficiencia energética, a la vez que proveen de mayores y más homogéneos niveles de QoS y QoE. Sin embargo, hasta el momento, las investigaciones realizadas se han limitado generalmente a estudios analíticos y de simulación, y existe por lo tanto la necesidad de demostrar los beneficios de las redes MCNs de manera experimental. En este contexto, una primera y significativa contribución de esta tesis es la evaluación experimental del rendimiento de las redes MCNs a través de pruebas de campo en redes

celulares comerciales. Las pruebas de campo llevadas a cabo persiguen validar y cuantificar los beneficios que las redes MCNs utilizando retransmisores móviles pueden proporcionar sobre los sistemas celulares tradicionales. Para ello, esta tesis ha diseñado e implementado una plataforma hardware con las herramientas software necesarias para monitorizar la operación y la QoS de los procesos de retransmisión en los enlaces multi-salto, y que permite investigar los beneficios de las redes MCNs y las condiciones en los que estos beneficios pueden obtenerse. Utilizando los datos obtenidos de las medidas de campo, esta tesis extrae un conjunto único de modelos empíricos que caracterizan el rendimiento de las comunicaciones MCN, y que pueden ayudar al diseño, testeo y optimización de protocolos de comunicación y de red para redes MCNs en estudios analíticos y de simulación. De manera complementaria a estos estudios, esta tesis propone mejorar la eficiencia en la transmisión del tráfico de datos tolerante a retardos por medio de la integración de técnicas de red oportunistas en las redes MCNs. Los mecanismos oportunistas explotan la tolerancia al retardo que caracteriza a alguno de los servicios de datos más relevantes para buscar las condiciones de transmisión más eficientes en las redes MCNs. En este contexto, esta tesis desarrolla primero un entorno analítico para redes MCNs oportunistas diseñado para identificar la configuración óptima en términos de eficiencia energética. Utilizando esta configuración óptima como referencia, esta tesis propone entonces un conjunto de mecanismos oportunistas que explotan información de contexto proporcionada por la red celular y que demuestran su potencial para contribuir de manera notable a alcanzar los requisitos de capacidad y eficiencia energética perseguidos en las redes 5G.

Acknowledgements

With thanks to:

Prof. Javier Gozalvez for supervising this thesis, for his continuous comments and suggestions that have significantly contributed to the quality of this thesis, for giving me the opportunity to join the UWICORE laboratory and for passing me on his passion to research.

UWICORE lab members (current and former) for their help, for their laughs and tears, for their coffee/lunch/dinner-breaks, and for doing this period unforgettable.

Prof. Vasilis Friderikos and people at CTR lab in King's College London for accepting me in this intense and live visiting period.

Dr. Miguel Sepulcre, Dr. Mari Carmen Lucas, Dr. Alberto Rodriguez-Mayol, Prof. Joaquín Sanchez-Soriano, Dr. Oscar Lázaro, Alejandro Moraleda-Soler, Juan Ramón Gutierrez-Agulló and Jónatan Muñoz Gelde (in addition to Prof. Javier Gozalvez and Prof. Vasilis Friderikos) for being co-authors of the publications produced in this thesis.

The Communications Engineering Department at UMH.

My sister and my brother for their continuous support. Thanks also to the rest of my family and family in law.

YOU for your love, patience and comprehension. Thanks for your differences that complement my life.

My friends for being always there when I needed them most.

Those who passed away that are the reason why I always try to do my best.

My mother for dedicating her life to doing mine easier.

UNIVERSITAS
Miguel
Hernández

Contents

UNIVERSITAS Miguel Hernández

List of Publications

To date, the work reported in this thesis has produced the following publications.

Publications in international peer-reviewed journals:

- B. Coll-Perales, J. Gozalvez, O. Lazaro and M. Sepulcre, "Opportunistic Multihopping for Energy Efficiency: Opportunistic Multihop Cellular Networking for Energy-Efficient Provision of Mobile Delay Tolerant Services", *IEEE Vehicular Technology Magazine*, *vol. 10, no. 2, pp. 93-101,* Jun. 2015. DOI: 10.1109/MVT.2015.2411414.
- B. Coll-Perales, J. Gozalvez and V. Friderikos, "Energy-efficient Opportunistic Forwarding in Multi-hop Cellular Networks using Device-to-Device Communications", *Wiley Transactions on Emerging Telecommunications Technologies, published online on Wiley Online Library*, Aug. 2014. DOI: 10.1002/ett.2855.
- J. Gozalvez and B. Coll-Perales, "Experimental Evaluation of Multihop Cellular Networks Using Mobile Relays", *IEEE Communications Magazine, vol. 51, no. 7, pp. 122-129*, Jul. 2013. DOI: 10.1109/MCOM.2013.6553688.

Publications under review in international peer-reviewed journals:

- B. Coll-Perales, J. Gozalvez and V. Friderikos, "Context-Aware Opportunistic Networking in Multi-Hop Cellular Networks", *under review*.
- B. Coll-Perales, J. Gozalvez and M. Sepulcre, "Empirical Models of the Communications Performance of Multi-hop Cellular Networks using D2D", *under review*.

Publications in international conferences with peer-review process of the full paper:

- B. Coll-Perales, J. Gozalvez and V. Friderikos, “Opportunistic Networking for Improving the Energy Efficiency of Multi-hop Cellular Networks”, *Proceedings of the 11th Annual IEEE Consumer Communications & Networking Conference (CCNC 2014), pp. 569-574*, Las Vegas, Nevada (USA), 10-13 Jan. 2014. DOI: 10.1109/CCNC.2014.6866628.

- B. Coll-Perales, J. Gozalvez and V. Friderikos, “Store, Carry and Forward for Energy Efficiency in Multi-hop Cellular Networks with Mobile Relays”, *Proceedings of the IEEE/IFIP Wireless Days Conference 2013 (WD 2013), pp. 1-6*, Valencia (Spain), 13-15 Nov. 2013. DOI: 10.1109/WD.2013.6686490.

- B. Coll-Perales, J. Gozalvez and J. Sánchez-Soriano, “Empirical Performance Models for P2P and Two Hops Multi-hop Cellular Networks with Mobile Relays”, *Proceedings of the 8th ACM Workshop on Performance Monitoring, Measurements and Evaluation of Heterogeneous Wireless and Wired Networks (PM2HW2N-2013), pp. 21-28*, Barcelona (Spain), 3-8 Nov. 2013. DOI: 10.1145/2512840.2512844.

- B. Coll-Perales, J. Gozalvez and V. Friderikos, “Context-Based Opportunistic Forwarding in Multi-hop Cellular Networks using Mobile Relays”, *Proceedings of the 2nd ACM/IEEE Workshop on High Performance Mobile Opportunistic Systems (HP-MOSys 2013), pp. 23-30*, Barcelona (Spain), 3-8 Nov. 2013. DOI: 10.1145/2507908.2507914.

- B. Coll-Perales and J. Gozalvez, "On the Capability of Multi-hop Cellular Networks with Mobile Relays to Improve Handover Performance", *Proceedings of the 8th IEEE International Symposium on Wireless Communication Systems 2011 (ISWCS 2011), pp. 207-211*, Aachen (Germany), 6-9 Nov. 2011. DOI: 10.1109/ISWCS.2011.6125339.

- J. Muñoz, B. Coll-Perales and J. Gozalvez, "Research Testbed for Field Testing of Multi-hop Cellular Networks using Mobile Relays", *Proceedings of the 35th IEEE Conference on Local Computer Networks (LCN), pp. 304-307*, Denver, Colorado (USA), 11-14 Oct. 2010. DOI: 10.1109/LCN.2010.5735728.

Publications in national conferences with peer-review process of the full paper:

- B. Coll-Perales, J. Gozalvez and O. Lazaro, “Eficiencia Energética a través de Procesos Oportunistas en Redes Multi-hop Celular”, *Libro de Actas del XXIX Simpósium Nacional de la Unión Científica Internacional de Radio (URSI), pp. 1-4,* Valencia (Spain), 3-5 Sept. 2014.

- B. Coll-Perales, J. Gozalvez and V. Friderikos, "Comunicaciones Oportunistas y Contextuales para Redes Multi-hop Celular con Retransmisores Móviles", *Libro de Actas de las XI Jornadas de Ingeniería Telemática (Jitel 2013), pp. 1-8*, Granada (Spain), 28-30 Oct. 2013.
  Publication selected among the top 4 out of the 80 papers published in the conference proceedings.

- B. Coll-Perales, J. Gozalvez and V. Friderikos, "Energy Efficiency in Multi-hop Cellular Networks with Mobile Relays", *Libro de Actas del XXVIII Simpósium Nacional de la Unión Científica Internacional de Radio (URSI), pp. 1-4*, Santiago de Compostela (Spain), 11-13 Sept. 2013.

- B. Coll-Perales and J. Gozalvez, "Modelo Empírico de Comunicaciones Multi-hop Celular con Retransmisores Móviles", *Libro de Actas del XXVII Simpósium Nacional de la Unión Científica Internacional de Radio (URSI), pp. 1-4*, Elche (Spain), 12-14 Sept. 2012.

- B. Coll-Perales, J. Muñoz and J. Gozalvez, "Plataforma Experimental y Estudio de la Calidad de Servicio en Redes Multi-hop Celulares con Retransmisores Móviles", *Libro de Actas del XXV Simpósium Nacional de la Unión Científica Internacional de Radio (URSI)*, pp. 1-4, Bilbao (Spain), 15-17 Sept. 2010.
  Publication selected among the top 5 candidates for the best young scientist award.

- B. Coll-Perales, J.R. Gutierrez, J. Muñoz, J. Gozalvez, M.A. Marhuenda and A. Rodriguez, "Plataformas Hardware para el Análisis de Redes Cooperativas Muti-hop Cellular Basadas en Retransmisores Móviles", *Libro de Actas de las XX Jornadas de Telecom I+D, pp. 1-6*, Valladolid (Spain), 27-29 Sept. 2010.

Related research publications:

- B. Coll-Perales and J. Gozalvez, “Contextual Optimization of Location-based Routing Protocols for Multi-hop Cellular Networks using Mobile Relays”, *Springer Telecommunication Systems*, accepted Mar. 2015. DOI: 10.1007/s11235-015-0036-3.

- J. Gozalvez, B. Coll-Perales, A. Rodriguez-Mayol and M.C. Lucas-Estañ, "Multi-hop Cellular Networks based on Mobile Relays: Capabilities and Enabling Technologies", *IEEE E-Letter of Multimedia Communications Technical Committee, vol. 6, no. 3, pp. 45-49*, Mar. 2011.

- A. Moraleda-Soler, B. Coll-Perales and J. Gozalvez. “Link-Aware Opportunistic D2D Communications: Open Source Test-bed and Experimental Insights into their Energy, Capacity and QoS Benefits”, *Proceedings of the 11th IEEE International Symposium on Wireless Communication Systems 2014 (ISWCS 2014)*, *pp. 606-610,* Barcelona (Spain), 26-29 August 2014. DOI: 10.1109/ISWCS.2014.6933425.

- M.C. Lucas-Estañ, J. Gozalvez, B. Coll-Perales, “Mode Selection for Mobile Opportunistic Multi-hop Cellular Networks", *Proceedings of the 79th IEEE Vehicular Technology Conference (VTC2014-Spring), pp. 1-5*, Seoul (Korea), 18-21 May 2014. DOI: 10.1109/VTCSpring.2014.7022988.

- J.R. Gutierrez-Agullo, B. Coll-Perales and J. Gozalvez, "An IEEE 802.11 MAC Software Defined Radio Implementation for Experimental Wireless Communications and Networking Research", *Proceedings of the 2010 IFIP/IEEE Wireless Days (WD'10), pp. 1-5*, Venice (Italy), 20-22 Oct. 2010. DOI: 10.1109/WD.2010.5657724.

- A. Moraleda-Soler, B. Coll-Perales, J. Gozalvez and O. Lázaro. “Comunicaciones D2D Oportunistas: Evaluación Experimental del rendimiento en términos de Energía, Capacidad y QoS”, *Libro de Actas del XXIX Simpósium Nacional de la Unión Científica Internacional de Radio (URSI)*, pp. 1-4, Valencia (Spain), 3-5 Sept. 2014.

- J.R. Gutierrez-Agullo, B. Coll-Perales and J. Gozalvez, "Plataforma Hardware Reconfigurable para el Estudio de Comunicaciones 802.11 Multi-hop", *Libro de Actas del XXVII Simpósium Nacional de la Unión Científica Internacional de Radio (URSI), pp. 1-4*, Elche (Spain), 12-14 Sept. 2012.

Related education publications:

- B. Coll-Perales, M. Sepulcre and J. Gozalvez, “Monitoring the Performance and Operation of Cellular Radio Interfaces using Professional Measurement Tools”, *Ed. Universidad Miguel Hernández de Elche*, Nov. 2014.

- B. Coll-Perales, M. Sepulcre and J. Gozalvez, “Monitoring and Analysis Tools for Mobile Communications Laboratory”, *Ed. Limencop*, S. L., Mar. 2013.

- B. Coll-Perales, M. Sepulcre and J. Gozalvez, “Innovative Mobile Communications Engineering Teaching Laboratory using Professional Network Testing Tools”, *Proceedings of the 3rd Annual International Conference on Education and New Learning Technologies (EDULEARN’11), pp. 5531-5535*, Barcelona (Spain), 4-6 Jul. 2011.

- B. Coll-Perales, M. Sepulcre and J. Gozalvez, "Uso de Herramientas Profesionales para una Docencia Práctica de Sistemas de Ingeniería de Telecomunicación", *Libro de Actas del XX Congreso Universitario de Innovación Educativa en las Enseñanzas Técnicas (CUIEET), pp. 1-7*, Las Palmas de Gran Canaria (Spain), 18-20 Jul. 2012.

UNIVERSITAS
Miguel
Hernández

List of Acronyms

3GPP	3rd Generation Partnership Project
1G – 5G	First Generation – Fifth Generation
5G PPP	5G Infrastructure Public Private Partnership
ACK	Acknowledgement
AMC	Adaptive Modulation and Coding
AODV	Ad-hoc On-demand Distance Vector
AP	Access Point
ARQ	Automatic Repeat Request
ASA	Authorized Shared Access
BLER	Block Error Rate
BO	Back-Off
BPSK	Binary Phase Shift Keying
BS	Base Station
C	Control plane
CCK	Complementary Code Keying
CoMP	Coordinated Multipoint Processing
CPICH	Common Pilot Channel
CQI	Channel Quality Indicator
CSMA/CA	Carrier Sense Multiple Access/Collision Avoidance
CTS	Clear To Send
CW	Contention Window
D-MN	Destination Mobile Node
D2D	Device-to-Device
DCF	Distributed Coordination Function
DIFS	DCF Inter-Frame Space
DL	Down Link
DRAM	Dynamic Random Access Memory
DSP	Digital Signal Processor
DSSS	Direct Sequence Spread Spectrum

DTN	Delay/Disruption Tolerant Network
EcNo	Energy per chip to Noise ratio
ESCC	Enhanced Serving Cell Changed
FDD	Frequency Division Duplex
FHSS	Frequency Hopping Spread Spectrum
FPGA	Field Programmable Gate Array
FTP	File Transfer Protocol
GPS	Global Positioning System
GPRS	General Packet Radio Service
GSM	Global System for Mobile communications
H-MN	Hybrid Mobile Node
HetNet	Heterogeneous Network
HHO	Hard Handover
HO	Handover
HSDPA	High Speed Downlink Packet Access
HSPA	High Speed Packet Access
HSUPA	High Speed Uplink Packet Access
HTML	HyperText Markup Language
HTTP	HyperText Transfer Protocol
IBSS	Independent Basic Service Set
IEEE	Institute of Electrical and Electronics Engineers
IMT	International Mobile Telecommunications
ISM	Industrial Scientific and Medical
KPI	Key Performance Indicator
LOS	Line Of Sight
LSA	Licensed Shared Access
LTE	Long Term Evolution
LTE-A	Long Term Evolution-Advanced
MAC	Medium Access Control
MANETs	Mobile Ad-hoc Networks
MCN	Multi-hop Cellular Network
MCS	Modulation and Coding Scheme
MIMO	Multiple-Input Multiple-Output
MMR	Mobile Multi-hop Relaying
MMS	Multimedia Messaging System
MN	Mobile Node
MR	Mobile Relay

MRN	Moving/Mobile relay node
MS	Mobile Station
NACK	Non-Acknowledgement
NAND	Negated AND
NAV	Network Allocation Vector
NLOS	Non-Line Of Sight
NTP	Network Time Protocol
ODMA	Opportunity Driven Multiple Access
OFDM	Orthogonal Frequency Division Multiplexing
PCF	Point Coordination Function
PDU	Packet Data Unit
PER	Packet Error Ratio
PHY	Physical
PLAID	Packet Link Adaptation Information for Downlink
PLAIU	Packet Link Adaptation Information for Uplink
PRB	Physical Resource Block
ProSe	Proximity Service
QAM	Quadrature Amplitude Modulation
QoE	Quality of Experience
QoS	Quality of Service
QPSK	Quadrature Phase Shift Keying
RNC	Radio Network Controller
RS	Relay Station
RSCP	Receive Signal Code Power
RSSI	Received Signal Strength Indication
RTS	Request To Send
RXPC	Reception Power Control
SCR	Scrambling Code
SDK	Software Development Kit
SDN	Software Defined Network
SDR	Software Defined Radio
SHO	Soft Handover
SIFS	Short Inter-Frame Space
SIR	Signal to Interference Ratio
SMS	Short Message Service
SON	Self-Organized Network
SSID	Service Set Identifier

TBS	Transport Block Size
TCP	Transmission Control Protocol
TDD	Time Division Duplexing
TDMA	Time Division Multiple Access
TTI	Time Transmission Interval
TTT	Time To Trigger
TXPC	Transmission Power Control
U	User plane
UARFCN	UMTS Terrestrial Radio Access Absolute Radio Frequency
UDP	User Datagram Protocol
UE	User Equipment
UL	UpLink
UMTS	Universal Mobile Telecommunications System
USB	Universal Serial Bus
VANETs	Vehicular Ad-hoc Networks
WAP	Wireless Application Protocol
Wi-Fi	Wireless Fidelity
WiMAX	Worldwide Interoperability for Microwave Access

UNIVERSITAS Miguel Hernández

List of Figures

UNIVERSITAS Miguel Hernández

List of Tables

UNIVERSITAS Miguel Hernández

1

Introduction

Cellular networks face significant capacity and energy challenges as a result of the continuous and exponential growth of cellular data traffic. The widespread adoption of smartphones and their pervasive use, along with the popularity of mobile video, web browsing and social networking applications among others, have been the main factors behind the significant increase in mobile data traffic. These growth levels are predicted to be maintained in the next decade, and Fifth Generation (5G) networks will be required to efficiently support them. The estimated growth in mobile data traffic (by a factor of 500 to 1000) is to a large extent expected to come from a 10 times increase in broadband mobile subscribers, and 50-100 times higher traffic per user [1]. Leading international organizations also expect that 5G networks should support, compared to current Fourth Generation (4G) networks, 10 to 100 times more connected devices, 10 to 100 times higher user data rates, and 5 times smaller end-to-end latency. All this should be achieved while saving up to 90% of energy per provided service [1]. A relevant contribution to the exponential growth of cellular data traffic will be the emergence and widespread adoption of Internet of Things (IoT), Machine-to-Machine (M2M) and connected vehicles applications. These applications have different characteristics and requirements than traditional cellular applications [2]. Industry and academia agree in that we have only yet begun the transition into a fully connected, networked society where everything that can benefit from a wireless connection will be connected [2]. The vision of the future is a *networked society with unconstrained access to information and*

sharing of data available anywhere and anytime to anyone and anything. In this context, future wireless networks should be able to handle diverse requirements and characteristics in an efficient way.

Current expectations and forecasts have launched the race towards the definition and design of efficient future 5G networks by 2020. Relevant efforts currently focus on the use of millimeter-wave (mmWave) frequency bands (i.e., tens of gigahertz and beyond), the (ultra)dense deployment of small cells and the design of advanced transmission technologies [3]. The motivation for these 5G research efforts includes the abundance of large spectrum blocks in the mmWave band, the proliferation of areas where extremely high data rates and/or extreme traffic capacity is required, and the need to provide higher system capacity and spectrum efficiency, respectively. On the other hand, key technological challenges and drawbacks are yet to be addressed including concerns regarding short-range and Non-Line-Of-Sight (NLOS) coverage issues due to propagation challenges, ensuring low-cost deployment and management despite a very large number of deployed nodes, and reducing complexity and computation resources for efficient transmission techniques. Traditional cell-centric solutions can though inherit the limitations to provide high and homogeneous Quality of Service (QoS) levels thorough the coverage area due to the signal attenuation with the distance in direct communications between the mobile station and the Base Station (BS). In this context, there is a trend in the research community [4] to explore and evolve from current solely cell-centric architectures to device-centric (or user-centric, machine-centric) architectures that exploit the intelligence, communications and computing resources of smart mobile devices. This trend will also lead to the design of device-centric networking schemes that aim to support efficient communications in dynamic wireless environments by exploiting the role that end users may have in the networking process by sharing network services and resources [5]. This device-centric perspective has been lately fostered by the identified benefits from Device-to-Device (D2D) communications that facilitate new value added services (including proximity based services), support critical public safety applications, help offload cellular traffic from the BSs, and increase the spatial frequency reuse and therefore the overall capacity of cellular networks [6]-[9].

In future device-centric wireless networks, smart mobile devices will provide wireless connectivity to other devices and will hence act as a bridge with the cellular infrastructure. The integration of cellular and ad-hoc or D2D communications is referred to as Multi-hop Cellular Networks (MCNs) using mobile relays or device-centric MCNs

[10]-[11]. This thesis will refer to MCNs using mobile relays as MCNs for simplification; actually the term MCNs may also refer to the use of fixed relay stations. MCNs (both fixed- and mobile-relay based) are capable of increasing and providing more homogeneous QoS levels by substituting long-distance (and generally NLOS) direct links between mobile users and the BS by various shorter links with improved link budgets using intermediate nodes. MCNs initially focused on the use of fixed relays [12]. However, MCNs that use mobile relays and D2D communications are characterized by a lower implementation cost, but a higher management complexity due to the participation of mobile terminals. In this context, the possibility to exploit the increasing processing power and communication/networking capabilities of mobile terminals in a decentralized and distributed manner increases the potential and future perspectives of MCNs using mobile relays and D2D communications. MCNs using mobile relays will transform mobile devices into *prosumers* of wireless connectivity in an underlay network that if efficiently coordinated with the cellular network has the potential for significant capacity, energy-efficiency and QoS benefits [11].

MCNs can increase QoS and network capacity, and reduce energy consumption by exploiting the communications, computing and networking capabilities of smart devices. MCNs can also benefit from the mobility and storing capacity of mobile devices to implement opportunistic networking schemes that exploit the store, carry and forward paradigm and obtain additional capacity and energy-efficiency gains [13].Traditionally, opportunistic networking has been proposed for disconnected networks that cannot always reliably ensure real-time end-to-end connections [13]. However, opportunistic networking can also be exploited in networks without disconnections (for example, in urban environments) in order to enhance the efficiency of device-centric wireless transmissions (whether D2D or MCN). In this case, two devices might not initiate a transmission (or even establish a connection) if such transmission is not sufficiently efficient, e.g. because of a low received signal level that would result in a high number of retransmissions and the use of low data rate transmission modes. Devices could hence benefit from the node's mobility and the store, carry and forward paradigm to establish communication links between mobile relays based on contact opportunities and waiting for more efficient transmission conditions to start their transmission. In this case, devices will reduce their energy consumption, while also improving the capacity of the network since less wireless resources will be needed to transmit a given amount of data. This opportunistic networking approach could result in some transmission delays, although it is not always the case as demonstrated in [14]. In any case, and according to Cisco estimates [15], delay tolerant services (including mobile video, social networking

services, emails, software/firmware updates, data metering, goods tracking, cloud services, and file sharing, among others) will represent a non-negligible portion of the expected mobile data traffic volume in the years to come. For example, Cisco estimates that mobile video will represent 72% of the mobile data traffic by 2019 [15]. The delay tolerance of certain services can then be exploited by opportunistic schemes to search for efficient contact opportunities, and thereby reduce energy consumption without reducing the end-user QoS. In this context, efficiency-driven opportunistic networking principles could be designed for delay tolerant mobile data traffic, and integrated into device-centric wireless networks in order to enhance the efficiency and capacity of future 5G wireless networks.

1.1 Objectives and Contributions

This thesis is aimed at investigating device-centric multi-hop cellular communications. Recent studies have investigated the benefits that the integration of cellular and D2D or ad-hoc networking technologies can provide over traditional cell-centric architectures in terms of capacity improvement [16]-[17], cell coverage [17], network scalability [17], infrastructure deployment cost [17], power consumption [18] and energy efficiency [19]. However, these studies are generally analytical or simulation-based and the challenges resulting from the use of mobile devices require empirical solid evidences of the performance benefits and the design of novel communication and networking solutions. In this context, it is important to highlight that the research studies conducted within this thesis have devoted significant efforts to demonstrate through field tests and using hardware platforms the potential benefits of MCNs. In fact, this thesis' contributions start with the report of the first experimental field tests over commercial live cellular networks that validate and quantify the benefits that MCNs using mobile relays and D2D communications can provide over traditional cellular systems. The first contributions can be summarized as follows:

- This thesis develops the first testbed with the necessary software tools to obtain real traces of the multi-hop connectivity in MCN systems, and investigate the performance improvements that can be achieved with MCN networks using mobile relays and D2D communications, and the operating conditions under which such improvements can be achieved.
- In addition, this thesis presents the first results of an extensive field test campaign that verify the performance benefits of MCN networks. The measurement campaign is aimed at analyzing the connectivity of MCN systems

in order to determine under which conditions it would be feasible to consider MCN transmissions and their QoS improvement with regards to traditional single-hop cellular communications.

The conducted field tests have provided very valuable data to evaluate and characterize the performance of MCNs using D2D communications. Field test measurements can also be used to characterize the multi-hop connectivity under various operating conditions. In this context, additional contributions of this thesis are:

- This thesis presents a unique set of empirical models of the communications performance of MCN systems that utilize D2D communications and take into account the impact of distance, propagation/visibility conditions, number of hops and communication settings.
- Using the measurements obtained for MCN communications, the thesis also reports D2D link-level models derived as function of the distance between communicating nodes.

A large portion of the cellular data traffic (present and future) can be deemed delay tolerant. In this context, this thesis investigates how to exploit this delay tolerance to further increase the MCN benefits through the integration of opportunistic networking policies. In particular, the main contributions of this thesis in this field are:

- The study of the energy and capacity benefits that can be obtained from the efficient integration of opportunistic networking mechanisms into MCNs that utilize D2D communications for delay tolerant services.
- An analytical framework for opportunistic MCNs that can be used to identify the optimal design of opportunistic MCNs with respect to energy efficiency.
- The study of the impact of the traffic characteristics of delay tolerant services on the energy-efficiency gains that can be achieved with opportunistic MCN communications, and how opportunistic MCN communications should be configured to exploit traffic characteristics in order to reduce the energy consumption.
- The proposal of a set of context-aware realistic opportunistic forwarding schemes for MCNs that exploit context data provided by the cellular infrastructure to significantly reduce the energy consumption compared to traditional single-hop cellular communications.

- The demonstration of how using context information per ring rather than per cell can further reduce the energy consumption of the proposed context-aware opportunistic schemes under non-uniform distribution of users per cell.

1.2 Outline

The outline of this thesis is as follows. Chapter 2 presents a brief overview of the evolution of traditional cell-centric cellular systems (Section 2.1). Device-centric solutions, including D2D and MCNs, are emerging alternatives to traditional cell-centric solutions that are being considered as part of the 5G ecosystem. This chapter hence presents the benefits and current state of the art in D2D communications (Section 2.2) considering cellular (Section 2.2.1) and IEEE 802.11 (Section 2.2.2) technologies. This thesis focuses on IEEE 802.11-based D2D communications (for experimental reasons), and hence a comprehensive description of the IEEE 802.11's physical (PHY) and Medium Access Control (MAC) layers is provided. This chapter presents then the benefits arising from the integration of cellular and ad-hoc or D2D technologies, usually referred to as MCNs, and reviews the studies conducted to demonstrate their capability to contribute towards overcoming certain limitations of traditional cell-centric architectures (Section 2.3). The standardization activities in the field of MCNs are summarized in Section 2.4, and Section 2.5 reviews current requirements and technical approaches that are being considered for the definition of future 5G networks and technologies[1].

The performance improvements that MCNs can achieve over traditional cellular systems have been empirically demonstrated in this thesis. Chapter 3 presents the experimental testbed for field testing of MCNs using mobile relays and D2D communications that has been implemented in this thesis. This chapter first presents the state of the art of recent research activities conducted to develop advanced multi-hop networking testbeds (Section 3.1). A detailed description of mHOP –the MCN research platform implemented in this thesis– is presented in Section 3.2. The platform integrates different types of mobile nodes, and the necessary software tools to monitor the operation of the cellular and ad-hoc multi-hop forwarding processes. The chapter also provides instructions on how to configure the mHOP testbed for field testing (Section 3.3). The testbed configuration includes: synchronization of mHOP devices (Section 3.3.1), configuration of the hybrid mobile node that acts as a bridge between

[1] The state of the art for the various research topics addressed in this thesis is included in each of the related chapters rather than in a single introductory chapter.

the cellular and ad-hoc networks (Section 3.3.2), configuration of the mobile relay nodes that forwards the data traffic to the destination mobile node (Section 3.3.3), and the configuration of the destination mobile node that executes the file download and receives the data (Section 3.3.4).

Chapter 4 presents the results of the field testing campaign that verifies and quantifies the benefits that MCNs using mobile relays and D2D communications can provide over traditional single-hop cellular systems. The field testing environment, including the configuration of mobile nodes, the employed technologies, localization of base stations and visibility conditions, etc., is described in Section 4.1. This chapter also presents how the performance of MCN communications is measured at the mobile destination node in order to minimize the impact of the radio resource management policies implemented by mobile network operators (Section 4.1.1). The experimental evaluation of the MCN performance is then presented in Section 4.2. This section focuses on the capacity of MCN technologies to increase the QoS while crossing handover areas (Section 4.2.1) and at large distances to the serving base station (Section 4.2.2), to extend the cellular radius (Section 4.2.3) and the outdoor QoS levels to indoor environments (Section 4.2.4), and to increase QoS under NLOS conditions to the BS (Section 4.2.5). The conducted field tests have also demonstrated the capacity of MCNs using mobile relays and D2D communications to reduce the energy consumption compared to traditional single-hop cellular communications (Section 4.2.6).

Chapter 5 exploits the valuable data obtained during the field tests measurements to characterize and model the communications performance of MCN using D2D. The experimental environment (Section 5.1.1) and considered performance metric (Section 5.1.2) are first presented. The chapter then presents the proposed models for two-hop MCN communications (Section 5.2). To this aim, the chapter presents first field tests measurements of the performance experienced at the destination node when the D2D link is characterized by LOS and NLOS conditions and for various distances between the hybrid mobile node and the base station (Section 5.2.1). The functions that best fit the performance measured at the mobile destination node are then identified (Section 5.2.2). Two different curve fitting methods, Least-Squares Parameter Estimation (Section 5.2.3) and Linear Programming (Section 5.2.4), are then used to derive the fitting parameters that best fit the selected functions to the communications performance of MCN measured at the destination mobile node. Performance models for 2-hop MCN communications are derived and validated in a different location with a different serving base station (Section 5.2.5). The two-hop MCN measurements are also used to derive

D2D link level models of the IEEE 802.11 communication between the hybrid node and the destination node (Section 5.2.6). MCN communications models are then presented for an increasing number of hops. In particular, this chapter presents new models derived for three-hop MCN connections that introduce an additional mobile node located between the hybrid node and the destination node (called intermediate node). The conducted field tests for three-hop MCN communications (Section 5.3.1) evaluate both the MCN performance at the intermediate node and the destination node, and the derived models are then presented in Section 5.3.2. This chapter finally presents, and justifies, MCN performance models for four-hop and five-hop MCN communications.

The benefits of integrating opportunistic networking principles into MCNs are analyzed in Chapter 6. This chapter first reviews related studies (Section 6.1) and then introduces some of the most relevant delay tolerant services that are driving the growth in cellular traffic data (Section 6.2). These services show the possibility to manage the tolerable delay towards an efficient integration of opportunistic networking and MCNs at no cost to the perceivable QoE. The study conducted in this chapter examines this possibility for a two-hop MCN scenario in which a static Source Node (SN) wants to transmit information to a Base Station (BS) using a Mobile Relay (MR) with store, carry and forward capabilities (Section 6.3). To this aim, the study first derives an analytical framework (Section 6.3.1) to identify the optimum MR location and the location at which the relay node needs to start forwarding the information to the cellular network in order to minimize the overall energy consumption (Section 6.4). Finally, this chapter analyzes the impact of the traffic characteristics on the energy efficiency and configuration of two-hop opportunistic MCN communications (Section 6.5); particular attention is paid to mobile video traffic given its large share over the total volume of cellular data traffic (Section 6.5.1).

Using the optimum configuration of opportunistic MCN communications derived in Chapter 6, Chapter 7 introduces novel context-aware opportunistic forwarding schemes for MCNs that exploit context information provided by the cellular infrastructure. First, related studies that highlight the important benefits that can be achieved using context information are presented (Section 7.1). The proposed opportunistic forwarding MCN schemes delay the start of the D2D communications (Section 7.2) or increase the search area where to look for potential mobile relays (Section 7.3) in order to increase their feasibility when no mobile relays are found at the identified optimum location and time instant. The operation of the two opportunistic MCN proposals require probabilistically estimating the time to delay the D2D transmission until an MR is found at the identified

optimum location and the radius of the search area around the optimum MR location that guarantees the presence of at least one mobile node; these estimations have been done for uniform and non-uniform distribution of nodes within the cell. This chapter also compares the performance of the two proposals (Section 7.4) under worst-case conditions (Section 7.4.1), and in terms of energy-efficiency (Section 7.4.2) and network capacity (7.4.3).

Finally, Chapter 8 summarizes the main conclusions that can be extracted from this thesis, and provides indications about possible future research directions.

UNIVERSITAS Miguel Hernández

UNIVERSITAS
Miguel
Hernández

2

Multi-hop Cellular Networks

Cellular systems have significantly evolved over the past decades with the emergence of new and efficient radio access technologies, and the implementation of advanced techniques to support the increased network capacity and the high data rates demanded by novel applications. The evolution has mainly focused around the traditional cell-centric approach where each Mobile Station (MS) directly communicates with the Base Station (BS). Despite the considerable efforts made in the research community, this approach is still challenged to provide high and homogeneous Quality of Service (QoS) levels throughout the cell area, in particular at the cell edges, due to the strong signal attenuation with the increasing distance and the highly variable propagation conditions caused by the presence of obstacles and interferers. These signal degradations result in that mobile users located at the cell boundaries experience poor QoS levels. This problem could be partially overcome by augmenting the number of BSs, although provisioning additional infrastructure bears significant costs at the deployment and management phases, and it has also a social cost. So, this solution in isolation might not be able to meet the data capacity demand for current and future networks. Other emerging alternatives currently being considered as part of Fifth Generation (5G) network evolution include the direct communication between devices, which is referred to as Device-to-Device (D2D) communications, and the integration of cellular, Wi-Fi and ad-hoc or D2D communications into what is referred to as Multi-hop Cellular Networks

(MCNs). The increasing processing power and networking capabilities of smartphones provide significant opportunities for the use of mobile relays in MCNs. MCNs substitute a direct MS-BS link by multiple hops, which reduces the path-loss and increases the link budget compared to long-distance single-hop cellular links. Despite the resulting management complexity, the implementation of MCNs using mobile relays and D2D communications could represent a significant technology breakthrough that could help progress from current cell-centric systems towards device-centric systems that exploit collaboratively the communication and computing resources available at mobile terminals. In this context, Section 2.1 summarizes the evolution of traditional cell-centric cellular systems, and highlights their main limitations to efficiently support the expected capacity demand of future 5G networks. Section 2.2 presents the two 3rd Generation Partnership Project (3GPP) variants for D2D communications that consider cellular (e.g. Long Term Evolution-Direct, LTE-Direct) as well as IEEE 802.11 technologies. Section 2.3 provides a comprehensive description of the benefits of MCNs in device-centric wireless networks, and summarizes prior and current standardization activities in this field. Finally, Section 2.5 summarizes the challenges and requirements for 5G networks along with key disruptive technologies that are being considered as part of the 5G ecosystem.

2.1 Cell-Centric Cellular Systems

Cellular systems have significantly evolved over the past decades. Second generation (2G) systems were developed to overcome First Generation (1G) limitations by means of the introduction of digital traffic channels, encryption, error detection and correction, and advanced channel access mechanisms among others. The objective of the Third Generation (3G) of cellular networks was to provide fairly high-speed wireless communications to support not only voice and Short-Messages Services (SMS), but also multimedia, data and video [20]. A significant breakthrough in mobile communications systems has been achieved with the introduction of 3.5G and Fourth Generation (4G) systems that have led to the emergence of new radio access techniques, and the implementation of advanced techniques designed to increase capacity and spectral efficiency, and the support of higher data rates. These (radio access) techniques include among others carrier aggregation, advanced smart antenna techniques, enhanced Multiple-Input Multiple-Output (MIMO), fast channel dependent scheduling, adaptive coding and modulation, and Coordinated Multipoint Processing (CoMP). Using these techniques, 3.5G and 4G systems offer high peak data rates in ideal conditions. However, the network capacity is not evenly distributed since the cell edge users

experience worse throughput levels than cell center users [21]. The introduction of 3.5G and 4G systems has also resulted in the modification of the cellular architecture. However, the introduced changes have generally been done in the framework of the traditional cell-centric architecture concept where each MS directly communicates with the BS. Under this cell-centric approach, and considering the fundamental limits of communication technologies and radio propagation, the transmit power of a data link increases with the data rate when a specific link quality is maintained. Consequently, and independently of the 3.5G or 4G radio interfaces being employed, data rates in a traditional cell-centric cellular architecture decrease with the distance to the serving BS. In this context, traditional cellular systems based on cell-centric architectures are likely to experience difficulties in providing high and homogeneous QoS levels throughout the cell area (in particular at the cell edge). This is mainly due to the singal attenuation with increasing distances, but also because of the highly variable propagation conditions caused by the presence of obstacles and interferers. Providing high and homogeneous QoS levels, as requested by future 5G systems (further deails on the 5G requirements and chellenges can be found in Section 2.5), would require to considerably increase the transmission power levels, or to limit the link to short distances between the MS and the BS which will in turn increase the number of BSs to be deployed. However, increasing the number of deployed BSs results in additional deployment and operational costs. It is also important to note that increasing the number of BSs has a social cost due to the social reaction against BSs.

A relevant novelty was introduced with the integration of relaying techniques into cellular systems. This new operational framework introduces new technical challenges to be solved, but represents a significant step towards overcoming the fundamental communication and radio propagation limits of traditional cellular architectures that difficult the provision of homogenous and high QoS levels across a coverage area. The integration of relaying techniques into cellular standards has initially focused on fixed relaying solutions. In fact, fixed relaying is part of both LTE-Advanced [22] and IEEE 802.16j [23]. Fixed relaying techniques are expected to significantly improve the system capacity and user-perceived QoS by means of serving user located close to the cell edge. Fixed relays are part of the network infrastructure, and have then to be considered during the network planning, design and deployment. Relevant field trials conducted at the Berlin LTE-Advanced testbed have experimentally demonstrated the benefits of fixed relaying in terms of cellular coverage and capacity [24]. Indoor coverage extension is also demonstrated in [25] using the EASY-C LTE-Advanced testbed. The benefits of fixed relaying solutions are obtained at the expense of an infrastructure deployment

cost, and the need to strategically locate fixed relays at the cell edge under LOS conditions with the BS in order to maximize capacity and end-user QoS.

2.2 Device-to-Device Communications

There is a common view in that future 5G systems will be accomplished through a group of radio technologies and advanced architectures that complement each other [26]. Several 5G research trends can be identified. On the one hand, relevant efforts focus on the use of higher frequency bands, the dense deployment of small cells, and the design of advanced transmission techniques [3]. These approaches build from traditional cell-centric architectures. On the other hand, there is a significant belief in the community [4] that future wireless networks need to explore and evolve from current cell-centric architectures to device-centric architectures that exploit the intelligence, increasing capabilities, communications and computing resources of smart mobile devices. This includes the offloading of cellular data traffic to Device-to-Device (D2D) connections [4]. D2D communications facilitate new value added services (including proximity based services), support critical public safety applications, help offload cellular traffic from the base stations, and increase the spatial frequency reuse and therefore the capacity of cellular networks [6]-[9].

D2D communications have received significant research attention during the last few years at the research (e.g. European research projects such as METIS -Mobile and wireless communications Enablers for the Twenty-twenty Information Society- [27] and MOTO -Evolving mobile internet with innovative terminal-to-terminal offloading technologies- [28]) and standardization levels (3GPP is already working on D2D communications in Release 12 [9], [29]-[34]). D2D communications have been proposed as a means of taking advantage of the physical proximity of communicating devices. Several technologies have been used for this purpose in the past, e.g. Bluetooth, Ultra-wideband (UWB), IEEE 802.15.4 (or Zigbee) and IEEE 802.11 (or Wi-Fi-Direct). Research efforts have been now mostly devoted to add cellular technologies (in particular LTE) to support D2D communications. The use of licensed bands and the provision of partial or total control of D2D links to the cellular network operator can increase the reliability and QoS levels of D2D communications. It is worth though noticing that 3GPP actually considers IEEE 802.11 technologies as well as cellular technologies (e.g. LTE-Direct) for the direct over-the-air data exchange between devices.

2.2.1 LTE-based D2D communications

D2D communications underlaying cellular networks will allow proximity users to communicate directly without having to be directed through the BS [35]. D2D communications may generate interference into the existing cellular network if not designed properly. Thus, interference management is one of the most critical issues for D2D underlaying cellular networks where D2D and cellular communications co-exist. Current solutions based on LTE focus on network-assisted approaches that target an interference-free integration of D2D communications within existing cellular networks. This co-existence is typically addressed by means of novel resource allocation schemes designed with the objective of maximizing the overall network capacity while guaranteeing the QoS requirements for both D2D users and traditional cellular users [36]. Approaches to limit the interference to the existing cellular users include restricting the transmission power of D2D links and the distance between the D2D users [37]. The aforementioned interference issues between D2D and existing cellular users can be also solved by dedicating part of the cellular spectrum to D2D communications, which is referred to as overlay in-band D2D communications [38]. Another alternative is to adopt out-band (i.e. a non-cellular portion of the spectrum, e.g. ISM –Industrial Scientific and Medical– bands) rather than in-band D2D communications in cellular networks. Hence, the D2D communications take place using a different radio interface than the cellular one, typically an IEEE 802.11 one (Section 2.2.2 is dedicated to IEEE 802.11-based D2D communications). In this context, the potential of D2D communications for enhancing the network performance and increasing the spectral efficiency is subject to an efficient management of the spectrum bands including the exploitation of licensed and unlicensed bands.

Another important issue to efficiently integrate D2D communications into the existing cellular networks is to detect nearby devices. To this aim, Qualcomm proposed LTE-Direct[2] that enables *always-on* discovery of devices in proximity (and their services), in a privacy sensitive and battery efficient way [39]-[41]. LTE-Direct uses radio signals –called *expressions*– that are (periodically) sent by the mobile devices showing the users profiles/preferences (privacy settings determine whether transmissions are targeted for private or public audience). LTE-Direct keeps discovery mechanisms on the device rather than in the network despite using licensed spectrum which is another example of the expected impact of device-centric solutions on future 5G wireless cellular networks.

[2] LTE-Direct is the basis of the 3GPP work item on D2D communications that is known as Proximity Services (ProSe).

LTE-based D2D communications have shown to possess unique capabilities that could lead to disruptive design changes towards the definition of future 5G cellular networks. However, it is important to highlight that the research conducted in this thesis is not focused on LTE-based D2D communications. This is motivated by the importance placed in this thesis not only to theoretical and simulation analyses, but most importantly to experimental validation through real-time hardware testbed. At the time this study was conducted, no D2D platforms based on LTE were available in commercial off-the-shelf mobile devices. The requested D2D platform should also allow its integration with cellular technologies and has to possess software tools to monitor the operation and QoS of the multi-hop forwarding processes, as it will be shown in Chapter 3. An interesting development is the Qualcomm's FlashLinQ solution [42] enabling mobile devices to discover automatically neighboring terminals and communicate with them with limited infrastructure support. FlashLinQ is implemented over licensed spectrum on a Digital Signal Processor (DSP)/Field Programmable Gate Array (FPGA) platform that enables distributed channel-aware spatial resource allocation in coordination with the cellular providers. All in all, FlashLinQ targets device-to-device communications, and not multi-hop cellular communications that is the focus of this thesis. FlashLinQ is now developed as LTE-Direct, and only a Software Development Kit (SDK) to develop proximal discovery solutions and proximity services has been recently released. This certainly represents an interesting progress towards the study of MCNs using LTE-based D2D communications that could be considered as future research.

2.2.2 IEEE 802.11-based D2D/Ad-hoc Communications

IEEE 802.11-based ad-hoc wireless networking has also received significant research attention as a technology alternative enabling nodes to form an infrastructureless network. Its capacity to enable high bit rates and provide multi-hop communications has fueled the emergence of novel solutions such as Mobile Ad-hoc Networks (MANETs), Vehicular Ad-hoc Networks (VANETs) and MCNs (Section 2.3). The success and penetration/availability of IEEE 802.11 technologies coincides with the increase of mobile data traffic. Offloading mobile data traffic to IEEE 802.11 networks has hence become an attractive solution to tackle the capacity challenge cellular networks are currently facing [43][44]. As cellular data traffic keeps on rising, it has been identified the need to further integrate cellular and IEEE 802.11 technologies. In fact, 3GPP is already working on the use of IEEE 802.11 technologies to support D2D communications and proximity services (ProSe) in cellular networks [9]. Figure 2-1 illustrates a specific use case scenario that is being considered within 3GPP where the integration between IEEE 802.11 and cellular technologies can help alleviate the cellular traffic load. In this

scenario, cellular networks do not only exploit IEEE 802.11-based technologies to offload cellular data traffic, but also have the capability to control and configure the establishment of the IEEE 802.11 network and IEEE 802.11-based D2D communications.

```
Pre-Conditions
   - Bob and John are subscribers to a mobile data service from an MNO
     (Mobile Network Operator);
   - Bob and John both carry UEs (User Equipments) that have IEEE 802.11
     capabilities;
   - Both UEs are enabled for ProSe (ProximityServices) Discovery and
     Communication;
   - Bob and John use ProSe-enabled applications on their UEs;
   - The 3GPP network has the capability to provide IEEE 802.11
     configuration information to ProSe-enabled UEs;
   - Bob has clicked the ProSe-enabled UE to send an HD (High-
     Definition) video to John.
Service Flows
   - The 3GPP EPC (Evolved Packet Core) determines proximity of Bob's
     and John's UEs and provides them with IEEE 802.11 configuration
     information to assist with IEEE 802.11 direct connection
     establishment.
   - Bob's and John's UEs use the configuration information to verify
     feasibility of the IEEE 802.11 direct connection and establish
     ProSe-assisted IEEE 802.11 direct communications.
   - The ProSe-enabled application on Bob's UE streams the HD video to
     the ProSe-enabled application on John's UE using the established
     IEEE 802.11 connection.
Post-Conditions
   - John has received Bob's HD video via the ProSe-enabled application
     on his UE.
```

Figure 2-1. 3GPP's use case that describes network-assisted IEEE 802.11-based D2D communications [9].

2.2.2.1 Physical Layer

The original IEEE 802.11 standard specified the use of three different PHY layers: (i) infrared, (ii) Frequency Hopping Spread Spectrum (FHSS) at 2.4 GHz, and (iii) Direct Sequence Spread Spectrum (DSSS) at 2.4 GHz [45]. The original goal was to achieve data rates of 2 Mbps which was only possible with DSSS. The DSSS PHY divided the available 80 MHz band at the 2.4 GHz range into three non-overlapping channels, each of them having around 20 MHz of bandwidth. This enabled the interference-free operation of three different ad-hoc networks/D2D links in the same spatial area. Revised amendments of the original IEEE 802.11 standard were released with the requirement of higher data rates. The goal of the IEEE 802.11b amendment was to increase the maximum data rate in the 2.4 GHz band up to 11 Mbps using Complementary Code Keying (CCK) at the PHY layer.

A significant breakthrough was achieved with the release of IEEE 802.11a at 5 GHz band, and especially with the introduction of Orthogonal Frequency Division Multiplexing (OFDM) at the PHY layer. IEEE 802.11a provides data rates of up to 54 Mbps (with fall-back rates of 48, 36, 24, 18, 12, 9 and 6 Mbps) using 8 non-overlapping channels of 20 MHz each (compared to three with IEEE 802.11b). With OFDM, the signal to be transmitted is modulated over several frequency carriers. In IEEE 802.11a, the 20 MHz bandwidth channel is divided into 52 subcarriers, each 312.5 KHz wide, that are modulated using Binary Phase Shift Keying (BPSK), Quadrature Phase Shift Keying (QPSK), 16-Quadrature Amplitude Modulation (16-QAM) or 64-QAM. Forward error correction coding (convolutional coding) is used with a coding rate of 1/2, 2/3, or 3/4.

IEEE 802.11g introduces the adoption of the OFDM technology at the 2.4 GHz band and thus enables transmission data rates of up to 54 Mbps, while it retains interoperability with IEEE 802.11b using DSSS and CCK (Table 2-1 summarizes the transmission modes defined for IEEE 802.11g and the resulting data rates). Since IEEE 802.11g operates at 2.4 GHz, it has the three-channel restriction of the original IEEE 802.11 standard giving its 20 MHz channel bandwidth.

Table 2-1. IEEE 802.11g transmission modes.

Data Rate [Mbps]	Modulation	Coding rate
1	DSSS-DBPSK	-
2	DSSS-DQPSK	-
5.5	CCK- 4 chipping seq.	-
11	CCK – 64 chipping seq.	-
6	OFDM-BPSK	1/2
9	OFDM-BPSK	3/4
12	OFDM-QPSK	1/2
18	OFDM-QPSK	3/4
24	OFDM-16-QAM	1/2
36	OFDM-16-QAM	3/4
48	OFDM-64-QAM	2/3
54	OFDM-64-QAM	3/4

2.2.2.2 Medium Access Control Layer

The IEEE 802.11 MAC layer for ad-hoc wireless networking specifies the use of the Carrier Sense Multiple Access (CSMA) protocol with Collision Avoidance (CA) to reduce packet collision on the network [46]. This is a contention-free service provided by the Distributed Coordination Function (DCF) defined at the IEEE 802.11 standard [47] – the IEEE 802.11 standard also defines the Point Coordinator Function (PCF) for Access Point (AP)/infrastructure network mode that cyclically polls stations, giving them the opportunity to transmit. An IEEE 802.11 node using CSMA/CA listens to (senses) the wireless medium before attempting to transmit its own data packets (see Figure 2-2). If the medium is sensed as busy (i.e. if another transmission is sensed), the IEEE 802.11 node defers its own transmission until the medium becomes available. In particular, the medium needs to be found as idle for an interval longer than the Distributed Inter-Frame Space (DIFS). The CA scheme in CSMA/CA provides a random Back-Off (BO) delay feature before a new transmission attempt is executed. This random delay helps avoid collisions from simultaneous multi-user transmissions, since other wireless nodes could also be waiting to send data over the network. The back-off time is an integer number of slots (e.g. the slot duration – t_{slot} – is equal to 9 μs in IEEE 802.11g) uniformly chosen in the interval (0, *CW*-1), where *CW* stands for Contention Window. At the first transmission attempt, *CW* = *CWmin*, and it is doubled at each retransmission up to *CWmax*. In the IEEE standard, *CWmin* and *CWmax* values depend on the physical layer adopted (e.g. *CWmin* and *CWmax* are equal to 15 and 1023 in IEEE 802.11g). The back-off timer is decreased as long as the medium is sensed as idle, but stopped when a transmission is detected on the channel (Figure 2-2). The back-off timer resumes its count down when the channel is sensed as idle again for more than a DIFS. When the back-off timer reaches zero, the station can transmit its frame (see Figure 2-2).

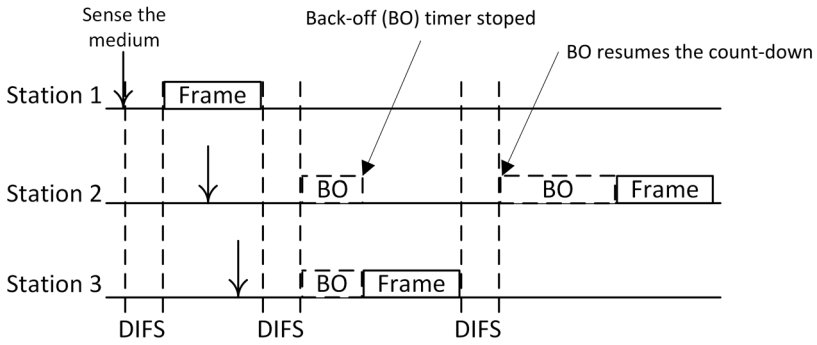

Figure 2-2. IEEE 802.11 basic medium access mechanism.

It may happen that two or more stations start transmitting simultaneously and a collision occurs. The IEEE 802.11 MAC layer defines then a mechanism to ascertain the correct reception of a frame. This mechanism is based on the transmission of an immediate positive acknowledgement frame (ACK) upon correct reception of a data frame. The ACK frame is transmitted by the destination station after a time interval called the Short InterFrame Space (SIFS). As depicted in Figure 2-3, the SIFS is shorter than the DIFS (e.g. SIFS is equal to 10 μs for IEEE 802.11g while DIFS is equal to SIFS+2· t_{slot}, i.e. 28 μs) in order to give priority to the receiving station over other possible stations waiting for transmission (Figure 2-3). If the ACK is not received by the transmitter station, the data frame is presumed to have been lost, and a retransmission is scheduled.

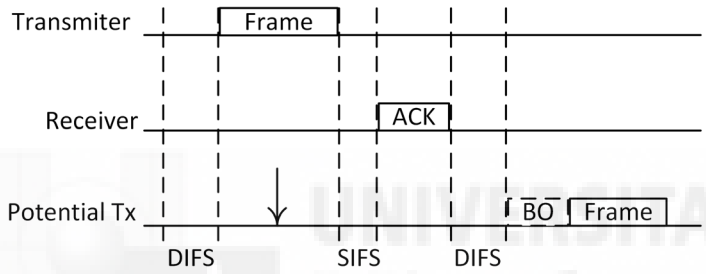

Figure 2-3. IEEE 802.11 mechanism to indicate positive acknowledgement of a frame. The figure also illustrates that the SIFS is shorter than the DIFS.

In addition, the IEEE 802.11 MAC layer defines the virtual carrier sensing mechanism to alleviate the problem known as hidden-station (Figure 2-4). The hidden-station problem occurs when a station (for example, station B) is in the transmitting range of two other stations (stations A and C), but stations A and C cannot hear each other. If station C has a frame to be transmitted to station B, it senses the medium and finds it free/idle because it is not able to hear station A's transmissions. Therefore, it starts transmitting the frame but this transmission will result in a collision at the station B if station A is also transmitting to B. The virtual carrier sensing mechanism is proposed to solve this issue. It is based on two control frames: Request To Send (RTS) and Clear To Send (CTS). Station A would then transmit a RTS frame to the receiving station B announcing the upcoming frame transmission. Upon receiving the RTS frame, station B replies by sending a CTS frame to indicate that it is ready to receive the data frame. Both the RTS and the CTS frames contain the total duration of the transmission (including the related ACK frame). This information can be also heard by any surrounding station (like station C) that uses this information to set up a timer called Network Allocation Vector (NAV) that indicates the remaining time the station must refrain from accessing the

wireless medium. Using the RTS/CTS mechanism, stations may become aware of transmissions from hidden stations, and learn how long the channel will be used for these transmissions.

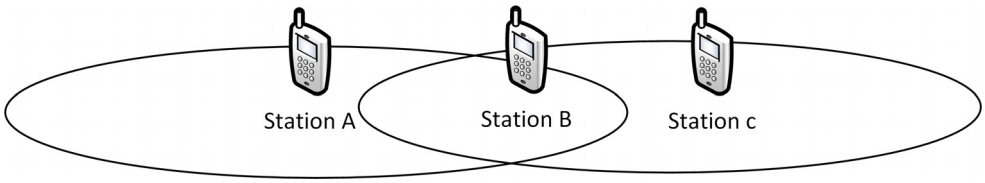

Figure 2-4. Representation of the hidden-station problem in IEEE 802.11.

2.3 Multi-hop Cellular Networks

MCNs are being considered as one of the alternative technology solutions for the future 5G ecosystems. MCNs integrate cellular with ad-hoc relaying technologies to substitute long-distance and NLOS cellular links for multiple hops with LOS propagation conditions and improved link budgets. MCNs use either fixed relays or mobile relays to reduce the communications distance and signal loss in each hop, and thereby offer the possibility to increase the overall multi-hop transmission rate. In this context, MCNs preserve the benefit of using a communications infrastructure while overcoming the limitations of cellular networks to provide homogeneous high bit rates over large areas through the use of multi-hop transmissions over short distances. The multi-hop operation in MCNs results in significant reductions in the transmit power requirements for the relay stations and in improved spectral efficiency per unit area of coverage [55]. As the relays can work in a decode-and-regenerate mode, they could also provide extra link gains by effectively reducing noise accumulation and bit error rates. Figure 2-5 illustrates the operation of MCNs for the cases that the multi-hop link between the MS and the BS uses Fixed Relays (FR) – Figure 2-5.a – or Mobile Relays (MR) – Figure 2-5.b. The figures show that the use of relaying nodes in MCNs can help replacing (NLOS) long-distance links between MS and BS with multiple hops with LOS propagation conditions and improved signal quality. On the other hand, MCNs using fixed relays (Figure 2-5.a) require that additional infrastructure elements are strategically deployed in order to ensure LOS conditions both with the MS and the BS. MCNs using mobile relays (Figure 2-5.b) do not require such deployment costs, but are characterized by a higher management complexity due to the participation of mobile terminals. While it has been suggested that introducing relaying capabilities can increase a mobile terminal's cost and complexity, [56] suggested that the required functionality for a mobile station to support relaying has a negligible impact on the terminal's cost. In addition, it has been

identified the need that future wireless networks explore and evolve from current cell-centric architectures to device-centric architectures which exploit the intelligence, communications and computing resources of smart mobile devices [4]. The expected potential of future device-centric wireless networks, together with the development of D2D or ad-hoc technologies (Section 2.2) and the flexibility of mobile relaying, have fuelled the interest on MCNs using mobile relays or device-centric MCNs (hereafter these terms will be referred to as MCNs for simplification). In future device-centric MCNs, smart mobile devices will provide wireless connectivity to other devices acting as a bridge with the cellular infrastructure. MCNs will transform mobile devices into *prosumers* of wireless connectivity in an underlay network that if efficiently coordinated with the cellular network has the potential for significant capacity, energy-efficiency and QoS benefits [8].

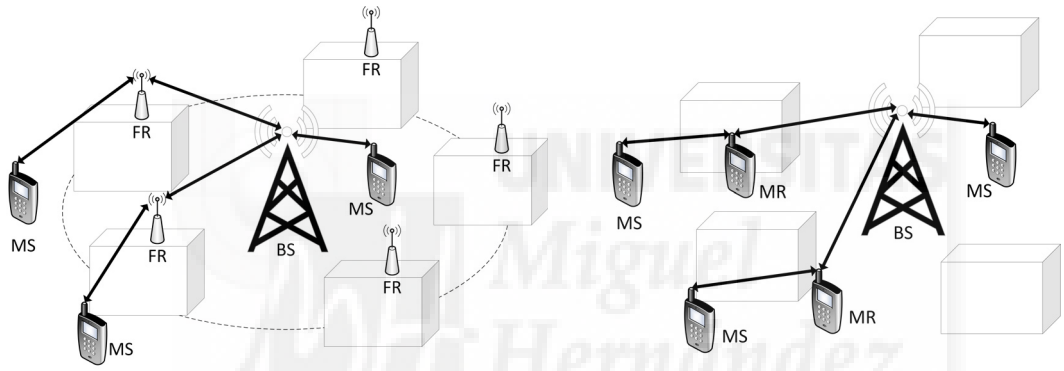

a) MCNs with fixed relays b) MCNs with mobile relays

Figure 2-5. Multi-hop cellular networks.

Previous publications have already reported the multiple advantages that MCN networks provide over traditional cell-centric architectures. In [16], the authors demonstrate the uplink capacity improvement that can be achieved using mobile relay stations in Universal Mobile Telecommunications Systems (UMTS) Frequency Division Duplex (FDD) systems. The uplink capacity is measured in [16] as the number of simultaneous accepted users, which reaches an improvement of 35% when using mobile relaying compared to a system without relaying. This is the case because in the scenario without relaying, the users that cannot reach the BS transmit at their maximum power. On the other hand, in the scenario with mobile relaying, they transmit to the mobile relays with lower transmission power resulting in lower interferences. Therefore, the system capacity improves as more users can be accepted into the system. In [17], the authors present an overview of important topics and applications in the context of

relaying. This work covers different approaches to exploiting the benefits of multi-hop communications via relays, such as solutions for radio range extension in mobile and wireless broadband cellular networks, and to combat shadowing at high radio frequencies. Furthermore, [17] presents multi-hop relaying as a means to reduce infrastructure deployment costs and enhance the capacity in cellular networks by exploiting spatial diversity. The capacity of MCNs using mobile relays to reduce the energy consumption was first highlighted in [18]. This study divided cells into concentric rings, and showed that the overall energy consumption can be reduced if only mobile relays located at the inner-most ring are allowed to directly transmit data to the cellular BS. On the other hand, users located in outer rings should find relays located at inner rings to reach the BS. Under the considered scenario and operating conditions, [18] shows a 20 dB energy reduction of multi-hop cellular communications using mobile relays compared with single-hop cellular communications. In addition, the study conducted in [18] demonstrates that the consumed energy decreases with the increase in number of hops until a certain number of hops (around 7 hops); with higher number of hops the energy saved in transmission does not compensate the increase in the energy consumption at intermediate nodes due to the forwarding operation. In [19], the authors demonstrate that multi-hop wireless networks can further reduce the total energy consumed by means of macro diversity (i.e. signals are jointly transmitted by two or more mobile terminals). In [57], the authors propose a mode selection scheme that decides whether to establish a single-hop or a multi-hop connection between a mobile user and the BS based on the signal strength of the pilot symbols from the BS. The study presented in [58] extends the mode selection alternatives to include connections that integrate opportunistic networking into MCNs. In this study, the mode selection criterion is partly based on the probability to find adequate mobile relays that provide the higher expected performance. It is also important to note that MCNs using D2D communications can provide a more efficient use of radio resources and increase the system's robustness by retransmitting combined data using network coding [59].

The consideration of mobile relays in MCN offers a plethora of novel communications possibilities by exploiting the resources of deployed mobile devices in an opportunistic and collaborative operational framework. MCNs that utilize mobile relays and D2D communications base their operation on the establishment of multi-hop paths to route the information from source to destination. To this aim, it is crucial the design of both adequate neighbor selection techniques and efficient multi-hop networking protocols that choose the most appropriate nodes over which to route the information and reduce the terminal's energy consumption. Various studies (e.g. [60]) have

demonstrated the importance and impact of the neighbor selection on the operation and performance of multi-hop wireless networks, including MCNs. Initial proposals to select the neighbor devices used selection criteria based on the received signal level from neighboring nodes [61], or the nodes proximity [62]. These proposals did not consider the particular characteristics of urban environments where non uniform density distributions of nodes and NLOS propagation conditions are frequent. In this case, an adequate selection of neighbor mobile nodes is even more crucial to increase the nodes connectivity and ensure that a multi-hop routing path from source to destination can be established. In this context, [63] proposed a set of neighbor selection techniques tailored for multi-hop wireless mesh networks (i.e. IEEE 802.11s), and that could be adequate for MCNs using D2D and mobile relays. The proposed schemes exploit spatial diversity to improve the performance and operation of multi-hop wireless networks. In particular, the proposals avoid selecting all neighbor devices in the same direction or closely located since they would not provide the multi-hop route diversity that is expected to improve the operation and performance of MCNs. The authors also proposed a set of novel multi-hop routing protocols that exploit the knowledge of the BS location to reduce network signaling and overall energy consumption [64]. The proposal is based on the reactive Ad-hoc On Demand Distance Vector (AODV) routing protocol [65], but modifies the route search process to reduce network flooding by ensuring that each hop progresses towards the destination node. This work is then extended in [66] to analyze the impact of the operating environment and the location of the source node within the cell on the optimum setting of the multi-hop routing protocol proposal.

2.4 Mobile Relaying Standardization Activities

A first attempt to include mobile relaying into cellular telecommunications networks was presented in 1996 with the name of Opportunistic Driven Multiple Access (ODMA) [67]. ODMA initially represented an enhancement for TDD-based UMTS technology, although some efforts were also devoted to examine its application to FDD-based UMTS technology [67]. The main purposes of ODMA were to reduce power consumption of User Equipments (UEs), to extend the base station's coverage area, and to support higher user data rates. To this aim, ODMA proposed to substitute large paths between the UE and the Base Station (BS) for smaller hops using the communication capabilities of intermediate mobile devices (Figure 2-6). In this context, user data was exchanged between the sending UE and the BS using other intermediate UEs. It should be noted that UEs located in the "Low Bit Rate Data TDD Coverage" area are those that benefit

from the ODMA operation since they communicate with the BS through UEs located in "High Bit Rate Data TDD Coverage" area. As the ODMA standard claims [67], in general, UEs located within the BS coverage area (i.e. UEs that receive layer 1 synchronization information) can be used as relays, even for those UEs located in the "Border Region – NO Coverage" area. The sending UE should establish a path through the intermediate UEs to BS prior to data exchange. One of the key objectives in ODMA was to efficiently route data in such multi-hop system without incurring in high overhead [68]. Unlike traditional MANETs where the communication generally occurs between any pair of nodes, ODMA exploited for this purpose the fact that a sending UE always communicates with the BS. ODMA standardization activities were finally dropped as a result of concerns over complexity, battery life of users on standby, and signaling overhead issues. However, it laid some foundations that are now re-appearing under device-centric 5G wireless proposals [69].

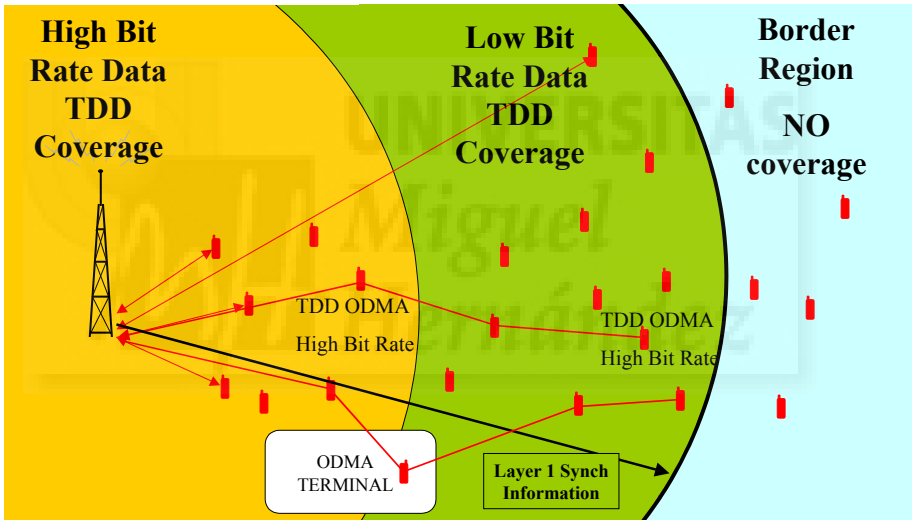

Figure 2-6. ODMA operation [67].

Other standardization efforts considering (mobile) relays took place between 2007 and 2009 for 3GPP LTE-Advanced [22] and WiMAX (through the established Mobile Multi-hop Relaying –MMR– IEEE 802.16j task group) [23] technologies. Relay Stations (RS) help to forward user information from mobile stations to a local BS. In addition to the fixed relay solutions already introduced in Section 2.1, LTE-Advanced and WiMAX also consider moving/mobile relay nodes (MRNs). However, such MRNs are dedicated terminals tailored to serve users inside public transportation vehicles (e.g. trains and buses) as illustrated in Figure 2-7. MRN-based systems face a number of challenges, including the user mobility management. Current standardization activities are to a large extent dealing with these issues, but still lack of many critical control management and

architectural aspects [70]. Their progress will though represent clear advances towards the definition of future 5G device-centric wireless networks.

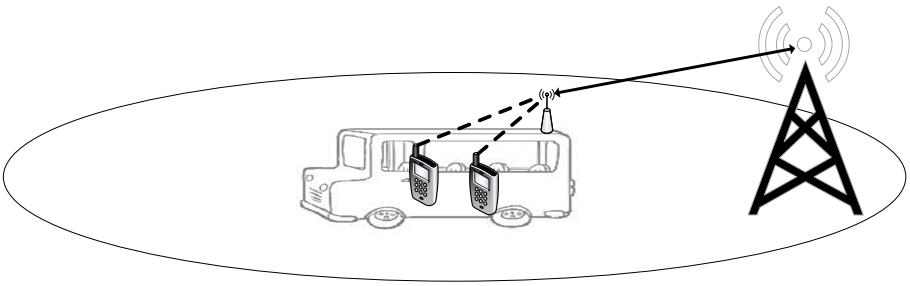

Figure 2-7. Mobile relay node scenario for LTE-Advanced and WiMAX.

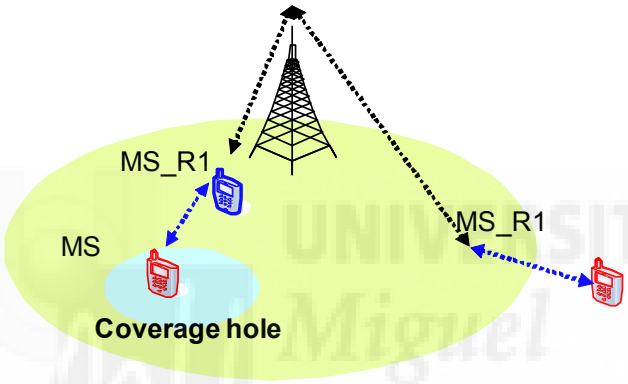

Figure 2-8. Emergency MS relay for IMT-Advanced [71].

The interest in using mobile terminals as relay nodes was already noted during the development of the LTE-Advanced standard and International Mobile Telecommunications (IMT)-Advanced, when Samsung considered this possibility initially for emergency calls when users were located in shadow areas or outside the coverage area of BSs [71], as depicted in Figure 2-8. 3GPP recent activities also focus on the definition of proximity-based services (ProSe) using D2D communications and mobile relays ([9], [29]-[34]) as part of 3GPP Release 12. The current 3GPP study activities cover the identification of use cases and potential requirements for operator-controlled discovery and communications between UEs that are in proximity, under continuous network control, and are under network coverage for commercial/social use, network offloading and public safety. Additionally, 3GPP is analyzing use cases and identifying potential requirements for public safety in case of absence of network coverage. For these purposes, 3GPP identifies potential benefits such as range extension via UE-to-UE relaying and self-organizing out-of-coverage D2D communications. The two basic functions for supporting 3GPP ProSe are D2D discovery and communications. D2D

discovery is broadly classified as restricted or open depending on whether permission from the network is needed or not. D2D communication enables the direct exchange of data between devices in proximity using a cellular radio interface in licensed bands (e.g. LTE) or radio interfaces in unlicensed bands (e.g. IEEE 802.11) [72].

2.5 5G Wireless Networks

There is yet not a clear vision of what 5G networks will be [73] and what technologies it will integrate [4]. What seems to be a consensus is that 5G will ultimately be a paradigm-shift. 5G will expand to accommodate a wide variety of use cases along with new types of connected devices and corresponding services (Figure 2-9, e.g. electricity meters, cars, household appliances, and industry devices). This will require 5G to be able to accommodate new and widely varying requirements. A *one technology fits all* solution will therefore likely not be the most efficient option, but rather a seamlessly integrated combination of evolved wireless technologies and complementary new ones. Considerable efforts are then being devoted to lay the base and foundation for 5G.

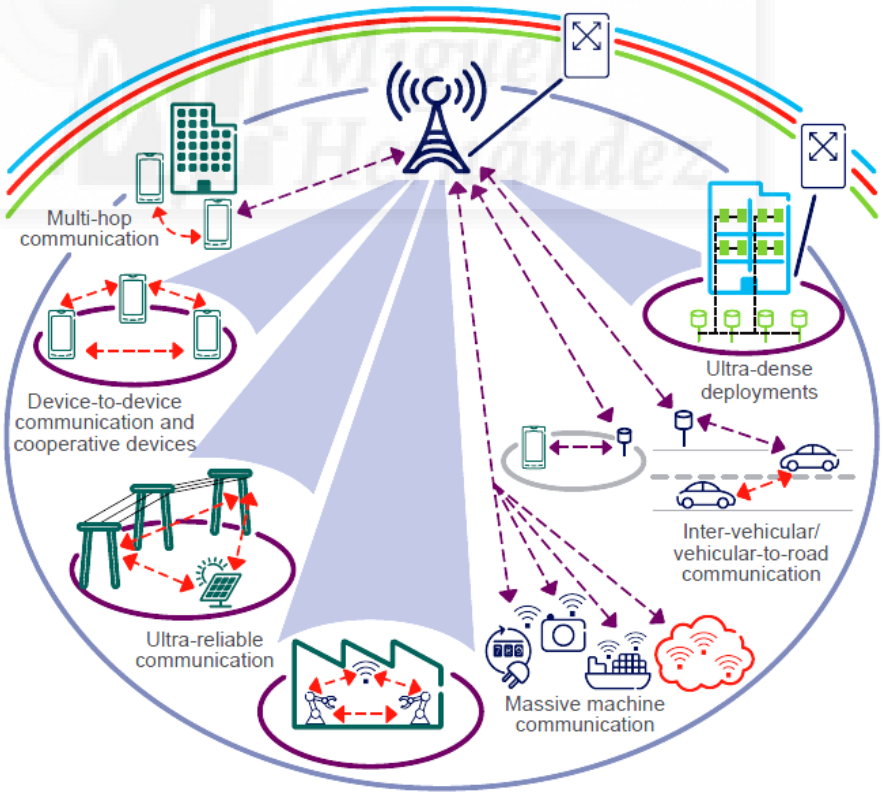

Figure 2-9. 5G as an integrated set of technologies addressing a wide variety of use cases and requirements [74].

These actions include for example the creation of the 5G Infrastructure Public Private Partnership (5G PPP) that is composed of leading EU industry manufacturers, telecommunications operators, service providers, Small Medium Enterprises (SMEs) and researchers. 5G PPP has set that the goal is to provide an initial 5G deployment by 2020. In fact, this coincides with the NTT DOCOMO's wish to showcase initial 5G progresses at the 2020 Olympic Games in Tokyo [75].

2.5.1 Challenges and Requirements

The first step in the definition of 5G has been to identify its requirements. Different applications will place different requirements on the performance; for example, multimedia applications may have more relaxed latency and reliability requirements than connected vehicles or public safety applications that do not necessarily require very high bit rates. The massive growth in the number of connected devices and their traffic volume, along with the requirements for affordability and energy efficiency, represent the most important challenges for the design of future mobile wireless networks. 5G networks will face significant challenges to support the expected growth (by a factor of 500 to 1000) in mobile traffic in the next decade [1]. These growth levels are expected to come from a 10 times increase in broadband mobile subscribers, and 50-100 times higher traffic per user. 5G networks should also support, compared to current 4G networks, 10 to 100 times more connected devices, 10 to 100 times higher user data rates, and 5 times smaller end-to-end latency. All this should be achieved while saving up to 90% of energy per provided service [1]. All in all, the following 5G performance and system-level challenges have been identified [76].

Performance challenges:

- Capacity: provide 1000x more available throughput in aggregate, as well as 10x to 100x more speed to individual users.
- Latency: provide service-level latency down to about 1 ms (i.e. 5x reduction end-to-end latency) when needed.
- Energy efficiency: reduce by 90% the energy consumption per provided service compared to 2010 levels.
- Battery lifetime: provide 10x better battery lifetime for low throughput services.
- Coverage: provide seamless extension of 5G services anywhere anytime.

System-level challenges:

- Quality of Service/Experience: provide differentiated services with different requirements in terms of throughput, latency, resilience, and cost per bit.
- Versatility: support a significant diverse range of uses cases.
- Density: increase number of diverse devices connected in proximity.
- Scalability: provide ability to support a wide range of requirements regardless of whether a large or low amount of traffic is present.
- Mobility: support for unlimited seamless mobility across all networks/technologies.
- Location and context: provide positioning and context capabilities in the sub-meter range in order to enable advanced (networking) solutions.
- Manageability: improve the manageability of networks in order to reduce the need for manual management and reduce the human intervention.
- Resource management: provide access agnostic control, policy and charging mechanisms and protocols for dynamic establishment, configuration, reconfiguration and release of any type of resource, for any type of device, and for any type of service.
- Flexibility: devise truly flexible control mechanisms and protocols for relocating functions, protocol entities and corresponding states in a truly end-to-end manner, leveraging programmable network technologies.

2.5.2 Enabler Technologies for 5G

In addition to technologies such as D2D (Section 2.2) and MCN (Section 2.3), other technologies are currently being investigated to be part of the 5G ecosystem [77]:

- Ultra dense deployments and small cells (HetNets). As the demand for higher data rates increases, one of the solutions available to operators is to reduce the size of the cell. By reducing the size of the cell, area spectral efficiency is increased through higher frequency reuse, and the transmission power levels can be reduced. Additionally, coverage can be improved by deploying small cells indoors where reception may not be good. Small cells also help offloading traffic from macro cells when necessary. The concurrent operation of different classes of base stations (e.g. macro-, pico-, and femto- base stations) is known as heterogeneous networks (or HetNets).

- Separation of user and control planes (phantom cells). The Control (C) plane provides the connectivity and mobility while the User (U) plane provides the data transport. In a possible envisioned C-/U-split scenario (which is also referred to as phantom cells), the mobile station will maintain connection with two different base stations (i.e. HetNets), a macro and a small cell, simultaneously. The macro cell will maintain connectivity and mobility (control plane) using lower frequency bands, while the small cell provides high throughput data transport using higher frequency bands. The macro cells will provide the signaling information, while the small cells can deliver data at higher spectrum efficiency, throughput, and energy savings. Additionally, small cells can be switched off when there is no data to transmit. The C-/U-split architecture can also provide additional benefits such as lower interference and improved cell edge user throughput.
- Self-Organized Networks (SONs). SONs are the first step towards the automation of (mobile) networks operation and management tasks, introducing closed control loop functions dedicated to self-configuration, self-optimization, and self-healing. A long-lasting dilemma has been to find the right balance between centralized controls versus distributed SONs. SONs imply cognitive processes (i.e. involve thinking, reasoning and remembering) and learning capabilities in order to achieve end-to-end goals.
- Software defined cellular networks (network virtualization). In parallel with the development of Software Defined Radio (SDR) in wireless communications, Software Defined Networking (SDN) has gained significant research attention. SDN enables abstraction of low level networking functionality into virtual services. In this way, the control plane can be decoupled from the user plane (C-/U-split architectures), which significantly simplifies network management and facilitates the introduction of new services or changes in configuration into the network. By means of SDN, network operators can dynamically configure, manage, and optimize network resources and adjust traffic flows to meet changing needs quickly via dynamic and automated SDN programs. SDN may help cellular operators simplify their network management and enable new services to support the exponential traffic growth envisaged for 5G networks. The flexibility offered by SDN can enable fine-grained resource control (e.g. based on subscriber/application attributes) to enhance user QoE while maximizing network utilization.

- Millimeter-wave (mmWave). A way to increase the throughput is by extending the allocated bandwidth. Since the available bandwidth below 6GHz is limited, significant research efforts are looking at exploring the millimeter-wave frequencies (i.e., tens of gigahertz and beyond) to evaluate their feasibility for future 5G wireless networks.
- Massive antenna (MIMO beamforming). Multi-antenna transmission/reception is now an established technology component. Current schemes can be extended towards massive multi-antenna configurations (in the extreme case consisting of several hundred antennas). Massive Multiple-Input Multiple-Output (MIMO) proposes multiplexing messages for several devices on each time-frequency resource, focusing the radiated energy towards the intended directions (i.e. beamforming) while minimizing intra- and intercell interferences. The use of massive MIMO technology is a potential solution to exploit higher frequency bands (mmWave) that allow reducing the antennas size.
- Smarter spectrum management (Licensed Shared Access – LSA, and Authorized Shared Access –ASA). Spectrum sharing between different technologies has long been seen as one way to increase the maximum contiguous chunks of spectrum available for mobile services. The objective behind spectrum sharing is to develop techniques that efficiently use the underutilized spectrum in many bands, and share it among different services and service providers. Research is focusing in providing a way in which all communication services can opportunistically use any portion of non-used available spectrum. The opportunistic use will led to maximum efficiency of spectrum use, and will require users to implement software defined radios. Regulatory concerns regarding the opportunistic use of licensed spectrum are also being considered under the Licensed Shared Access (LSA) and Authorized Shared Access (ASA) concepts.

2.6 Summary

Future wireless networks will be required to efficiently provide high and homogeneous QoS levels thorough the cell for the exponentially increasing data traffic and connected devices. Leading international organizations, as well as research experts from industry and academia, agree to recognize that the expectations and requirements are so high that it might be necessary to complement traditional cell-centric architectures with novel device-centric solutions. Current solutions that are being

considered as part of the 5G ecosystem include D2D communications and MCNs. These device-centric solutions exploit the intelligence, processing power and networking capabilities of smart mobile devices to create an underlay network that if efficiently coordinated with the cellular network has the potential for significant capacity, energy-efficiency, and QoS benefits. However, these benefits need yet to be demonstrated through experimental hardware testbeds and field trials. In this context, this thesis will help towards a better understanding of the real performance of MCNs using mobile relays and D2D communications. In addition, the integration of opportunistic networking into MCNs when dealing with relevant mobile delay tolerant services can significantly contribute towards achieving the capacity and energy efficiency gains sought for 5G networks, as it will be also demonstrated in this thesis.

UNIVERSITAS Miguel Hernández

3

mHOP: Experimental MCN Testbed

Multi-hop Cellular Networks (MCNs) are attracting significant research attention due to the multiple advantages that the integration of cellular and Device-to-Device (D2D) or ad-hoc networking technologies can provide over traditional cellular architectures. Section 2.2 has reviewed previous publications that demonstrate the benefits of MCNs using mobile relays over traditional single-hop cellular architectures in terms of capacity [16]-[17], radio cell extension [17], lower infrastructure deployment cost [17], power saving [18] and energy efficiency [19], among others. Despite their significant value, these studies are either analytical or based on simulations, and there is yet the need to validate the potential of multi-hop cellular networking through experimental field trials. To this aim, this thesis has designed and implemented what, to the author's knowledge, is the first MCN testbed developed to investigate the performance improvements that can be achieved with MCNs using mobile relays and D2D communications, and the operating conditions under which such improvements can be achieved. The testbed developed in this thesis is an improved version of an initial work conducted by Jónatan Muñoz and Baldomero Coll-Perales. This testbed is presented and described in detail in this chapter. The chapter starts with a review of recent research activities focused on the development of advanced multi-hop networking testbeds (Section 3.1). Then, the chapter provides a comprehensive description of mHOP, the novel research hardware

platform presented in this thesis for the study of MCNs using mobile relays (Section 3.2). The description of mHOP includes both the hardware equipment (requirements, devices, design, etc.) and the specific software tools that have been developed with the purpose of monitoring and geo-referencing the multi-hop links' performance. Finally, Section 3.3 presents a generic description of the steps needed to configure the mHOP testbed for conducting field tests.

3.1 Multi-hop Networking Platforms

There is a growing interest in the research community to design and develop hardware platforms to investigate the potential, performance and operation of multi-hop communication systems. Most of the activities focus around IEEE 802.11 networks and the study of cooperative mechanisms in multi-hop ad-hoc communications. A practical demonstration of the potential of cooperative networks is shown in [78], where the authors implement the Cooperative Medium Access Control (MAC) protocol (CoopMAC); firstly presented in [79]. CoopMAC is a cross-layer mechanism for IEEE 802.11 that allows selecting neighboring helper stations for MAC layer forwarding. The implementation is performed in two programmable cooperative communication testbeds using open-source platforms (i.e. open-source drivers and software defined radio). The results shown in [78] suggest that cooperative techniques perform more efficiently than legacy IEEE 802.11 networks. The work reported in [80] presents the MadMAC platform that was developed for building reconfigurable MAC protocols in commodity IEEE 802.11x hardware. The platform was then used to develop a Time Division Multiple Access (TDMA)-based MAC protocol that, according to the tests carried out by the authors, improves (20% throughput improvement) the performance of the Carrier Sense Multiple Access (CSMA) protocol proposed in the IEEE 802.11 standard under the considered scenario. Another interesting multi-hop networking testbed was developed in [81] to investigate the impact of adjacent channel interference on the multi-hop QoS achieved with legacy IEEE 802.11 nodes. The paper also proposes practical solutions (e.g. channel separation, antenna distance) to mitigate the effects of such interference that considerably improve the multi-hop performance.

These studies have demonstrated the feasibility of cooperative multi-hop ad-hoc communications, and therefore represent a significant encouragement for the experimental investigation of MCN networks using mobile relays. However, few activities to develop hybrid cellular and ad-hoc networking research platforms can yet be found in the literature. Although not focused on MCN using mobile relays, an

interesting research is that reported in [82], where the authors study the performance of mixed cellular and IEEE 802.11 architectures. In particular, [82] introduces the Cool-Tether platform that provides Internet access to laptop clients using cellular handsets as Internet gateways, thereby creating Wi-Fi hotspots on-the-fly. The reverse infrastructure-mode adopted in Cool-Tether defines that one of the laptop clients must act as Access Point (AP). As a result, the coordination processes are carried out by this laptop and the energy consumption of mobile stations is minimized. Considering the Cool-Tether topology, it is important to note that the QoS that Internet users will experience will be highly dependent on the cellular link quality of the mobile station acting as gateway. This quality will be in turn influenced by the distance to the base station and the Line-of-Sight (LOS)/Non-LOS (NLOS) propagation conditions of the cellular link. The work presented in [83] progresses towards the integration of cellular and ad-hoc networking technologies. In [83], the authors develop a hardware node that integrates a Global System for Mobile communications (GSM)/General Packet Radio Service (GPRS) wireless modem module and a Bluetooth module into a Linux embedded platform (S3C2410 microprocessor). The nodes also implement an on-demand routing protocol that enables multi-hop communications. Static field trials conducted in indoor environments validate the implementation, but reveal that the experimental studies that can be conducted with this testbed are limited mainly due to the Bluetooth's bandwidth constraint.

It is also important to highlight the activities conducted to develop LTE-Advanced hardware testing platforms; these activities are focused on fixed relaying solutions. The work reported in [24] presents a prototype (Berlin LTE-Advanced testbed) installed in the center of Berlin that consists of three LTE base stations and a fixed relay node. The fixed relay node is placed inside a measurement van in order to test different locations. The measurement results reported in [24] demonstrate that relaying techniques have a high impact on the coverage (they allow extending the radio range) and on the capacity of cellular systems by means of delivering high date rates to the cell-edge. Indoor coverage extension is also demonstrated in [25] using the EASY-C LTE-Advanced testbed. These two LTE-Advanced platforms corroborate the benefits that fixed relaying schemes can achieve at the expense of an infrastructure deployment cost, and the need to strategically locate the relay nodes at the cell edge in LOS conditions to the BS in order to achieve the maximum capacity and end-user QoS. Another interesting development is the release of Qualcomm's FlashLinQ solution [42]. FlashLinQ is a synchronous (time-slotted) Orthogonal Frequency Division Multiplexing (OFDM)-based system that enables node discovery, channel allocation, and link scheduling with power control with limited

infrastructure support. Through simulation and experimental studies, FlashLinQ has demonstrated its capability to increase system performance. FlashLinQ is being standardized as LTE-Direct (or ProSe) as part of 3GPP Release 12 (see Section 2.2) with the main aim of achieving battery efficient and privacy sensitive *always-on* proximal discovery solutions. However, FlashLinQ and LTE-Direct target device-to-device communications, and not multi-hop cellular communications.

This section has reviewed relevant initiatives to create hardware platforms over which to investigate cooperative multi-hop and relaying-based communications. However, to the author's knowledge, no MCN testbed using mobile relays has yet been reported in the literature. In this context, this thesis presents mHOP, a novel research platform designed to experimentally investigate the operation, performance and benefits of MCNs using mobile relays and D2D communications.

3.2 mHOP Research Testbed

The mHOP testbed has been designed with the objective to investigate the performance benefits of MCNs using mobile relays over traditional cellular systems, and the conditions under which such benefits can be obtained. As a result, the platform includes MCN and conventional single-hop cellular links. Figure 3-1 illustrates the mHOP architecture, and shows how the destination Mobile Node (MN) can be reached through a single-hop cellular connection or an MCN connection. The platform focuses on downlink transmissions, although uplink transmissions can also be performed. The MCN connection requires access to the cellular infrastructure through a hybrid MN capable of forwarding cellular data in real-time to the destination MN without downgrading the overall network performance. In particular, the hybrid MN forwards the data to the destination node using other mobile relay nodes and D2D communications. The nodes that integrate the mHOP platform should also have the capability to continuously monitor their radio performance, and their design should guarantee the platform's scalability and capacity to integrate an increasing number of mobile nodes. Their configuration should also ensure the flexibility to investigate various communication settings, such as advanced multi-hop routing protocols, different IEEE 802.11 standards, frequencies, etc.

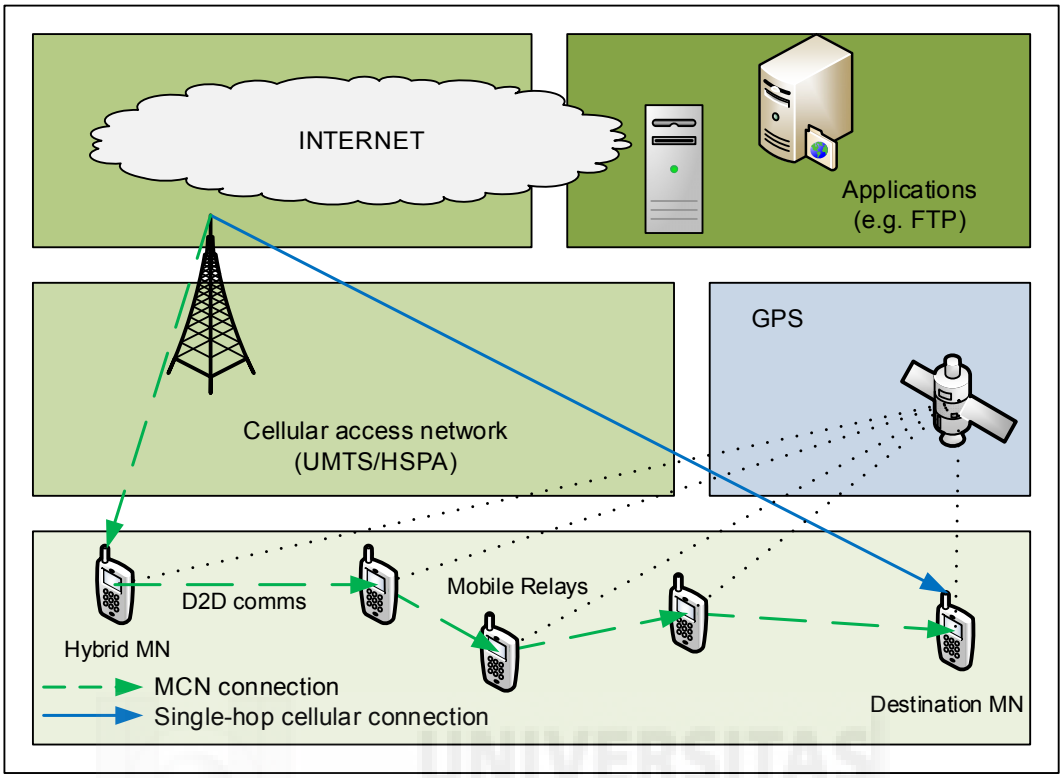

Figure 3-1. mHOP architecture.

The implemented mHOP platform integrates three different types of MNs, with different connectivity capabilities: the hybrid and destination MNs with cellular and ad-hoc D2D connectivity, and the mobile relays with ad-hoc D2D connectivity. Figure 3-2 shows the fully equipped mobile nodes that integrate the mHOP testbed.

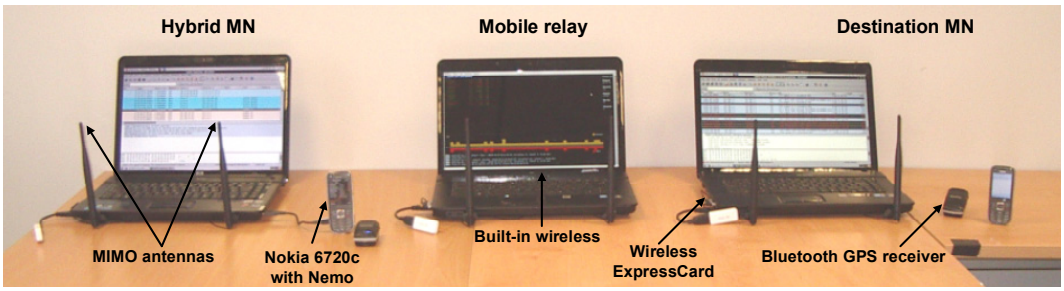

Figure 3-2. mHOP platform.

3.2.1 Cellular Connectivity

The mHOP platform includes cellular connectivity into the hybrid MN and the destination MN using a Nokia 6720c handset. The Symbian-based terminal supports the radio access technologies shown in Table 3-1 and that include GSM/GPRS and Universal Mobile Telecommunications System (UMTS)/High Speed Packet Access (HSPA) – HSPA

was the most advanced radio access technology at the time the mHOP testbed was developed. It also incorporates the Nemo Handy application [84], which provides the terminal with a powerful radio monitoring capability. Nemo Handy is a state-of-the-art professional network testing tool used to extensively monitor in real-time the operation of cellular networks and the QoS and QoE of mobile applications. To this end, Nemo Handy provides a large set of parameters and measurement data captured over voice and video calls, File Transfer Protocol (FTP)/HyperText Transfer Protocol (HTTP) data transfers, iPerf testing, HyperText Markup Language (HTML)/Wireless Application Protocol (WAP) browsing, video streaming, Short Message Service (SMS)/Multimedia Messaging Service (MMS) messaging, e-mail and ping services.

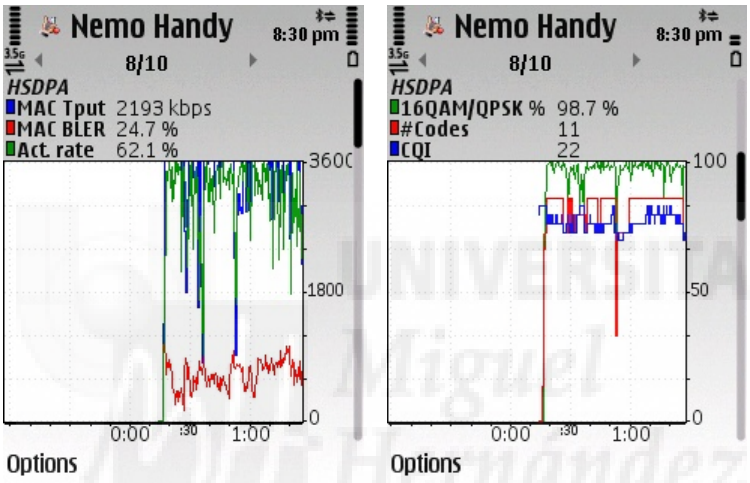

Figure 3-3. Two examples of the real-time capabilities of Nemo Handy to monitor the HSPA performance.

Figure 3-3 shows an example of the capabilities of Nemo Handy to monitor in real-time the network performance. In particular, Figure 3-3 shows two Nemo Handy's screenshots of High Speed Downlink Packet Access (HSDPA) performance. The screenshots display parameters such as the MAC throughput, Block Error Rate (BLER) or activity rate (Figure 3-3-left), and the ratio of 16-Quadrature Amplitude Modulation (QAM) and Quadrature Phase Shift Keying (QPSK) modulations, number of channelization codes and Channel Quality Indicator (CQI) (Figure 3-3-right). In addition to its real-time monitoring capabilities, Nemo Handy also offers the possibility to store all the network parameters monitored by the mobile handset (including signaling messages) for post-processing. The processing of the logged measured data is done using the professional Nemo Outdoor tool (it could also be done using Nemo Analyze or any other 3rd party software). Nemo Outdoor offers a valuable set of Key Performance Indicators (KPIs), e.g. throughput, BLER or Received Signal Strength Indication (RSSI) that

have been very valuable to analyze the cellular QoS in the mHOP testbed. Another important feature of Nemo Handy is the possibility to lock the cellular connection to a specific radio access technology and Base Station (BS). This results in that a Mobile Station (MS) cannot select another BS (i.e. it cannot perform a cell reselection or handover) even if its performance degrades, for example if the user moves away from the serving BS. This feature facilitated a more stable testing environment to compare single-hop cellular and MCN connections. Finally, Nemo Handy also provides spatial and time synchronized measurement results through an external Global Positioning System (GPS) connected via Bluetooth (Table 3-1.). The GPS data has been used to track the MS position and geo-reference all the performance measurements.

Table 3-1. Hardware characteristics of the cellular mobile node.

Cellular Mobile Station	**Nokia 6720 classic with Nemo Handy**
Radio Access Technologies	GSM 850/900/1800/1900 MHz GPRS/EGPRS class B (max. speed DL/UL = 298/178.8 Kbps) EDGE class A (max. speed DL/UL =178.8/118.2 Kbps) UMTS FDD 2100 MHz (max. speed DL/UL = 384/384 Kbps) HSDPA category 9 (max. speed DL = 10.2 Mbps) HSUPA category 5 (max. speed UL = 2 Mbps) Bluetooth v.2.0 Enhanced Data Rate
Memory	2GB MicroSD Card
Accessories	GPS Bluetooth RoyalTek

Figure 3-4 shows a fragment of the measurement file produced by the Nemo Handy application. As it can be appreciated, the captured network parameters are saved in a specific format. All Nemo tools produce this type of measurement files that can be post-processed using the Nemo Outdoor playback functions, as mentioned previously, or any other 3rd party post-processing tool (e.g. this thesis uses Matlab for the post-processing of the Nemo Handy's measurement files). The file in Figure 3-4 is organized following events (GPS, Receive Power Control –RXPC–, Transmit Power Control –TXPC–, etc.) in different rows. Most of these events are generated every 200 ms, and provide statistics recorded during the last 200 ms. The first parameter, after the event identifier, is common to all events and indicates the time instant at which the event was created. The other parameters for each of the depicted events are:

- GPS: this event captures the GPS information including longitude, latitude, height, GPS satellites monitored, and velocity.

- RXPC: this event shows information related to the power control mechanism in reception, and it includes parameters such as the target Signal to Interference Ratio (SIR), measured SIR and number or percentage of power up/down commands in the downlink.

- TXPC: this event shows information related to the power control mechanism in transmission, and it includes parameters such as the MS's total transmitted power, transmit power control step size, and number or percentage of power up/down commands in the uplink.

- PLAIU: the Packet Link Adaptation Info for Uplink (PLAIU) event contains statistical information on the usage of the uplink link adaptation. It includes parameters such as the High Speed Uplink Packet Access (HSUPA) throughput, HSUPA modulation, HSUPA transport block size, HSUPA spreading and channelization codes, and HSUPA retransmission rate, among others.

- PLAID: the Packet Link Adaptation Info for Downlink (PLAID) event contains statistical information on the usage of the downlink link adaptation. It includes parameters such as the HSDPA throughput, HSDPA modulation, HSDPA effective coding, HSDPA transport block size, HSDPA channelization codes and HSDPA MAC-hs BLER, among others.

- CQI: this event indicates the distribution of HSDPA CQI transmitted from the MS to the network. It includes information such as the HSDPA physical layer requested throughput, the HSDPA CQI value and the percentage of this CQI value from the total sampling duration. It is important to note that the Nemo Handy's event is generated every 200 ms, whereas the HSDPA Time Transmission Interval (TTI) is 2 ms. Therefore, each CQI event contains information of 100 TTIs.

- MACRATE: this event is related to the MAC layer throughput and contains information such as the HSDPA MAC-hs throughput, HSDPA MAC-hs block rate, and HSDPA MAC-hs 1st, 2nd and 3rd retransmission rates.

- MACBLER: this event is related to the MAC layer block error rate and contains information such as the HSDPA MAC-hs Acknowledgement (ACK)/Non-ACK (NACK) count, HSDPA MAC-hs block error rate in the downlink and the number of HSDPA MAC-hs data block transferred.

- CELLMEAS: the cell measurement event contains information such as the channel number, carrier RSSI, band, Energy chip on the Noise spectral density (Ec/No), Receive Signal Code Power (RSCP) of the active cell(s), and the criterion established to perform a cell reselection.

```
…
GPS,10:45:49.708,,-0.686620,38.273712,96,0,1,7,0
RXPC,10:45:49.767,,5,,8.0,,1,119,0.8,
TXPC,10:45:49.767,,5,-36.0,0,1.0,0,59,61,49.2
PLAIU,10:45:49.817,,5,7,200,3720,,,,,,2,8,90.0,,,,,,,,10.0,1,3
72,4,4,0.0,21,13.0
…
PLAID,10:45:49.828,,5,3,200,6653245,0.0,26,13,5.0,,,,,,,0,,,,,
1,1.0,1,0.35,1356,6,4,0.0,1,…
CQI,10:45:49.828,,5,5,200,8589405,1,2,,6,5,1.0,24,2,,1,10.0,26
,2,,1,16.0,27,2,,1,38.0,28,2,,1,25.0,29,2,,1,10.0,30,2,,1
MACRATE,10:45:49.828,,5,0,1,8,,3,5867685,95,11.6,0.0,0.0,0.0
MACBLER,10:45:49.828,,5,0,1,6,,3,95,10.5,85,0.0
…
CELLMEAS,10:45:49.862,,5,0,1,2,10688,-46.9,1,17,0,50001,10688
,186,-6.4,,-53.5,,,,,,,,, ,
…
```

Figure 3-4. Example of network parameters monitored by the Nemo Handy application.

3.2.2 Ad-hoc D2D Connectivity

3.2.2.1 Mobile Relay Nodes

mHOP mobile relay nodes consist of conventional laptops transmitting over IEEE 802.11. In addition to their built-in wireless interface, the laptops have been equipped with a wireless ExpressCard integrating the AR9280 Atheros chipset. Table 3-2 summarizes the hardware characteristics of the mHOP's mobile relays. The wireless ExpressCard interface was chosen due to its outdoor range, data rate, reliability and capacity to operate under ad-hoc mode using IEEE 802.11a/b/g/n. The laptops use their wireless ExpressCard for the ad-hoc D2D communications, and they monitor the transmitted and received packets using both their built-in wireless interface and a virtual interface created using the wireless ExpressCard (see below the explanation for the need of the two interfaces to capture the IEEE 802.11 traffic). This monitoring capability allows continuously evaluating the performance of the ad-hoc IEEE 802.11 D2D links. As shown in Table 3-2, the laptops have also been equipped with a Universal Serial Bus (USB) GPS receiver that, together with the Network Time Protocol (NTP), allows time-synchronizing all mHOP devices. In addition, the GPS is used to geo-reference all the logged radio measurements.

The mobile relay nodes operate under Linux using the Ubuntu distribution. This solution was chosen due to the need to configure parameters of the IEEE 802.11 physical (PHY) and MAC layers, and the availability of open tools to configure such parameters under the Linux operating system. In particular, mHOP uses the *Backports* and *iw* packages to configure the wireless interfaces. The *Backports* package includes the Ath9k driver used to control the wireless ExpressCard. Using the *iw* package, it is possible to configure: the operation channel (*channel*) or frequency (*freq*), the transmission power (*txpower*) –including the power save mode–, the data rate (*bitrates*), the size of the smallest packet to send a Request To Send (RTS) message (*rts*), the maximum size of the transmitted packets without fragmentation (*frag*), the transmission modulation (*modulation*), the encryption type (*enc*), or the number of allowed retries (*retry*) of the wireless ExpressCard. The *iw* package is also used to configure the wireless ExpressCard in ad-hoc mode, create virtual wireless interfaces, and configure the built-in and virtual wireless interfaces in monitor mode. The *iw* package is used to create the ad-hoc network that mHOP's mobile relays will join to establish the MCN end-to-end connection.

Table 3-2. Hardware characteristics of mHOP's mobile relays.

Mobile relay nodes	**HP Compaq 6730s**
Operating system	Ubuntu
Built-in wireless interface	Intel® Wifi Link 5100 AGN
Wireless ExpressCard	Ubiquiti SR71-X IEEE 802.11a/b/g/n MIMO with Atheros AR9280 chipset
USB GPS receiver	GlobalSat ND-100 GPS USB Dongle with NMEA 0183v3 protocol

The mobile relays also incorporate a packet sniffer software developed in this thesis to capture the IEEE 802.11 traffic through the laptop's built-in and virtual wireless interfaces operating in monitor mode. The sniffer uses the open source *libpcap* library provided by Linux and employed in tools such as Wireshark/T-Shark [85] or Kismet [86]. Having access to the raw captured packets allows a much faster and customized filtering and post-processing than using certain network testing tools. Figure 3-5 illustrates an example of the captured packets using the virtual interface of the wireless ExpressCard. Each row corresponds to a captured packet, and the columns contain the following information:

1) Epoch time: this is the Unix time that represents the number of seconds that have elapsed since Thursday, 1 January 1970 (epoch date). The *epoch* then serves as a reference point from which time is measured.

2) Capture time: this is the elapsed time since the wireless interface was launched to capture packets.

3) Packet size: it corresponds to the size of the IEEE 802.11 frame including headers and payload.

4) Radiotap header size: this is the size of the radiotap header in the IEEE 802.11 packet. The radiotap header is attached to the IEEE 802.11 frame when the packet is received at the PHY layer and it supplies additional information about IEEE 802.11 frames from the driver to user space applications such as *libpcap*. It includes information such as the RSSI of the received packet, the data rate and the channel frequency. Radiotap header can be also created at the user space to include information useful for the driver for transmission. It is important to note that the radiotap header is not transmitted to the wireless air interface; it is only used to transfer information between the driver and the user space.

5) Data rate: it indicates the data rate or transmission mode used in the ad-hoc D2D communication between the IEEE 802.11 devices. For the case of IEEE 802.11g, the twelve possible data rates resulting from the combination of different modulation and coding schemes are: {54, 48, 36, 24, 18, 12, 9, 6; 11, 5.5, 2, 1} Mbps. Figure 3-5 shows that, for this example, the data rate is initially set to 54 Mbps, but after some packets are received with the retransmission flag set to 1 (see column ‘7) Retry’ below) the data rate is reduced to 48 Mbps. The IEEE 802.11 card’s driver (Ath9k in this case) dynamically selects the IEEE 802.11 data rate based on the link quality conditions.

6) RSSI: it represents the received signal strength (in dBm) at which the IEEE 802.11 packets are correctly received. It is important to note that the values of the RSSI can be only considered if the mobile relay node is the destination of the D2D transmission (see column ‘9) Destination’ below), although an arbitrary value is also attached when the mobile relay node is the source node (see column ‘8) Source’ below) of the D2D transmission.

7) Retry: this parameter indicates whether the IEEE 802.11 received packet has been retransmitted before (‘1’) or not (‘0’). A data packet retransmission is required if the transmitter does not receive an ACK from the destination (see Section 2.2.2). This can be caused by an error in the transmission of the data packet from the transmitter to the destination, or an error in the ACK sent from the destination to the transmitter. It is important to note that the destination cannot know how many times the packet has been retransmitted because this information is not attached in the packet/headers. In addition, the number of retransmissions can be configured. In the mHOP platform, the built-in wireless interface is used to log the retransmitted packets. Figure 3-7 illustrates, for the example shown in Figure 3-5, the packets that were captured in the built-in wireless interface of the hybrid MN (for the example, the hybrid MN would be the transmitter and the destination MN the destination). Figure 3-5 shows that a packet identified by the sequence number 16 (see column ’10) Sequence number’ below) is received at the destination MN (see column ‘9) Destination’ below) with the flag indicating that the packet is a retransmission (column 7). The captured packets at the hybrid MN using the built-in wireless interface (Figure 3-7) show that the packet identified with the sequence number 16 was first transmitted by the hybrid MN (see column ‘8) Source’ below) with the retransmission flag set to 0 (column 7), and after with the flag set to 1. The captured packets in Figure 3-7 also show that the packet identified with the sequence number 17 was retransmitted twice. To illustrate the need of the built-in wireless interface to monitor the retransmitted packets, Figure 3-8 shows the captured packets by the virtual interface of the wireless ExpressCard at the hybrid MN (the transmitter in this example). It can be appreciated that packets with different sequence number (column 10) are only captured once with the retransmission flag set to 0 (column 7). This is the case because packet retransmissions are carried out at a very low level (out of the action range of the *libpacp* library) and therefore they cannot be logged using the virtual interface of the wireless ExpressCard. mHOP testbed then uses the built-in wireless interface in the same node (i.e. the hybrid MN) to capture through the air interface the retransmissions conducted by the wireless ExpressCard interface (Figure 3-7).

8) Source: it indicates (‘1’) whether the wireless ExpressCard interface that captures the IEEE 802.11 packet is the origin of the D2D transmission or not (‘0’).

9) Destination: it indicates (‘1’) whether the wireless ExpressCard interface that captures the IEEE 802.11 packet is the destination of the D2D transmission or not (‘0’).

10) Sequence number: this is a unique identifier of the IEEE 802.11 packet. Using the examples shown in Figure 3-8, Figure 3-7 and Figure 3-5, it is possible to follow the flow of every single packet using the sequence number; for example, it is possible to know whether a retransmission was required, the number of retransmissions, the data rate in each transmission, the RSSI, etc.

11) More fragments: this parameter indicates (‘1’) whether the IEEE 802.11 packet has been fragmented and therefore more fragments are to follow. In the examples illustrated in Figure 3-8, Figure 3-7 and Figure 3-5, the fragmentation was not used. As indicated previously, the fragmentation size can be configured using the *iw* package.

12) Beacon: it indicates (‘1’) whether the captured packet is a beacon subtype management frame or not (‘0’). Figure 3-6 illustrates an example of a portion of beacon packets captured at the destination MN. The example shows beacons transmitted (column 8)/received (column 9) at the destination MN.

13) Data: it indicates (‘1’) whether the captured packet is a data subtype data frame or not (‘0’). The IEEE 802.11 packets shown in Figure 3-5, Figure 3-7 and Figure 3-8 correspond to data packets.

14) Ack: it indicates (‘1’) whether the captured packet is an ACK subtype control frame or not (‘0’).

1	2	3	4	5	6	7	8	9	10	11	12	13	14
1319711655.703692	1.473588	623	13	54	-68	0	1	0	2	0	0	1	0
1319711655.703937	1.473833	623	13	54	-24	0	1	0	3	0	0	1	0
1319711655.704215	1.474111	623	13	54	-24	0	1	0	4	0	0	1	0
1319711655.704407	1.474303	623	13	54	-24	0	1	0	5	0	0	1	0
1319711655.739778	1.489674	1562	26	54	-24	1	0	1	16	0	0	1	0
1319711655.742786	1.492682	1562	26	54	-25	1	0	1	17	0	0	1	0
1319711655.742809	1.492705	1562	26	54	-24	0	0	1	18	0	0	1	0
1319711655.744599	1.494495	1562	26	54	-25	1	0	1	19	0	0	1	0
1319711655.745598	1.495494	1562	26	54	-25	1	0	1	20	0	0	1	0
1319711655.748527	1.498423	1562	26	48	-23	1	0	1	21	0	0	1	0
1319711655.750075	1.499971	1562	26	48	-23	1	0	1	22	0	0	1	0
1319711655.750095	1.499991	1562	26	48	-24	0	0	1	23	0	0	1	0
1319711655.752676	1.502572	1562	26	48	-24	0	0	1	24	0	0	1	0

Figure 3-5. Example of data packets captured using the virtual interface of the wireless ExpressCard at the destination MN of a two-hop MCN communication.

1	2	3	4	5	6	7	8	9	10	11	12	13	14
1319711654.300560	0.098506	96	18	1	-18	0	0	1	217	0	1	0	0
1319711654.402837	0.200783	96	18	1	-16	0	0	1	218	0	1	0	0
1319711654.404897	0.202843	96	18	1	-4	0	1	0	200	0	1	0	0
1319711654.504873	0.302819	96	18	1	-16	0	0	1	219	0	1	0	0
1319711654.606951	0.404897	96	18	1	-84	0	0	1	220	0	1	0	0
1319711654.709991	0.507937	96	18	1	-16	0	0	1	221	0	1	0	0
1319711654.811252	0.609198	96	18	1	-15	0	0	1	222	0	1	0	0
1319711654.913983	0.711929	96	18	1	-15	0	0	1	223	0	1	0	0
1319711655.016515	0.814461	96	18	1	-16	0	0	1	224	0	1	0	0
1319711655.119530	0.917476	96	18	1	-16	0	0	1	225	0	1	0	0

Figure 3-6. Example of beacon packets captured using the virtual interface of the wireless ExpressCard at the destination MN of a two-hop MCN communication.

1	2	3	4	5	6	7	8	9	10	11	12	13	14
1319711655.707470	3.859270	628	18	54	-30	0	0	1	5	0	0	1	0
1319711655.720551	3.873253	1550	18	54	-9	0	1	0	16	0	0	1	0
1319711655.721453	3.873253	1550	18	54	-9	1	1	0	16	0	0	1	0
1319711655.723073	3.874873	1550	18	54	-10	0	1	0	17	0	0	1	0
1319711655.723975	3.875775	1550	18	54	-10	1	1	0	17	0	0	1	0
1319711655.725482	3.877282	1550	18	54	-10	1	1	0	17	0	0	1	0
1319711655.725983	3.877783	1550	18	54	-9	0	1	0	18	0	0	1	0
1319711655.726375	3.879077	1550	18	54	-10	0	1	0	19	0	0	1	0
1319711655.727277	3.879077	1550	18	54	-10	1	1	0	19	0	0	1	0
1319711655.727846	3.879646	1550	18	54	-10	0	1	0	20	0	0	1	0
1319711655.728287	3.880087	1550	18	54	-9	1	1	0	20	0	0	1	0

Figure 3-7. Example of data packets captured using the built-in wireless interface at the hybrid MN of a two-hop MCN communication.

1	2	3	4	5	6	7	8	9	10	11	12	13	14
1319711655.707316	3.807298	640	26	54	-27	0	0	1	5	0	0	1	0
1319711655.721602	3.821584	1545	13	54	-11	0	1	0	16	0	0	1	0
1319711655.722589	3.824571	1545	13	54	-11	0	1	0	17	0	0	1	0
1319711655.724687	3.825069	1545	13	54	-11	0	1	0	18	0	0	1	0
1319711655.725781	3.826363	1545	13	54	-11	0	1	0	19	0	0	1	0
1319711655.727419	3.827401	1545	13	54	-11	0	1	0	20	0	0	1	0

Figure 3-8. Example of data packets captured using the virtual interface of the wireless ExpressCard at the hybrid MN of a two-hop MCN communication.

The mobile relay nodes time- and geo-reference all the captured packets using an USB-based GPS module and a simple application developed in this thesis (using the Linux

libgps library) to collect the time, latitude and longitude with a refresh periodicity of 1 Hz. Figure 3-9 illustrates an example of the information collected from the GPS at each mobile node. Each row corresponds to an event, and the columns contain the following information:

1) Reference: this is an identifier of the number of GPS events collected.
2) Epoch time: this is the Unix time that represents the number of seconds that have elapsed since Thursday, 1 January 1970 (epoch date). Having this *epoch* time in the GPS information and in the captured packets (see above) allows geo-referencing the captured IEEE 802.11 data packets.
3) Latitude: this is the geographic latitude coordinate.
4) Longitude: this is the geographic longitude coordinate.

1	2	3	4
73,	1319711655.764811,	38.273810,	-0.686597
74,	1319711656.464675,	38.273795,	-0.686610
75,	1319711657.464920,	38.273780,	-0.686627
76,	1319711658.468783,	38.273780,	-0.686627
77,	1319711659.468700,	38.273780,	-0.686627
78,	1319711660.468861,	38.273780,	-0.686627
79,	1319711661.769092,	38.273775,	-0.686640
80,	1319711662.468765,	38.273775,	-0.686640
81,	1319711663.472637,	38.273775,	-0.686640
82,	1319711664.469107,	38.273770,	-0.686670
83,	1319711665.473371,	38.273757,	-0.686692
84,	1319711666.476775,	38.273757,	-0.686692
85,	1319711666.777136,	38.273748,	-0.686713
86,	1319711667.472718,	38.273750,	-0.686735

Figure 3-9. Example of GPS information captured at mobile relay nodes.

3.2.2.2 Hybrid Mobile Node

The hybrid MN is a mobile relay node that also acts as a gateway between the cellular and IEEE 802.11 ad-hoc D2D links. To this aim, the hybrid MN is also implemented on a laptop with all previously described IEEE 802.11 features and ad-hoc D2D connectivity functions, and uses a Nokia 6720c terminal as modem to provide the cellular link required in MCN connections. To allow for the real-time forwarding of information from the cellular to the multi-hop ad-hoc D2D links, the hybrid MN's routing table has been modified (detailed information on how the routing table is modified is presented in Section 3.3). Finally, the hybrid MN includes two GPS receivers and the cellular and ad-hoc D2D software monitoring tools previously described.

3.3 Testbed Configuration and Set-Up

The mHOP tested has been implemented to demonstrate through field tests the conditions under which MCNs using mobile relays can overcome the limitations of traditional cellular architectures. To this aim, field trials need to be conducted at different locations and under different configurations. As it will be shown in Chapters 4 and 5, the site selection and mHOP testbed configuration (including number of hops in the MCN connection, hop distance, mobility pattern, traffic configuration, etc.) are carefully chosen based on the test requirements and the conditions under which it is intended to verify the capabilities of MCN technologies to overcome the limitations of single-hop cellular systems. This section presents then a generic example of the steps needed to configure the mHOP testbed for conducting field tests.

3.3.1 Synchronization of mHOP Devices

An adequate post-processing of the data obtained from the field measurements requires all mHOP devices to be perfectly synchronized. This is the case because measurement files from different devices are gathered together when the field tests finish for post-processing. This requires all the mHOP devices to use the same time reference for the proper post-processing of the measurements. To this aim, all mHOP devices execute the command <`ntpdate pool.ntp.org`> to synchronize their internal clocks over the Internet using the Network Time Protocol (NTP). The *epoch* times that all mHOP devices save in the measurement files of the IEEE 802.11 packets (Figure 3-5) and GPS (Figure 3-9) are then synchronized.

3.3.2 Configuration of the Hybrid MN

The configuration of the Hybrid MN starts with the execution of the Nemo Handy application. Some field tests may require the cellular link of the MCN connection to be locked to a specific radio access technology and BS (it allows a more stable testing since it prevents the cell-reselection and handover execution). If this is the case, Nemo Handy is used to force the carrier, using the UARFCN (UTRA –UMTS Terrestrial Radio Access– Absolute Radio Frequency Channel Number) parameter, and the scrambling code of the cellular link. Figure 3-10 illustrates an example of the views in Nemo Handy to force the cellular link of the hybrid MN to an UMTS/HSPA BS characterized by the UARFCN 10663 and scrambling code 26. The Nemo Handy terminal is then configured to start logging data, and it is connected to the Hybrid MN through an USB cable. Using the Ubuntu's network-manager functionality, a mobile broadband connection is then activated in the laptop to enable the HSPA cellular link.

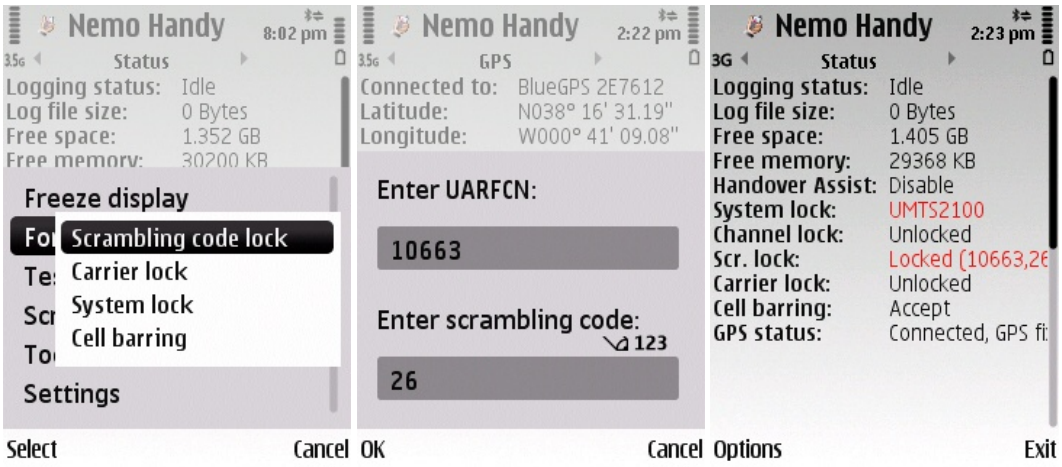

Figure 3-10. Example of Nemo Handy views when the mobile terminal is locked to a specific radio access technology and BS.

The configuration of the IEEE 802.11 ad-hoc network in the hybrid MN node starts by setting the wireless ExpressCard interface as ad-hoc or Independent Basic Service Set (IBSS) type (<`iw dev $wlanext set type ibss`>); '`$wlanext`' refers to the MAC address of the wireless ExpressCard interface. Then, this IBSS-type interface is used to create the ad-hoc network that the rest of mHOP's mobile nodes will join to establish the MCN end-to-end connection (<`iw dev $wlanext ibss join $SSID $freq fixed-freq $ap`>). The command used to configure the ad-hoc network includes the frequency/channel (`$freq`) where the ad-hoc D2D communications will operate, and the name of the IBSS network (`$SSID`). The configuration of the IBSS-type interface in the Hybrid MN also includes the selection of the transmission power (<`iw dev $wlanext set txpower auto`>)[3], and the data rate (<`iw dev $wlanext set bitrates legacy-2.4 12 18 24`>)[4]. Using the command <`iw dev $wlanext interface add $wlanextmon type monitor`>, we create the virtual interface of the wireless ExpressCard that is configured in monitor mode. Using the command <`iw dev $wlanint set type monitor`>, the built-in wireless interface is also configured in monitor mode to capture the IEEE 802.11 traffic. The

[3] In the command used as example the transmission power is set automatic ("`auto`"). This means that the Ath9k driver will automatically select the transmission power based on the radio channel conditions.

[4] By default the data rate is set automatically, i.e. dynamically modified based on the link quality conditions and the adaptive mechanisms implemented in the Ath9k driver. However, as shown in the command used as example, the data rate can be set to vary among specific values (in the example 12, 18, 24 Mbps).

forwarding of packets is activated by setting '1' in the file 'ip_forward' within the folder '/proc/sys/net/ipv4'. The hybrid MN is assigned an IP address by using the command <`ifconfig $wlanext 192.168.1.1`>, and its routing table is modified to enable the real-time data forwarding from/to the cellular link (<`route add default dev ppp0`>) to/from the IEEE 802.11 ad-hoc network (<`route add -host 192.168.1.2 dev $wlanext`> and <`route add -net 192.168.1.0/24 gw 192.168.1.2`>). Finally, the GPS application is executed to track the location of the hybrid MN and the packet-sniffer software to capture the IEEE 802.11 traffic through both the built-in and virtual interfaces configured in monitor mode.

3.3.3 Configuration of the Mobile Relays

The mobile relay nodes are located between the hybrid MN and the destination MN. These nodes act as relays of the IEEE 802.11 traffic (they do not have a cellular link to the BS), and therefore their configuration starts by setting the wireless ExpressCard interface in IBSS mode (<`iw dev $wlanext set type ibss`>). In the conducted field tests, the multi-hop path is predefined at the start of each field trial. To this aim, the mobile relay nodes (first the one closer to the hybrid MN) join the ad-hoc network created by the hybrid MN. This is done using the command <`iw dev $wlanext ibss join $SSID $freq fixed-freq $ap`> and indicating the same parameters for the SSID (`$SSID`), frequency (`$freq`) and AP identifier (`$ap`) as the ones used by the hybrid MN. The mobile relay nodes can also configure their transmission power and data rates using the commands presented previously in the configuration of the hybrid MN. The mobile relay nodes also create the virtual interface of the wireless ExpressCard, and configure this virtual interface and the built-in wireless interface in monitor mode. The forwarding of packets is also activated in the mobile relay nodes by setting '1' in the file 'ip_forward' within the folder '/proc/sys/net/ipv4'. Then, a different IP address is assigned to each of the mobile relay nodes' wireless ExpressCard (<`ifconfig $wlanext 192.168.1.$node`>, where `$node` varies depending on the location of the mobile relay. `$node` will be equal to 2 for the mobile relay that is located closer to the hybrid MN, and an increasing number is set as mobile nodes are closer to the destination MN). Once the IP address is assigned, the routing table of the mobile relays is modified to establish that the wireless ExpressCard is used to reach the precursor and successor mobile relay nodes (<`route add -host 192.168.1.$[$node+1] dev $wlanext`> and `route add -host 192.168.1.$[$node-1] dev $wlanext`>). New entries are also added to the routing table to indicate that the traffic targeted to the destination MN is routed via the successor mobile relay (<`route add -host 192.168.1.$nodes gw`

`192.168.1.$[$node+1]`>) and the traffic that goes to Internet –default traffic– is routed via the precursor mobile relay towards the hybrid MN (<`route add default gw 192.168.1.$[$node-1]`>). *`$nodes`* refers to the number of hops in the end-to-end MCN connection. Finally, the GPS application is executed to track the location of the mobile relay nodes, and the packet-sniffer software is configured in monitor mode.

3.3.4 Configuration of the Destination MN

The configuration of the destination MN is similar to that described above for the hybrid MN and mobile relay nodes. If the field tests involve simultaneous downloads through both the MCN connection and the single-hop cellular connection to the destination MN, the configuration of the destination MN starts by connecting the Nemo Handy terminal to the PC and activating the mobile broadband connection. Then, the wireless ExpressCard of the destination MN joins the ad-hoc network, and the virtual and built-in wireless interfaces are set in monitor mode. The destination MN's routing table needs also to be modified to indicate the path that the traffic (cellular, IEEE 802.11 or both) will follow. For example, in the case of the MCN connection it has to be added an entry in the routing table to indicate that the traffic goes via the successor MN towards the hybrid MN using the wireless ExpressCard (<`route add -host 192.168.1.$[$node-1] dev $wlanext`>). The destination MN also has to activate the GPS application and execute the packet sniffer software.

At this point in time, the mHOP testbed is configured and ready to start a field test. The test starts when the destination MN launches a script that executes the download of the traffic from the server. A server located at the UWICORE laboratory has been used for the field tests. The server is configured to allow for an unlimited number of users, and it has no limit in the download speed. In addition, the flexibility of the mHOP platform allows testing a wide range of traffic applications including UDP and TCP traffic, ping, web browsing, FTP downloads and iPerf.

3.4 Summary and Discussion

This chapter has introduced the mHOP testbed, the first research platform designed and implemented to investigate the performance benefits of MCNs using mobile relays compared to traditional single-hop cellular communications, and to analyze the conditions under which such benefits can be obtained. The testbed will allow complementing current analytical or simulation-based MCN research studies with field

trials. Field trials are not constrained by simplifications or assumptions usually made in analytical or simulation studies.

The mHOP platform includes a single-hop cellular connection and a MCN connection to allow for their performance comparison. In addition, it is fully equipped with the software tools necessary to monitor and evaluate the performance of the cellular and multi-hop links, and with GPS receivers that allow time and geo-reference all the performance measurements. The design of the mHOP platform also guarantees the platform's scalability and flexibility to investigate various communications settings. These mHOP functionalities are exploited in the experimental MCN evaluation presented in Chapter 4 and the MCN performance modeling described in Chapter 5. These chapters do not only verify the performance benefits of MCNs, but also the potential of the implemented mHOP testbed to conduct advanced research on multi-hop cellular networking.

UNIVERSITAS Miguel Hernández

4

Experimental Evaluation of Multi-hop Cellular Networks

Future 5G wireless networks are expected to support high bandwidth multimedia services in extended areas with homogeneous QoS levels. Conventional single-hop cellular architectures might not be able to satisfy these requirements due to the effect of surrounding obstacles and the signal attenuation with distance, in particular at large distances and under NLOS propagation conditions. MCNs are expected to significantly improve the system capacity and user-perceived QoS through the substitution of long-distance (and generally NLOS) cellular links by various multi-hop links with improved link budgets. Although there are still significant challenges to be solved, MCNs represent a significant step towards overcoming the fundamental communication and radio propagation limits of traditional single-hop cellular architectures. Several analytical and simulation-based studies have proved the benefits that MCNs using mobile relays can provide in terms of capacity, cell coverage, network scalability, infrastructure deployment cost, power consumption and energy efficiency. This thesis complements this study, and this chapter reports the first experimental field trials that validate and quantify the benefits that MCNs using mobile relays and D2D communications can provide over traditional cellular systems. The field trials have been conducted using the mHOP testbed presented in Chapter 3. Section 4.1 describes the testing conditions and metrics, and the configuration of the mHOP testbed. Section 4.2 provides a

comprehensive description of the obtained experimental results that demonstrate the scenarios and conditions under which MCNs using mobile relays outperform traditional single-hop cellular communications.

4.1 Testing Conditions and Metrics

The field trials presented in this chapter were conducted over commercial live cellular networks. Orange Labs in Spain supported the field trials conducted over different locations in the city of Elche (Spain). The locations were carefully chosen to identify and evaluate the conditions under which MCN technologies using mobile relays and D2D communications can overcome the limitations of traditional single-hop cellular systems. Additional details about the locations where the field trials were conducted are provided in Section 4.2 for each of the scenarios.

The field trials consider downlink transmissions of long-size files using the mHOP platform (Chapter 3, Figure 3-1) from a local FTP server located at the UWICORE Laboratory. The configuration of the server allows an unlimited number of users, and has no limit in the download speed. The cellular links are configured to operate over HSPA, and the ad-hoc D2D links over IEEE 802.11g at 2.4 GHz that provides a theoretical maximum bit rate of 54 Mbps and established a maximum transmit power of 27 dBm. IEEE 802.11g was selected over IEEE 802.11a to benefit from the better propagation conditions experienced at 2.4 GHz compared to 5 GHz [87][5]. The IEEE 802.11 data rate and the transmission power at which the mobile relay nodes operate are dynamically modified based on the link quality conditions as implemented by the network driver (Ath9k). In the tests, the IEEE 802.11 transmission power of the mobile relay nodes has been limited to a maximum of 19 dBm in compliance with the Spanish regulations (limit is established at 20 dBm).

The field trials have been carried out under diverse configurations combining different number of hops and hop distances. For example, a 3hops-40m configuration refers to an MCN connection composed of one cellular link and two IEEE 802.11g ad-hoc D2D links with a distance between Mobile Nodes (MNs) of 40 meters. If the tests involve mobility, the MNs approximately maintain the distance during the route. The tests start when the destination MN launches a script that executes a file download through the MCN link. The MCN link requires that the hybrid MN transforms the transport blocks

[5] Ath9k is not yet providing a stable operation in ad-hoc mode for the IEEE 802.11n variant.

received through the cellular link to IEEE 802.11g Packet Data Units (MAC PDU); the MAC PDU size has been set to 1564 bytes. As a result, the hybrid MN stores the cellular transport blocks in a buffer until an IEEE 802.11g MAC PDU is filled. Once the IEEE 802.11g packet is formed, the hybrid MN transmits the MAC PDU to the next mobile node using its IEEE 802.11g wireless ExpressCard interface. Mobile nodes located between the hybrid MN and the destination MN act as relays with the multi-hop path being predefined at the start of each field trial following the configuration steps described in Section 3.3.

4.1.1 Performance Metric

The MCN performance is measured in terms of the throughput experienced by the destination MN. The throughput is commonly used as a performance indicator in cellular systems[6]. In the case of single-hop cellular transmissions, it would have been reasonable to expect that as the destination MN moves away from the BS and the link quality degrades (measured in HSPA through the CQI parameter), the throughput decreases. However, it is important to note that the testing BSs are not barred, and therefore other users might be active. Although this configuration guarantees realistic operating conditions, it requires a careful treatment to adequately interpret the field measurements. Initial tests showed that the operator's radio resource management policy compensates link degradations with more HSPA radio resources (Figure 4-1). Figure 4-1 depicts the QoS experienced by a single-hop cellular user as a function of the distance to its serving BS; the results are shown as relative performance since the actual measurements have been divided by the maximum value experienced for each parameter during the test. The dotted line represents the percentage of time that the user was assigned radio resources (*usage*), and the dash-dotted line represents the user's CQI. The HSPA standard uses CQI estimates to provide an indication of the channel quality and recommend transmission modes (transport block size, number of parallel codes, modulation scheme, etc.). High CQI values indicate good channel quality conditions. Figure 4-1 shows that the CQI decreases with the increasing distance to the serving BS. However, the user throughput (dashed line in Figure 4-1) remains relatively constant despite the degradation of the channel quality conditions. This is the case because the network detects the channel degradation and compensates it by increasing

[6] Other metrics such as the delay or the energy efficiency might have been used to measure the MCN performance. However, since the field trials consider downlink transmissions they would require access to the operational BSs which was not possible for the authors at the time this study was conducted.

the *usage* of radio resources as the user moves away from the serving BS. This results in the user throughput level being relatively independent of the distance to the serving BS for the measurements reported in Figure 4-1. However, if the throughput is divided by the *usage* parameter (*normalized throughput* in Figure 4-1 represented by solid line), it is then possible to observe the dependence of the cellular performance with the channel quality (and distance). To reduce the impact of the radio resource management policies on the conducted study, the *normalized throughput* has been selected as the reference parameter. In addition, and despite the fact Nemo Handy evaluates the cellular QoS every 0.2 seconds, the reported *normalized throughput* will correspond to measurements averaged over time periods of one second given the GPS updating rate (1 Hz).

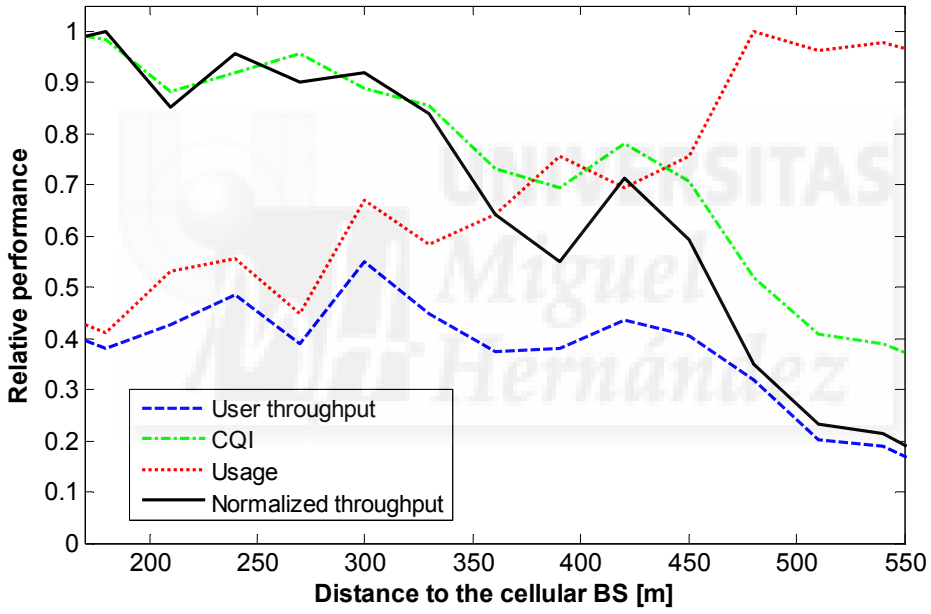

Figure 4-1. Cellular performance as a function of the distance to the serving BS.

It should be also noted that in the MCN connection the cellular technology represents the bottleneck. The Nemo Handy's HSPA release uses for downlink transmissions a 5 MHz bandwidth, Quadrature Phase Shift Keying (QPSK) and 16-Quadrature Amplitude Modulation (QAM) modulations, and variable transport block size. On the other hand, IEEE 802.11g uses a 20 MHz bandwidth, Orthogonal Frequency Division Multiplexing (OFDM) modulation and a fixed transport block size. These features result in that HSPA is characterized by lower data rates than IEEE 802.11g, and therefore downlink transmissions are upper-bounded by the cellular performance. As a result, the throughput at the destination MN should not be higher than the maximum

theoretical cellular data rates. If the throughput at the destination MN was normalized considering the IEEE 802.11g resources (time and frequency), normalized throughput values higher than the maximum theoretical HSPA data rates could be obtained which is not realistic. However, it is possible that the operating conditions make the IEEE 802.11g ad-hoc performance decreases significantly and becomes the bottleneck of the MCN connection (for example when the IEEE 802.11 ad-hoc D2D links experience NLOS conditions). Independently of which technology (HSPA or IEEE 802.11) represents the bottleneck of the MCN connection, the normalization process considering the *usage* parameter is valid since the MCN throughput is normalized only considering the cellular radio resources assigned to the hybrid MN; these resources do not depend on the performance of the IEEE 802.11 ad-hoc D2D link. This procedure results in that any performance degradation in the IEEE 802.11 ad-hoc link will also represent a reduction of the MCN *normalized throughput*. In this context, and following the observations derived from Figure 4-1, the MCN throughput is here reported as the ratio between the MCN user throughput measured at the destination MN and the *usage* of the cellular link experienced by the hybrid MN. For simplification, the *normalized throughput* at the destination MN of the MCN connection will be hereafter referred to as throughput.

4.2 Experimental MCN Performance Evaluation

This section describes the field tests conducted to evaluate the performance of MCNs using mobile relays, and the conditions under which MCNs can help overcome the limitations of traditional single-hop cellular networks. The field tests have been conducted under different operating conditions (e.g. NLOS and large distances to the serving BS) and scenarios, including handover or cell overlaid areas and indoor environments.

4.2.1 Handover

MCN technologies using mobile relays and D2D communications could help improve the cellular QoS experienced in handover (HO) areas. In cellular systems, a handover process is launched when the quality of a cellular connection with a given cell degrades, and other nearby cells can provide better quality levels. To this aim, mobile terminals perform continuous measurements of the serving cell and the neighboring cells' signal quality, and report the results to the Radio Network Controller (RNC). Using the reported measurements, the RNC decides whether a handover is executed based on pre-established network policies. UMTS allows for both Hard Handover (HHO) and Soft Handover (SHO) mechanisms. In HHO, the connection with the serving BS is released

before establishing a new connection with the target BS. On the other hand, SHO allows for mobile terminals to be simultaneously connected to the serving and target BSs. HSDPA does not support SHO. This is the case because HSDPA introduces a number of enhancements for faster packet scheduling and retransmission that require data packets to be buffered in the BS. In this case, multiple BSs cannot transmit simultaneously to a mobile terminal.

The first release of HSDPA (3GPP Release 5) only allows performing a handover between cells belonging to the mobile user's active set as shown in Figure 4-2. In the illustrated example, a mobile station (MS) is conducting a HSDPA file download through BS_1 (identified with scrambling code SCR_1). During the file download, the MS executes a number of measurements of the active cell (SCR_1) and the monitored cells (Figure 4-2 assumes that the monitored set only includes BS_2 identified with SCR_2). When the signal level from BS_2 increases, the MS sends a measurement report to the RNC through its serving BS indicating that BS_2 fulfills the criteria for being added to the active set (event 1A). Once this process is completed, the RNC sends the ACTIVE_SET_UPDATE message including BS_2 in the active set, and the MS acknowledges the receipt of this message by

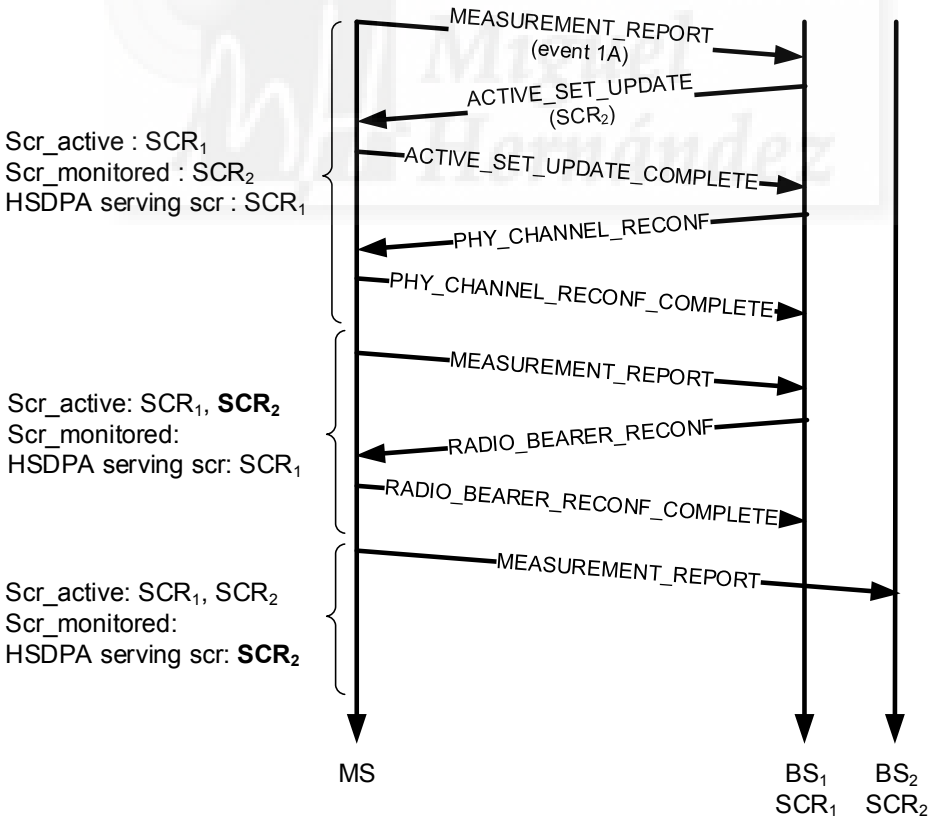

Figure 4-2. Messages exchanged in the HSDPA-release 5 handover process.

replying with the ACTIVE_SET_UPDATE_COMPLETE message. The active set process is completed with the establishment of the physical channel (PHY_CHANNEL_RECONF). Although BS_2 belongs now to the MS's active set, the file download is still conducted through BS_1. When the criteria to perform a handover are fulfilled, the RNC sends the RADIO_BEARER_RECONF message that contains the new configuration parameters for the radio bearer and the lower layers. The reconfiguration procedure, including the change of serving cell, is completed when the MS acknowledges the receipt of this message.

In 3GPP Release 6, the active set update procedure also allows carrying out a HSDPA serving cell change. However, to increase reliability, 3GPP Release 8 introduces the Enhanced Serving Cell Changed (ESCC) procedure [88]. In ESCC, mobile terminals receive the signaling message to change the HSDPA serving cell through the target cell. This has been done in order to exploit the stronger signal strength of the target cell, and thereby increase the reliability with which key signaling messages are exchanged. The communications between the MS and the target cell is possible thanks to the configuration information received by the MS during the active set update procedure.

Independently of which 3GPP release is being considered, the RNC decides whether a handover should be triggered or not based on the measurement reports sent by the MSs; these reports contain the Common Pilot Channel (CPICH) strength of the active and monitored cells. It is important to note that handover algorithms are not specified in the standards, and are proprietary to each operator. However, a possible method to decide whether a handover procedure should be triggered is by comparing the CPICH strength of the active and monitored cells. In order to avoid frequent changes of serving cell, handover algorithms use a *hysteresis* (*H*) parameter that identifies the required CPICH power difference between the target cell and the serving cell that must be experienced in order to trigger a handover. In addition, the reliability of the handover procedure is enhanced through the *Time To Trigger* (*TTT*) parameter, which defines the uninterrupted period of time during which the target cell's CPICH strength has to fulfill the hysteresis condition to trigger the handover. The *H* and *TTT* parameters are critical factors to guarantee high performance and avoid frequent connection outages during the serving cell change procedure. If these parameters are not adequately optimized, the HSDPA throughput and user-perceived QoS may significantly decrease. In fact, previous studies have analyzed how to optimize HSDPA performance in cell overlaid areas. The work reported in [89] studies two different handover methodologies. The first one simply changes the HSDPA serving cell when entering the handover area (i.e.

HHO). On the other hand, the second method implies switching from HSDPA to UMTS when the MS moves into the handover area (active set size is larger than one), and then switches back again to HSDPA when the MS leaves the handover area. This method was proposed to exploit UMTS macro diversity capability during the handover procedure (i.e. SHO). The results obtained in [89] indicate that switching to UMTS is not an optimum solution, whereas minimizing the handover area (using small *H* and *TTT* parameters) results in a higher data rate and a lower connection outage probability. However, the results reported in [90] show that very low values for *H* and *TTT* decrease the user-perceived QoS because of frequent handovers in the cell overlaid area. The studies conducted in [90] also demonstrate that the optimization of handover parameters is not easy, and that a trade-off exists between the *H* and *TTT* parameters based on the mobile user's speed.

The benefits of using MCNs to enhance the handover procedure have been previously highlighted in the literature [91]. Multi-hop handover conditions and the necessary signaling messages are being defined in the baseline documents for standards such as IEEE 802.16j and LTE-Advanced [92]. The efforts focus initially on fixed relay solutions, and only a few studies have slightly addressed the handover issues from the mobile relay point of view [93][94]. In this context, this thesis discusses a proposal on how to conduct handovers exploiting the features of MCNs using mobile relays and D2D communications. The proposal discussed in this thesis concentrates on downlink transmissions, and thereby will be compared with the HSDPA handover management.

In a traditional HSDPA single-hop cellular network, the decisions to trigger a handover can be based on the measurement reports sent by the MS to the RNC. These reports contain the CPICH signal strength of the monitored and active cells. Based on these measurements, the RNC can dynamically compare the signal strength of the serving HSDPA BS and the potential BS candidates. Figure 4-3 shows an example of the monitored CPICH Energy per chip over the Noise (Ec/NO) parameter for an HSDPA serving BS (source cell), and the target BS (target cell) over which a handover is to be conducted. This example has been obtained during some field tests conducted using Orange's HSDPA network (implemented 3GPP Release 5 at the time of the measurements) at the city of Elche in Spain. The pre-established network policies to decide the *H* and *TTT* values that trigger the handover process are not standardized, and the operator fixes them according to the characteristics of the cellular environment. In this case, the specific algorithm used by Orange to decide and execute handovers was not public. However, using the monitoring capabilities of Nemo Handy (described in

Section 3.2.1), it has been possible to determine the moment at which Orange's handover algorithm decides to transfer the active connection from the HSDPA source cell to the target cell (depicted in Figure 4-3 with the vertical arrow ①). The Nemo Handy monitoring tool has also allowed measuring the time between the moments at which the target cell's CPICH Ec/NO is better than the one measured at the source cell and the handover is executed (*TTT*), and the CPICH Ec/NO difference (*H*) between the source cell and the target cell.

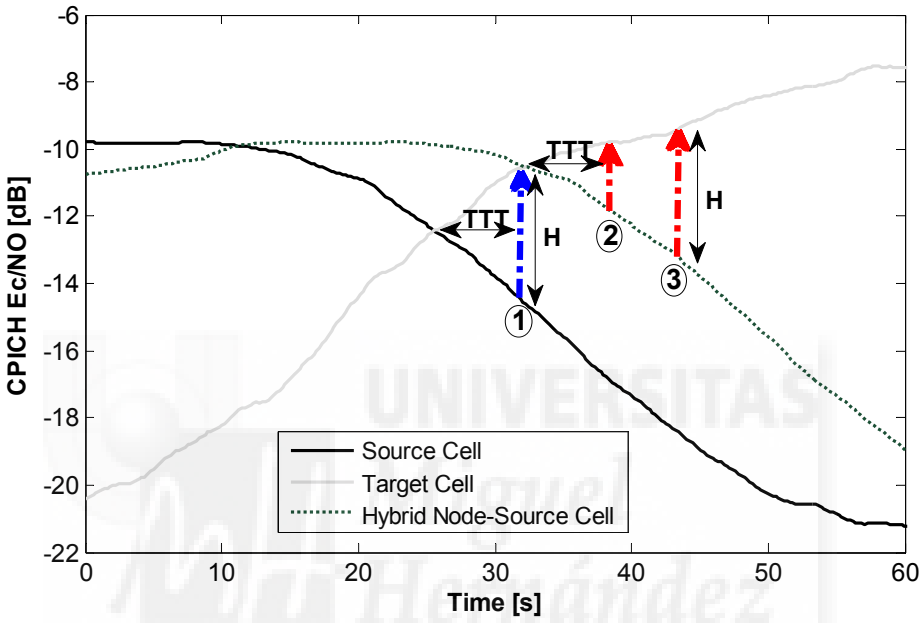

Figure 4-3. CPICH Ec/NO example.

Although the destination MN is the end-point of the MCN link, it is important to note that the cellular transmission in a MCN connection is actually conducted through the hybrid MN and not the destination MN. Since the cellular link represents the QoS bottleneck in a MCN connection, the quality experienced at the hybrid MN can be extended to the destination node through the MCN link. In this context, an unresolved question is how and when to launch a cellular handover process in MCN transmissions. If such process was to be launched based on the (single-hop) cellular link quality experienced at the destination MN, the handover of the MCN connection would take place at the same distance to the BS as the handover in traditional single-hop cellular networks. On the other hand, this thesis proposes to execute MCN handovers (i.e. changing the serving cellular BS in a MCN link) at the RNC based on the comparison of the destination MN's cellular signal quality with the target BS (labeled 'Target Cell' in Figure 4-3), and the hybrid MN's cellular signal quality with the serving BS (labeled

'Hybrid Node-Source Cell' in Figure 4-3). Although the cellular transmission in a MCN connection is conducted through the hybrid MN, the destination MN also sends periodically its measurements reports to the BS. As a result, the RNC can execute the proposed MCN handover process by comparing the signal quality for the link destination MN-target BS and the link hybrid MN-source BS. Using the example reported in Figure 4-3, it is then possible to identify the times at which the MCN handover process would be executed following this thesis' proposal. The vertical arrow ② represents the time at which the MCN handover would be conducted if the handover was based on the *TTT* parameter. If the handover was based on the measured *H* parameter, vertical arrow ③ would represent the time at which the MCN handover would be executed. It is important to note that in both cases, the MCN handover will significantly improve the end-user QoS. This is the case because the destination node leaves the source cell with higher signal strength than in a traditional single-hop cellular architecture, and it also perceives a stronger signal when it connects to the target cell. The impact of this MCN handover process in the end-user performance (estimated by means of the throughput) has been illustrated through field test measurements.

4.2.1.1 Testing Environment

Urban field trials have been conducted in the scenario shown in Figure 4-4 in order to demonstrate how MCN technologies could help improve the QoS in HO areas. Figure 4-4 illustrates the location of the serving BS and the target BS, and the initial position of the hybrid MN (H-MN) and the destination MN (D-MN) which are placed linearly under LOS conditions. One MCN configuration with 2 hops and a distance between the hybrid MN and the destination MN equal to 40 meters is tested (i.e. 2hops-40m MCN link). In this scenario, MNs move from one cell to a neighboring cell in order to force a handover (in this case, Nemo Handy did not lock to a specific BS). Figure 4-4 represents the HO area as the area with cellular coverage from the two cells.

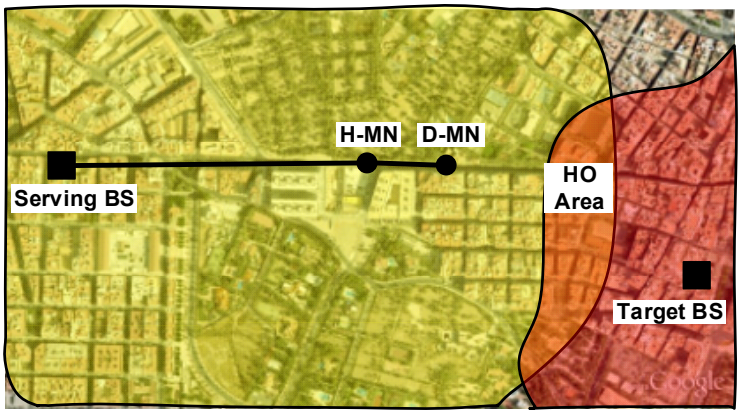

Figure 4-4. Handover field testing environment.

4.2.1.2 Field Test Results

The HSDPA performance strongly depends on the implemented radio resource management algorithms. HSDPA adapts its operation to the link quality through the use of mechanisms such as Adaptive Modulation and Coding (AMC) and Hybrid-Automatic Repeat Request (ARQ). These mechanisms require the mobile terminal to transmit estimates of the experienced channel quality conditions in the uplink direction; the channel quality is measured in HSDPA through the CQI parameter. Based on such estimates, the BS will modify its transmission parameters to ensure a certain QoS target. In this context, it is important to note that the lower the channel quality, the higher the number of resources needed to achieve a QoS target.

Figure 4-5 represents the CQI measurements reported by a MS while it moves from the serving cell to the target cell and forces the handover execution (Figure 4-4). As expected, the channel quality significantly degrades in the HO area, which thereby requires a significant increase of the mobile terminal's transmission power in order to communicate with the BS and send its CQI reports (Figure 4-6). HSDPA's link adaptation mechanism aims at maintaining a BLER between 10% and 20% [20]. Based on the uplink CQI reports (Figure 4-5), the HSDPA BS adjusts the transmission power and transmission mode (modulation, transport block size and number of parallel codes) to guarantee that the downlink performance is within the target limits. Figure 4-7 shows that the link adaptation algorithm implemented in Orange's network is able to achieve the BLER target outside the HO area. On the other hand, the worse propagation conditions and higher interference levels experienced in the HO area difficult the adaptation of the transmission parameters and results in higher BLER values. As a consequence of the low channel quality conditions (Figure 4-5) and the resulting high BLER (Figure 4-7), the HSDPA throughput significantly degrades in the HO area (Figure 4-8). Figure 4-8 shows the throughput measured in the case of a single-hop HSDPA cellular link as the MS moves from the source cell to the target cell. As shown in Figure 4-8, the performance significantly degrades (60-70% on average) in the HO area due to the lower signal level. The performance improves rapidly when the HO process ends and the MS connects to the target cell offering better signal quality.

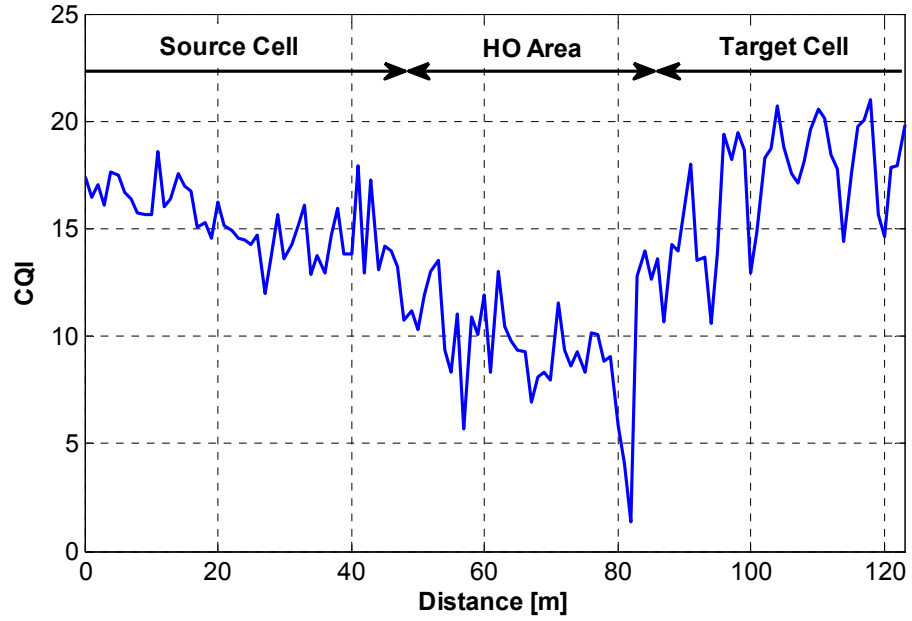

Figure 4-5. Measured CQI for the HSDPA cellular link.

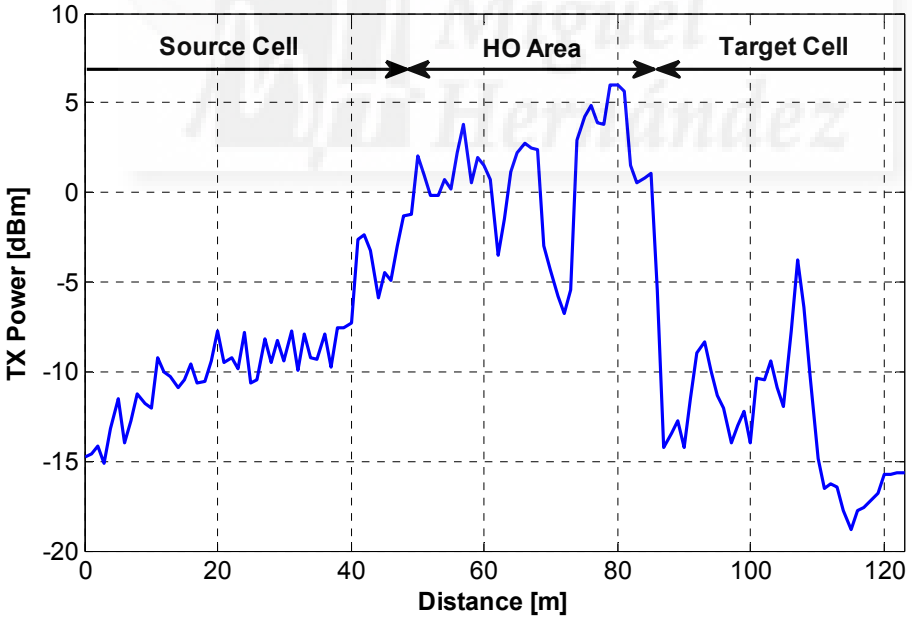

Figure 4-6. MS transmission power for the HSDPA cellular link.

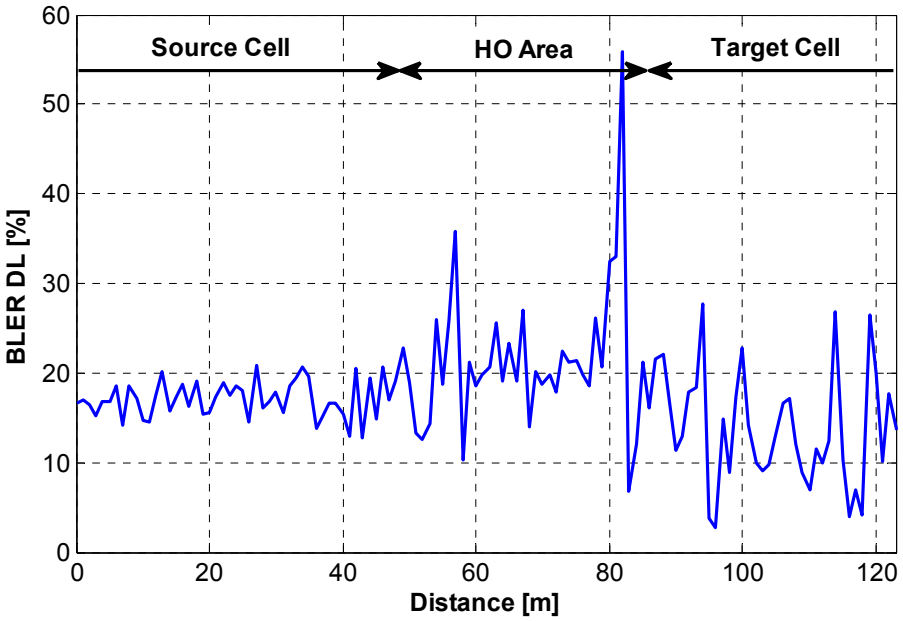

Figure 4-7. BLER for the HSDPA cellular link.

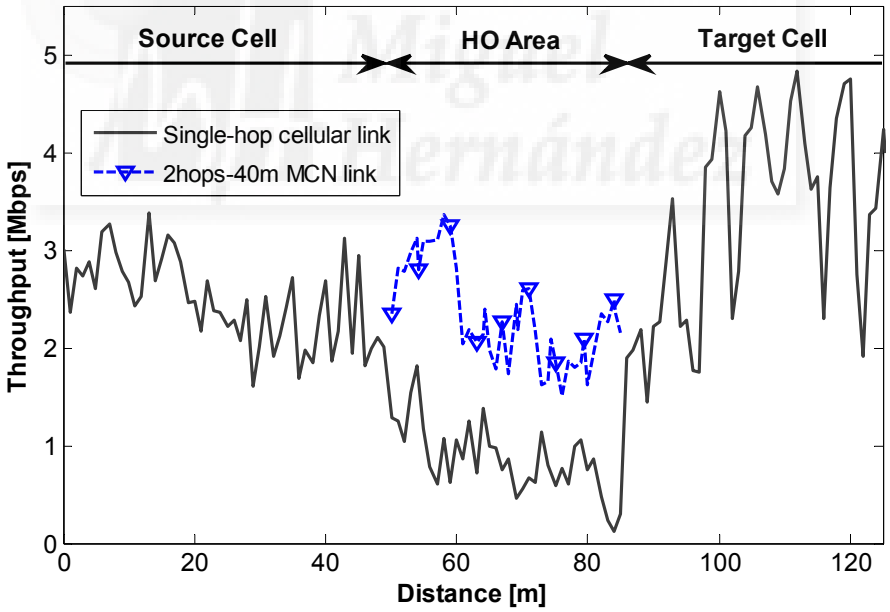

Figure 4-8. MCN capacity to improve QoS in handover areas.

MCN technologies can help improve the QoS during a HO by replacing the single-hop cellular connection when the MS enters the HO area with an MCN connection using a hybrid MN located outside the HO area and with good propagation conditions to the destination node (for example, a hybrid MN located in the same street). This scenario

was reproduced in the conducted field tests using a hybrid MN that is 40 meters closer to the serving BS than the destination node. The throughput as the destination MN crosses the HO area is significantly higher than in the case of a single-hop cellular link (Figure 4-8). It is important to note that the destination MN is connected to the serving BS through the hybrid MN, and that the distance between the destination and hybrid MNs was selected so that the hybrid MN does not enter the HO area during the test. This results in that the MCN connection is capable of guaranteeing to the destination MN the same quality in the HO area as experienced by the hybrid MN outside the HO area. Based on the throughput measurements reported in Figure 4-8, the adoption of the MCN handover strategy discussed in Section 4.2.1 would then result in that the destination MN is capable of experiencing a high throughput performance even in the HO area. In fact, the MCN handover will not be triggered until the hybrid MN reaches the HO area. If the distance between the hybrid and destination MNs is adequately selected, the MCN handover would then be triggered when the destination MN has left the HO area and entered the target cell area, which would again guarantee a high throughput level when the handover is executed. These unique experimental results show that MCN technologies could significantly improve the QoS as mobile nodes cross HO areas in comparison to traditional single-hop cellular communications.

4.2.2 QoS at Large Distances to the Serving BS

A major motivation behind the development of relaying techniques in cellular systems is the possibility to provide the same QoS experienced by users close to a BS to users at larger distances across the cell area. This can be done by substituting long-distance and NLOS single-hop cellular links by MCN connections using mobile relays and D2D communications. To extend the QoS experienced close to the BS to larger distances from the serving BS, multi-hop MCN links need to experience good LOS conditions and/or shorter distances among the communicating nodes.

4.2.2.1 Testing Environment

The field measurements were carried out in the scenario illustrated in Figure 4-9. In this scenario, three different MCN configurations composed of 2, 3 and 4 hops with increasing distances between mobile relay nodes (from 60 to 120 meters) were tested. Figure 4-9 depicts one example of each of these configurations. Figure 4-9.a corresponds to the 2hops-60m MCN link configuration; there is one cellular link and one IEEE 802.11g ad-hoc D2D link, and the distance between the destination MN (D-MN) and the hybrid MN (H-MN) is 60 meters. Figure 4-9.b and Figure 4-9.c show two examples of the 3hops and 4hops MCN links configurations with separation distances between MNs of 90 meters and 120 meters, respectively. As it can be appreciated from the examples, the

location of the destination MN was always fixed at 780 meters distance to the BS. On the other hand, the location of the hybrid MN and intermediate mobile relay nodes vary depending on the MCN configuration. Figure 4-9 shows that the higher the number of hops, the closer is the hybrid MN to the BS. The D2D links between mobile relay nodes are characterized by LOS conditions with pedestrians continuously crossing over. In this scenario, Nemo Handy was locked to the Serving BS in order to prevent cellular handovers.

a) 2hops-60m MCN link

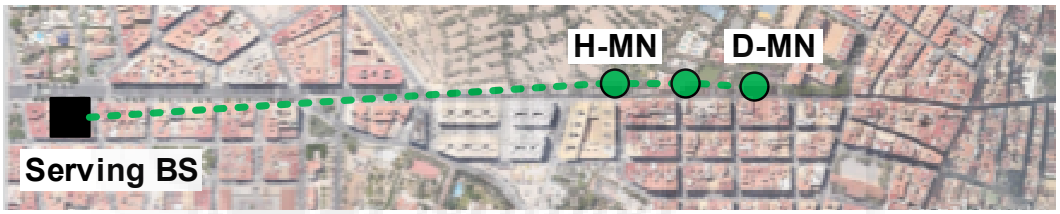

b) 3hops-90m MCN link

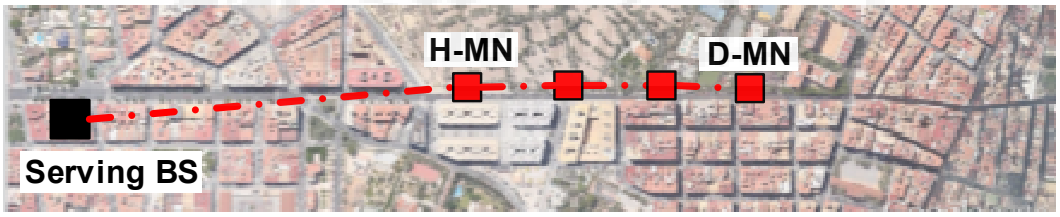

c) 4hops-120m MCN link

Figure 4-9. QoS at large distances - field testing environment.

4.2.2.2 Field Test Results

Figure 4-10 represents the throughput experienced by a single-hop cellular link and MCN links under various configurations in the scenario shown in Figure 4-9. The solid line in Figure 4-10 represents the throughput experienced by a single-hop cellular user walking away from the BS. As demonstrated in Section 4.2.1 for the Handover scenario, the cellular QoS decreases with the distance as a result of the higher signal losses and lower link quality. The cellular HSDPA link can reach data rates above 10 Mbps using various channelization codes (up to a maximum of 15) and the 16QAM modulation.

Table 4-1. Cellular QoS at three different distances to the BS.

a) Close to the BS

%	Modulation	# Ch. Codes
79	16QAM	10
1	QPSK	6
20	n/a	n/a

b) Intermediate location

%	Modulation	# Ch. Codes
2	16QAM	10
2	QPSK	10
5	QPSK	8
15	QPSK	6
22	QPSK	4
42	QPSK	2
5	QPSK	1
7	n/a	n/a

c) Cell edge

%	Modulation	# Ch. Codes
5	QPSK	6
28	QPSK	4
48	QPSK	2
9	QPSK	1
10	n/a	n/a

However, the HSDPA performance depends on the link quality conditions, and thereby on the distance between the cellular user and its serving BS. This can be appreciated in Table 4-1 that shows the usage percentage ('%') of modulation schemes ('Modulation') and number of channelization codes ('# Ch. Codes') at three different locations: close to the BS (Table 4-1.a), at an intermediate location (Table 4-1.b) and at the cell edge (Table 4-1.c). These measurements correspond to three different samples of Nemo Handy that evaluates the cellular QoS every 200 ms. Since the HSDPA's TTI is equal to 2 ms, Nemo Handy's samples correspond to 100 TTIs. When the user was located close to the BS (Table 4-1.a), the MS used 16QAM and 10 channelization codes in 79 out of the 100 TTIs. At the intermediate location (Table 4-1.b), 91 out of the 100 TTIs used QPSK, and at the cell edge (Table 4-1.c) more than 50 TTIs used 2 or fewer channelization codes. On average, the cellular link used the high level modulation mode (i.e. 16QAM) and 10 channelization codes close to the BS. As the user walked away from the BS and the channel conditions degraded, the cellular link was characterized by a more robust modulation scheme (i.e. QPSK) and a lower number of channelization codes.

Figure 4-10 also depicts the throughput measured at the destination MN of the three MCN configurations. As previously explained, the measured MCN performance is generally upper-bounded by the cellular QoS given the lower HSDPA data rates compared to IEEE 802.11g (this was actually the case for the measurements reported in Figure 4-10). As a result, the destination MN achieved the same throughput as the hybrid MN for all the analyzed MCN configurations. The throughput of the destination node is therefore depicted at the position at which the hybrid MN was located. For example, the destination MN located 780 meters away from the BS achieved a throughput of approximately 4.2 Mbps when operating an MCN link with 4 hops and distances among mobile relay nodes of 120 meters (i.e. 4hops-120m MCN

configuration). This performance is reduced to 3.5 Mbps if the distance among mobile relay nodes decreases to 90 meters (i.e. 4hops-90m MCN configuration) since the hybrid MN is further away from the BS compared to the case in which the distance between mobile relay nodes is equal to 120 meters. These experimental results clearly show that MCN technologies using mobile relays and D2D communications can provide nodes located at large distances from the serving BS with high QoS levels close to those perceived by nodes located at shorter distances to the serving BS. This will in turn result in a more efficient use of the radio resources.

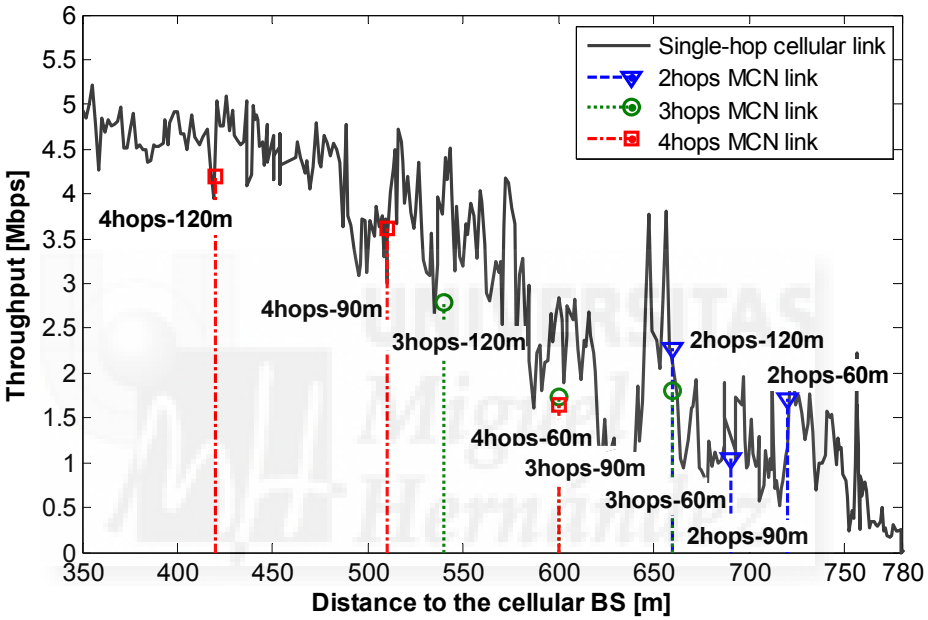

Figure 4-10. MCN capacity to improve QoS at large distances from the serving BS.

4.2.3 Coverage Extension

MCNs allow distant nodes to connect to a cellular BS through other relaying mobile nodes using D2D communications. This feature can facilitate extending the radio cell coverage area compared to single-hop cellular networks, which can be attractive to provide service in shadow areas or disaster areas where part of the infrastructure is temporarily unavailable. The MCN cell extension capability could also be beneficial to balance traffic among neighboring BSs under traffic congestion scenarios. For example, a node located under a congested cell could connect to the cellular network using a hybrid mobile relay node located at the cell edge of a less congested neighboring cell.

4.2.3.1 Testing Environment

A large set of field trials with varying MCN configurations were conducted to verify the capacity of MCNs using D2D communications to extend the cell radius. Figure 4-11 shows the scenario where these field trials were conducted under two MCN configurations composed of 3 and 5 hops, and a distance between MNs of 60 and 85 meters respectively. The hybrid MN and mobile relay nodes (including the destination MN) were all located on the same street with the hybrid MN being the closest to the serving BS and the destination node the farthest. In the case of an MCN link with 3 hops, the hybrid MN was at a distance of 400 meters to the BS at the start of the trial. This distance decreased to 180 meters in the case of an MCN link with 5 hops. When the destination MN executes the file download, all the mobile nodes move in the direction of the cell boundary to increase the distance to the BS. The download continues until the hybrid MN reaches the cell boundary where the cellular coverage from the serving BS is lost. To prevent the hybrid MN to perform a handover to a neighboring BS, the Nemo Handy capability to force the terminal to the serving BS was used.

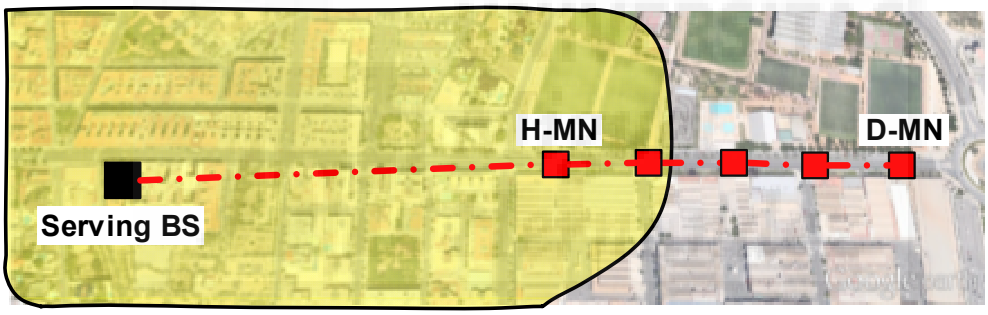

a) 5hops-85m MCN link

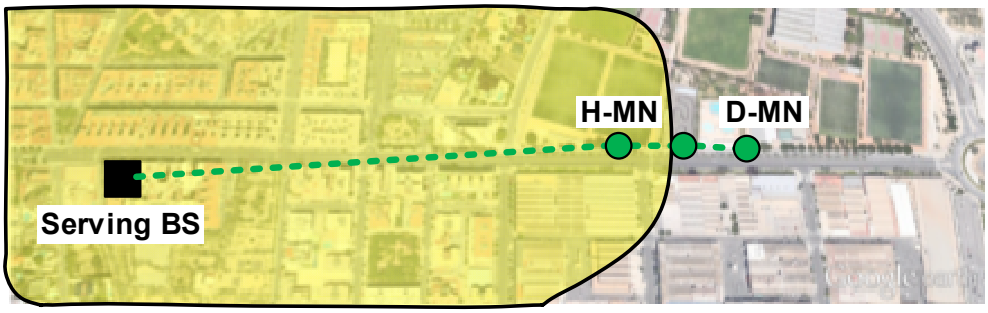

b) 3hops-60m MCN link

Figure 4-11. Coverage extension – field testing environment.

4.2.3.2 Field Test Results

Initial tests were conducted using the Nemo Handy tool to measure the actual radius of a typical urban cell in the city of Elche. To this aim, the testing MS was forced to connect to the BS under study using Nemo Handy. Figure 4-12 shows the throughput of the single-hop cellular link as a function of the distance to the BS. The reported measurements show that the cell radius for the conventional HSDPA single-hop cellular link is equal to approximately 650 meters.

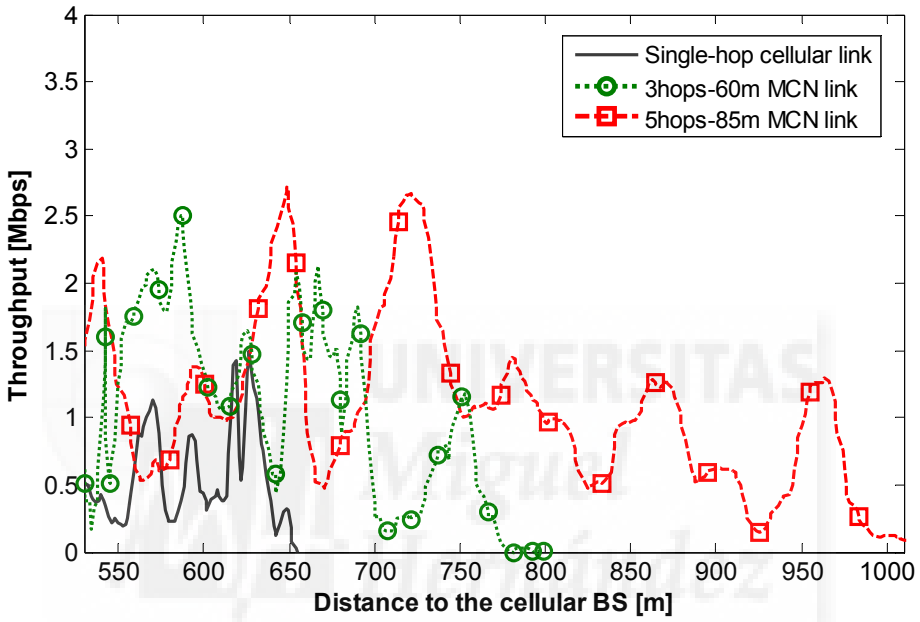

Figure 4-12. MCN capacity to extend the radio coverage.

Figure 4-12 also shows the MCN throughput at the destination MN of the two MCN configurations. It should be noted that the MCN performance exhibits larger variations than conventional single-hop cellular links. This is due to the fact that the mobile nodes had to cross several streets during the experiments (when all the MNs move in the direction of the cell boundary) resulting in temporary loss of the LOS conditions. When the hybrid MN reaches the cell boundary, the destination MN is located 120 meters beyond the cell limit (the cell limit is approximately 650 meters) in the case of the 3hops-60m MCN link configuration. The 5hops-85m MCN link configuration increases the distance the destination MN is located beyond the cell limit by approximately 340 meters. The obtained results thereby demonstrate the capacity of MCNs to extend the cell radius compared to conventional single-hop cellular networks (Figure 4-12). In fact, the results depicted in Figure 4-12 not only highlight the cell extension capability, but also the acceptable QoS levels that MCNs using mobile relays and D2D communications

can provide over the extended coverage areas. As previously discussed, the lower cellular performance typically results in the QoS level experienced by the destination node being similar to that experienced by the hybrid MN. The hybrid MN is closer to the BS in the case of the five-hop MCN link than in the case of the three-hop one. As a result, the 5hops-85m MCN link configuration provides higher QoS levels than the conventional single-hop cellular link and the 3hops-60m MCN link configuration.

4.2.4 Indoor QoS

Traditional single-hop cellular transmissions served by outdoor BSs can experience a notable QoS degradation when entering indoor environments. Cellular operators therefore have to consider hybrid deployments of macro and small cells. Such hybrid deployments result in several issues including interference, mobility management and energy efficiency [95]. In addition, it is required to plan where to strategically place the small cells based on coverage and capacity needs. An alternative that can help increase indoor QoS is the use of MCN connections that utilize D2D communications to extend outdoor QoS levels to indoor environments through the use of mobile relaying nodes.

4.2.4.1 Testing Environment

Field trials have been conducted in a shopping center of Elche (Figure 4-13). The outdoor cellular BS used for the experiments was located at 500 meters to the entrance of the shopping center under LOS conditions.

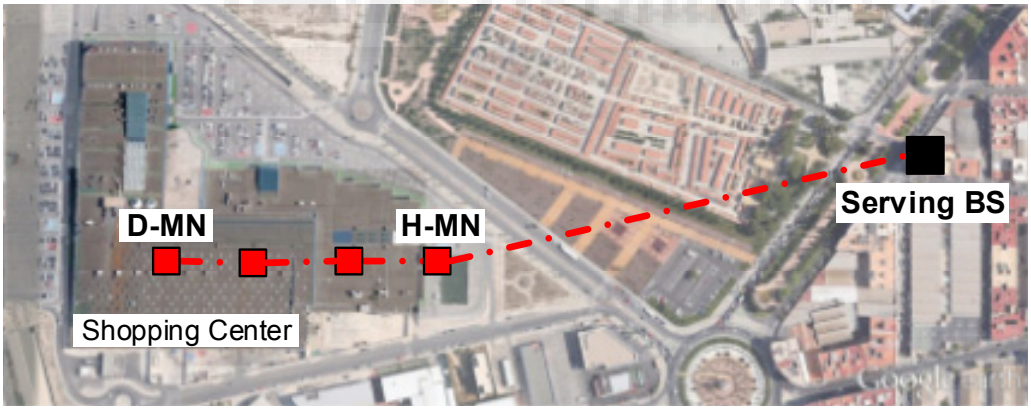

Figure 4-13. Field testing environment for indoor QoS provisioning using MCNs (example of 4hops-75m MCN link configuration).

Three different MCN configurations with 2, 3 and 4 hops, and a distance between MNs of 75 meters were tested. Figure 4-13 shows an example of the 4hops-75m MCN link configuration. At the start of the tests, the hybrid MN (H-MN) is located outside the shopping center (75 meters away from the entrance), while the mobile relay nodes and

the destination MN (D-MN) are located inside. The distance of the destination node to the entrance of the shopping center increases with the number of intermediate mobile nodes in the MCN configuration. When the destination node executes the file download, all the MNs move 75 meters inward (the hybrid MN ends up just inside the shopping center). Indoor markers using Nemo Handy were necessary to measure distances due to the poor indoor GPS signal. At the time of the experiments, the shopping center was crowded and people were continuously blocking the LOS conditions between the D2D links.

4.2.4.2 Field Test Results

Figure 4-14 shows the RSSI level experienced by a conventional single-hop HSDPA connection as the MS walks inside the shopping center and is locked to the outdoor BS (the negative distances represent the distance to the shopping center entrance). The conducted experiments show how the RSSI levels sharply decrease as the user walks inside the shopping centre. The signal attenuation as the user walks inside the shopping center also results in the rapidly decrease of the throughput experienced by the single-hop HSDPA connection depicted in Figure 4-15. Figure 4-15 shows that the single-hop HSDPA connection is able to maintain the outdoor QoS next to the entrance, but not inside the shopping center. The obtained results also show that the single-hop cellular connectivity is lost (the throughput value is equal to 0) when the MS moves 175 meters inwards. On the other hand, the results depicted in Figure 4-15 show that MCN technologies are capable of increasing indoor QoS performance to levels close to that experienced in outdoor conditions with better cellular signal quality. For example, Figure 4-15 shows that the 2hops-75m MCN link configuration can provide QoS levels close to those experienced outdoor when the D-MN is 75 meters inwards. Figure 4-15 also shows that the higher number of hops in the MCN configuration results in better QoS levels at inner regions in the shopping center. The 4hops-75m MCN link configuration increases the distance at which outdoor QoS levels can be provided to 225 meters inwards. The capacity to extend the cellular radio coverage is also observed in the results depicted in Figure 4-15 since MCNs are capable of maintaining active communication links at higher distances than single-hop cellular systems.

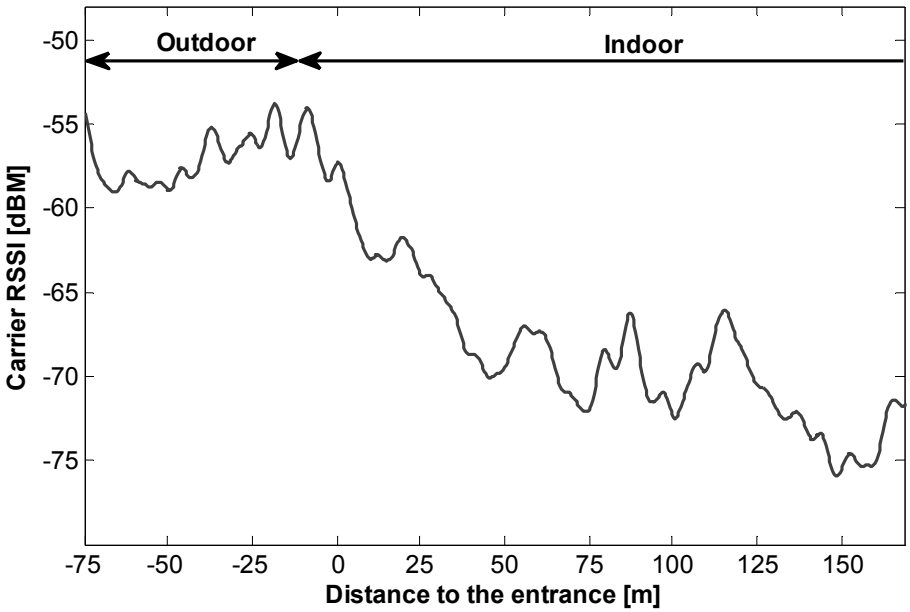

Figure 4-14. Cellular carrier RSSI as the user walks inside the shopping center.

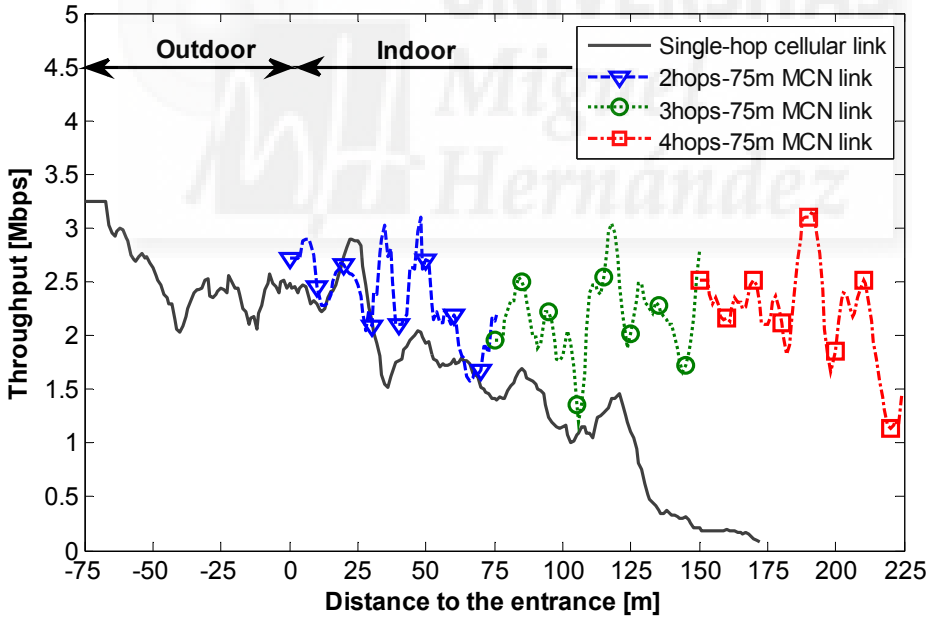

Figure 4-15. MCN capacity to improve indoor QoS levels.

4.2.5 QoS under NLOS Conditions

The presence of obstacles can significantly attenuate wireless signals and result in shadow areas that can prevent providing homogeneous QoS levels across a cell. The field experiments reported in [24] for LTE-Advanced with fixed relays showed that the use of relay nodes can help reduce the disadvantages experienced under single-hop

cellular NLOS conditions. To do so, relaying technologies, including MCNs, should replace large-distance NLOS single-hop cellular links by shorter-distance LOS multi-hop communications. In this context, the aim of this section is to complement the conclusions reported in [24], and demonstrate that MCNs using mobile relays and D2D communications can also enhance the single-hop cellular performance when a MS operates under NLOS conditions.

4.2.5.1 Testing Environment

The field trials have been conducted in a typical urban cell in the city of Elche with the destination node turning around an intersection corner (Figure 4-16). This setting allows reproducing the traditional signal attenuation experienced when passing from LOS to NLOS conditions. To do so, the cellular link is locked to the same BS providing service under LOS conditions, i.e. a cellular handover is not allowed when turning around the corner. The MCN performance has been analyzed under two different multi-hop configurations. Both of them consider a hybrid MN (H-MN), two mobile relay nodes, and a destination MN (D-MN), but with different distances among the mobile nodes (40 and 50 meters). At the start of the experiments (Figure 4-16.a), the hybrid, mobile relays and destination MNs are placed linearly under LOS conditions with the serving BS. Once the file download is executed, the MNs walk towards the intersection corner, with the destination node being the first to turn around the corner (Figure 4-16.b). As the file download continues the mobile relay nodes and finally the hybrid MN reach the corner (Figure 4-16.c).

4.2.5.2 Field Test Results

Figure 4-17 shows the RSSI levels experienced by a single-hop cellular link when experiencing LOS and NLOS conditions as the MS turns around the intersection corner. The negative distances represent the distance to the corner under LOS conditions, and the positive ones the NLOS distances after turning the corner. The reported measurements show how the single-hop RSSI levels maintain an acceptable level under LOS conditions, but rapidly decrease after turning around the corner and the MS enters NLOS conditions with the serving BS. The low RSSI levels after the MS enters NLOS conditions result in the low throughput measurements reported in Figure 4-18. The obtained measurements show that the single-hop cellular QoS cannot be maintained under NLOS conditions.

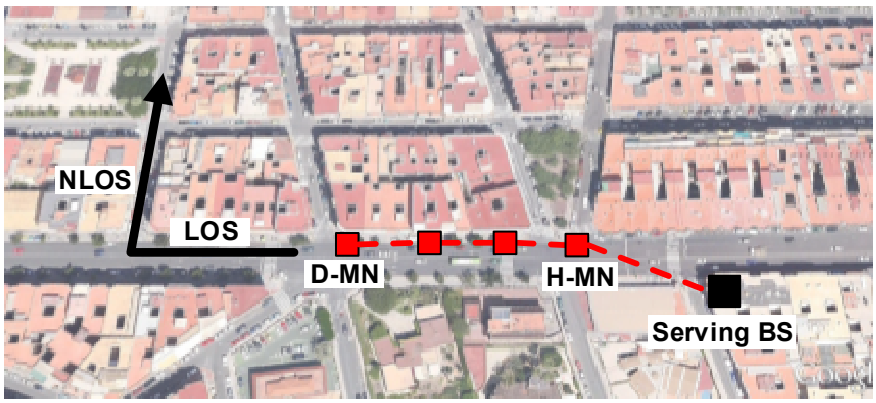

a) Initial deployment with all MNs under LOS conditions

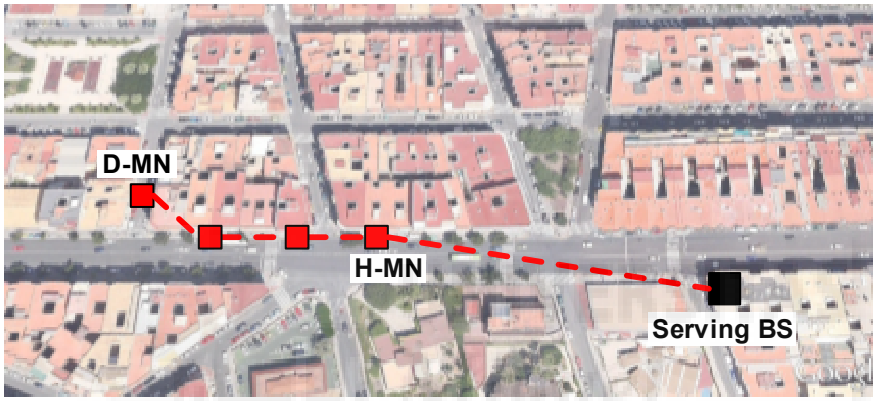

b) The D-MN reaches the intersection corner and experiment NLOS conditions with its precursor mobile node

c) The H-MN reaches the intersection corner and experiences NLOS conditions with the BS

Figure 4-16. QoS under NLOS conditions - field testing environment.

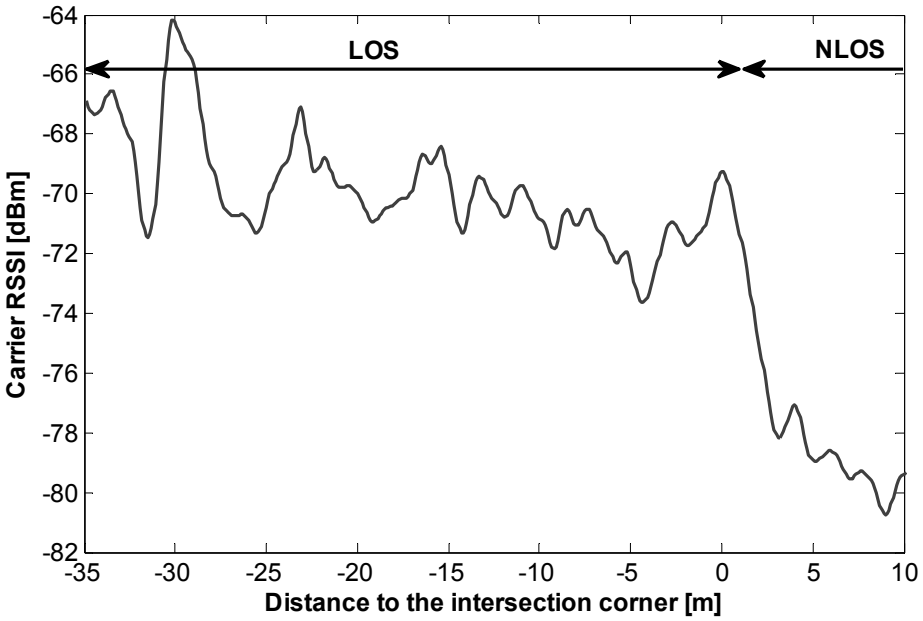

Figure 4-17. A cellular carrier RSSI level experienced by the MS as it walks from LOS to NLOS conditions with the BS.

Figure 4-18 also represents the throughput experienced at the destination MN for the two MCN configurations. The point at which the hybrid MN reaches the corner is marked in Figure 4-18 for each MCN configuration. The reported measurements show that MCN technologies can improve the NLOS QoS performance to levels experienced under LOS when adequately selecting the relay nodes (the mechanisms and criteria to select relay nodes are out of the scope of this study). The performance difference between both MCN configurations is a result of the varying distance among mobile relay nodes. A higher distance allows maintaining the connection during larger distances after turning the intersection corner. However, it also increases the time during which an IEEE 802.11g ad-hoc D2D link experiences NLOS conditions when one of the mobile relays turns the corner. This condition results in temporary deeper QoS degradations observed for the configuration with 50 meters between mobile relays (i.e. 4hops-50m MCN link configuration in Figure 4-18 around 40 meters).

ith the BS to shadow areas or locations with NLOS conditions with the BS. In this context, MCNs can contribute towards providing homogeneous QoS levels across a cell.

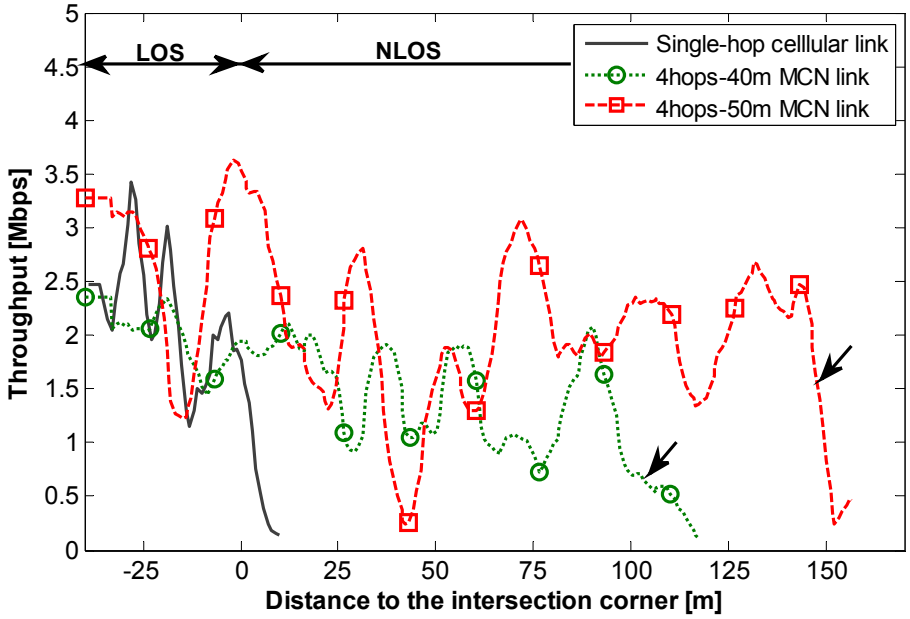

Figure 4-18. MCN capacity to improve NLOS QoS levels.

4.2.6 Energy Efficiency

Previous analytical and simulation-based studies (e.g. [18] and [96]) emphasized the possible energy consumption benefits of MCN communications. To experimentally evaluate this benefit, additional field tests have been conducted. These tests concentrate on uplink transmissions since energy gains for downlink transmissions are expected from the power management and saving techniques implemented at BSs. To measure such gains in downlink transmissions, access to operational BSs would have been necessary which was not possible for the authors at the time this study was conducted.

4.2.6.1 Testing Environment

The field tests conducted at the Miguel Hernández University of Elche compare the energy consumed by a single-hop uplink HSUPA cellular connection with that consumed by a two-hop MCN connection (Figure 4-19). In the case of the single-hop uplink HSUPA connection, the MS was static and located inside a building (the MS was 30 meters away from the entrance of the building). The serving cellular BS was located 200 meters away from the entrance of the building. The BS had LOS conditions with the entrance of the building and NLOS conditions with the MS. In the case of the two-hop MCN connection, the destination MN is located at the same location than the MS in the single-hop uplink HSUPA connection. It is important to note that the destination MN (D-MN in Figure 4-19) is actually the source of information since the field tests concentrates on uplink

transmissions. The D-MN in the two-hop MCN connection gains access to the BS through a hybrid MN (H-MN) separated 30 meters and located at the entrance of the building and experiencing LOS conditions with both the BS and the D-MN. The energy consumption was measured using Nokia's Energy Profiler application [97].

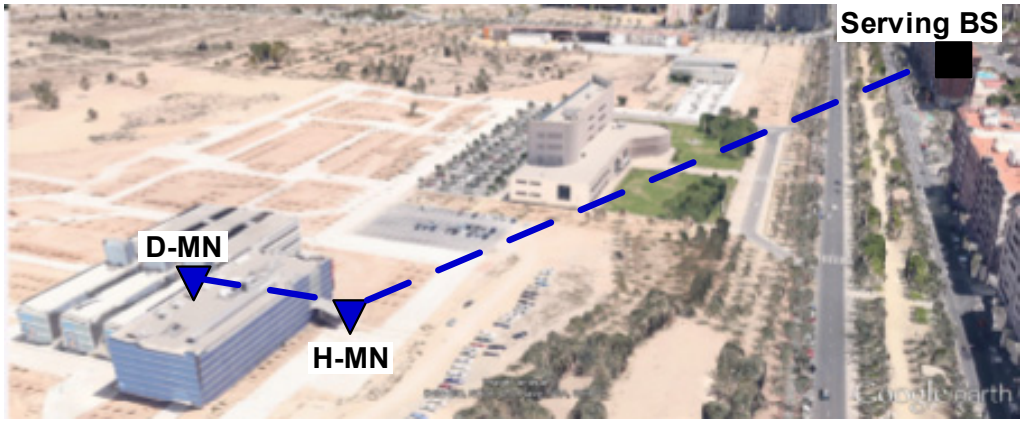

Figure 4-19. Field testing environment for the experimental demonstration of the energy efficiency benefits of MCNs using mobile relays.

4.2.6.2 Field Test Results

The conducted field tests aim at measuring the transmission energy consumption. Therefore, the measured energy consumption does not consider the energy consumed by screen-backlight, Bluetooth and other applications/processes running in the MS's background. The conducted field tests showed that the single-hop uplink HSUPA cellular transmission from the MS to the BS required on average a transmission power of 15 dBm and consumed 1.06 μJ/bit. On the other hand, the cellular transmission from the hybrid MN to the BS required on average a transmission power of -20 dBm and consumed on average 0.23 μJ/bit. The IEEE 802.11g D2D transmission from the MS to the hybrid MN consumed 0.29 μJ/bit. In this case, the IEEE 802.11g transmission was performed using a Nokia N97 handset in order to measure the energy consumption using Nokia's Energy Profiler application. As a result, the MCN connection only consumed 0.52 μJ/bit, which represents a 50% reduction in the consumed energy compared to the single-hop uplink HSUPA cellular transmission. Figure 4-20 shows the evolution of the energy consumption with time for the single-hop cellular link and the MCN link.

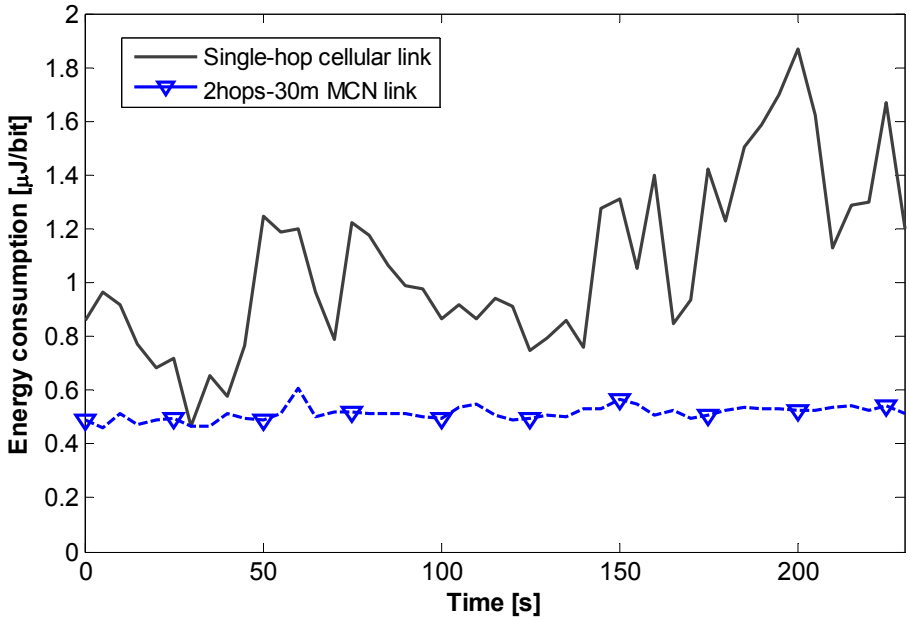

Figure 4-20. MCN capacity to reduce energy consumption.

4.3 Summary and Discussion

Multi-hop cellular networks have been proposed to overcome certain limitations of conventional cellular architectures in terms of QoS, capacity and energy consumption among others. However, to date, no study had ever experimentally evaluated the QoS benefits of multi-hop cellular networking using mobile relays. In this context, this thesis has presented the results of an extensive field testing campaign conducted to evaluate the performance of MCN networks, and the conditions under which they can overcome the limitations of conventional single-hop cellular systems. These results represent therefore the first field trials measurements that validate the potential of MCNs using mobile relays and D2D communications. The study has been conducted using HSPA and IEEE 802.11g for the cellular and D2D links of the MCN connection. However, the reported trends with regards to the benefits of MCNs with respect to single-hop cellular systems are likely to be maintained using different radio access technologies, as long as the MCN connection is upper-bounded by the cellular link between the H-MN and the BS. In particular, the conducted field tests have experimentally proved the capacity of MCN technologies to increase the QoS while crossing handover areas and at large distances to the serving BS. The obtained results have also demonstrated that the use of mobile relays and D2D communications in MCNs can help extend the cellular coverage area beyond its physical limits and from outdoor to indoor environments. Finally, the conducted field tests have also experimentally demonstrated the capacity of MCN networks using mobile relays to reduce the energy consumption.

5

Empirical Models of the MCN Communications Performance

The field tests reported in Chapter 4 have provided very valuable data to evaluate and characterize the performance of MCNs using D2D communications. Field test measurements can also be used to derive models useful to the community. In this context, this thesis presents a unique set of empirical models of the communications performance achieved with MCNs that utilize D2D communications. The models take into account the impact of distance, propagation/visibility conditions, number of hops and communication settings. The proposed models can help design, test and optimize in analytical and simulation studies, novel communications and networking protocols tailored for MCNs. For example, the derived models could help design:

- *Techniques to integrate MCNs in heterogeneous wireless networks.* Future cellular/wireless ecosystems will be characterized by the coexistence of multiple but complementary radio access technologies [58]. Mechanisms are necessary to select the most adequate technology at each point in time. The inclusion of MCNs in heterogeneous wireless networks needs to take into account both their benefit (e.g. QoS, capacity, and energy-efficiency) and cost (e.g. communications overhead). In this context, the models here presented could help identify the conditions under which MCNs would be a viable communications alternative in heterogeneous wireless networks.

- *Routing protocols for MCNs using D2D communications.* MCNs networks utilizing D2D communications require establishing a path between source and destination using intermediate mobile devices to forward the information [64], [98]. The selection of forwarding nodes can strongly influence the end-to-end performance. The proposed models could help select relay nodes that ensure reliable routes that guarantee the target end-to-end performance. The models can also be used to compare the performance of different routing protocols.

- *Opportunistic networking in MCNs using D2D communications.* Opportunistic networking mechanisms can be designed to exploit the delay tolerance of mobile data services in order to reduce the energy consumption and improve the network's capacity [99], [100]. These mechanisms need to determine the conditions and time instant at which mobile devices storing information could forward it to the final destination. The proposed models can be used to identify the conditions under which opportunistic networking schemes can help improve the operation and performance of MCNs.

The rest of this chapter is organized as follows. Section 5.1 describes the conditions under which the field trials used to derive the empirical models have been conducted. Section 5.2 proposes an empirical model for the communications performance of two-hop MCNs using D2D communications. The modeling process is then extended to a larger number of hops in Sections 5.3 and 5.4.

5.1 Experimental Conditions

5.1.1 Testing Environment

The field tests have been conducted in the city of Elche (Spain) using Orange's live network and the mHOP testbed. The field tests analyze the impact of propagation conditions, distance and number of hops, and communication settings on the performance of MCNs using D2D communications. Tests are conducted for different distances between the Hybrid Mobile Node (HN) and the Base Station (BS). During the tests, the mobile relays and the Destination Mobile Node (DN) vary their locations depending on the number of hops and the conditions under study. The field tests were conducted in a long and straight four-lane avenue close to the Miguel Hernandez University of Elche. The avenue ensured LOS conditions between the HN and the mobile relays when they were located at the same side of the avenue. The NLOS conditions were achieved locating the HN and the mobile relay nodes in opposite sidewalks of the

avenue, with vehicles continuously crossing over and dense vegetation in the avenue's median.

The tests start when all nodes execute a script that establishes the cellular connection from the HN to its serving BS, and the D2D links between the mobile relay nodes (see Section 3.3). During the tests, the *iperf* network testing tool [101] is used to transfer UDP packets from a server located at the UWICORE lab to the mobile DN. UDP traffic was used since it allows identifying the radio link that represents the bottleneck of a multi-hop transmission. This feature was very valuable to analyze separately the performance of various links of a MCN connection. *Iperf* allows specifying the size of the UDP packets that were set to the largest allowed Ethernet size at the network layer, i.e. 1548 bytes including headers. The cellular connection uses HSPA[7]. D2D links are established using IEEE 802.11g. This technology was selected over IEEE 802.11a to benefit from the better propagation conditions experienced at 2.4 GHz compared to 5 GHz [87]. IEEE 802.11g provides a theoretical maximum bit rate of 54 Mbps and defines a maximum transmission power of 27 dBm. However, the transmission power was limited to 19 dBm in compliance with the Spanish regulations (limit is established at 20 dBm). Unless otherwise specified, the data rate and transmission power in D2D links were dynamically modified based on the link quality conditions and the adaptive mechanisms implemented in the IEEE 802.11 cards' driver. Additional field tests were conducted fixing the data rate and the transmission power.

5.1.2 Performance Metric

The communications performance of the single-hop and MCN connections is measured in terms of the throughput experienced at the mobile DN. As it has been described in Section 4.1.1, the throughput performance (whether single-hop cellular or MCN) is here computed as the ratio between the measured throughput and the *usage* parameter in order to reduce the impact of the radio resource management policies on the conducted study. The selected metric results in that the MS located close to the BS would experience a higher throughput than the MS located at the cell edge (the empirical demonstration is presented in Section 4.1.1).

[7] LTE was not available in Elche at the time these field tests were conducted. The study defines the conditions to extend the derived models to other cellular technologies.

5.2 Two-Hop MCN Communications

This study considers the scenario illustrated in Figure 5-1. During the tests, the HN remains in a static position, while the DN moves away from the location of the HN until the D2D link with the HN is lost. Various locations of the HN at different distances from the BS have been analyzed. Field tests have been conducted for LOS and NLOS conditions between the HN and DN nodes.

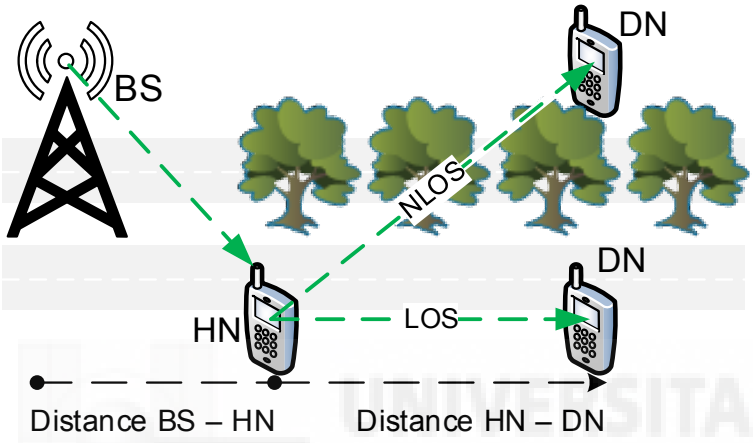

Figure 5-1. Testing environment for two-hop MCN communications.

5.2.1 Field Tests

Figure 5-2.a shows two examples of throughput experienced at the DN for the two-hop MCN connection when the HN-DN D2D link is characterized by LOS conditions. The HN was located 200 meters (left figure) and 500 meters (right figure) away from the BS. The throughput is depicted as a function of the distance between the HN and the mobile DN (the DN begins the tests close to the HN). The MCN throughput at the DN is first upper-bounded by the cellular performance of the BS-HN link ($\overline{Thr_{\mathrm{HN}}}$) for short HN-DN distances. The IEEE 802.11g throughput performance of the D2D link between HN and DN is high when the distance between the two nodes is small. In this case, the MCN throughput at the DN is upper bounded by the lower throughput experienced in the BS-HN cellular link. The performance at the mobile DN starts decreasing when the D2D link quality starts degrading as the distance between HN and DN increases (this distance will be referred to as critical distance). This happens at an approximate distance between HN and DN of 140-160 meters. From this distance onwards, the MCN throughput at the DN of the two-hop MCN connection is upper-bounded by the D2D performance. Similar trends are observed under NLOS conditions (Figure 5-2.b). The main difference lies in

the HN-DN distance from which the throughput at the mobile DN decreases (approximately 45 meters). This difference is explained by the more challenging NLOS propagation conditions between HN and DN, and the consequent lower received signal levels.

A large set of field trials have been conducted for various HN locations. In particular, trials have been conducted with the HN located 200, 500 and 800 meters away from the BS. Varying the location of the HN resulted in different average HSPA throughput levels at the HN ($\overline{Thr_{\mathrm{HN}}}$) and MCN throughput performance at the mobile DN. However, similar trends to that depicted in Figure 5-2 were always observed.

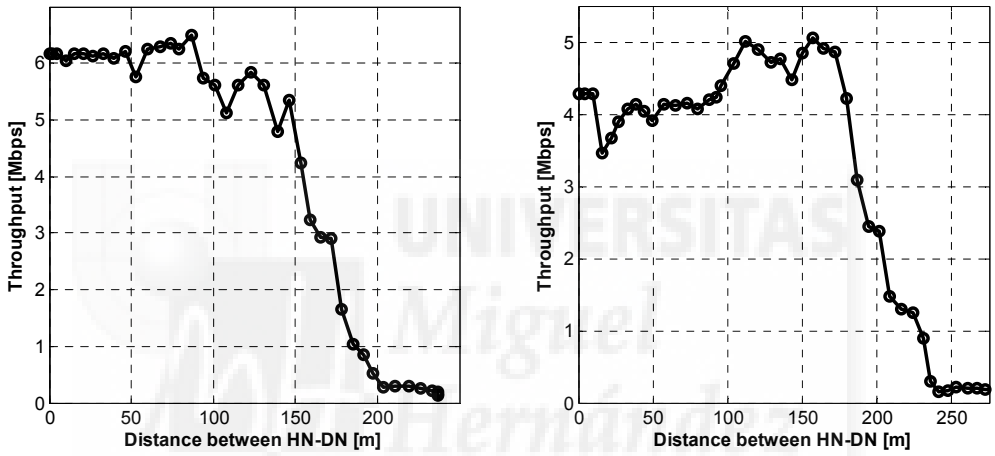

a) HN-DN link under LOS conditions.

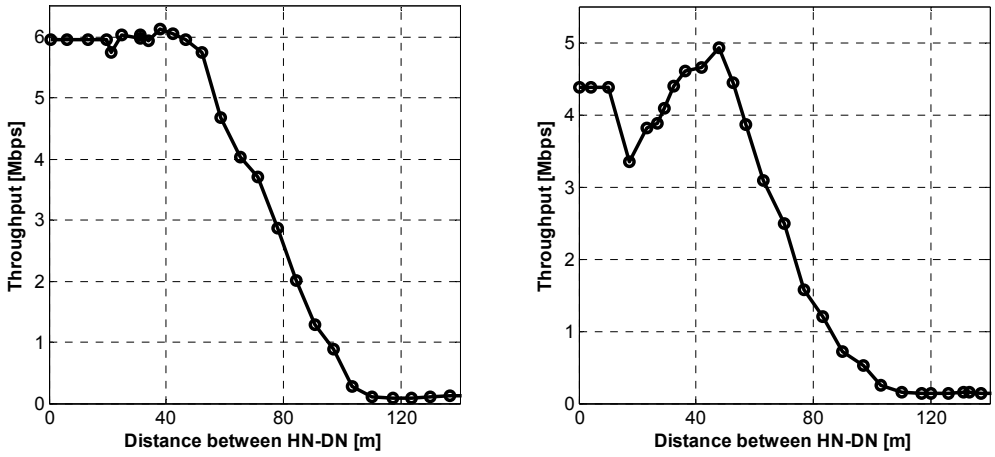

b) HN-DN link under NLOS conditions.

Figure 5-2. Two-hop MCN throughput at the mobile DN with HN located 200 (left) and 500 (right) meters away from the BS.

5.2.2 Modeling Functions

The first step to derive performance models for MCNs using D2D communications is to identify the functions that best fit the throughput measured at the mobile DN of the two-hop MCN connection. This process is based on an average processing of measurements like those reported in Figure 5-2. The performance depicted in Figure 5-2 has a symmetric S shape. There are several mathematical functions that can model such shape, and that can be grouped into three broad categories: sigmoid, piecewise-defined and exponential functions. A function from each of these categories has been selected based on the possibility to adequately fit its expression to the field measurements, and the simplicity of its expression for facilitating future analytical and simulation uses. More complex functions could also provide good fits, but the selected ones provide a reasonable trade-off between accuracy and analytical-simulation tractability. In particular, the following functions have been selected:

- The *Sig* function (equation (5-1)) has asymptotes y=*A* and y=*0*, and is symmetric at $d=p_2$ (*d* represents the distance in meters). The parameters *A* and p_1 determine the maximum slope ($A \cdot p_1/4$) of the *Sig* function at $d=p_2$.

$$Sig\left(p_1, p_2, d\right) = A \cdot \left[1 - \frac{1}{1+e^{-p_1 \cdot \left(d-p_2\right)}}\right], \ \forall d \in \{0,...,M\} \tag{5-1}$$

To calculate the distance *d* at which the *Sig* function decreases below *y=A* (critical distance), it is first necessary to define the maximum curvature point or upper knee (K_u) of the *Sig* function [102]. This parameter can be calculated using the curvature (*Curv*) function:

$$Curv\left(d\right) = \frac{Sig''(d)}{\left(1+(Sig'(d))^2\right)^{3/2}} = \frac{\frac{A \cdot p_1^{\,2} \cdot t \cdot \left(1-t\right)}{\left(1+t\right)^3}}{\left(1+\left(\frac{-A \cdot p_1 \cdot t}{(1+t)^2}\right)^2\right)^{3/2}} \tag{5-2}$$

Where $t=exp(-p_1 \cdot (d-p_2))$. Computing the critical distance also requires defining the utility (*U*) function:

$$U\left(d\right) = \begin{cases} Sig\left(d\right) - P\left(d\right) & d \le K_u \\ Sig\left(d\right) & d > K_u \end{cases} \tag{5-3}$$

In equation (5-3), *P(d)* is a monotonically increasing function ($P(d)=\alpha \cdot (d-K_u)$) that represents the penalty assigned to $d \le K_u$. The critical distance is then obtained by setting *U*'(d)=0 and solving the equation $Sig'(d)=P'(d)=\alpha$ where $|\alpha| < |Sig'(K_u)|$.

- The *Part* function (equation (5-4)) is defined by the asymptotes y=*A* and y=*0* when *d* is smaller than p_1 and higher than p_2 respectively. Otherwise, *Part* function is characterized by a slope equal to ($-A/(p_2-p_1)$). The *Part* function is symmetric in $d=(p_2-p_1)/2$ and its critical distance is located at p_1.

$$Part(p_1,p_2,d)=\begin{cases}A & d<p_1\\ k\cdot\left(\frac{1}{d}-\frac{1}{p_2}\right) & p_1\le d<p_2\\ 0 & p_2\le d\end{cases},\quad \forall d\in\{0,\ldots,M\} \tag{5-4}$$

  where $k=A/(1/p_1-1/p_2)$.

- The *Exp* function (equation (5-5)) is defined as:

$$Exp(p_1,p_2,d)=A\cdot e^{-(p_1\cdot d)^{p_2}},\forall d\in\{0,\ldots,M\} \tag{5-5}$$

  Following a similar analysis to that conducted for the *Sig* function, it is possible to determine the critical distance for the *Exp* function.

The three selected functions are defined by the parameters *d*, *A*, p_1 and p_2. When applied to modeling the throughput of the MCN connection, *d* is defined as the distance between the HN and the mobile DN. *A* represents the average cellular throughput measured at the HN ($\overline{Thr_{\mathrm{HN}}}$) for distances smaller than the critical distance. Finally, p_1 and p_2 are the variables or fitting parameters that modify the characteristics of the S-shaped functions:

- Length of the upper asymptote, i.e. the distance at which the MCN throughput starts decreasing or critical distance.
- Slope of the curve, i.e. how fast the MCN throughput decreases with the distance from the critical distance point.
- The start of the lower asymptote, i.e. the distance at which the MCN throughput is negligible because the D2D connectivity is lost.

Curve fitting is one of the common techniques used to derive the fitting parameters of a modeling function from empirical data. This method seeks minimizing the residue/difference between the measured data and the proposed modeling function. Different estimators can be used to calculate the residue. The least-squares estimator produces the maximum-likelihood estimate of the parameters when the errors are distributed along the modeling function [103], which is actually the case for the MCN

field measurements here reported. In this context, two different curve fitting methods using least-squares estimators are here used to derive the (p_1, p_2) parameters that best fit the selected functions (*Sig, Part* and *Exp*) to the MCN throughput measured at the DN.

5.2.3 Least-Squares Parameters Estimation

The Least-Squares Parameter Estimation (LSPE) technique seeks minimizing the residue *e*:

$$e_j = \sqrt{\frac{\sum_{d_1}^{d_M} \left(f_j(p_1, p_2, d) - g(d) \right)^2}{M}} \quad , j \in \{Sig, Part, Exp\} \tag{5-6}$$

where $f_j(p_1, p_2, d)$ represents the modeling functions, and *g(d)* the measured data (in this case, the MCN throughput experienced at the mobile DN[8]). LSPE derives the fitting parameters $(p^i_1, p^i_2)_j$ that minimize the residue e^i_j for each of the selected functions *j* ($j \in$ {*Sig*, *Part*, *Exp*}) and the measurement test *i*.

Figure 5-3 depicts an example showing that LSPE is capable to achieve a good match between the MCN throughput at the mobile DN and the selected functions under LOS and NLOS conditions. The measurements analyzed in Figure 5-3 correspond to those reported in Figure 5-2 with the HN located 200 meters away from the BS. The LSPE scheme has been applied to all field measurements, which results in a set of fitting parameters $(p^i_1, p^i_2)_j$ and residues e^i_j ($\forall\ i \in \{1, \ldots, T\}$, with *T* representing the number of conducted field tests (in total, more than 100 field measurements were conducted). For each of the selected functions, the results are grouped based on the visibility conditions between the HN and the DN, and the different locations of the HN. The average of the resulting fitting parameters is shown in Table 5-1. Clear differences are appreciated between the (p_1, p_2) parameters obtained under LOS and NLOS conditions. However, only small differences are obtained for the different locations of the HN despite the fact that the HN throughput varies with the distance to the BS (Figure 5-4). For example, the difference is smaller than 10 meters for the *Part* function (Table 5-1). As a result, the fitting (p_1, p_2) parameters for the different locations of the static HN have been grouped. Table 5-2 shows the resulting average fitting parameters (p_1, p_2) under LOS and NLOS conditions for each of the selected functions. Table 5-1 and Table 5-2 also depict the average residues e^i_j ($\langle e \rangle$) between the selected functions (when using the derived fitting

[8] The measurements are averaged over time periods of 1s since the GPS has an updating rate of 1 Hz, and are processed using a simple moving average scheme with 5 samples [104].

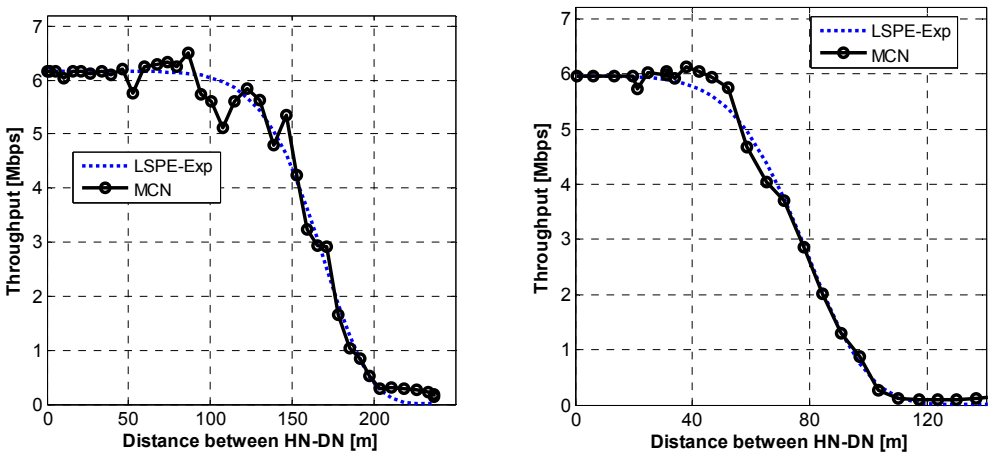

a) LSPE fitting with *Exp* function.

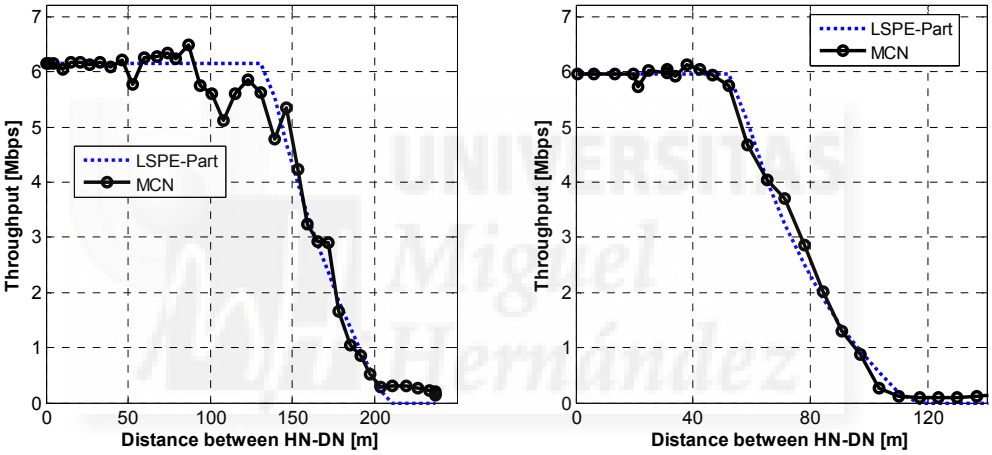

b) LSPE fitting with *Part* function.

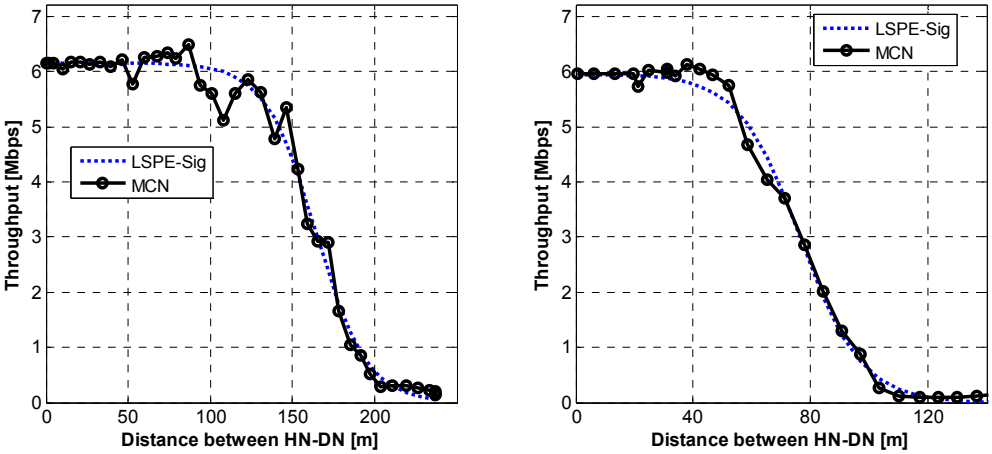

c) LSPE fitting with *Sig* function.

Figure 5-3. LSPE fitting of the two-hop MCN throughput measured at the mobile DN as it moves away from the location of the HN under LOS (left) and NLOS (right) conditions.

parameters shown in Table 5-1 and Table 5-2) and the measured data under LOS and NLOS conditions. The reported results show that the *Sig* function provides the lower differences with the measured data under LOS and NLOS conditions.

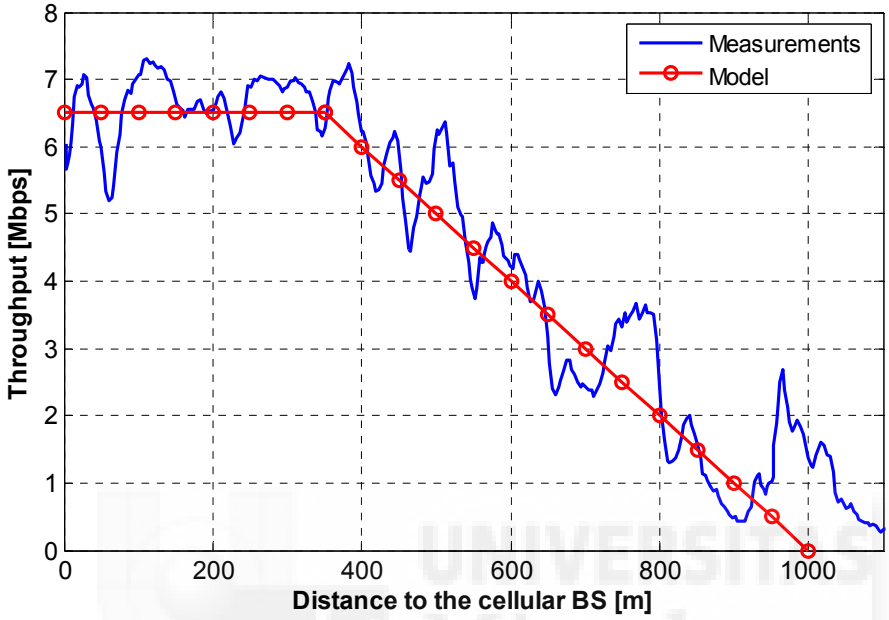

Figure 5-4. HSPA throughput.

Table 5-1. Two-hop MCN LSPE (p_1, p_2) as a function of LOS/NLOS conditions and distance of HN to the Serving BS (in meters).

			Function					
			Exp		***Part***		***Sig***	
			(p_1, p_2)	**⟨e⟩ [Mbps]**	**(p_1, p_2)**	**⟨e⟩ [Mbps]**	**(p_1, p_2)**	**⟨e⟩ [Mbps]**
LOS	**Distance BS-HN**	200	(0.005, 11.46)	0.146	(156.5, 234.6)	0.146	(0.107, 177.6)	0.140
		500	(0.005, 13.8)	0.119	(162.1, 232.5)	0.114	(0.12, 194.9)	0.107
		800	(0.005,13.98)	0.175	(151.7, 229.2)	0.143	(0.12, 179.8)	0.142
NLOS	**Distance BS-HN**	200	(0.012, 6.44)	0.061	(58.9, 102.6)	0.057	(0.13, 75.96)	0.055
		500	(0.011, 6.57)	0.119	(62.4, 108.2)	0.114	(0.10, 85.25)	0.112
		800	(0.012,6.9)	0.078	(59.55, 107)	0.074	(0.12, 78)	0.074

Table 5-2. Two-hop MCN LSPE (p_1, p_2) as a function of LOS/NLOS conditions.

	LOS		NLOS	
Function	**(p_1, p_2)**	**⟨e⟩ [Mbps]**	**(p_1, p_2)**	**⟨e⟩ [Mbps]**
Exp	(0.005, 12.05)	0.129	(0.012, 6.53)	0.088
Part	(157.9, 230.8)	0.128	(60.6, 113.8)	0.089
Sig	(0.12, 186.99)	0.126	(0.12, 79.67)	0.087

5.2.4 Linear Programming

The fitting (p_1, p_2) parameters can also be derived using Linear Programming (LP) techniques. LSPE calculated the fitting parameters by averaging the $(p^i_1, p^i_2)_j$ values. On the other hand, LP techniques derive the fitting parameters using all the measurements obtained under similar conditions (e.g. LOS or NLOS conditions). To this aim, LP techniques seek optimizing a linear objective function subject to a set of constraints. This thesis analyzed three common objective functions that are intended to provide the fitting parameters $(p_1, p_2)_j$ that minimize the residue e_j[9] between the selected functions $j \in$ {*Sig*, *Part*, *Exp*} and the measured data (i.e. the MCN throughput experienced at the mobile DN):

- *Minimize the maximum (min-max) of the residues*. The first LP scheme derives the fitting parameters $(p_1, p_2)_{min\text{-}max}$ that minimize the maximum residue (e) between the selected function ($j \in$ {*Sig*, *Part*, *Exp*}) and the entire set of measurements obtained under similar conditions ($i \in$ {1,…,N}). The objective function can be expressed as:

$$\min \max_{i\in\{1,\ldots,N\}} e^i_j \tag{5-7}$$

  Equation (5-7) must be expressed as a linear equation to solve it using linear programming techniques. To this aim, a new real variable z, equal to z=max e^i_j, is defined. The objective function and its constraints can now be expressed as:

$$\min \quad z \;;\;\; s.t: e^i_j \le z \;\; \forall i \in \{1,\ldots,N\} \;;\;\; p_1, p_2, z \in \Re \tag{5-8}$$

- *Minimize the sum (min-sum) of the residues*. The second LP scheme derives the fitting parameters $(p_1, p_2)_{min\text{-}sum}$ that minimize the sum of the residues (e) between the selected function ($j \in$ {*Sig*, *Part*, *Exp*}) and the entire set of measurements obtained under similar conditions ($i \in$ {1,…,N}). The *min-sum*

[9] e_j has also been computed following the mean of the least-squares estimator reported in equation (5-6).

objective function shown in equation (5-9) is already linear, and no additional changes are required.

$$\min \quad \left(\sum_{i=1}^{N} e_j^i\right); \quad s.t: p_1, p_2 \in \Re \tag{5-9}$$

- *Minimize the multiplication (min-mul) of the residues*. The third LP scheme computes the fitting parameters $(p_1, p_2)_{min\text{-}mul}$ that minimize the multiplication of the residues (e) between the selected function ($j \in \{Sig, Part, Exp\}$) and the entire set of measurements obtained under similar conditions ($i \in \{1,\ldots,N\}$). In this case, the objective function is expressed as:

$$\min \quad \left(\prod_{i=1}^{N} e_j^i\right) \tag{5-10}$$

Since equation (5-10) is not a linear equation, the following equivalent objective function is selected:

$$\min \quad \left(\sum_{i=1}^{N} \ln\left(1+e_j^i\right)\right); \quad s.t: p_1, p_2 \in \Re \tag{5-11}$$

Table 5-3 shows the (p_1, p_2) parameters obtained using the *min-max*, *min-sum* and *min-mul* LP techniques. The results only differentiate between LOS and NLOS conditions between the HN and the mobile DN following the observations reported in the LSPE analysis. Table 5-3 also shows the average residues e_j^i ($\langle e \rangle$) obtained with each of the LP schemes. The depicted results show that the *Sig* function minimizes $\langle e \rangle$ in most cases.

Table 5-3. Two-hop MCN LP (p_1, p_2) as a function of LOS/NLOS conditions.

Function		**LOS**		**NLOS**	
		(p_1, p_2)	**$\langle e \rangle$ [Mbps]**	**(p_1, p_2)**	**$\langle e \rangle$ [Mbps]**
min-max	***Exp***	(0.0047, 4.2)	0.174	(0.011, 4.6)	0.105
	Part	(153.5, 251)	0.174	(59, 144.5)	0.113
	Sig	(0.03, 194)	0.174	(0.06, 85)	0.108
min-sum	***Exp***	(0.0051, 5.6)	0.137	(0.012, 5.2)	0.093
	Part	(141.5, 244.5)	0.138	(56, 113)	0.094
	Sig	(0.05, 180.5)	0.136	(0.09, 77.5)	0.091
min-mul	***Exp***	(0.0053, 6)	0.126	(0.012, 5.2)	0.083
	Part	(141, 240.5)	0.128	(56, 111.5)	0.084
	Sig	(0.05, 177)	0.125	(0.11, 77)	0.081

5.2.5 Two-hop MCN Performance Models and Validation Tests

Two different methods (LSPE and LP) have been used to derive the (p_1, p_2) parameters that best fit the selected functions (*Exp, Part* and *Sig*) to model the MCN throughput measured at the DN. LSPE derives fitting parameters for each measurement set, and averages them all to obtain the final (p_1, p_2) values. The LSPE averaging process reduces the impact of the measurement data variations that are usually observed in field tests. The impact of these variations is higher in the LP case since LP techniques take into account the entire set of measurement at once. The *min-max* LP technique derives the fitting parameters that minimize the maximum distance (residue) to the entire set of measurements. However, only the lowest and the highest fitting parameters have an impact on the *min-max* LP optimization problem, which may explain the largest average residues reported in Table 5-3 for the *min-max* scheme. The *min-sum* and *min-mul* LP schemes are also influenced by measurement variations, but they only cause deviations from the general trend. These variations have a slightly larger effect in the case of the *min-sum* scheme since *min-mul* mitigates large residues (e^i_j) using a logarithmic function in its objective function.

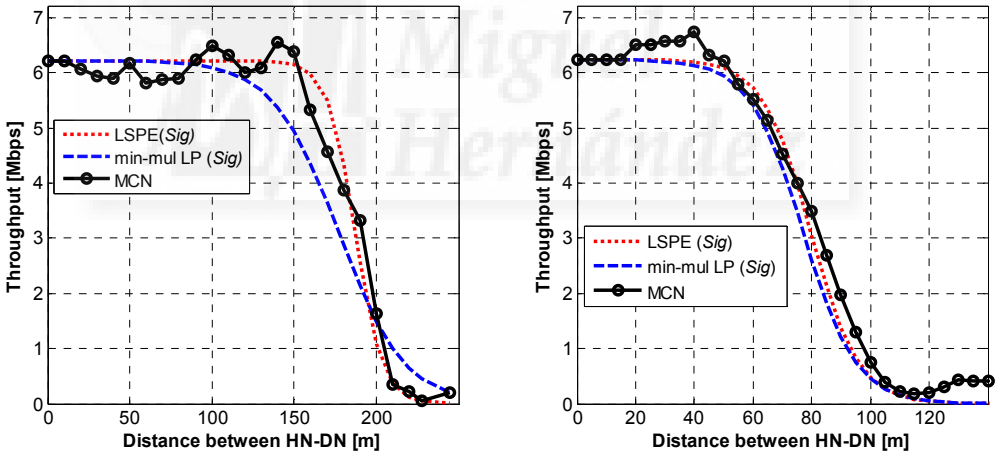

a) LOS conditions b) NLOS conditions

Figure 5-5. Two-hop MCN throughput measured at the DN as it moves away from the location of the HN under LOS (a) and NLOS (b) conditions. The measurements were obtained using a different serving BS as that used for Figure 5-2. The HN was located 200 meters away from the BS. The figure also shows the *Sig* functions derived using LSPE and *min-mul* LP schemes.

The results reported in Table 5-2 and Table 5-3 show that the *Sig* function minimizes the average residue ⟨*e*⟩ for the LSPE and LP techniques under LOS and NLOS conditions[10]. The *min-mul* LP scheme results in the lower residue. Additional tests were carried out due to the small differences observed between LSPE and LP schemes (except for *min-max*). The additional tests were carried out in a different location with a different serving BS. Figure 5-5 shows examples of the two-hop MCN throughput measurements obtained at DN in these additional tests (the HN was located 200 meters away from the BS in these examples; additional tests with the HN located at different distances to the BS were also conducted). Figure 5-5 also compares the measured throughput with the *Sig* models obtained using the fitting parameters derived using the LSPE and *min-mul* LP schemes. The figure shows that the *Sig* functions provide a good fit with the measured performance despite changing locations and serving BS. Table 5-4 compares the average residue e_i (⟨*e*⟩) obtained with the LSPE and *min-mul* LP schemes for all the additional tests conducted with a different serving BS. The reported ⟨*e*⟩ values for LSPE are in line with those listed in Table 5-2. However, Table 5-4 shows that *min-mul* LP derived fitting parameters perform worse when using a different BS. This can be appreciated when comparing the reported ⟨*e*⟩ values in Table 5-3 and Table 5-4. As a result, this study proposes to model the two-hop MCN throughput performance experienced at a mobile DN using the *Sig* function in equation (5-12) with the LPSE fitting parameters reported in Table 5-2 for LOS and NLOS conditions:

$$\text{MCN-MR } Thr\left(p_1, p_2, d\right)_{\text{2-hop DN}} = \overline{Thr_{\text{HN}}} \cdot \left[1 - \frac{1}{1 + e^{-p_1 \cdot \left(d - p_2\right)}}\right] \tag{5-12}$$

where *d* represents the HN-DN separation distance. For these fitting parameters, the critical distance is 156 meters and 52 meters under LOS and NLOS conditions respectively. The $\overline{Thr_{\text{HN}}}$ parameter represents the average HSPA throughput measured at the HN. Figure 5-4 reports HSPA throughput measurements at a node located at different distances to the BS. The throughput depends on the actual position of the HN. Using this figure, it is possible to model the $\overline{Thr_{\text{HN}}}$ throughput parameter as follows:

$$\overline{Thr_{\text{HN}}}(d) = \begin{cases} 6.5 & d < 350m \\ -0.01 \cdot d + 10 & d \geq 350m \end{cases} \tag{5-13}$$

[10] The only exception is the *min-max* LP scheme, but this scheme is discarded since it results in the higher residue values.

with *d* representing the distance between the HN and the serving BS. Those interested in using the two-hop MCN throughput performance model proposed in equation (5-12) could use the $\overline{Thr_{\mathrm{HN}}}$ measurements depicted in Figure 5-4 and modeled in equation (5-13), or use their own cellular measurements. It is important emphasizing that the derived model can be used for different locations of the HN since as previously discussed the (p_1, p_2) parameters do not depend on $\overline{Thr_{\mathrm{HN}}}$.

Table 5-4. LSPE and LP Comparison.

Function	⟨*e*⟩ [Mbps]	
	LOS	NLOS
LSPE (*Sig*)	0.132	0.102
***min-mul* LP (*Sig*)**	0.158	0.110

5.2.5.1 IEEE 802.11g Fixed Transmission Mode

The previous models were obtained using the default configuration of the IEEE 802.11g cards used in the mHOP testbed. This configuration adapts the transmission parameters (data rate and transmission power) based on the experienced link quality conditions. The operation of these adaptive mechanisms is driver-dependent (the employed IEEE 802.11g cards use the Ath9k driver), and detailed information about their implementation is generally not provided. In this context, it is of interest checking whether the two-hop MCN throughput performance models follow similar trends when operating with fixed transmission power levels and data rates. Additional field tests have therefore been conducted under similar conditions as those reported in previous sections and illustrated in Figure 5-2. The HN remains static (again, different locations of the HN were also tested with similar results), while the DN moves away from the location of the HN under LOS and NLOS conditions. The IEEE 802.11g transmission power was fixed to 19 dBm (19 dBm was previously the power limit, but the actual transmission power was dynamically modified by the IEEE 802.11 cards). The tests were conducted using the 54 Mbps and 48 Mbps IEEE 802.11g data rates. The obtained measurements showed indeed similar trends as those observed when the IEEE 802.11g adaptive scheme was active. As a result, the same LPSE curve fitting process using the *Sig* function has been applied to these measurements. Figure 5-6 represents the derived model with the obtained fitting parameters and the average residue (*p1*, *p2*, ⟨*e*⟩) for each plotted configuration. The MCN throughput curves have been obtained using the model presented in equation (5-12). Following the procedure described in Section 5.2.2, it is possible to calculate the critical distance, or distance at which the MCN throughput

operates below the $\overline{Thr_{\mathrm{HN}}}$. The analysis reveals that when the mobile nodes communicate using the 54 Mbps data rate, the critical distance is equal to 125 (LOS) and 50 (NLOS) meters. The 48 Mbps data rate increments the critical distance to 143 (LOS) and 65 (NLOS) meters. In addition, the decreasing slope of the MCN throughput at the DN (related with the p_1 parameter) is greater when the mobile nodes use the 54 Mbps data rate than when using the 48 Mbps one. This is due to the more robust modulation and coding scheme used by the 48 Mbps data rate. When activating the IEEE 802.11g adaptive schemes, the critical distance was equal to 156 meters and 52 meters for the LSPE *Sig* function under LOS and NLOS conditions respectively. It is interesting noting that the critical distance with active adaptive schemes is higher for LOS conditions than when using the 48 Mbps data rate, but is smaller under NLOS conditions. The different pattern could be due to the challenging NLOS propagation conditions that difficult a successful operation of the IEEE 802.11g adaptive schemes.

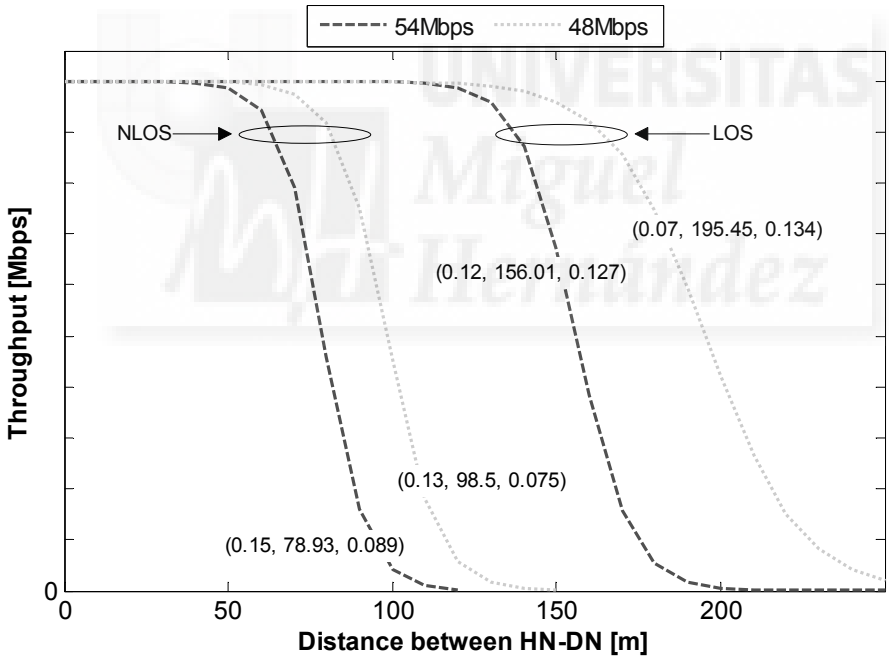

Figure 5-6. Two-hop MCN throughput models at the DN with fixed IEEE 802.11g transmission modes for LOS and NLOS conditions and a transmission power of 19 dBm. The figure shows for each configuration the fitting parameters and the average residue (*p1*, *p2*, ⟨*e*⟩).

5.2.6 D2D Link Level Modeling in MCN Communications

The communications performance of MCN systems has been shown to strongly depend on the conditions experienced between mobile relays. It is therefore of interest to analyze and characterize the D2D communications between the HN and the DN in the two-hop MCN scenario illustrated in Figure 5-1. The conducted field tests focused on downlink MCN transmissions from the BS to the DN. In this context, it is important remembering that the MCN performance is upper-bounded by the cellular throughput, and so is the D2D IEEE 802.11 throughput performance. The D2D communications characterization and modeling focuses then on the IEEE 802.11g Data Rate, Packet Error Ratio (PER) and Receive Signal Strength Indicator (RSSI). Other studies have previously modeled different aspects of IEEE 802.11 communications. For example, [105] characterizes the performance of Minstrel (the algorithm implemented on the mHOP IEEE 802.11 nodes to select the data rate) for different transmission power configurations and fixed separation distances between the IEEE 802.11g devices. PER and RSSI IEEE 802.11 models can be found in the literature, although PER models are mainly derived as a function of the packet-length and/or physical-level metrics (e.g. Signal to Noise Ratio –SNR) [106][107]. The IEEE 802.11 D2D models here presented complement existing models by modeling IEEE 802.11 D2D communications as a function of the distance between mobile relays. Characterizing the D2D communications as a function of the distance between mobile relays can facilitate the use of the models in analytical and simulation-based studies.

5.2.6.1 D2D IEEE 802.11g Data Rate

The IEEE 802.11g data rate represents the transmission mode used in the ad-hoc D2D communication between the static HN and the mobile DN. IEEE 802.11g defines twelve possible combinations of modulation and coding schemes that result in the following set of eligible data rates: {54, 48, 36, 24, 18, 12, 9, 6; 11, 5.5, 2, 1} Mbps. As previously mentioned, the IEEE 802.11 card's Ath9k driver dynamically selects the IEEE 802.11g data rate based on the link quality conditions. Figure 5-7 shows, for one of the conducted tests, the measured data rate when the IEEE 802.11g D2D link between the HN and mobile DN operates under LOS and NLOS conditions. The data rate is depicted as a function of the distance between the HN and the mobile DN. The depicted results show that the IEEE 802.11g data rate is initially set to 54 Mbps. However, more robust transmission modes are used with the increasing distance between the HN and the DN. The more challenging NLOS propagation conditions result in the adaptation of the data rate at smaller distances, which is consistent with the earlier MCN throughput reduction depicted in Figure 5-2 under NLOS conditions. The extracted measurements show

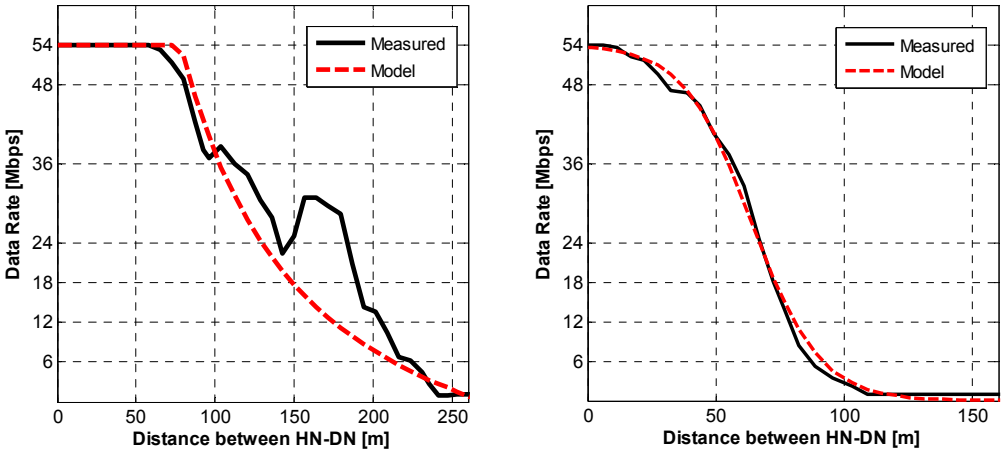

a) LOS conditions between HN-DN

b) NLOS conditions between HN-DN

Figure 5-7. IEEE 802.11g data rate.

similar properties to the S-shaped mathematical functions used to model the communications performance of two-hop MCNs that utilize D2D communications. As a result, the LSPE curve fitting process using the *Exp*, *Part* and *Sig* functions has also been applied to derive the IEEE 802.11g data rate models for D2D communications. The smoother pass from the upper asymptote to the slope of the curve (Figure 5-7.b) results in that the *Sig* function provides the best match with the IEEE 802.11g data rate under NLOS conditions. The IEEE 802.11g data rate model for D2D communications is therefore represented in equation (5-14) with the fitting (p_1, p_2) parameters equal to (0.076, 63.97) (resulting in an average residue equal to 1.3 Mbps). The measurements reported in Figure 5-7.a for LOS conditions were better fitted with the *Part* function. As a result, the IEEE 802.11g data rate under LOS conditions is modeled by equation (5-15), with the fitting parameters being equal to (78.47, 270.85) (resulting in an average residue equal to 3.95 Mbps). In both models (equations (5-14) and (5-15)), *d* represents the distance between the HN and the DN, and the upper asymptote (*A*) is set to 54 Mbps. The derived models are also depicted in Figure 5-7 showing an adequate match with the measurements.

$$DataRate_{NLOS}(p_1, p_2, d) = 54 \cdot \left[1 - \frac{1}{1 + e^{-p_1 \cdot (d - p_2)}} \right] \quad (5\text{-}14)$$

$$DataRate_{LOS}(p_1, p_2, d) = \begin{cases} 54 & d < p_1 \\ k \cdot \left(\frac{1}{d} - \frac{1}{p_2} \right) & p_1 \le d < p_2 \\ 0 & p_2 \le d \end{cases} \quad (5\text{-}15)$$

5.2.6.2 D2D IEEE 802.11g Packet Error Ratio

The PER has been measured in the HN as the ratio between the data packets retransmitted and the total number of data packets transmitted (including retransmissions) [106]. A data packet retransmission is required if the HN does not receive an ACK from the DN. This can be caused by an error in the transmission of the data packet from the HN to the DN or an error in the ACK sent from the DN to the HN. An example of the PER measured at the HN as a function of the separation distance between the HN and DN is shown in Figure 5-8. The obtained measurements show that the PER augments with the distance (both for LOS and NLOS conditions) even if more robust data rates are being used with increasing distances (Figure 5-7). The upper PER limit is reached at the distance at which the MCN throughput measured at the DN is negligible (Figure 5-2). The PER modeling analysis has considered the original (not symmetric) S shape of the *Sig*, *Part* and *Exp* functions and the LSPE curve fitting technique. The conducted fitting process resulted in the *Sig* function providing the lower error between the theoretical functions and the measured data both under LOS and NLOS conditions. The PER is therefore model as shown in equation (5-16). The fitting (p_1, p_2) parameters are equal to (0.019, 115.15) under LOS conditions (resulting in an average residue of 9.58%) and equal to (0.0475, 54.38) under NLOS conditions (resulting in an average residue of 5.01%). The *d* parameter in equation (5-16) represents the distance between the HN and the mobile DN. The measured upper PER limit/asymptote (U_{PER}) is on average 75% both under LOS and NLOS conditions. The derived models are also depicted in Figure 5-8. The worse IEEE 802.11g D2D performance under NLOS conditions is highlighted by the higher value of p_1 and the lower value of p_2. This fact also explains the lower critical distance of the MCN throughput under NLOS conditions.

$$PER(p_1, p_2, d) = \frac{U_{PER}}{1 + e^{-p_1 \cdot (d - p_2)}} \quad (5\text{-}16)$$

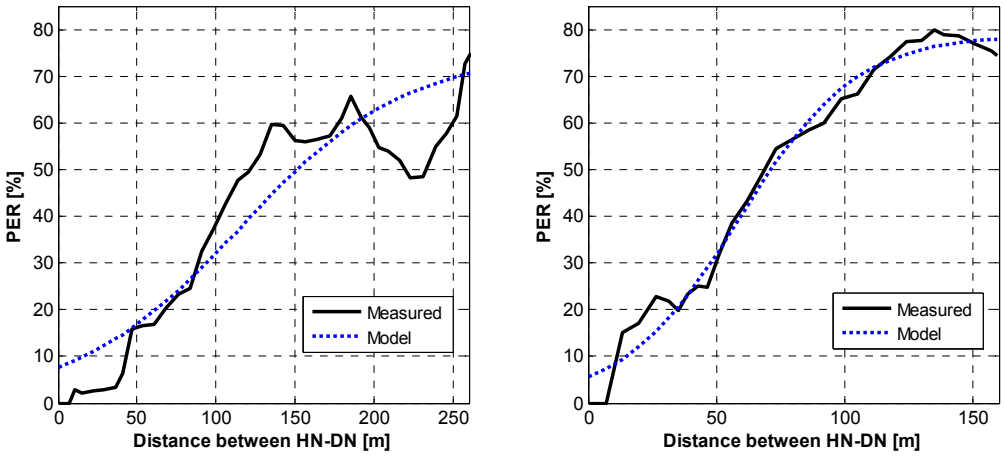

a) LOS conditions between HN-DN b) NLOS conditions between HN-DN

Figure 5-8. IEEE 802.11g PER.

5.2.6.3 D2D IEEE 802.11g Received Signal Strength Indicator

The RSSI represents the signal strength at which IEEE 802.11g data packets are correctly received at the DN (Figure 5-9). It is common to represent the average strength of the RSSI in dBm as a log-distance function (equation (5-17)) [107][108], where $RSSI_o$ is the RSSI at a reference distance (d_o) and α is the RSSI exponent. The fitting ($RSSI_o$, α) parameters derived using the LSPE curve fitting technique are equal to (-37.95, 1.73) for LOS conditions, with an average residue of 4.07 dBm. The fitting parameters under NLOS were found to be equal to (-34.88, 2.21), with an average residue of 3.95 dBm. For both scenarios, d_o is set to 1 meter. Using equation (5-17), it is possible to detect the RSSI levels characterizing the HN-DN critical distance. For example, in the case of a D2D link (two-hop MCN with adaptive transmission schemes) under LOS conditions, the RSSI level at which the throughput is below $\overline{Thr_{\mathrm{HN}}}$ is found to be equal to -75.8 dBm. Under NLOS conditions, this value is equal to -72.8 dBm.

$$RSSI\left(RSSI_0, \alpha, d\right) = RSSI_0 - 10 \cdot \alpha \cdot Log\left(d / d_0\right) \tag{5-17}$$

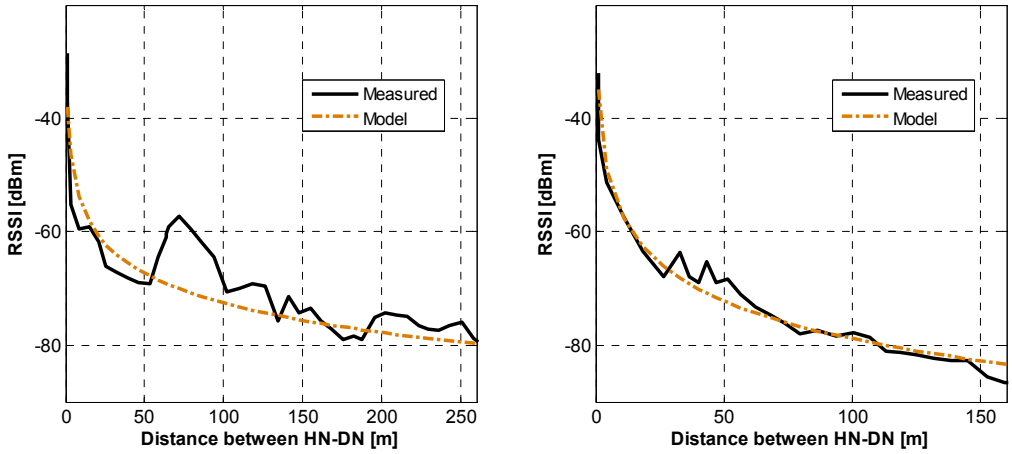

a) LOS conditions between HN-DN b) NLOS conditions between HN-DN

Figure 5-9. IEEE 802.11g RSSI.

5.2.6.4 IEEE 802.11g Fixed Transmission Mode

Using equations (5-16) and (5-17), it is also possible to model the D2D link level communications for a two-hop MCN connection using IEEE 802.11g fixed transmission modes. The resulting model parameters are summarized in Table 5-5. As it can be appreciated, using the data rate and transmission power configuration (54 Mbps-19 dBm) results in higher PER values than using the (48 Mbps-19 dBm) configuration; this is reflected in the higher values of U_{PER} and p_1. The use of adaptive schemes for the IEEE 802.11g D2D connection results in lower U_{PER} and p_1 values. Fixing the transmission power to 19 dBm results in that the RSSI fitting parameters do not show significant differences under similar propagation conditions (despite using a different data rate). However, the worse NLOS conditions are captured in the RSSI fitting parameters. The comparison with the RSSI fitting parameters obtained with adaptive schemes reveals the

Table 5-5. PER and RSSI (p_1, p_2) parameters with fixed IEEE 802.11g transmission modes for LOS and NLOS conditions and transmission power of 19dBm.

Function		LOS		NLOS	
		(p_1, p_2)	$\langle e \rangle$	(p_1, p_2)	$\langle e \rangle$
PER	54 Mbps	(0.043, 123.4), U_{PER}=95.2%	6.4%	(0.068, 48), U_{PER}=93.24%	6.7%
	48 Mbps	(0.041, 137), U_{PER}=91.78%	6.8%	(0.051, 54), U_{PER}=88.67%	7.9%
RSSI	54 Mbps	(-30.5, 1.69)	3.67 dBm	(-33.3, 2.17)	3.88 dBm
	48 Mbps	(-29.9, 1.75)	3.66 dBm	(-34.6, 2)	3.8 dBm

higher signal strength levels measured when fixing the transmission power to 19 dBm. Although 19 dBm is the power limit when using adaptive schemes, the transmission power is dynamically modified based on the link quality conditions.

5.3 Three-Hop MCN Communications

This section derives models of the communications performance of three-hop MCN in the scenario illustrated in Figure 5-10. The 3-hops scenario considers the presence of an additional mobile node (Intermediate Node, IN) located between the HN and the DN. The mobile IN acts as a relay and forwards the packets coming from the HN to the DN through its IEEE 802.11g D2D link. The HN-IN and IN-DN IEEE 802.11g D2D links have been set up by modifying the routing tables of each mobile node. The HN remains in a static position during the tests, whereas the DN is a mobile node. The IN would be either static or mobile. The three-hop MCN communication models need to take into account the possibility that the HN-IN and IN-DN links operate under LOS or NLOS conditions.

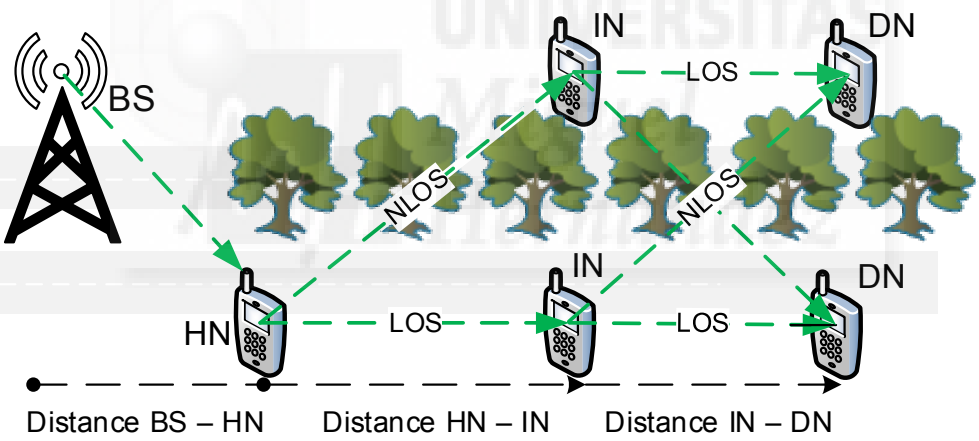

Figure 5-10. Testing environment for three-hop MCN communications.

5.3.1 Field Tests

The three-hop MCN performance observed at the DN does not only depend on the real-time data forwarding process from the HN to the IN, but also on the forwarding capability of the IN. In this context, it is important that the field tests, and consequent communications performance models, thoroughly analyze the impact of the mobile IN on the end-to-end MCN performance. To this aim, this section analyzes the MCN performance at the IN and the DN under different configurations varying the propagation conditions (LOS and NLOS) and the distance between mobile nodes.

5.3.1.1 MCN Throughput at the IN

The first tests analyzed the MCN performance at the IN under LOS and NLOS conditions with the HN. During the tests, the DN is located in the same sidewalk as the IN and they both move away from the location of the HN while maintaining a separation distance of approximately 30 meters. This short separation distance was selected to minimize the impact of the IN-DN D2D link on the performance measured at the IN (the D2D connection experienced negligible PER levels and used consistently a 54 Mbps data rate). Figure 5-11 shows an example of the MCN throughput measured at the IN with the HN located 500 meters away from the BS (additional field tests were conducted for different distances between BS and HN). The measurements reported in Figure 5-11 show that the MCN throughput measured at the IN initially exhibits similar performance levels to those experienced by the HN. As the IN walks away from the location of the HN and the HN-IN link quality degrades, the MCN throughput at the IN decreases. As expected, the throughput degradation starts at smaller distances to the HN under NLOS conditions than under LOS conditions. The distance at which the degradation starts is the IN critical distance. For the measurements reported in Figure 5-11, the IN critical distance at which the IN performance decreases below the throughput performance at the HN is 154 and 54 meters under LOS and NLOS conditions respectively. Figure 5-11 does not represent the throughput measured at the DN. However, the throughput was

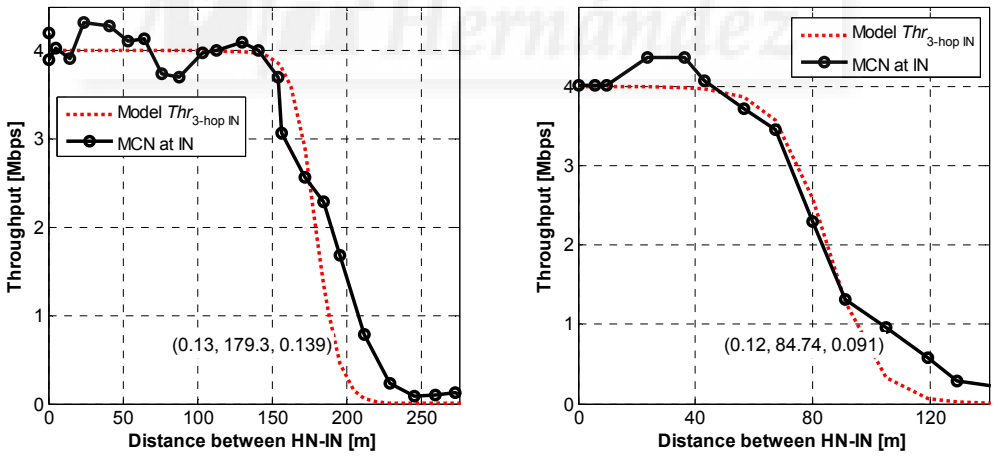

a) LOS conditions b) NLOS conditions

Figure 5-11. MCN throughput measured at the IN under a three-hop MCN configuration, and considering LOS (a) and NLOS (b) conditions between the HN and IN. The DN maintains a separation distance of 30 meters under LOS conditions with the IN. The HN is located 500 meters away from the BS. The figure also shows the three-hop MCN throughput model at IN (Section 5.3.2). The throughput is modeled using the *Sig* function with the LPSE fitting parameters and residue plotted in the figures.

very similar to that measured at the IN due to the short separation distance and the LOS conditions between the IN and DN nodes. In this context, whenever the distance between the HN and IN is smaller than the IN critical distance, the MCN throughput measured at the DN is again upper-bounded by the HSPA cellular performance experienced at the HN. However, when such distance is exceeded, the performance is upper-bounded by the HN-IN IEEE 802.11g D2D link.

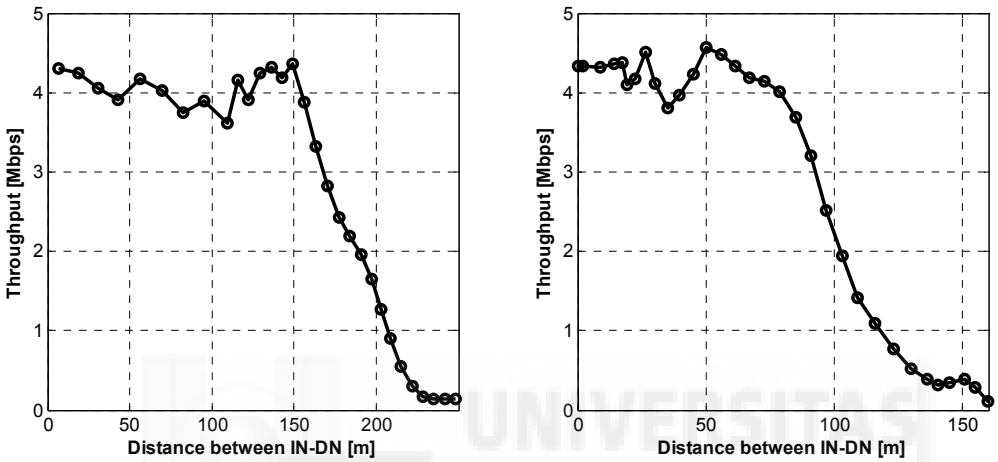

a) Distance HN-IN < IN critical distance

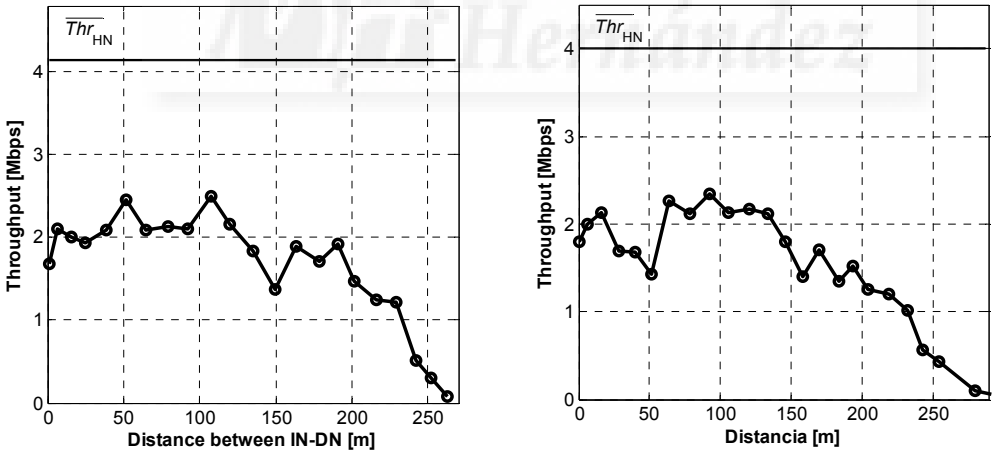

b) Distance HN-IN > IN critical distance

Figure 5-12. Three-hop MCN throughput measured at the DN when the IN-DN link experiences LOS (left) and NLOS (right) conditions. The IN remains static and under LOS conditions with the HN. The HN-IN distance is 50 (a) or 175 (b) meters. The HN is located 500 m away from the BS.

5.3.1.2 MCN Throughput at the DN

Additional field tests were conducted to analyze the MCN performance at the DN. In this case, the HN and IN nodes remain static and under LOS conditions, with their separation distance being equal to 50 or 175 meters. These two values were selected to consider scenarios where the separation distance is above or below the IN critical distance. During the tests, the DN moves away from the location of the IN under LOS or NLOS conditions until the IEEE 802.11g D2D link is lost. The results depicted in Figure 5-12.a show that when the HN-IN distance is shorter than the IN critical distance, the MCN throughput measured at the DN follows similar patterns as those discussed in the two-hop scenario (Figure 5-2). On the other hand, when the HN-IN distance is above the IN critical distance, the IN performance is seriously degraded (Figure 5-11), and so is the MCN throughput measured at the DN. Figure 5-12.b shows that, in this case, the MCN throughput experienced at the DN is not limited by the average HSPA throughput measured at the HN ($\overline{Thr_{\mathrm{HN}}}$), but by the MCN throughput measured at the IN. However, it can further decrease as the distance between the IN and DN increases. Then, the MCN throughput measured at the DN is upper-bounded by the IN-DN IEEE 802.11g D2D link[11].

5.3.2 Three-hop MCN Performance Models

The models of the three-hop MCN throughput performance experienced at the DN have been derived using the *Sig* function and the LSPE scheme described in Section 5.2.3. These models are represented in Figure 5-13 together with the fitting parameters and average residue values (*p1*, *p2*, ⟨*e*⟩). The three-hop MCN throughput at the DN has been modeled as follows:

$$\mathrm{MCN}\,Thr\left(p_1,p_2,d\right)_{\text{3-hop DN}}=\begin{cases}\overline{Thr_{\mathrm{HN}}}\cdot\left[1-\dfrac{1}{1+e^{-p_1\cdot\left(d-p_2\right)}}\right] & \text{if HN-IN dist} < \text{IN critical dist}\\ \mathrm{MCN}\,Thr_{\text{3-hop IN}}\cdot\left[1-\dfrac{1}{1+e^{-p_1\cdot\left(d-p_2\right)}}\right] & \text{if HN-IN dist} \geq \text{IN critical dist}\end{cases} \tag{5-18}$$

[11] As the number of hops increases, MCN connections would be mainly attractive if good link quality conditions can be guaranteed for the D2D links (further details are provided in Section 5.4). As a result, field tests with the HN-IN link under NLOS conditions were not conducted. Anyway, similar trends to those reported for the HN-IN link under LOS conditions (with the HN-IN distance shorter/above the IN critical distance) are likely to be observed.

where *d* represents the distance between IN and DN, and (p_1, p_2) are the fitting parameters shown in Figure 5-13.

Previous results have shown that the MCN throughput measured at the DN is upper-bounded by the average HSPA throughput at the HN ($\overline{Thr_{\mathrm{HN}}}$) when the separation distance between the HN and IN nodes is smaller than the IN critical distance. When the HN-IN separation distance is higher than the IN critical distance, the MCN throughput at the DN is upper-bounded by the MCN throughput at the IN (MCN $Thr_{\text{3-hop IN}}$) that can be computed as follows:

$$\mathrm{MCN}\,Thr\left(p_1, p_2, d\right)_{\text{3-hop IN}} = \overline{Thr_{\mathrm{HN}}} \cdot \left[1 - \frac{1}{1 + e^{-p_1 \cdot \left(d - p_2\right)}}\right] \qquad (5\text{-}19)$$

where *d* represents the distance between HN and IN, (p_1, p_2) the fitting parameters reported in Figure 5-11, and $\overline{Thr_{\mathrm{HN}}}$ the average HSPA throughput at the HN that can be derived from the measurements reported in Figure 5-4 and modeled in equation (5-13). For these fitting parameters, the IN critical distance at which the IN performance decreases below $\overline{Thr_{\mathrm{HN}}}$ is 154 and 54 meters under LOS and NLOS conditions respectively.

The conducted study has shown that when the distance between HN and IN is smaller than the IN critical distance, the three-hop MCN performance at the DN is not significantly influenced by the presence of the IN node. In fact, the fitting (p_1, p_2) parameters for the MCN throughput at the DN are similar to those derived for two-hop MCN communications (Table 5-2). Using the two-hop MCN fitting parameters to model three-hop MCN communications when the HN-IN distance is smaller than the IN critical distance will only marginally increase the average residue (approximately 7%). On the other hand, when the distance between HN and IN is larger than the IN critical distance, the fitting parameters significantly differ, in particular under LOS conditions. An analysis of the measurements suggests that the main reason for the lower p_1 (related to the slope of the curve) and higher p_2 parameters (related to the distance at which the curve is symmetric) is the challenging HN-IN link quality conditions that result in the IN using more robust transmission modes. Under NLOS conditions, the adaptive link level techniques do not perform as well as under LOS conditions, which results in the NLOS fitting (p_1, p_2) parameters being similar to those derived for the two-hop MCN communications.

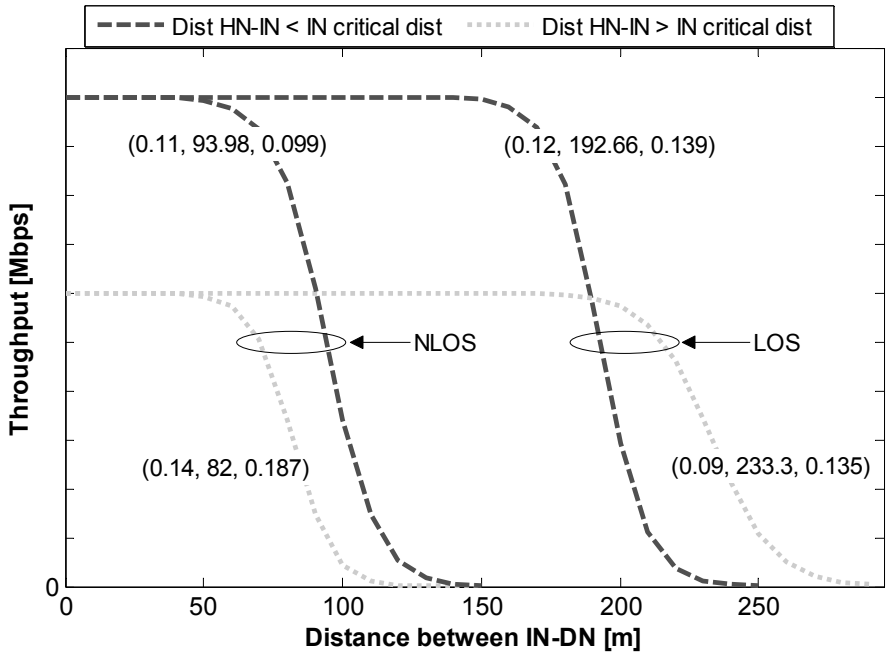

Figure 5-13. Three-hop MCN throughput models at the DN when the IN-DN D2D link experiences LOS and NLOS conditions, and for HN-IN distances smaller (50 m) and higher (175 m) than the IN critical distance. The models are derived with IN static and under LOS conditions with the HN.

5.4 x-Hop MCN Communications

The previous sections have derived MCN performance models for likely deployment scenarios with 2 and 3 hops. A higher number of hops would increase the probability to have an unstable MCN connection as a result of a higher probability that at least one of the D2D links experiences bad link quality conditions [109]. MCN connections with a high number of hops would hence be mainly attractive if good link quality conditions can be guaranteed for the D2D links. In fact, the previous sections showed that if the distance between relay nodes was shorter than their critical distance, the HN-IN and IN-DN D2D performance was superior to the HSPA cellular performance measured at the HN. In this case, the MCN performance at the DN would be at its highest level and would be upper-bounded by the cellular performance[12]. It is then of interest analyzing whether this performance level and model could be extended to a larger number of hops, and the conditions under which such extension would be feasible. In this context, it is important to note that even if the D2D link quality is good, the processing at each

[12] In addition, the results showed than in this scenario the three-hop MCN performance at the DN can be modeled using the two-hop MCN model and its fitting parameters, with a small residue.

intermediate relay decreases the multi-hop D2D performance, which could actually decrease below the cellular performance at the HN. It is then of interest determining the maximum number of hops that would guarantee that the multi-hop ad-hoc D2D performance (and thereby the end-to-end MCN performance) is upper-bounded by the cellular performance at the HN. To this aim, we can use the channel efficiency *E* of an IEEE 802.11 ad-hoc D2D link defined in [110] as follows:

$$E = \frac{t_d}{DIFS + t_{cont} + t_d + SIFS + t_{ack}} \tag{5-20}$$

where t_d, t_{cont} and t_{ack} represent the transmission time of the data packet, the contention period and the transmission time of the ACK frame, respectively. Distributed Coordination Function Inter Frame Space (*DIFS*) represents the period of time that the wireless channel has to be sensed as idle to initiate the transmission. Short Inter Frame Space (*SIFS*) represents the time interval between the reception of the data frame and the transmission of the ACK. *DIFS* and *SIFS* are equal to 28 μs and 10 μs for IEEE 802.11g (additional details can be found in Section 2.2.2). The value of t_{cont} has been set to 67.5 μs following the indications reported in [110].

Let's suppose that the IEEE 802.11g D2D links operate with the 54 Mbps data rate[13], and the size of the data packets and the ACK frame[14] is 1548 bytes and 14 bytes respectively. In this case, the efficiency *E* of an D2D link would be equal to 0.675, which results in a maximum throughput for a single hop IEEE 802.11g D2D link of 36.48 Mbps. We can then extend the efficiency computation to various hops E_{nhops}. In this case, it would be possible to identify the maximum number of hops that guarantees an end-to-end multi-hop performance higher than the cellular performance at the HN. To estimate the efficiency of a multi-hop (*n*-hop) ad-hoc D2D link, we assume that nodes cannot transmit simultaneously over the link[15]. In this case, the E_{nhops} efficiency needs to consider the processing time introduced by intermediate relay nodes (t_{pro}). Such time has been extracted from the three-hop MCN trials that included the intermediate IN node. t_{pro} measures the time difference at the IN between the reception (from the HN)

[13] In this case, the efficiency would represent the best case scenario. However, as previously discussed, MCN connections with a high number of hops should try guaranteeing good link quality conditions for D2D connections. When this was the case, the measurements showed that the D2D links mainly operated with the 54 Mbps data rate.

[14] In the conducted measurements, the ACK was transmitted at 24 Mbps.

[15] This assumption results in a lower-bound of the multi-hop channel efficiency since a single data packet can be transmitted at each point in time over the multi-hop D2D link.

and the transmission (to the DN) of IEEE 802.11 data packets. Table 5-6 summarizes the obtained results considering the LOS or NLOS conditions experienced at the IN-DN link. The results differentiate the measurements obtained when the HN-IN distance was higher or smaller than the IN critical distance. Several reasons explain the higher processing delay at the IN when the distance was above the IN critical distance: lower data rates, higher retransmission rates, an increase in the back-off/contention timers at the MAC layer, and the overflow of the transmission/reception buffers, among others. The channel efficiency of *n* multi-hop ad-hoc D2D links (E_{nhops}) can be computed as follows:

$$E_{nhops} = \frac{t_d}{\left(DIFS + t_{cont} + t_d + SIFS + t_{ack}\right) + \left(n-1\right)\cdot t_{pro}} \quad (5\text{-}21)$$

Assuming that the distance between nodes is shorter than their critical distance, and using the average processing time values reported in Table 5-6, the channel efficiency is equal to $E_{nhops}=0.2255$ for a two-hop IEEE 802.11g D2D link (three-hop MCN), $E_{nhops}=0.1353$ for a three-hop IEEE 802.11g D2D link, and E_{nhops}=0.0967 for a four-hop IEEE 802.11g D2D link. This results in a maximum throughput for a two-hop IEEE 802.11g D2D link of 12.17 Mbps, a maximum throughput for a three-hop IEEE 802.11g D2D link of 7.31 Mbps, and a maximum throughput for a four-hop IEEE 802.11g D2D link of 5.22 Mbps. The HSPA throughput measurements showed maximum values between 5 and 6.5 Mbps. In this case, a MCN connection with up to 4 IEEE 802.11 D2D hops could be upper-bounded by the HSPA cellular performance at the HN. Taking into account this result, and the fact that a higher number of hops can result in unstable MCN connections, this section analyzes and models the performance of 4 and 5 hops MCN connections with the separation distance between the relay nodes being shorter than their critical distance.

Table 5-6. Average processing delay at the intermediate IN node.

IN-DN link under LOS		**IN-DN link under NLOS**	
HN-IN dist < IN critical dist	HN-IN dist > IN critical dist	HN-IN dist < IN critical dist	HN-IN dist > IN critical dist
0.67 ms	8.6 ms	0.77 ms	7.2 ms

5.4.1 Four-hop and Five-hop MCN Field Tests and Performance Models

The performance of four-hop and five-hop MCN connections has been tested under similar conditions to those described for the two-hop and three-hop MCN scenarios. In the case of the four-hop MCN connection, two intermediate MNs (IN_1 and IN_2) are located between the HN and the DN. Three INs (IN_1, IN_2 and IN_3) are needed for the five-hop MCN connection. The HN and INs remain static during the field tests, and they maintain a separation distance of 50 meters[16] under LOS conditions (this distance is below the critical distance of each D2D link). The DN moves away from the location of its closer IN (IN_2 for four-hop MCN and IN_3 for five-hop MCN) under LOS or NLOS conditions. The obtained results showed similar trends to that analyzed previously for two-hop and three-hop MCN communications. The four-hop and five-hop MCN performance models have hence been derived using the *Sig* function and the LSPE fitting process, and can be expressed as:

$$\text{MCN } Thr\left(p_1, p_2, d\right)_{\text{4-hop or 5-hop DN}} = \overline{Thr_{\text{HN}}} \cdot \left[1 - \frac{1}{1 + e^{-p_1 \cdot \left(d - p_2\right)}}\right] \qquad \text{(5-22)}$$

where *d* represents the distance between IN_2 and DN for the four-hop scenario, and the distance between IN_3 and DN for the five-hop scenario. The models together with the fitting parameters and average residues (*p1*, *p2*, ⟨*e*⟩) for the two scenarios are plotted in Figure 5-14 and Figure 5-15 respectively. The average residues for four-hop MCN communications increase about 17% and 25% under LOS and NLOS conditions compared to the average residues obtained for two-hop MCN communications. The increment for the five-hop MCN scenario compared to the two-hop MCN one is equal to 25% and 30% under LOS and NLOS. The obtained results show that MCN connections with a high number of hops can still be attractive if good link quality conditions are guaranteed for the D2D links. In fact, the average residues for four-hop and five-hop MCN communications are smaller under the considered conditions than with the three-hop MCN scenario when the distance between IN and DN was higher than the IN critical distance.

[16] The scenario where the distance between relay nodes is higher than their critical distance has not been reproduced for four-hop and five-hop MCN communications. This was decided following the discussion about the need to guarantee D2D links with good link quality conditions in order to ensure stable multi-hop MCN connections.

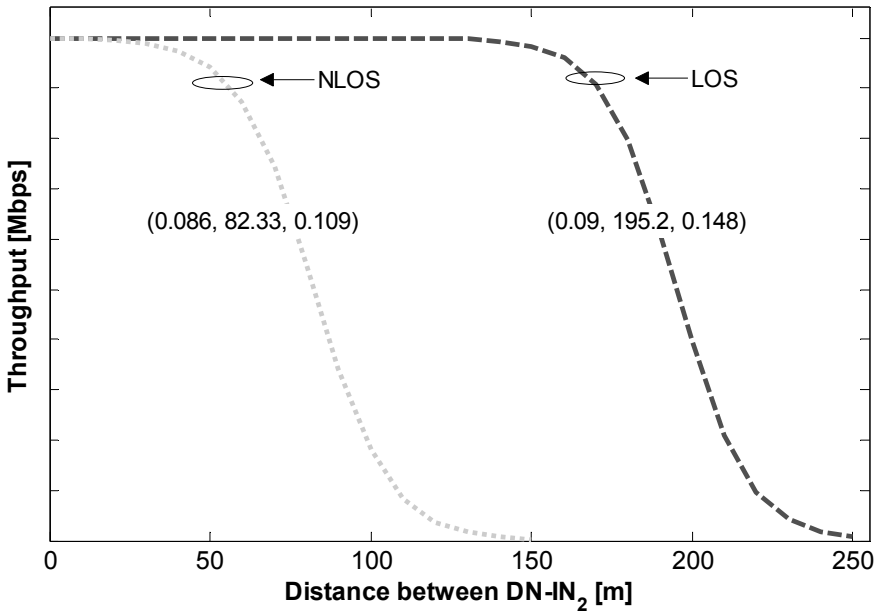

Figure 5-14. MCN throughput model at the DN under a four-hop MCN configuration, and considering LOS and NLOS condition between IN_2 and DN.

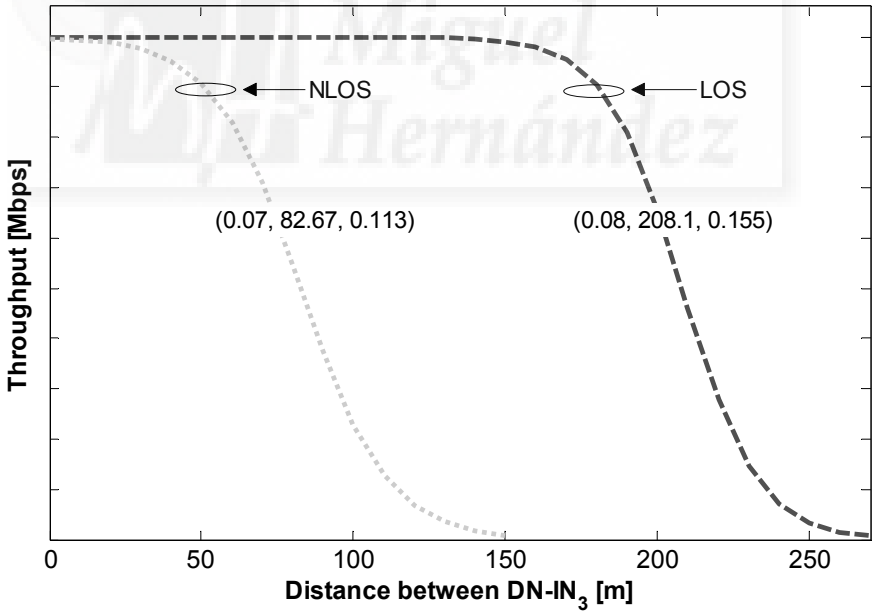

Figure 5-15. MCN throughput model at the DN under a five-hop MCN configuration, and considering LOS and NLOS conditions between IN_3 and DN.

5.5 Summary and Discussion

This chapter has presented novel and unique models for the communications performance of MCNs using mobile relays and D2D communications. The proposed models can be significantly valuable to support the design, test and optimization of novel communications and networking protocols tailored for MCNs. The models have been obtained following a large field testing campaign using an active cellular network in the city of Elche in Spain. The reported models represent the MCN throughput experienced at a mobile destination node as a function of the distance, propagation/visibility conditions, number of hops and communication settings. The performance metric was selected with the objective to reduce the impact of cellular resource management policies that may vary from operator to operator. The MCN throughput performance has been modeled with a sigmoid function that is a function of the cellular throughput experienced at the hybrid or gateway mobile node. The models' fitting parameters have been shown to depend on key factors such as the propagation conditions and number of hops. The models have been derived considering HSPA cellular transmissions and IEEE 802.11g D2D communications. Extending the models to other cellular technologies could be feasible as long as the MCN performance is upper-bounded by the cellular link between the BS and the hybrid mobile node. Using the MCN measurements, this chapter also reports D2D link-level models derived as function of the distance between communicating nodes.

6

Opportunistic Multi-hop Cellular Networks

Cellular networks face significant capacity and energy challenges as cellular data keeps on rising. Cellular data traffic is significantly growing with the pervasive use of smartphones and the popularity of mobile video, web browsing and social networking applications among others. This trend will keep on exponentially growing with the adoption of Machine-to-Machine (M2M), Internet of Things (IoT) and connected vehicles applications, among others [2]. As experimentally demonstrated in Chapter 4, Multi-hop Cellular Networks (MCNs) can help address the increasing capacity and energy constraints of traditional cellular systems through the integration of cellular and ad-hoc or D2D communications. MCNs can also benefit from the adoption of opportunistic networking solutions. Opportunistic schemes exploit the nodes' mobility and the store, carry and forward paradigm to establish communication links between mobile relays when favorable communication conditions are found [13]. Opportunistic schemes can then reduce the overall energy consumption [111], but can result in possible end-to-end transmission delays and their use should concentrate on delay tolerant services. The integration of opportunistic networking and MCNs represents then an interesting option to provide quality of service while improving energy-efficiency by taking advantage of the delay tolerance or non-real-time properties of certain traffic services, e.g. email, file sharing, social networking, software/firmware updates, mobile video, cloud services,

data metering, goods tracking; according to the Cisco's global mobile data traffic forecast for 2014-2019 [15], these services represent some of the most popular applications driving the mobile data growth. In this context, this chapter investigates the capacity of opportunistic store, carry and forward techniques in MCNs to exploit the data delivery margins offered by delay tolerant services to improve the energy-efficiency of cellular networks.

Section 6.1 reviews related studies and Section 6.2 introduces the most popular delay tolerant applications. Section 6.3 presents a detailed mathematical framework for the study and design of energy-efficient opportunistic MCN communications. Section 6.4 derives the optimum configuration of opportunistic forwarding in a two-hop MCN scenario, including the identification of the optimum mobile relay location, and the location at which the relay needs to start forwarding the information to the cellular network in order to minimize the overall energy consumption. Finally, Section 6.5 analyzes the impact of traffic characteristics of delay tolerant services on the energy gains that can be reached with opportunistic MCN communications, and how opportunistic MCN communications should be configured to exploit traffic characteristics in order to reduce the energy consumption.

6.1 Opportunistic Networking in Multi-hop Cellular Networks

MCNs using mobile relays and D2D communications possess unique capabilities to overcome the limitations of traditional single-hop cellular communications by means of exploiting the communications, computing and networking capabilities of smart devices. MCNs can also benefit from the mobility and storing capacity of mobile devices to implement opportunistic networking schemes that exploit the store, carry and forward paradigm. Opportunistic networking was initially proposed for disconnected wireless networks. In the absence of forwarding opportunities, mobile nodes could store the message and carry it until they can forward it to other nodes. Opportunistic networking can reduce the energy consumption [111] at the cost of possible higher transmission delays [112]-[113]. For example, the study reported in [114] investigates the problem of optimal opportunistic forwarding for Delay/Disruption-Tolerant Networks (DTNs) under energy constraints (the study considers that the energy for transmitting a message is limited). To maximize the delivery probability while satisfying the energy constraint, the study controls the probability of transmitting a message upon the opportunistic connectivity between devices. A similar approach is presented in [115], where the forwarding probability between encountering nodes is determined by the node density

estimation. When the density is high, the forwarding probability is reduced to avoid excessive simultaneous message copy transmissions. Important efforts have also been devoted to estimate the periodicity in the encounters between mobile nodes [116], as well as the duration of opportunistic connections and the nodes' inter-contact time [117]-[118]. These studies have been further extended to consider the impact of duty-cycle operation that results in that nodes can miss contact opportunities when they operate under sleep state for saving energy [119].

Opportunistic networking principles can be extended to networks that do not suffer frequent disconnections. In fact, opportunistic networking can be utilized for searching for the most efficient transmission conditions between devices. For example, the adoption of opportunistic networking principles has been proposed to extend the coverage of cellular networks, offload cellular traffic using D2D communications, or increase the capacity [117]. The studies reported in [120] and [121] show that opportunistic policies can significantly enhance the efficiency of D2D transmissions by pausing communications under unreliable and low efficiency link-quality conditions, and re-starting them when channel conditions improve. This feature was proven in [122] using queuing theory, and has been recently experimentally demonstrated in [14]. Opportunistic networking can also help offloading data traffic from cellular networks to metropolitan Wi-Fi access points without degrading the QoS [43]. The benefits of integrating opportunistic networking and MCNs was first discussed in [99], where the authors present novel routing policies that use information about the relays' mobility to reduce energy consumption, increase spatial capacity, reduce co-channel interference, balance the load across cells, and switch-off low-utilization base stations. To do so, the authors formulate a finite space-time network graph that includes all possible routes for forwarding information towards a cellular BS. Such graph is constructed taking into account the delay tolerance acceptable for different services. The vertexes of the graph represent the location of the mobile relays with time, and the edges the transmission links. The authors claim that using the graph, a BS can identify end-to-end opportunistic forwarding paths to achieve an established QoS target. The study was then extended in [123] where the authors highlight the importance of considering the power consumption of storage units in mobile relays when studying opportunistic networking.

6.2 Delay Tolerant Mobile Traffic Services

Cisco estimates that mobile video represented 55% of the mobile data traffic by the end of 2014. This percentage is expected to increase to 72% by 2019. Even uplink mobile

video traffic is increasing thanks to the popularity of applications such as Ustream [124], Bambuser [125] or Livestream [126] that allow users to broadcast live events using their mobile devices. Mobile video content delivery technologies currently utilize Adaptive Streaming (AS) schemes that divide video content into fragments. These fragments are delivered to the user on demand to ensure that sufficient content (in the order of tens of seconds) is constantly buffered at the user device ahead of playback time. This buffering policy avoids freezing of video streaming, thereby improving the user's Quality of Experience (QoE). The study in [127] showed that YouTube adaptive streaming delivers approximately 1 Megabyte (MB) of data to the user's player every 10 seconds, with the data being received in multiple fragments. However, video content fragments could also be grouped to postpone their transmission at no cost to the perceivable QoE as long as the playback is not interrupted [128]. The work presented in [128] utilizes mobility information to control the download rate of video content fragments and thereby the amount of fragments in the user's buffer. When the mobile user is far away from the BS, the buffer size is maintained at a minimum level (only a few seconds ahead of playback time) in order to minimize the radio transmissions conducted under low QoS levels. On the other hand, the content is aggressively downloaded when the mobile station is close to the BS and the link quality conditions are good. The scheme proposed in [128] has shown to considerably reduce the energy consumption compared to traditional mobile video content deliver schemes in high mobility networks. However, videos are not always watched from start to finish (actually 80% of video sessions are interrupted [129]) and therefore downloading all the video data, even at good channel conditions, might be inefficient (considerable resources are wasted in the case that user

Figure 6-1. YouTube screenshot - example of delay tolerant traffic.

decides not to watch part or the whole media file after it has been downloaded). In this context, the adoption of opportunistic forwarding schemes in MCNs represents an interesting alternative to provide quality of service while improving energy-efficiency for mobile video traffic. Figure 6-1 illustrates a real example of the buffering policy implemented on YouTube. In this case, the buffered data is equivalent to 50 seconds of playback. Therefore, the download of the remaining data could be postponed/delayed at no cost to the user's QoE as long as the playback time does not pass the buffered data.

Mobile email is another example of popular service that can tolerate certain transmission delay. Mobile email data traffic has increased over the last years due to the availability of renewed email client applications on mobile devices and smartphones that have improved the user experience. Based on Cisco's estimates, email traffic will grow at a compound annual growth rate of 39 percent from 2014 to 2019 in mobile networks [15]. Email traffic (in general) does not require synchronous end-to-end communications and can tolerate delays (>>10 s) according to the International Telecommunication Union (ITU) QoS classification [130]. The delay tolerance is expected from the polling frequency at which email clients check for emails at servers. For example, Gmail clients check for emails approximately once per hour and the polling frequency reduces as long as emails are found on the server; the polling interval can be reduced to approximately 5 minutes intervals. Gmail has also recently released an application that is intended to let users use email service offline. This Gmail Offline application stores messages created offline to be sent when the connectivity opportunities arise. Microsoft Outlook also allows configuring when to schedule an automatic send/receive command. The minimum send/receive schedule is 1 minute and the maximum is 1440 minutes (1 day).

Social networks and messaging applications generate a significant amount of photo sharing and messaging (text and multimedia) traffic. For example, recent figures published in [131] show that more than 250 billion photos have been uploaded to Facebook since the site was launched, and more than 350 million photos are uploaded every day on average. It is also worth noting the recent WhatsApp figures: users are sending 19 billion messages a day and sharing 600 million photos every 24 hours. Uploading photos to social networks is not necessarily an instantaneous process, and can be configured considering factors such as the synchronization frequency, battery level and technology (e.g. synchronizing over WiFi and cellular network, or over WiFi only). Mobile messaging applications (e.g. WhatsApp, Line [132], Viber [133] or HeyTell [134]) require a data connection at the transmitter and receiver for the exchange of

messages. Mobile messaging applications are delay tolerant from their design since they postpone the transmission or reception of the messages if such connections are not available.

Other relevant delay tolerant applications include Over-The-Air (OTA) updating and cloud file hosting services. OTA updating services are becoming increasingly popular in smartphones and tablets for updating applications, software or firmware as well as configuration settings on mobile devices [135]. These services are delay tolerant in nature since software updates are generally delivered to the users gradually once released. Therefore, OTA updating services can be designed to exploit connectivity and offloading opportunities. Cloud file hosting services allow (mobile) users to store content in the cloud and access it at any time and place using different (mobile) devices/platforms. These services can be configured to automatically upload files of any type for backup or just for sharing with other users and platforms (e.g. files, photos or videos). This process can again be configured to exploit the characteristics and efficiency of connectivity conditions. The possibility to optimize the configuration of mobile uploading processes is also present in the vehicular environment. For example, car insurance companies are introducing pay-as-you-drive policies that calculate the drivers' insurance premiums based on the vehicle usage (speed, acceleration, time of day, type of road, and milestone). Vehicles are equipped with an accelerometer and a GPS to track the vehicle location/acceleration, and a cellular modem to collect the measurements at the control center. The frequency with which the vehicle uploads the information is managed at the control center [136]. Therefore, the upload of information from the vehicle can be deemed as delay tolerant.

6.3 Opportunistic Forwarding in Multi-hop Cellular Networks

The services introduced in Section 6.2 offer the possibility to manage the tolerable delay towards a desired outcome at no cost to the perceivable QoE. This can be of particular interest for the integration design of opportunistic networking into MCNs since delay tolerant mobile traffic services offer the possibility for mobile devices to delay the transmission of the information to the base station. In the case of this thesis, the desired outcome for the integration of opportunistic store, carry and forward mechanisms in MCNs is to reduce the total energy consumption.

The study conducted in this thesis considers a two-hop MCN scenario in which a static Source Node (SN) wants to transmit information to a Base Station (BS) using a

Mobile Relay (MR) with store, carry and forward capabilities (Figure 6-2). To start with, the study does not focus on any particular delay tolerant service but a generic one that requires the information to be transmitted to the BS within a time *T*. The time needed to transmit the information from SN to BS is computed taking into account: 1) the time needed for the D2D transmission from SN to MR (*D2D tx*), 2) the time that the MR stores and carries the information (*Store and carry*), and 3) the time needed by the MR to transmit the information to the BS (*Cellular tx*). As depicted in Figure 6-2, estimating the time needed for each one of these processes requires determining the MR location at which the D2D transmission should start (Opt_X_i), and the MR location at which the cellular transmission should start (Opt_Y_i). This section focuses then on estimating these two locations with the final objective to reduce the total energy consumption.

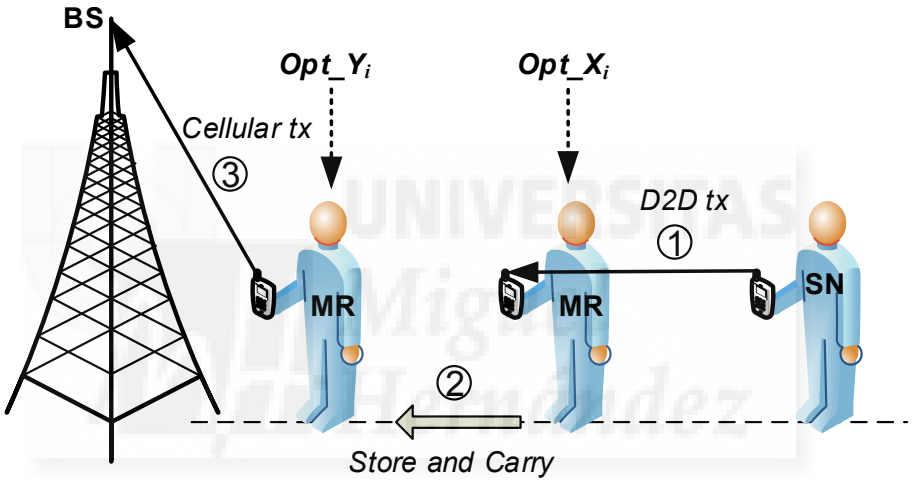

Figure 6-2. Two-hop opportunistic MCN scenario.

6.3.1 Problem Formulation

A multi-objective constrained optimization problem is defined to identify the optimum MR location and the location at which the relay needs to start forwarding the information to the cellular network in order to minimize the overall energy consumption (equations (6-1) to (6-4)). The objective function shown in equation (6-1) has been defined together with two constraints (equations (6-2) and (6-3)), and the requirement that the BS receives the information before a service-dependent deadline *T* (equation (6-4)). This deadline *T* is discretized in the optimization framework as $\{\tau_0, \tau_1 \ldots \tau_r\}$.

$$o.f:\min\left(\begin{array}{l}\underbrace{\sum_{\tau=\tau_0}^{\tau_{b-1}}\left(E_{D2D}\left(d_{SN-MR},\tau\right)+\tau\cdot\left(P_R+P_W\right)\right)}_{①}+\\ \underbrace{\sum_{\tau=\tau_b}^{\tau_{c-1}}\tau\cdot P_{IDLE}}_{②}+\\ \underbrace{\sum_{\tau=\tau_c}^{\tau_{c+m}}\left(E_{cell}(d_{MR-BS},\tau)+\tau\cdot P_W\right)}_{③}\end{array}\right) \quad (6\text{-}1)$$

$$st:$$

$$\sum_{\tau=\tau_0}^{\tau_{b-1}}TR_{D2D}\left(d_{SN-MR}\right)\cdot\tau\geq F \quad (6\text{-}2)$$

$$\sum_{\tau=\tau_c}^{\tau_{c+m}}TR_{cell}\left(d_{MR-BS}\right)\cdot\tau\geq F \quad (6\text{-}3)$$

$$\tau_0<\tau_{b-1}<\tau_b\leq\tau_{c-1}<\tau_c<\tau_{c+m}\leq\tau_T \quad (6\text{-}4)$$

The objective function (equation (6-1)) is formulated considering the energy consumed by the D2D transmission from SN to MR ①, the store and carry process ② and the cellular transmission ③ carried out by the MR. In ①, $\sum_{\tau=\tau_0}^{\tau_{b-1}}E_{D2D}\left(d_{SN-MR},\tau\right)$ is the energy consumed in the D2D transmission between SN and MR within the time interval {τ_0, τ_1… τ_{b-1}}, and considering that SN and MR are separated by d_{SN-MR} at τ. $\sum_{\tau=\tau_0}^{\tau_{b-1}}\tau\cdot\left(P_R+P_W\right)$ represents the storage power consumption at the SN while transmitting the information, and the storage power consumption at the MR while receiving the information during the D2D transmission [123]. In ②, $\sum_{\tau=\tau_b}^{\tau_{c-1}}\tau\cdot P_{IDLE}$ represents the power consumption at the MR when the node stores and carries the information while moving towards the BS [123]. This process takes place within the time interval {τ_b, τ_{b+1}… τ_{c-1}}. Finally, $\sum_{\tau=\tau_c}^{\tau_{c+m}}E_{cell}\left(d_{MR-BS},\tau\right)$ represents in ③ the energy consumed in the cellular transmission from MR to BS within the time interval {τ_c, τ_{c+1}… τ_{c+m}}, and considering that MR and BS are separated by d_{MR-BS} at τ. $\sum_{\tau=\tau_c}^{\tau_{c+m}}\tau\cdot P_W$ represents the storage energy consumption at MR while transmitting the information to the BS during the time interval {τ_c, τ_{c+1}… τ_{c+m}} [123].

The objective function is complemented with two constraints for the message (of size *F*) to be completely transmitted in the D2D (equation (6-2)) and cellular (equation (6-3)) transmissions. TR_{D2D} and TR_{cell} represent the D2D (from SN to MR) and cellular

transmission (from MR to BS) rates respectively. $\sum_{\tau=\tau_0}^{\tau_{b-1}} TR_{D2D}\left(d_{SN-MR}\right)\cdot\tau$ in equation (6-2) represents then the data transmitted in the D2D connection between SN and MR within the time interval {τ_0, τ_1… τ_{b-1}}, and considering that SN and MR are separated by d_{SN-MR} at τ. $\sum_{\tau=\tau_c}^{\tau_{c+m}} TR_{cell}\left(d_{MR-BS}\right)\cdot\tau$ in equation (6-3) represents the data transmitted in the cellular communication from MR to BS within the time interval {τ_c, τ_{c+1}… τ_{c+m}} considering that MR and BS are separated by d_{MR-BS} at τ. The last constraint (equation (6-4)) guarantees for the derived solution that the end-to-end transmission is completed before the service-dependent deadline *T*.

The defined optimization framework (equations (6-1) to (6-4)) allows identifying the optimum two-hop opportunistic MCN configuration that minimizes the overall energy consumption. For a given location of the SN, the optimization problem derives the time instances τ_0, τ_{b-1}; τ_b, τ_{c-1}; and τ_c, τ_{c+m} at which the D2D transmission, store and carry and cellular transmission processes take place, respectively. This is in fact equivalent to identifying the optimum mobile relay location (*Opt_X*$_i$ in Figure 6-2) and the location at which the relay needs to start forwarding the information to the cellular network (*Opt_Y*$_i$ in Figure 6-2) in order to minimize the overall energy consumption. The optimization process (represented by θ) can then be expressed as follows:

$$\begin{aligned}&\left[\tau_0,\tau_{b-1},\tau_b,\tau_{c-1},\tau_c,\tau_{c+m};Opt\_X_i,Opt\_Y_i\right]=\\&\arg\min\left(\vartheta\left(F,T,TR_{D2D},TR_{cell},E_{D2D},E_{cell},P_R,P_W,P_{IDLE}\right)\right)\end{aligned} \tag{6-5}$$

6.3.1.1 Transmission Energy Consumption

This study models the energy consumed in the transmissions between SN and MR, and between MR and BS, using the urban WINNER propagation model [137]; to the author's knowledge, this model is one of the most complete ones for urban environments with low transmitter and receiver's antennas height. The WINNER's Path Loss (*PL*) model is of the form presented in equation (6-6), where *d* is the separation distance between the transmitter and the receiver (in meters), *f* is the carrier frequency (in GHz), the fitting parameter *A* includes the path loss exponent, *B* is the intercept, *C* describes the path loss frequency dependence, and *X* is an optional environment-specific parameter [137]. For urban scenarios with low antennas height, and under LOS conditions between the transmitter and the receiver, *A* = 22.7, *B* = 41.0 and *C* = 20 if *d* is smaller than the break point distance d_{bp} (d_{bp} = 4(h_{TX} -1)(h_{RX} -1)/λ; h_{TX} and h_{RX} are the

transmitter and receiver antenna heights, and λ is the carrier wavelength, all of them in meters). If d is higher than d_{bp}, PL= 40·log$_{10}$(d)+41-17.3·log$_{10}$(d_{bp})+20·log$_{10}$(f/5).

$$PL = A\log_{10}(d) + B + C\log_{10}\left(\frac{f}{5}\right) + X \tag{6-6}$$

The study also considers that the signal power level at the receiver can be computed as:

$$P_{RX} = G_{TX} + G_{RX} + P_{TX} - PL \tag{6-7}$$

where G_{TX} and G_{RX} represent the transmitter and receiver antenna gain, and P_{TX} is the transmission power (PL is the propagation loss of the form presented in equation (6-6)). The transmission energy consumption is here computed considering that the transmission power (P_{TX}) is the necessary one to guarantee that the receiver's signal power level (P_{RX}) is equal to the threshold required for a successful communication between two nodes. It is then possible to estimate the transmission power under LOS conditions using the WINNER propagation model as follows:

$$P_{TX}^{LOS}(d) = \begin{cases} \dfrac{P_{RX}\cdot 10^{4.1}\cdot (f/5)^2}{G_{TX}\cdot G_{RX}} d^{2.7} & if\ d < d_{bp} \\ \dfrac{P_{RX}\cdot 10^{4.1}\cdot (f/5)^2}{G_{TX}\cdot G_{RX}\cdot d_{bp}^{1.73}} d^{4} & if\ d \geq d_{bp} \end{cases} \tag{6-8}$$

The energy consumed in the D2D (E_{D2D}) and MR to BS cellular (E_{cell}) transmissions under LOS can then be expressed as:

$$E(d) = \left(e_{rx} + e_{tx} + e_{LOS}(d)\right)\cdot TR \tag{6-9}$$

where e_{tx} and e_{rx} represent the energy consumption per bit in the transmitter and receiver electronics respectively, and TR is the throughput (TR_{D2D} or TR_{cell}). e_{LOS} represents the transmission energy consumption per bit under LOS conditions and is equal to P_{Tx}^{LOS}/TR. A similar process can be followed to estimate the NLOS transmission energy consumption.

6.3.1.2 Storage Energy Consumption

As recommended in [123], this study considers the energy consumed by storage units in mobile relays. Data packets received from wireless interfaces are automatically stored in the Dynamic Random Access Memory (DRAM) storage unit. The data packets could be transferred to internal units such as Negated AND (NAND) flash to reduce energy consumption. This decision usually depends on the time that the information is stored, and the transfer speed and power cost. If the information is transferred from DRAM to

NAND, it must be transferred back to the DRAM when the mobile device decides to start any transmission process (D2D transmission or cellular transmission). This work considers that the information is always transferred from DRAM to NAND flash (it is out of the scope of this study to determine when it is worth transferring data from DRAM to NAND). As a result, the power state transitions of the two storage units needs to be considered when computing the storage energy consumption. These state transitions are depicted in Figure 6-3 [123]. P_R includes the power consumed by the DRAM and NAND flash when these storage units Read (*R*) and Write (*W*) the information, as well as the power consumed for transferring the information from DRAM to NAND flash at speed *Transf_DF*. P_{IDLE} includes the power consumed by the NAND flash that is storing the information in *Idle* state, and the power consumed by the DRAM that is in *Idle_self-refresh* state. Finally, P_W is the power consumed by the two storage units when they transfer the information back to the DRAM for transmission at speed *Transf_FD*.

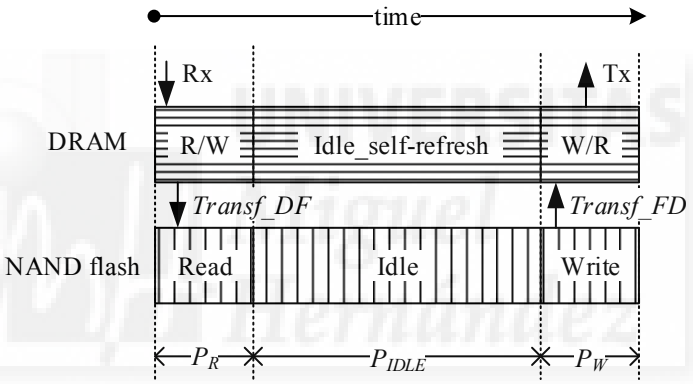

Figure 6-3. Transition states of the storage units as a function of the time when the data is transferred from DRAM to FLASH, and sent back to DRAM [123].

6.4 Optimum Configuration of Opportunistic Forwarding in MCN

Considering the optimization framework presented in Section 6.3, this section derives optimum configurations of opportunistic forwarding in MCNs that identify for a two hop scenario the optimum mobile relay location and the location from which the mobile relay should start forwarding the information to the cellular base station in order to minimize the overall energy consumption.

6.4.1 Evaluation Scenario

The numerical resolution of the analytical framework described in the previous section is done considering the parameters summarized in Table 6-1. The evaluation

Table 6-1. Evaluation parameters.

Parameter	Description	Value
R	Cell radius	1000 m
v	Mobile nodes' speed	2 m/s
F	File size	10 Mb
T	Transmission deadline	100 s
G_{TX}, G_{RX}	Transmitter and receiver antenna gain	1
e_{tx}, e_{rx}	Energy consumed per bit by the transmitter/receiver	50 x 10^{-9} J/b
P_{RX}	Power reception threshold	-62 dBm
h_{SN}, h_{MR}, h_{BS}	Antenna height of SN, MR and BS	1.5 m, 1.5 m, 10 m
DRAM P_R, P_W, $P_{Idle\_self\text{-}refresh}$	DRAM power consumed for Reading, Writing and in Idle_self-refresh state	252 mW, 252 mW, 1.35 mW
NAND Eff_{Read}, Eff_{Write}, P_{Idle}	NAND efficiency for Reading and Writing, and Power consumed in Idle state	1.83 nJ/b, 11.92 nJ/b, 0.4 mW
Transf_DF, Transf_FD	Transfer speed from the DRAM to the NAND flash and vice versa	4.85 MiB/s, 927.1 KiB/s

considers LTE at 2 GHz for the cellular transmissions, and IEEE 802.11g at 2.4 GHz for the D2D transmissions[17]. These technologies have been selected based on the availability of the necessary models. In any case, the conclusions reported in this study are not dependent on the selected radio access technologies. In fact, the analysis has been replicated considering HSPA for the cellular radio access, and the same conclusions have been observed (see Annex A). Following the model reported in [138], the LTE throughput for the cellular link between MR and BS can be approximated as:

$$TR_{cell}(d) = r(N_{PRB}, l_{MCS}) \cdot (1 - p_{BLER}(N_{PRB}, l_{MCS})) \quad (6\text{-}10)$$

where $r(N_{PRB}, l_{MCS})$ is defined in [138] as the maximum instantaneous data rate achievable by the user on a frequency chunk of size N_{PRB} Physical Resource Blocks (PRB), and modulation and coding scheme (MCS) index l_{MCS}. N_{PRB} has been set to 6 as in [139] and following the 3GPP guidelines in [140]. In addition, $p_{BLER}(N_{PRB}, l_{MCS})$ is the Block Error Rate (BLER) experienced for an allocation size of N_{PRB} and MCS index l_{MCS}. As established in [138], this study considers a target BLER of 10% that coincides with that for the

[17] It is important to recall that 3GPP considers IEEE 802.11 technologies as well as cellular technologies (e.g. LTE-Direct) for device-to-device communications [9].

reported CQI values as described in the 3GPP physical layer procedures [141]; $p_{BLER}(N_{PRB}, I_{MCS})$ is hence set to 0.1 in equation (6-10). This study considers 15 MCS indexes (coinciding with the available CQI indexes in LTE) that are set according to the distance (d) between the MR and the BS (more robust MCS are needed as the distance to the serving BS increases). The cell is hence divided into 15 equally spaced and concentric rings identified by the MCS indexes. MCS indexes for the allocated N_{PRB} are finally mapped to the Transport Block Size (TBS) indexes (I_{TBS}) using the table reported in [141]. The $r(N_{PRB}, I_{MCS})$ used in equation (6-10) can then be calculated as:

$$r\left(N_{PRB}, I_{MCS}\right) = TBS \Big/ T_{TBS} \tag{6-11}$$

where T_{TBS} is the TBS duration which is equal to 0.5 ms in LTE, and *TBS* is the size of the transport block associated with I_{TBS}.

Using the model reported in [110], the IEEE 802.11g throughput for the D2D link between SN and MR can be expressed as follows:

$$TR_{D2D}\left(d\right) = DataRate(d) \cdot Eff \cdot \left(1 - PER\left(d\right)\right) \tag{6-12}$$

where *DataRate*, *PER* and *Eff* represent the IEEE 802.11g transmission mode, Packet Error Ratio and channel efficiency, respectively. d is the distance between the transmitter and receiver (in meters). IEEE 802.11g defines twelve possible combinations of modulation and coding schemes that result in the set of data rates: {54, 48, 36, 24, 18, 12, 9, 6; 11, 5.5, 2, 1} Mbps. The data rate control algorithm dynamically selects the IEEE 802.11g data rate based on the link quality conditions. The IEEE 802.11g *DataRate* model used in this study is the one empirically derived by this thesis in Section 5.2.6:

$$DataRate\left(d\right) = \begin{cases} 54 & d < 78.47m \\ \dfrac{54}{\dfrac{1}{78.47} - \dfrac{1}{270.85}} \cdot \left(\dfrac{1}{d} - \dfrac{1}{270.85}\right) & 78.47m \le d < 270.85m \\ 0 & 270.85m \le d \end{cases} \tag{6-13}$$

Equation (6-13) indicates that the IEEE 802.11g *DataRate* is set to 54 Mbps at short distances. More robust data rates are then used with increasing distances between SN and MR. The IEEE 802.11g *PER* model is also derived empirically in this thesis and has been presented in Section 5.2.6:

$$PER\left(d\right) = \frac{0.75}{1 + e^{-0.019 \cdot (d - 115.15)}} \tag{6-14}$$

Equation (6-14) indicates that the PER augments with the distance (d, in meters) between transmitter and receiver (despite using more robust modulation and coding

schemes as shown in equation (6-13)), although an upper PER limit (0.75) is reached. The IEEE 802.11g channel efficiency (*Eff*) represents the effective time that the IEEE 802.11g channel is used to transmit data, and depends on the transmission time of data packets (t_d) and ACK packets (t_{ack}), the contention period (t_{cont}), and the inter-frame guard times (*DIFS* and *SIFS*)[110]:

$$Eff = \frac{t_d}{DIFS + t_{cont} + t_d + SIFS + t_{ack}} \quad (6\text{-}15)$$

The energy consumption values for the DRAM and NAND flash storage units have been obtained from [142] and [143] respectively. The energy consumed per bit in the transmitter and receiver electronics (e_{tx} and e_{rx}), and the power reception threshold (P_{Rx}), have been obtained from [123]. The scenario considers the MR is in line with the SN, and moving towards the BS with a speed *v* of 2 m/s. The considered pedestrian scenario represents a worst-case scenario. This is the case because the faster the MR moves towards the BS, the closer to the BS will start the cellular transmission, which will result in higher cellular data rates and lower energy consumption. The SN needs to transmit to the BS a 10 Mb (*F*) file before a 100 seconds deadline *T* [99].

6.4.2 Numerical Evaluation

The optimization problem presented in Section 6.3 has been implemented in Matlab. Brute force has been used to solve the optimization problem for all possible distances between SN and BS. Figure 6-4.a shows the optimum MR location at which to start the D2D transmission as a function of the distance between SN and BS (labeled 'Optimum'). The MR location is represented by means of the distance between SN and MR. For example, if SN is located 400 meters away from the BS, the MR should be ideally located 50 meters away from the SN in the direction of the BS in order to minimize the total energy consumption. Figure 6-4.a shows that the distance between SN and the optimum MR that minimizes the energy consumption increases with the distance between SN and BS. This is to reduce the distance at which the MR starts forwarding the information towards the BS (and therefore the cellular transmission energy consumption). The peaks shown in Figure 6-4.a correspond to the case when the SN selects an MR closer to the BS and that could reach a ring with higher cellular data rate; the use of higher data rates reduces the cellular transmission energy consumption. However, the D2D transmission energy consumption increases as the MR is selected closer to the BS. As a result, the distance between SN and the optimum MR location only increases when the energy saving of the store and carry process (that allows reducing the cellular transmission distance from MR to BS) can compensate the increase in the D2D transmission energy consumption. Figure 6-4.a shows a small increase in the MR location when the SN is

located very close to the BS. This is because the optimum MR does not store and carry the information when the SN is close to the BS (further details are provided below), and therefore the SN selects an MR as close as possible to the BS. The energy consumption levels for the D2D transmission from SN to the optimum MR location are reported in Figure 6-4.b in logarithmic scale as a function of the distance between SN and BS. The increasing distances between SN and the optimum MR location (Figure 6-4.a) result in that the D2D transmission energy consumption levels increase with the distance between SN and BS.

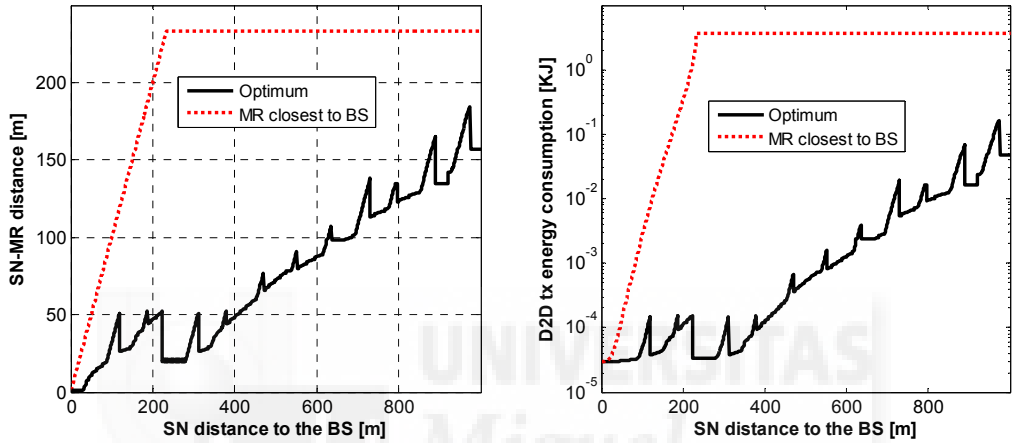

a) Optimum MR location b) D2D transmission energy consumption

Figure 6-4. Optimum configuration of two-hop opportunistic MCN communications: D2D transmission.

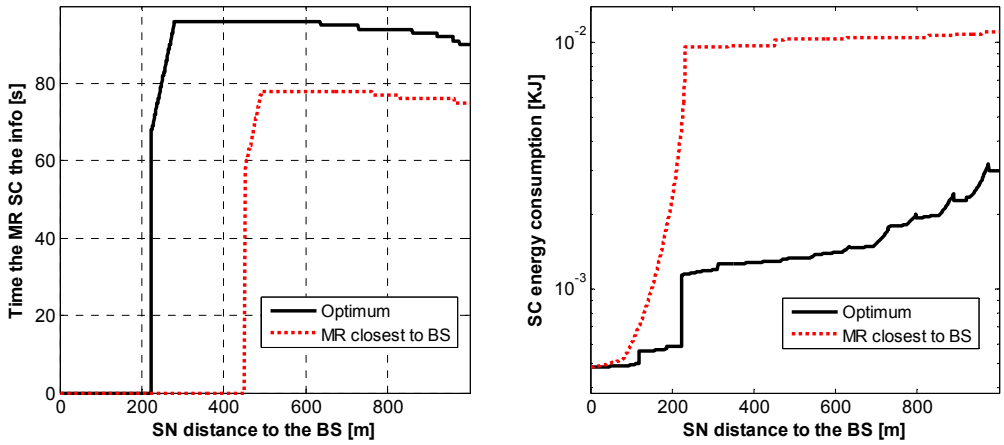

a) Time the MR stores and carries the information while moving towards the BS b) Store and Carry energy consumption

Figure 6-5. Optimum configuration of two-hop opportunistic MCN communications: Store and Carry (SC).

To demonstrate how important is to adequately select the MR, Figure 6-4 also shows the results obtained with a greedy forwarding scheme in which the SN selects the MR that is located closest to the BS [144]. This scheme is referred to as 'MR closest to BS' in this study. For a fair comparison, a similar optimization process to that reported in Section 6.3 is conducted for the 'MR closest to BS' scheme. In particular, the optimization process derives for this scheme the MR location that provides the highest progress towards the BS and still allows the MR to upload the information to the BS before the deadline *T*. The location at which the MR should start forwarding the information to the BS is also derived in the optimization problem. In this case, if the SN is located 400 meters away from the BS, the MR should be located 230 meters away from the SN in the direction towards the BS (Figure 6-4.a). The higher D2D transmission distances of the 'MR closest to BS' scheme with respect to the 'Optimum' proposal (Figure 6-4.a) result in the significant increase in the D2D transmission energy consumption depicted in Figure 6-4.b.

Once the D2D transmission from SN to the optimum MR is completed, the MR needs to store and carry the information towards the BS from the location identified in Figure 6-4.a. Figure 6-5.a shows the time that the optimum MR stores and carries (SC) the information in order to minimize the total energy consumption ('Optimum' in Figure 6-5). Figure 6-5.a shows that if an SN is located 500 meters away from the BS, the optimum MR needs to store and carry the information for 96 seconds before transmitting it to the BS using cellular communications. The obtained results indicate that when the SN is close to the BS, the optimum MR does not need to store and carry the information. The MR should instead forward it to the BS as soon as received from the SN. This is because the energy consumption of the store and carry process does not compensate the energy savings resulting from forwarding the information at distances closer to the BS. Despite the fact that the optimum MR does not store and carry the information, the results depicted in Figure 6-5.b show non null SC energy consumption levels when SN is close to the BS. This is because the SC energy consumption also includes the storage energy consumption at SN and MR while transmitting and receiving the information (P_R and P_W in Figure 6-3). As the distance from SN to the BS increases, the optimum MR needs to store and carry the information so that its cellular transmission starts closer to the BS where higher cellular data rates are possible. However, for high distances between SN and BS, the time the MR stores and carries the information to minimize the total energy consumption slightly decreases. The results depicted in Figure 6-5.b also show that the SC energy consumption levels increase with the distance between SN and BS. These two effects are due to the increase in the time

needed to complete the D2D (Figure 6-4.a) and cellular transmissions (Figure 6-6.a). Figure 6-6.a shows the time the optimum MR needs to transmit the information to the BS using its cellular radio interface, while Figure 6-6.b reports the resulting cellular transmission energy consumption levels. The results depicted in Figure 6-6.a also show that an optimum configuration of opportunistic forwarding reduces the time needed to complete the MR-BS cellular transmission compared to the time needed by traditional single-hop cellular communications to complete the SN-BS cellular transmission ('1-hop cellular'). This actually demonstrates that the use of opportunistic MCN communications can also provide significant capacity gains at the network level.

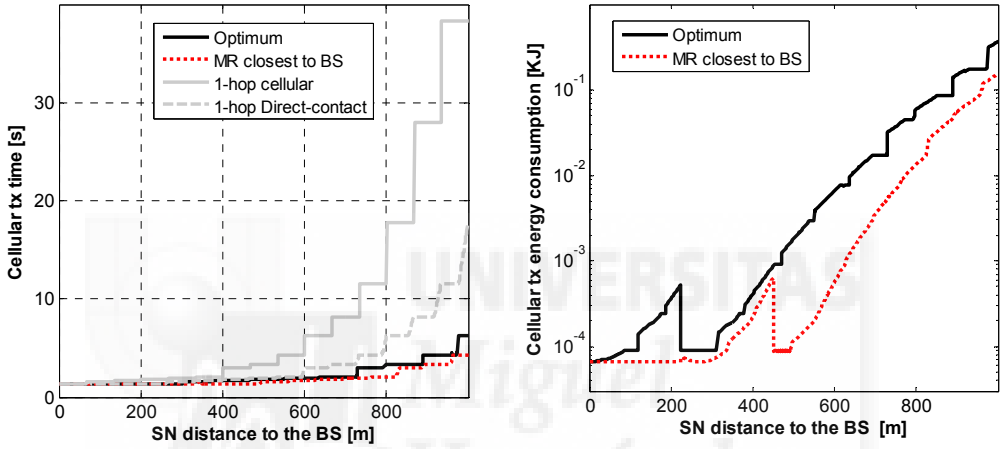

a) Time the MR requires to transmit the data to the BS

b) Cellular transmission energy consumption

Figure 6-6. Optimum configuration of two-hop opportunistic MCN communications: cellular transmission.

The impact of selecting the MR that provides the highest progress towards the BS ('MR closest to BS' in Figure 6-5) on the store and carry process is twofold. First, the time the MR stores and carries the information (Figure 6-5.a) is reduced compared with the optimum configuration ('Optimum'). For example, if SN is located 500 meters away from the BS, the time the MR stores and carries the information is reduced to 78 seconds. Second, the SC energy consumption levels (Figure 6-5.b) increase compared to the optimum configuration despite reducing the time the MR stores and carries the information (Figure 6-5.a). These two trends are observed because of the higher time necessary for finishing the D2D transmission from SN to MR when MR is selected as close as possible to the BS (Figure 6-4.a). This reduces the time needed to upload the information to the BS (Figure 6-6.a), and therefore the cellular transmission energy

consumption (Figure 6-6.b). However, it also results in shorter times available for the MR to store and carry the information, and therefore increases the energy consumption at SN and MR while transmitting and receiving the information (P_R and P_W), respectively.

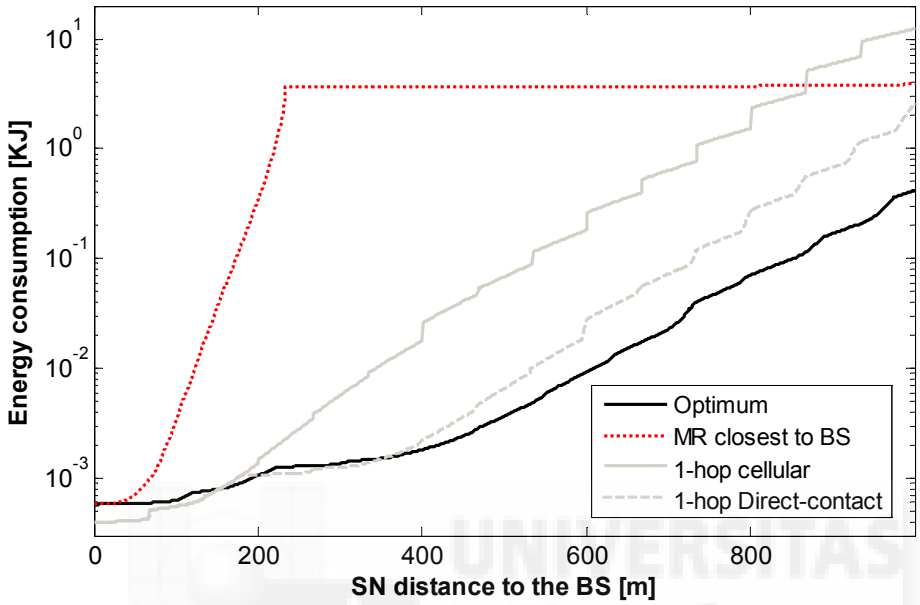

Figure 6-7. Optimum configuration of two-hop opportunistic MCN communications: Total energy consumption.

Using the configurations illustrated in Figure 6-4, Figure 6-5 and Figure 6-6, the optimum MR location ('Optimum') results in significant total energy savings for the end-to-end transmission of the file before *T* from SN to BS (Figure 6-7). On average, the total energy consumption can be reduced by 98% when using the derived optimum configuration for opportunistic MCN communications with respect to the 'MR closest to BS' approach. The lower cellular transmission energy consumption levels (Figure 6-6.b) obtained when selecting the MR as close as possible to the BS cannot compensate the higher D2D transmission (Figure 6-4.b) and SC (Figure 6-5.b) energy consumption levels. The obtained results clearly demonstrate the need to adequately configure opportunistic MCN communications to achieve the desired objectives in terms of energy efficiency.

The energy consumption of traditional single-hop cellular communications has also been evaluated and is reported in Figure 6-7. The '1-hop cellular' configuration refers to the case in which the static SN transmits the file directly to the BS. In the '1-hop Direct-contact' configuration, the SN is mobile, and can store, carry and forward the

information to the BS without using a mobile relay; this scheme is usually referred to as Direct-contact in the literature [111]. For a fair comparison, the '1-hop Direct-contact' configuration follows a similar optimization process to that reported in Section 6.3 to derive the optimum location at which the moving SN should start forwarding the information to the BS in order to minimize the total energy consumption. The obtained results show that when SN is very close to BS, there are no energy benefits from using opportunistic MCN communications compared to single-hop cellular schemes. However, as the distance increases, an optimum configuration of opportunistic MCN communications can significantly reduce the total energy consumption compared to single-hop cellular schemes; please note that energy consumption levels in Figure 6-7 are shown in logarithmic scale. For example, when SN is 300 meters away from the BS, the optimum configuration ('Optimum') reduces the total energy consumption by approximately 75% compared to traditional single hop cellular communications ('1-hop cellular'). The reduction augments to approximately 98% at the cell edge. The Direct-contact scheme ('1-hop Direct-contact') reduces the total energy consumption compared to traditional single-hop cellular communications (on average by 85%), but cannot achieve the total energy consumption levels that an optimum configuration of opportunistic MCN communications can reach. In fact, such optimum configuration can reduce the total energy consumption by up to 85% (on average by 77%) compared to the Direct-contact scheme. In addition, the '1-hop Direct-contact' scheme cannot reach the capacity benefits shown by the optimum configuration in Figure 6-6.a in terms of the time needed to upload the information to the BS.

6.5 Influence of Traffic Characteristics on the Energy Consumption of Opportunistic MCN

The study conducted in Section 6.4 has derived optimum configurations of opportunistic MCN communications (i.e. the optimum MR location and the location at which the MR should start forwarding the information to the BS) and their corresponding energy consumption levels. The analytical framework presented in Section 6.3 showed that the optimum opportunistic MCN configuration depends on the traffic characteristics (T and F) of the mobile delay tolerant service. This section therefore investigates the impact of such traffic characteristics on the total energy consumption, and how opportunistic MCN communications should be configured to exploit traffic characteristics in order to reduce the energy consumption. This study also considers that a static SN wants to upload a message of size F to the BS before a

deadline *T*. The term message will refer in this section to the information data that needs to be uploaded to the BS before the service-dependent delay tolerance (*T*) elapses. For example, it could represent the entire file in the case of cloud/email services, or a set of grouped fragments in the case of mobile video traffic (see Section 6.2). This analysis is also conducted through numerical resolution of the analytical framework described in Section 6.3. The optimization problem has been thus solved by means of brute force techniques implemented in Matlab for all possible distances between SN and BS, and for a wide set of traffic characteristics *T* and *F* representing different delay tolerant mobile traffic services.

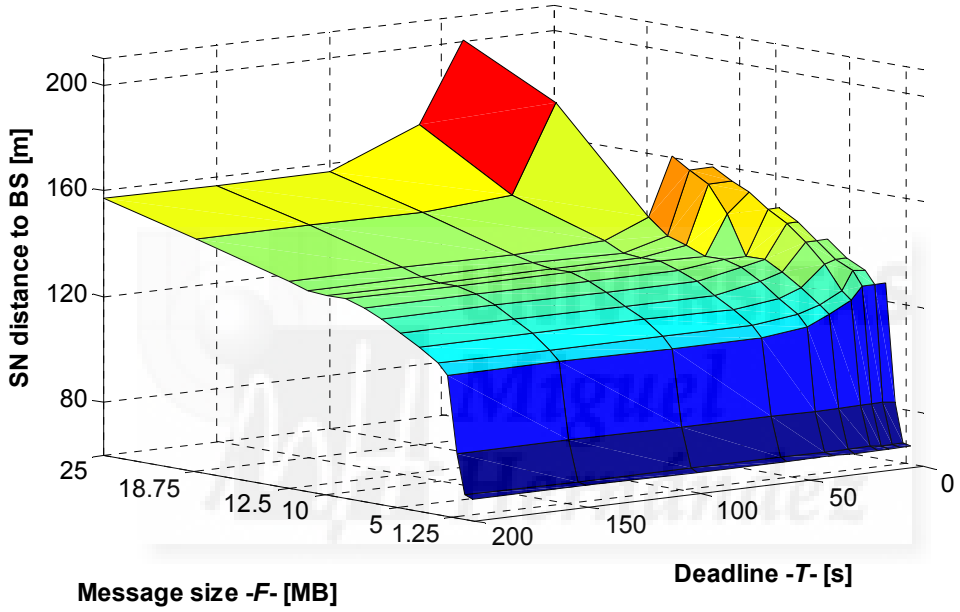

Figure 6-8. SN distance to the BS from which two-hop opportunistic MCN communications are more energy efficient than single-hop cellular communications. The distance is depicted as a function of the size of the message to be transmitted (*F*) and the traffic-dependent deadline (*T*).

The energy consumed by opportunistic MCN communications is first compared against that consumed in traditional single-hop cellular ('1-hop cellular', direct cellular connection between SN and BS). Figure 6-8 shows the SN distance to the BS from which two-hop opportunistic MCN communications are more energy efficient than 1-hop cellular communications. The results are shown for a variety of *F* and *T*, and have been obtained considering a cell radius of 1000 meters and mobile MRs moving towards the BS at pedestrian speed (2 m/s)[18]. The depicted results show that the SN distance to the

[18] The rest of parameters for the evaluation conducted in this section are those already presented in Table 6-1.

BS from which opportunistic MCN communications are more efficient than single-hop communications increases with increasing values of *F*. This means that with messages of larger size, opportunistic MCN communications can be more energy efficient if SN is not close to the BS. This is due to the fact that large messages increase the E_{D2D} and E_{SC} energy consumption levels in the opportunistic MCN connection. To reduce the overall energy consumption with respect to single-hop cellular communications, high energy savings from the MR-BS cellular transmission are hence necessary to compensate the increased E_{D2D} and E_{SC} levels. Opportunistic MCN communications can achieve such savings with increasing SN-BS distances because of the lower single-hop energy efficiency at large distances to the BS, and the use of store, carry and forward schemes with mobile relays. This is actually reflected in Figure 6-9 that shows the total energy consumption for 1-hop cellular and opportunistic MCN communications as a function of the SN-BS distance (*F*=5 MB and *T*= 150 seconds)[19]. Figure 6-9 shows that an optimum configuration of opportunistic MCN communications can significantly reduce the total energy consumption for SN-BS distances larger than 140 meters. For example, when SN

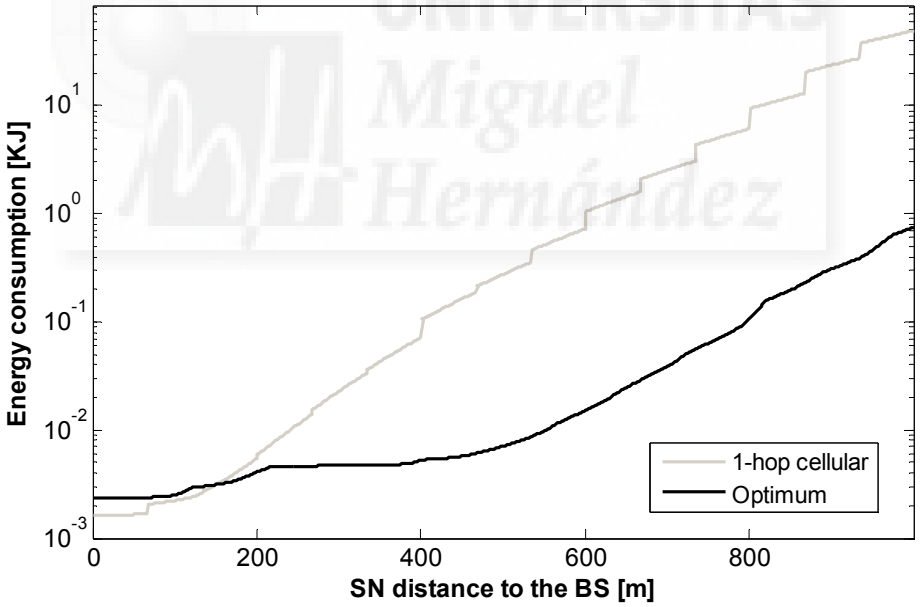

Figure 6-9. Total energy consumption as a function of the distance between SN and BS when *F*=5 MB and *T*=150 seconds.

[19] Note that the results presented in Figure 6-9 are similar to those already shown in Figure 6-7 for different traffic characteristics. While the results shown in Figure 6-7 were obtained with *F*=10 Mb and *T*=100 s, the results in Figure 6-9 are obtained with *F*=5 MB and *T*=150 s. However, similar trends are observed in both figures.

is located 250 meters away from the BS, opportunistic MCN communications reduce by 60% the energy consumption compared with traditional single-hop cellular communications. This gain increases above 90% for distances between SN and BS higher than 350 meters. Figure 6-9 has been obtained considering LTE for the cellular transmissions. Simulations were also conducted with HSPA (see Annex A), and the same trends were observed with slightly smaller energy gains for opportunistic MCN communications compared to when using LTE. This is the case because of the higher LTE transmission rates that benefit opportunistic MCN communications as the MR moves towards the BS and forwards the information to the cellular network.

Figure 6-8 also shows that the SN distance to the BS from which opportunistic MCN communications are more energy efficient than single-hop cellular communications increases when the message deadline *T* is small. This is the case because small deadlines do not provide sufficient time to exploit the store and carry process, and the MR forwards the message to the BS as soon as received. When *T* increases, the SN-BS distance from which opportunistic MCN communications achieves higher energy efficiency than single-hop cellular communications does not vary with *T*. However, *T* has an impact on the average reduction in total energy consumption of opportunistic MCNs compared to single-hop cellular communications. Such impact is shown in Table 6-2 as a function of the distance between SN and BS. As previously discussed, opportunistic MCN communications do not provide an energy gain when SN is close to the BS (SN-BS distances below 100 meters); Table 6-2 shows that this trend is independent of the deadline *T*. When the SN-BS distance increases, opportunistic MCN communications can significantly reduce the energy consumption compared to single-hop cellular communications, reaching reduction levels near 100% under certain conditions. In fact, the obtained results show that for a fixed deadline *T*, opportunistic MCN communications achieve its higher energy gains compared to single-hop cellular communications when the distance from SN to the BS increases. When this distance increases, opportunistic MCN communications achieve their higher possible energy gains compared to single-hop cellular communications when *T* also increases, but up to a certain limit. For example, when SN is at a distance to the BS between 401 and 500 meters, the maximum energy reduction is reached for *T*=200 seconds, and no further gains are achieved for higher values of *T*. Increasing *T* allows reducing the D2D distance at which SN should start the transmission to MR, as well as the distance to the BS at which MR should start the cellular transmission to reduce the total energy consumption. Reducing such distances decreases the energy consumption in the D2D and cellular transmissions (see Figure 6-4 and Figure 6-6 in Section 6.4) but increases the energy

consumption of the store and carry process at the MR (see Figure 6-5 in Section 6.4). The results depicted in Table 6-2 clearly show that for a given SN-BS distance, there is a *T* threshold (T_{thr}) from which the D2D and cellular transmission energy savings do not compensate the increased store and carry energy consumption levels. For the scenario under study, it can be derived such *T* threshold (T_{thr}) that depends on the location of SN (represented by means of the SN-BS distance – X_i), the distance from the SN to the optimum MR location ($dist_{SN\text{-}MR}$), and the speed at which MR moves towards the BS (v), as follows:

$$T_{thr} \approx \frac{X_i - dist_{SN-MR}}{v} \quad (6\text{-}16)$$

It should be also noted that Table 6-2 does not show any values when *T*=40 seconds and the SN-BS distance increases beyond 700 meters. This is the case because under these conditions, it is not possible to establish an opportunistic MCN connection that can transmit the complete 10 MB message before the *T* deadline expires. Since such connection is not possible, a comparison with traditional single-hop cellular communications is not feasible.

Table 6-2. Average energy reduction (in %) of opportunistic MCN communications compared to single-hop cellular communications for different values of *T* and *F*= 10 MB.

SN-BS distance [m]	***T* [s]**			
	40	**100**	**200**	**300**
1-100	-33.0	-33.0	-33.0	-33.0
101-200	3.1	3.1	3.1	3.1
201-300	50.3	58.0	58.7	58.7
301-400	70.2	85.5	88.3	88.3
401-500	80.8	93.7	97.1	97.1
501-600	80.5	94.3	98.7	99.2
601-700	82.7	95.4	99.3	99.7
701-800	-	95.5	99.4	99.8
801-900	-	95.7	99.5	99.9
901-1000	-	94.9	99.4	99.9

The energy gains of opportunistic MCN communications depend on an adequate selection of the MR. For example, Section 6.4.2 showed that selecting an MR as close as possible to the BS (referred to as 'MR closest to BS' in this study) can reduce the energy consumed in the cellular transmission (Figure 6-6), but this is done at the expense of higher energy consumption levels in the D2D transmission (Figure 6-4) that can increase

the total energy consumption (Figure 6-7). It is therefore necessary to derive the optimum MR location that minimizes the overall energy consumption, and analyze its dependence with the traffic service characteristics. Figure 6-10 shows the optimum MR location to start the D2D transmission as a function of the distance between SN and BS. The MR location is represented by means of the distance between SN and MR. Figure 6-10.a shows for example that if SN is located 600 meters away from the BS, the MR should be ideally located 88 meters away from SN in the direction of the BS in order to minimize the total energy consumption. The results depicted in Figure 6-10.a show that the distance between SN and MR that minimizes the energy consumption increases with the distance between SN and BS, and that it does not vary with the message size *F* (fixing the message deadline *T* to 100 seconds). On the other hand, Figure 6-10.b shows that, for a given location of SN, the distance from SN to MR that minimizes the overall energy consumption decreases as *T* increases (*F* is set to 6.25 MB). With increasing values of *T*, MR has more time to store and carry the information, and therefore can reduce the D2D distance with SN, and hence the total energy consumption. On the other hand, when the traffic service is characterized by lower *T* deadlines, opportunistic MCN communications should increase the D2D distance to start the cellular forwarding process closer to the BS and reduce the total energy consumption. In this context, for the scenario under study, it is possible to derive an expression to calculate the optimum MR location (represented by means of the distance between SN and MR – $dist_{SN\text{-}MR}$) as a function of the SN-BS distance (X_i) and the time available to upload the message to the BS (T) as follows:

$$dist_{SN-MR} \approx \left(-5 \cdot 10^{-4} \cdot T + 0.2\right) \cdot X_i + 1 \qquad (6\text{-}17)$$

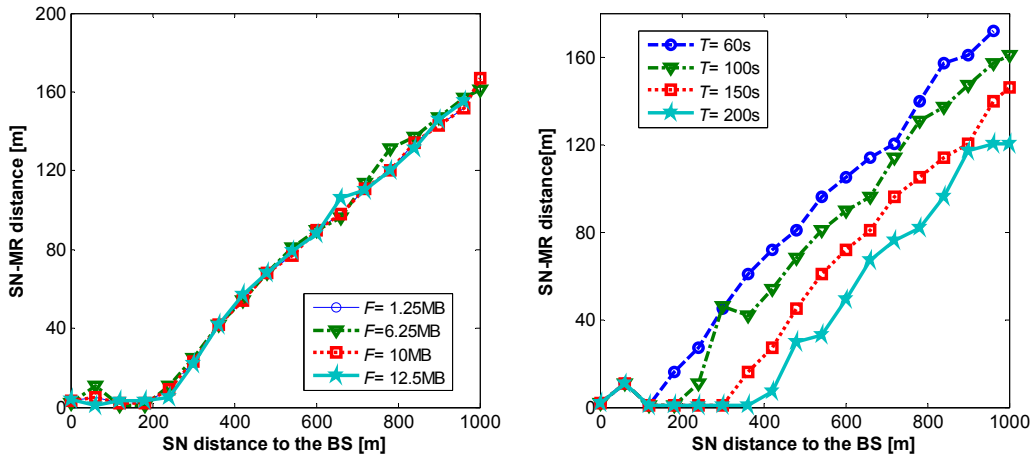

a) *T*=100 seconds b) *F*=6.25 MB

Figure 6-10. Optimum MR location that minimizes the total energy consumption for opportunistic MCN communications. The MR location is shown as a function of the distance between SN and BS and varying service characteristics (*F* and *T*).

6.5.1 Mobile Video Traffic

The relevance of mobile video traffic in current and forecasted cellular data traffic statistics requires a specific analysis of the energy benefits that could be achieved when using opportunistic MCN communications to transmit mobile video traffic. In fact, opportunistic MCN communications can take advantage of the buffers that video players implement to keep the video content ahead of playback time. This allows grouping the video content fragments to postpone their transmission at no cost to the perceivable QoE as long as the playback is not interrupted. Figure 6-11 compares the average energy consumption in the transmission of a mobile video file using traditional single-hop cellular communications and opportunistic MCN communications (results are shown in relative units). The results are shown for the case in which a traditional Adaptive Streaming (AS) scheme is used to upload the multiple video fragments [127] (bars marked as AS). The opportunistic MCN energy consumption is also evaluated when video content fragments are grouped into messages of 1 MB, 2 MB, 3 MB and 4 MB. In this case, the video messages are equivalent to 10 seconds, 20 seconds, 30 seconds and 40 seconds of playback [127] respectively. As a result, a 1MB-10s traffic configuration requires that the opportunistic MCN transmission of the 1 MB message from SN to BS concludes before 10 seconds to avoid the video playback to freeze. This study considers the average YouTube video size (7.6 MB) reported in [145]. In the case of the 1MB-10s

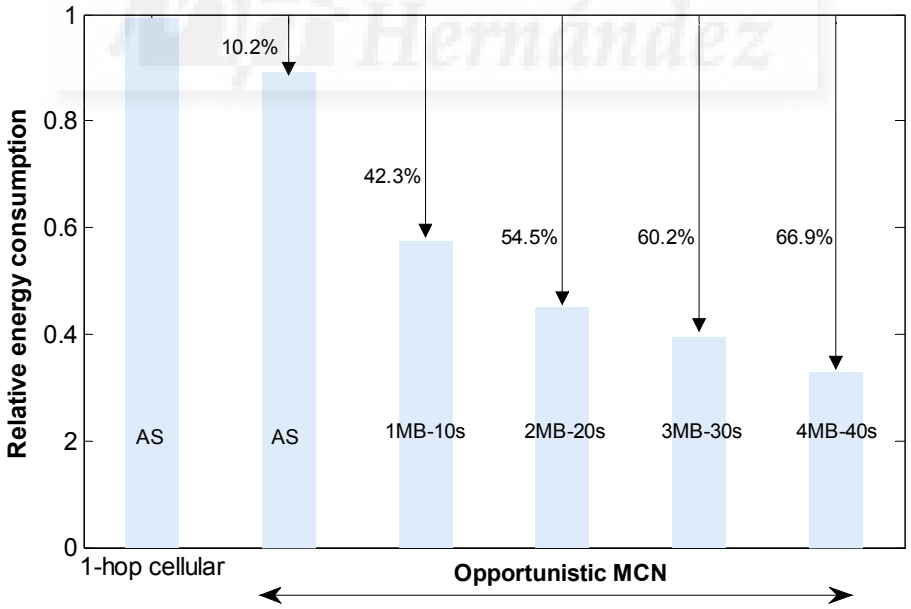

Figure 6-11. Average energy consumption to transmit a 7.6 MB video file (results shown in relative units). Video content fragments of 1 MB, 2 MB, 3 MB and 4 MB (equivalent to 10 s, 20 s, 30 s and 40 s of playback) are grouped in the case of opportunistic MCN.

traffic configuration, eight opportunistic MCN transmissions from SN to BS are necessary to complete the video transmission (seven transmissions of 1 MB plus one transmission of 0.6 MB). It is considered that the time available to transmit the 0.6 MB video fragment from SN to BS is also equal to 10 seconds. This is the case because the time available to transmit this fragment is related to the buffered data in the playback from the previous transmission (1 MB video fragment with 10 seconds of playback). A 4MB-40s traffic configuration would only require two transmissions (1x4 MB + 1x3.6 MB) with the maximum time available (deadline *T*) for each one equal to 40 seconds. Each of these opportunistic MCN transmissions is initiated at the same location of the SN but uses different MRs (always at the same location for a given traffic configuration, Figure 6-10.a) as MRs are mobile. The energy consumption levels shown in Figure 6-11 for opportunistic MCN communications correspond then to the sum of the energy consumption in each one of the transmissions necessary to complete the video file transference. The energy consumption values shown in Figure 6-11 have been averaged for all possible distances between SN and BS considering a cell radius of 1000 meters and MRs moving towards the BS at 2 m/s[20].

Figure 6-11 shows that opportunistic MCN communications can considerably reduce the average energy consumption with respect to single-hop cellular communications. The reduction is particularly relevant when video content fragments are grouped. In fact, the reduction increases with the number of video content fragments that are grouped. For example, the reduction increases from 42.26% with the 1MB-10s traffic configuration to 66.87% with the 4MB-40s traffic configuration. This is due to the fact that opportunistic MCN communications can benefit from increasing values of the transmission deadline *T* since the MR would have more time to store and carry the information, and therefore reduce the D2D distance, the cellular distance with the BS, and finally the total energy consumption (as analyzed in Section 6.5). The message deadline *T* in mobile video traffic, and therefore the energy benefits of opportunistic MCN communications, increase with the amount of video content fragments that are grouped. It should be noted that this is at the expense of a higher delay in the transmission of the first message, which can determine the start of the playback. For example, the first message (set of grouped video content fragments) is uploaded to the BS before 10 seconds elapse in the case of the 1MB-10s traffic configuration. On the other hand, it could take up to 40 seconds to receive the first 4 MB message in case of the 4MB-40s traffic configuration.

[20] The rest of parameters used in the study are the same as those already presented in Table 6-1.

6.6 Summary and Discussion

5G cellular networks will require innovative solutions to tackle with the capacity and energy challenges resulting from the exponential growth of data traffic as mobile users are increasingly taking a *prosumer* role. Such innovative solutions should not solely rely on new radio access technologies and the massive deployment of small BSs, but also need to exploit the characteristics of the cellular data traffic at no cost to the user QoE. Some of the services driving the mobile data growth are characterized by certain delay tolerance. In this context, this chapter investigates how the adoption and design of opportunistic store, carry and forward mechanisms in MCNs can help significantly decrease the energy consumption for delay tolerant traffic. To this aim, the study first derives an analytical framework to identify in two hop scenarios the optimum mobile relay location and the location from which the mobile relay should start forwarding the information to the cellular base station in order to minimize the overall energy consumption. The obtained results show that significant energy gains can be achieved (on average up to 90%) compared to traditional single-hop cellular transmissions. This study has also analyzed the impact of traffic characteristics of delay tolerant services on the energy gains that can be reached with opportunistic MCN communications, and how opportunistic MCN communications should be configured to exploit the traffic delay tolerance in order to reduce the overall energy consumption. The obtained results have shown that the energy reduction levels with respect to traditional single-hop cellular communications can be above 95% under certain conditions (e.g. with increased traffic delay tolerance thresholds and the increased distance of the source node to the serving base station). Particular attention has been paid to the case of mobile video traffic that accounts for a very significant portion of current and forecasted mobile data traffic. The conducted analysis has shown that by grouping video content fragments, mobile video traffic and opportunistic MCN communications can provide significant energy savings in cellular networks at no cost to the perceived QoE. The conducted study has focused on deriving optimum configurations that can be used as performance bounds. This is the case because it is hardly likely that in a real scenario an MR can be found at the identified optimum location and time instant. The optimum locations should then be considered as reference points from where to look for other neighboring MRs. In this context, the derived analytical framework can be used as a benchmark for the design of more realistic opportunistic forwarding schemes in MCN systems exploiting D2D communications.

UNIVERSITAS
Miguel
Hernández

7

Context-Aware Opportunistic Forwarding in MCN

The study conducted in Chapter 6 has identified optimum configurations for two-hop opportunistic MCNs using mobile relays and D2D communications. In particular, the study has identified the optimum MR location and the location at which the MR should start forwarding the information to the BS in order to minimize the overall energy consumption. This optimum configuration can help establish an energy-efficiency performance bound. This is the case because the derived optimum configuration assumes that an MR can be found when needed at the identified optimum location, which might not always be the case in a real world network deployment. To address this scenario, this chapter presents novel context-aware opportunistic forwarding schemes designed to facilitate the selection of an MR when no device is available at the identified optimum location and time instant. The proposed solutions build from the optimum MCN configuration and MR location identified in Chapter 6, and exploit context information provided by the cellular infrastructure to search for candidate MRs. The first proposal –that is presented in Section 7.2 and that is referred to as 'Time-dependent opportunistic forwarding' (DELAY, in short)– delays the start of the D2D transmission until an MR is found at the identified optimum location. The second proposal –that is presented in Section 7.3, and that is referred to as 'Space-dependent opportunistic forwarding' (AREA, in short)– increases the search area where to look for potential MRs

around the optimum MR location. These two approaches improve the feasibility of integrating opportunistic forwarding schemes into cellular networks in a practical setting since they relax the need for an MR to be located at the identified optimum location and time instant. Section 7.4 compares the performance of the two context-aware opportunistic forwarding proposals under different evaluation settings, and analyzes the conditions under which each proposal outperforms the other.

7.1 Context-Awareness in MCNs

Context-awareness is increasingly gaining research attention as a means of taking advantage of context-information (user preferences, social relationships, network state, spectrum availability and characteristics, link conditions, interference levels, operating conditions) to improve the operation and efficiency of networks in general, and MCNs in particular. For example, the study reported in [146] proposes a centralized scheme where the cellular BS selects the mobile relay for a two-hop MCN connection with the longest multi-hop link duration. To do so, the BS collects GPS information about the location of mobile nodes using measurement report messages. The infrastructure-assisted selection of mobile relays is shown to minimize the relay switching rate and increase the system throughput. In [147], the authors exploit context information to reduce inter-cell interference in MCNs. In particular, the study presented in [147] divides cells into sub-cells characterized by a radius of several orders of magnitude smaller than the cell radius. By adjusting the sub-cell-radius (using context-information such as intercell and intersession interferences), the proposal jointly optimizes scheduling, routing and power control to obtain the optimum tradeoff between throughput, delay and power consumption in MCNs.

Leading international activities [148] have also recognized the importance to exploit context information in cellular networks in order to manage the adequate time or location where certain wireless transmissions should take place in order to optimize spectral and energy efficiency. A first approximation towards this assessment is presented in [149] where the authors demonstrate that the performance of opportunistic networking can be improved when exploiting context information. In particular, the authors propose to exploit the spatial and temporal features of context information for more efficient forwarding decisions. The study proposes a social context-based routing scheme that is used to predict the context of nodes, so that devices know when and where they should start forwarding messages in order to minimize the transmission delay and network overhead. The benefits of using context

information and device's storing capabilities have been also demonstrated in [150] to reduce peak traffic demands. In particular, the authors explore in [150] the proactive caching concept through which files are proactively cached on users' smart mobile devices during off-peak periods based on the file popularity and correlations among user and file patterns. Files are then disseminated to other users via D2D communication. Numerical results demonstrate that the proposed proactive caching paradigm can increase by up to 25% the ratio of satisfied users. A similar approach is presented in [151] that exploits context-information to predict mobile user behavior related to consumption of content. Content prediction and mobility information is exploited in [151] to change the time and location where content is delivered to the user in order to increase network efficiency and improve user service perception. The work presented in [152] also exploits opportunistic D2D sharing to offload the traffic from cellular links to local communications among users. In [152], a subset of mobile users is initially selected as seeds based on their content spreading impact (extensive study on the selection of the target set of mobile users is presented in [153]). Then, selected users share the content via opportunistic local connectivity using WiFi-Direct. The conducted evaluation shows that the cellular traffic can be reduced by 63-85% while satisfying the users' delay requirements.

Previous studies have shown that the use of context information can result in important benefits for opportunistic networking and mobile relaying solutions. In this context, this study investigates the design of realistic opportunistic forwarding schemes in MCNs that exploit context information already available in cellular networks to reduce the energy consumption and increase the system capacity in MCNs that utilize mobile relays and D2D communications.

7.2 Time-dependent Opportunistic Forwarding: DELAY

The DELAY proposal uses the optimum MR location identified in Chapter 6, but delays the start of the D2D transmission until an MR is found at the identified optimum location. The space-time graph shown in Figure 7-1 is used to represent and compare the operation when considering the optimum configuration identified in Chapter 6 ('Optimum'), and the time-dependent proposal that delays the D2D transmission until an MR reaches the identified optimum location ('DELAY'). For the optimum configuration, the D2D transmission between SN_i and the optimum MR located at Opt_X_i starts at time instant τ_0. MR then stores and carries the information from Opt_X_i until it reaches the Opt_Y_i location at time instant τ_c, and initiates the cellular transmission. The

DELAY proposal considers the scenario in which SN_i cannot find an MR at the optimum location (Opt_X_i) at time instant τ_0. In this case, the proposed scheme delays the D2D transmission until an MR arrives at Opt_X_i. We denote as t the time SN_i should delay the D2D transmission to guarantee with certain probability that an MR reaches the identified optimum location (additional details are presented below). When such node reaches the optimum location, SN_i can start the D2D transmission. MR would again store and carry the information before starting the cellular transmission to the BS. The cellular transmission cannot start at the location Opt_Y_i and time τ_c when implementing the DELAY proposal since SN_i had to delay the start of the D2D transmission. However, the complete transmission has to still end before the deadline T. In this case, MR would start the forwarding process to the cellular BS at location Y'_i (further away from the BS than Opt_Y_i) and time τ'_c.

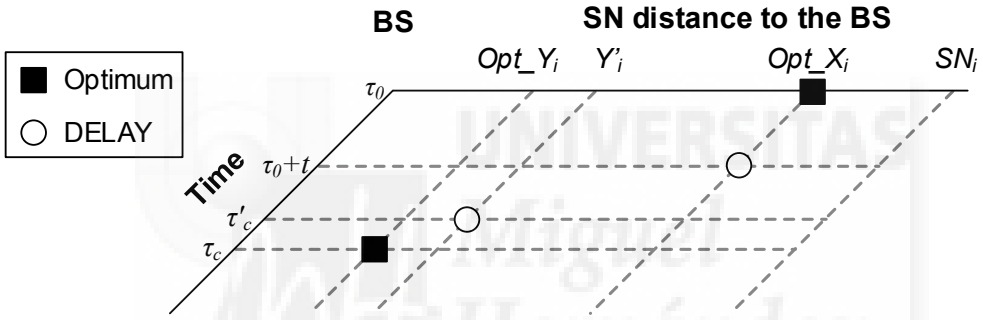

Figure 7-1. A graphical representation of two-hop opportunistic MCN communications for the optimum configuration and the DELAY proposal.

The DELAY scheme requires SN to delay the D2D transmission for t seconds until an MR reaches the optimum MR location identified in Chapter 6. The time t has to be selected conditioned to the fulfillment of the following two conditions. First, it is necessary to guarantee with certain probability that at least one MR reaches the identified optimum MR location before t seconds elapse. This thesis proposes to define and establish this probabilistic requirement using context information that can be extracted from cellular networks, in particular statistical information about the spatial density and distribution of mobile nodes within a cell. This information is already available in current cellular systems and can be obtained at no further cost since mobile terminals are required to register their location with the serving BS. Even a more accurate identification of the mobile devices location can be achieved with cellular standards such as HSPA and LTE that define concentric rings where mobile users utilize different transmission modes based on radio link quality parameters (e.g. signal strength

or CQI). The second condition is that, despite the delay in the D2D transmission, the BS must still receive the complete file before the service-dependent deadline *T*. This condition must be satisfied independently of whether SN has to exhaust or not the delay time *t* to find an MR at the identified optimum location. If these two conditions are not fulfilled, a satisfactory opportunistic MCN transmission is considered unfeasible, and SN should directly transmit the information to the cellular BS through a traditional single-hop cellular link.

7.2.1 Uniform Distribution of Nodes within the Cell

The parameter *t* represents the time SN needs to delay the start of the D2D transmission in order to guarantee with certain probability the arrival of at least one MR at the identified optimum MR location. To determine its value, this study first considers that mobile devices are uniformly distributed within the cell. Using the Poisson distribution[21], the probability that an MR reaches the identified optimum MR location can be calculated as follows [154]:

$$P_{Opt\_X_i} = P\left(x>0;\mu' t\right) = 1 - P\left(x=0;\mu' t\right) = \\ 1 - \frac{\left(\mu' t\right)^0 \cdot \exp\left(-\mu' t\right)}{0!} = 1 - \exp\left(-\mu' t\right),\ \forall Opt\_X_i \in \left(1,\ldots,R\right) \quad (7\text{-}1)$$

where μ' represents the average arrival rate of MRs to the identified optimum MR location (actually to any location within the cell), and *t* corresponds to the inter-arrival delay time or the time to the next arrival of an MR to the identified location. μ' is computed using the average number of MRs (μ) uniformly distributed within a cell of radius *R* and the nodes' speed *v* as follows:

$$\mu' = \frac{\mu \cdot v}{R} \quad (7\text{-}2)$$

The time *t* that guarantees with probability δ (i.e. $P_{Opt\_Xi} = \delta$) the arrival of an MR at the identified optimum MR location Opt_X_i can be expressed as shown in equation (7-4):

$$P_{Opt\_X_i} = 1 - \exp\left(-\mu' \cdot t\right) = \delta \quad (7\text{-}3)$$

$$t = \frac{R \cdot \ln\left(1-\delta\right)}{-\mu \cdot v} \ \ iff\ \exists\ Y'_i = \underset{\tau'_{b-1}=\tau_{b-1}+t}{\arg\min}\left(\vartheta\left(\ldots\right)\right) \quad (7\text{-}4)$$

[21] Poisson methods have been demonstrated to correctly model the number of isolated points that are expected to fall within a particular region, and also the arrival rate and inter-arrival time of nodes to a specific location based on characteristics such as the node's speed [154][155].

As shown in equation (7-4), the time *t* that guarantees the arrival of at least one MR at the identified optimum MR location is proportional to the cell radius (*R*) and inversely proportional to the average spatial density of nodes within the cell (μ/R) and to the nodes' speed (*v*). In addition, *t* increases with the probability δ guaranteeing the presence of the MR at the identified optimum MR location. It is important to note that the derived delay time *t* represents the worst case, i.e. the maximum time the SN should delay the D2D transmission waiting for an MR to reach the optimum MR location. In this context, the time *t* can be found if and only if (*iff*) the condition shown in equation (7-4) is also fulfilled. The condition requires that there exists a suboptimum solution Y'_i of the optimization problem (θ) presented in Chapter 6. This solution is obtained considering that the D2D transmission would finish at time instant $\tau_{b-1}+t$ (the optimum configuration needs τ_{b-1} to conclude the D2D transmission from SN to MR). If this condition is met, it is possible to establish the two-hop opportunistic MCN link to transmit the information from SN to the BS before the service-dependent deadline *T*. If the condition is not met, SN will transmit the information directly to the BS through a traditional single-hop cellular link.

7.2.2 Non-uniform Distribution of Nodes within the Cell

The time *t* can also be computed when the distribution of users within the cell is non-uniform. Without loss of generality, this study considers a distribution in which the spatial density of nodes is higher close to the BS. This is actually a common assumption in the literature since it represents scenarios where BSs are deployed to provide coverage to frequently visited places. Following [156], the mathematical model of this non-uniform distribution has been represented by means of a truncated Normal distribution centered at the position of the cellular BS. The truncated Normal distribution can be expressed as follows [154]:

$$P(x;s,\sigma,a,b)=\begin{cases}\dfrac{\phi\left(\dfrac{x-s}{\sigma}\right)}{\sigma\cdot Z}, & if \quad x\in[a,b]\\ 0 \qquad\qquad , & if \quad x\notin[a,b]\end{cases} \tag{7-5}$$

where $\emptyset(x\text{-}s/\sigma)$ represents the probability density function of the standard Normal distribution. The Normal distribution of a random variable *x* with mean *s* and variance σ^2 can be expressed as [154]:

$$P(x;s,\sigma)=\frac{1}{\sqrt{2\cdot\pi}\sigma}\exp\left(-\frac{(x-s)^2}{2\sigma^2}\right), \quad -\infty\le x<\infty \tag{7-6}$$

In equation (7-5), *Z* is the Cumulative Distribution Function (CDF) difference at the upper (*b* \ *x* ∈ [-∞, *b*]) and lower (*a* \ *x* ∈ [*a*, ∞]) bounds:

$$Z = \Phi\left(\frac{b-s}{\sigma}\right) - \Phi\left(\frac{a-s}{\sigma}\right) \tag{7-7}$$

being the CDF defined as:

$$\Phi(x) = F(x) = P(X \le x) = \int_{-\infty}^{x} P(x; s, \sigma)\, dx \tag{7-8}$$

The probability to find one MR at the identified optimum MR location Opt_X_i can be calculated using equation (7-5) as:

$$P_{Opt\_X_i} = \int_{Opt\_X_i - \varepsilon/2}^{Opt\_X_i + \varepsilon/2} P(x; s, \sigma, a, b)\, dx \tag{7-9}$$

where ε represents the spatial discretization unit. Considering that the average spatial density of nodes in the cell is equal to μ/R, the average spatial density of nodes at Opt_X_i can then be computed as $\mu_{Opt\_Xi} = (\mu/R) \cdot P_{Opt\_Xi}$. Following the indications in [157], the truncated Normal distribution can be discretized into many Poisson distributions as shown in Figure 7-2. In Figure 7-2, μ_i represents the parameter that characterizes the Poisson distribution (i.e. the expected value in general). This allows carrying out a similar analysis to that presented in Section 7.2.1 for the uniform distribution of nodes within the cell (equations (7-1) to (7-4)). In particular, we can calculate the time *t* the SN needs to delay the D2D transmission to guarantee with probability δ the arrival of an MR at the identified optimum location under non-uniform distribution of nodes within the cell. *t* can be calculated as follows:

$$t = \frac{R \cdot \ln(1-\delta)}{-\mu \cdot P_{Opt\_X_i} \cdot v} \;\; iff \;\; \exists\, Y'_i = \underset{\tau'_{b-1} = \tau_{b-1} + t}{\arg\min} \left(\vartheta(\ldots)\right) \tag{7-10}$$

It is important to note that equation (7-10) depends on P_{Opt_Xi} and thus on the optimum MR location (Opt_X_i) within the cell; this is not the case when nodes are uniformly distributed within the cell. The definition of equation (7-10) is also subject to the fulfillment of the condition that there exists a suboptimum solution of the optimization problem (θ) presented in Chapter 6. It this condition is not met, the SN transmits the file to the BS using a traditional single-hop cellular link.

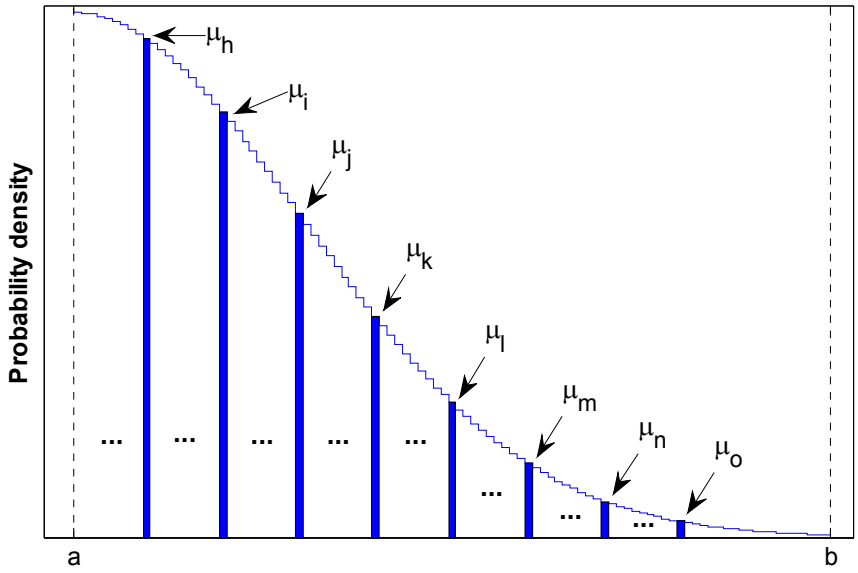

Figure 7-2. Discretization of the truncated Normal distribution into many Poisson distributions.

7.3 Space-dependent Opportunistic Forwarding: AREA

The AREA proposal addresses the scenario in which an MR cannot be found when needed at the identified optimum location by increasing, around the optimum MR location, the search area where to look for potential MRs. The search area is defined using context information provided by the cellular infrastructure (spatial density and distribution of mobile nodes within the cell). It could be the case that more than one MRs are found within the search area. If this is the case, the AREA proposal would select the one that is closer to the optimum MR location (Opt_X_i). Figure 7-3 illustrates the search area around Opt_X_i. In Figure 7-3, r denotes the radius of the search area around Opt_X_i. X'_i represents the location of the selected MR within the search area, and Y'_i the location at which the selected MR will start the cellular transmission to BS. The position Y'_i at which the selected MR will start the cellular transmission to the BS (closer or further away to the BS than the optimum configuration) depends on the initial location of the selected MR (i.e. X'_i).

The area of interest to find potential MRs around the identified optimum MR location needs to satisfy two conditions. The first one is that it must guarantee with certain probability the presence of at least one MR. To compute this probability, and similarly to the process for the DELAY proposal (Section 7.2), this thesis proposes to exploit context information provided by the cellular infrastructure, in particular, statistical information about the spatial density and distribution of mobile nodes within the cell. The second

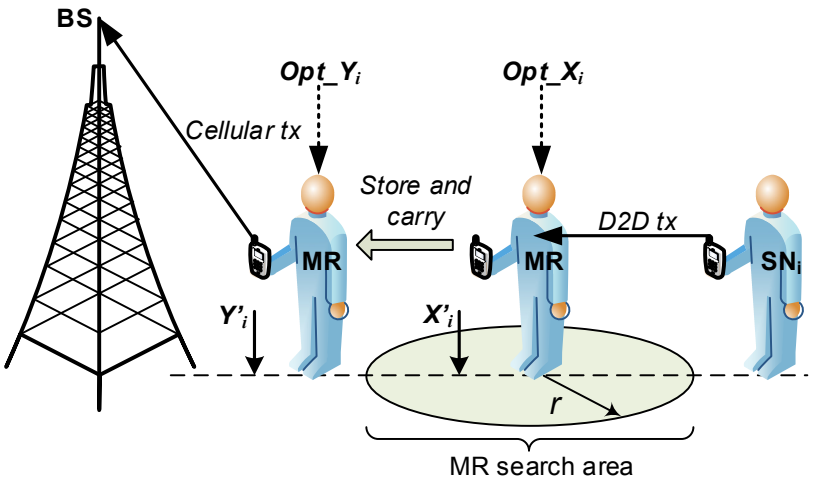

Figure 7-3. Two-hop opportunistic MCN communications for the optimum configuration and the AREA proposal.

condition to define the search area is that it must satisfy the established QoS restriction, i.e. independently of the selected MR within the search area, BS must receive the complete file before the service-dependent deadline *T*. This condition must be satisfied for any possible MR location within the search area. It might then happen that the search area is so large that the end-to-end MCN transmission cannot be completed before the deadline *T*. This may be due to a significant increase of the D2D transmission time when the distance from SN to the selected MR is much larger than the distance from SN to the optimum MR. It might also happen that the distance between the selected MR and SN exceeds the D2D transmission radio coverage limit. When it is not possible to define a search area that fulfills the two conditions, a satisfactory opportunistic MCN transmission is considered unfeasible, and SN transmits the information to the cellular BS using traditional single-hop cellular communications.

7.3.1 Uniform Distribution of Nodes within the Cell

The MR search area is first estimated considering a uniform distribution of mobile devices within the cell. Assuming an average density of μ/R mobile devices uniformly distributed within a cell, and using the Poisson distribution as in equation (7-1), the probability to find at least one MR around an identified optimum location (*Opt_X*$_i$) can be computed as [154]:

$$\begin{aligned} P_{Opt\_X_i} &= P\left(x>0;\frac{\mu}{R}\cdot\phi\right) \\ &= 1-\exp\left(-\frac{\mu}{R}\cdot\phi\right),\ \forall Opt\_X_i \in (1,\ldots,R) \end{aligned} \tag{7-11}$$

where μ is the average number of MRs within the cell of radius R, and $\emptyset$ corresponds to the diameter of the MR search area. It is important to note that equation (7-11) is valid for any Opt_X_i location within the cell. Following equation (7-11), the radius r around Opt_X_i that guarantees with probability δ the presence of at least one MR can be estimated as:

$$r = \frac{R \cdot \ln(1-\delta)}{-2 \cdot \mu} \quad iff \ \exists \ Y'_i = \underset{\forall X'_i \in o(Opt\_X_i, r)}{\arg\min} \ (\vartheta) \tag{7-12}$$

with the diameter of the search area ($\emptyset$) being equal to $2r$. The condition defined in equation (7-12) requires that for every possible location of the selected MR within the search area (X'_i), the optimization problem formulated in Chapter 6 (represented by θ in equation (7-12)) provides the location (Y'_i) at which the MR should start the cellular transmission to the BS that minimizes the total energy consumption and satisfies that the transmission is completed before T. If this condition is met, it is possible to define the MR search area $o(Opt\_X_i, r)$ centered in Opt_X_i and with radius r. If the condition is not met, the SN will transmit the information directly to the BS through a traditional single-hop cellular link.

7.3.2 Non-uniform Distribution of Nodes within the Cell

The search area (defined by the radius r around Opt_X_i) has also been computed when the distribution of users within the cell is non-uniform. As indicated in the definition of the DELAY proposal (Section 7.2), this study considers a non-uniform distribution in which the spatial density of nodes is higher close to the BS. This distribution is mathematically modeled by means of a truncated Normal distribution (equation (7-5)). Equation (7-9) estimates the probability P_{Opt_Xi} that one MR is located at the identified optimum MR location. Using equation (7-9), the probability to find one MR within the search area can be defined as a function of r:

$$P_{SearchArea}(r) = \int_{Opt\_X_i - \varepsilon/2 - r \cdot \varepsilon}^{Opt\_X_i + \varepsilon/2 + r \cdot \varepsilon} P(x; \mu, \sigma, a, b)\, dx \tag{7-13}$$

where ε represents the spatial discretization unit. If we consider that there are on average μ MRs within the cell, the probability to find at least one MR within the search area around the identified optimum MR location Opt_X_i can be calculated as:

$$\left(1 - \left(1 - P_{SearchArea}(r)\right)^{\mu}\right) \tag{7-14}$$

In this context, the minimum radius r ($r \in \mathbb{N}$) around Opt_X_i that guarantees with probability δ the presence of at least one MR can be defined using the following conditions:

$$\left(1-\left(1-P_{SearchArea}\left(r-1\right)\right)^{\mu}\right)<\delta$$
$$and\ \left(1-\left(1-P_{SearchArea}\left(r\right)\right)^{\mu}\right)\geq\delta \qquad iff\ \exists\ Y'_i=\underset{\forall X'_i\in o(Opt\_X_i,r\cdot\varepsilon)}{\arg\min}\left(\vartheta\right) \tag{7-15}$$

It should be noted that that equation (7-15) depends on $P_{SearchArea}$ and thus on the optimum MR location (Opt_X_i) within the cell; this is not the case when nodes are uniformly distributed within the cell. It should be also noted that the same condition to that analyzed in equation (7-12) must be satisfy in equation (7-15) in order to define the MR search area $o(Opt\_X_i, r\cdot\varepsilon)$; i.e. for every possible location of the selected MR within the search area (X'_i), the optimization problem formulated in Chapter 6 (represented by θ in equation (7-15)) provides the location (Y'_i) at which the MR should start the cellular transmission to the BS that minimizes the total energy consumption and satisfies that the transmission is completed before T. If the condition is not met, the SN will again transmit the information directly to the BS through a traditional single-hop cellular link.

7.4 Performance Comparison of the DELAY and AREA proposals

7.4.1 Worst Case Conditions

This section is aimed at numerically comparing the performance of the two proposed context-aware opportunistic forwarding strategies considering their worst case operation conditions. In particular, we consider that the DELAY scheme needs to wait for the complete time t to elapse before an MR reaches the optimum MR location (Opt_Xi), and that AREA founds the MR at the limit of the search area. The evaluation under these worst case conditions allows identifying the minimum energy gains that the proposed strategies can achieve with respect to traditional single-hop cellular communications. Annex B complements this study by means of deriving the configuration of opportunistic forwarding for the DELAY and AREA proposals under worst case conditions.

The comparison is first conducted considering a uniform distribution of nodes within the cell. The probability δ used to guarantee the presence of the MR at the identified location and time instant is set to 0.9. The performance has been evaluated in Matlab for all possible distances between SN and BS. The study considers a cell with a radius of 800 meters. The cell is divided into 15 equally spaced and concentric rings with a LTE transmission mode assigned to each ring (Section 6.4.1). The energy consumption values for the DRAM and NAND flash storage units have been obtained from [142] and [143] respectively. The file that the static SN needs to upload to the BS has initially a nominal

Table 7-1. Evaluation parameters.

Parameter	Description	Value
R	Cell radius	800 m
BW	LTE system bandwidth	5 MHz
G_{TX}, G_{RX}	Transmitter and receiver antenna gain	1
e_{tx}, e_{rx}	Energy consumed per bit by the transmitter/receiver	50 x 10^{-9} J/b
P_{RX}	Power reception threshold	-62 dBm
h_{SN}, h_{MR}, h_{BS}	Antenna height of SN, MR and BS	1.5 m, 1.5 m, 10 m
DRAM P_R, P_W, $P_{Idle\_self\text{-}refresh}$	DRAM power consumed for Reading, Writing and in Idle_self-refresh state	252 mW, 252 mW, 1.35 mW
NAND Eff_{Read}, Eff_{Write}, P_{Idle}	NAND efficiency for Reading and Writing, and Power consumed in Idle state	1.83 nJ/b, 11.92 nJ/b, 0.4 mW
Transf_DF, Transf_FD	Transfer speed from the DRAM to the NAND flash and vice versa	4.85 MiB/s, 927.1 KiB/s

size of 10 Mb. The study considers the following range of deadlines T={60 s, 100 s, 150 s, 200 s}. We consider that the MR is in line with the SN, and move towards the BS with a speed of 2 m/s. The rest of parameters are summarized in Table 7-1.

Figure 7-4 compares the energy consumed by DELAY and AREA as a function of the distance between SN and BS. The results are depicted in logarithmic scale, and have been obtained for an average spatial density of users within the cell equal to μ/R=0.03 MRs/m. Figure 7-4.a represents the energy consumed in the D2D transmission from SN to MR, while Figure 7-4.b represents the energy consumed in the store and carry process, and Figure 7-4.c the energy consumed in the cellular transmission from MR to BS. Figure 7-4.a shows that the DELAY proposal reduces the energy consumed in the D2D transmission with respect to AREA. However, AREA reduces the energy consumed in the store and carry (Figure 7-4.b) and cellular transmission (Figure 7-4.c) processes with respect to DELAY. The delay introduced by DELAY on the D2D transmission results in that MR starts the cellular transmission to the BS at a higher distance to the BS than the AREA scheme. This results in that DELAY increases the time MR needs to upload the

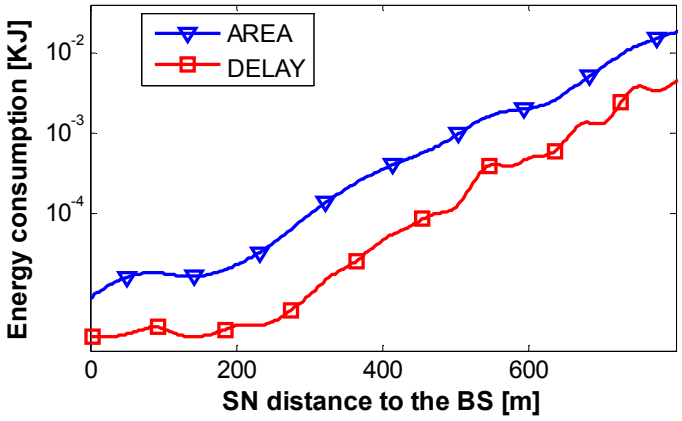

a) D2D transmission

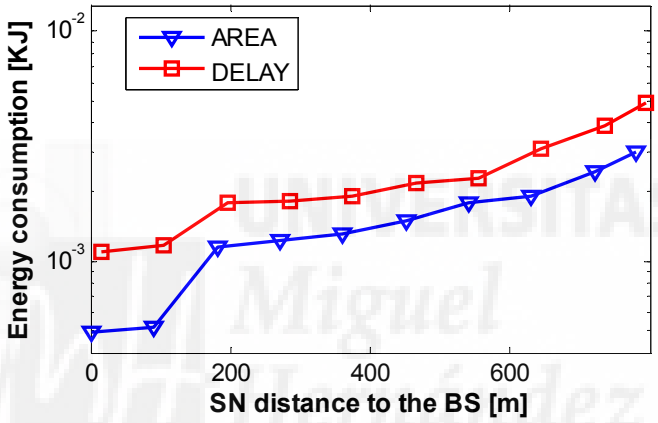

b) Store and Carry (SC)

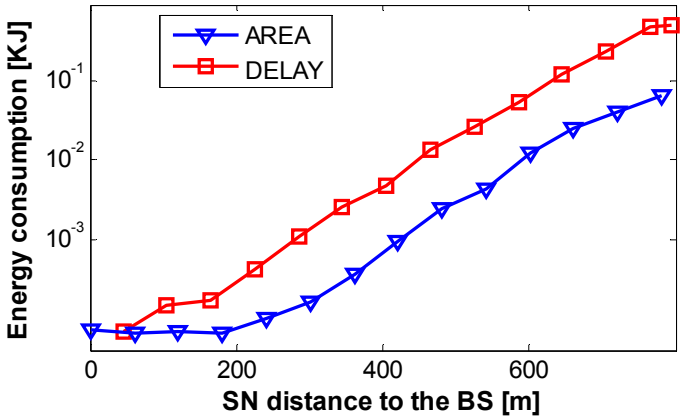

c) Cellular transmission

Figure 7-4. Comparison of the DELAY and AREA energy consumption (uniform distribution of nodes within the cell, v=2 m/s, T=60 s, F=10 Mb, μ/R=0.03 MRs/m).

information to the BS, and therefore the energy consumed in the cellular transmission to the BS (Figure 7-4.c). The comparison of Figure 7-4.a and Figure 7-4.c shows that the reduction in energy consumed in the D2D transmission process by DELAY cannot compensate the increase in the energy consumed during the cellular transmission.

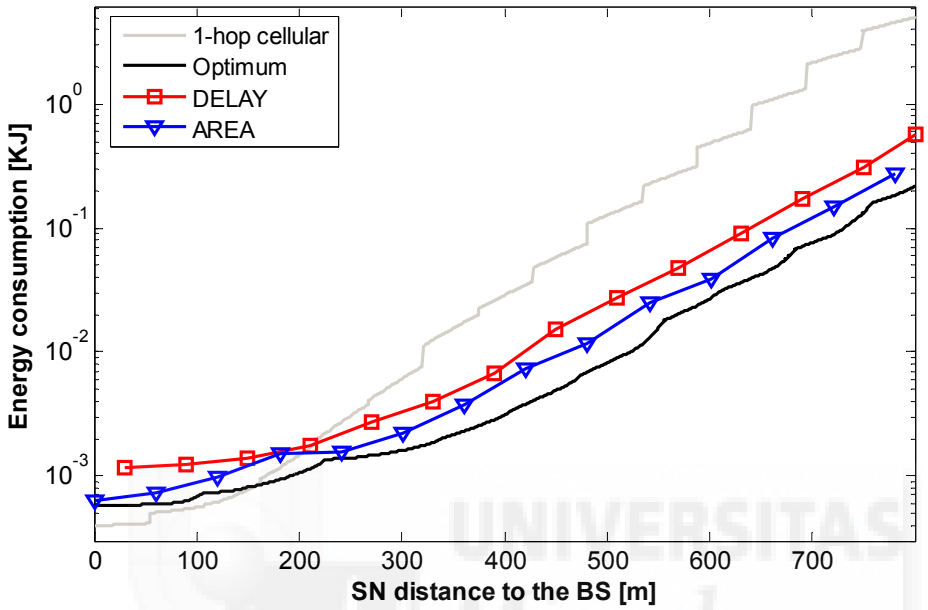

Figure 7-5. Total energy consumption (uniform distribution of nodes within the cell, v=2 m/s, T=60 seconds, F=10 Mb, μ/R=0.03 MRs/m).

The total energy consumed under the evaluated worst-case scenario and conditions is depicted in Figure 7-5. Both schemes decrease the energy consumption compared to traditional single-hop cellular communications. It is also important to highlight that AREA and DELAY only result in minor degradations of the energy performance compared to the optimum configuration. On average, AREA reduces the energy consumption compared to single-hop cellular communications by 91.8%, and DELAY by 88.1%. The optimum configuration reduces on average the energy consumption compared to single-hop cellular communications (from SN to BS) by 95.6%. The results also show that AREA achieves better energy performance than DELAY. In fact, Figure 7-5 shows that the AREA proposal can reduce, on average, the total energy consumption compared to DELAY by 17.4%. This trend is observed for (almost) all the distances between SN and BS[22], and for different values of the deadline T.

[22] Under a uniform distribution of mobiles within the cell, t and r are constant for any location of the SN within the cell following equations (7-4) and (7-12).

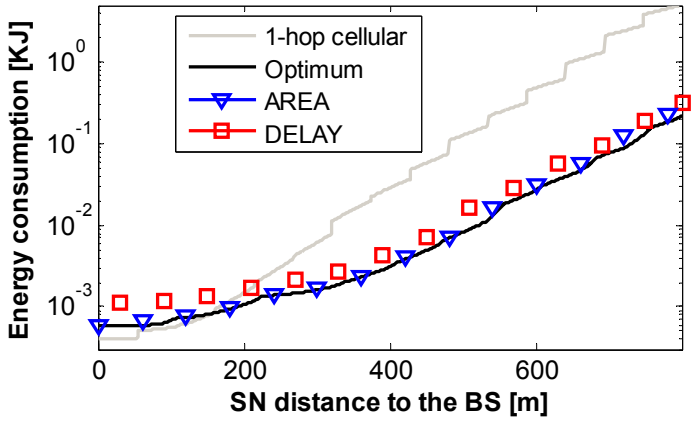

a) v=2 m/s, T=60 s, F=10 Mb, μ/R=0.09 MRs/m

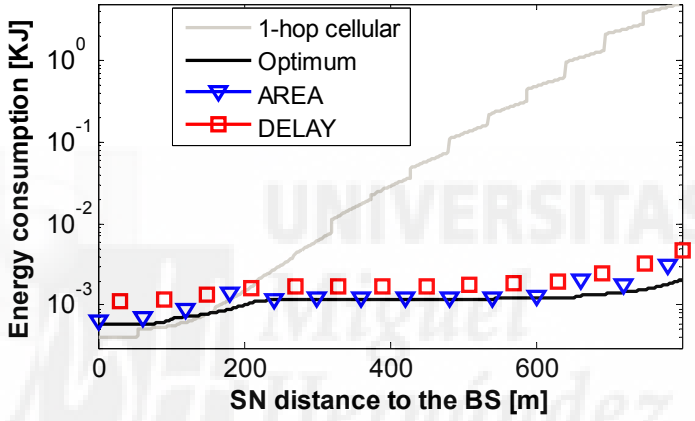

b) v=10 m/s, T=60 s, F=10 Mb, μ/R=0.03 MRs/m

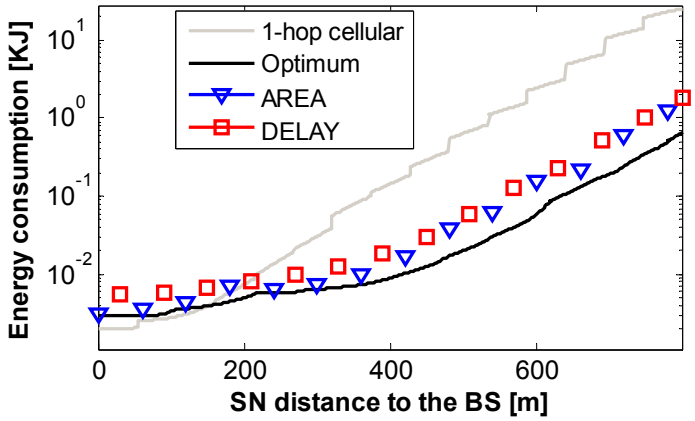

c) v=2 m/s, T=60 s, F=50 Mb, μ/R=0.03 MRs/m

Figure 7-6. Total energy consumption (uniform distribution of nodes within the cell).

However, we observe that the differences between AREA and DELAY decrease as the deadline T increases. For example, if we increase T from 60 s to 100 s, 150 s and 200 s,

the reduction in average energy consumption obtained by AREA compared to DELAY is equal to 14.4%, 9.2%, and 6.2%, respectively. As the deadline *T* increases, DELAY compensates the delay experienced for the D2D transmission, which allows reducing the distance at which MR starts the cellular transmission to the BS, and therefore the energy consumption. The reduction in the differences between the AREA and DELAY proposals are also observed if we increase the spatial density of nodes, the speed at which MR moves, or the size of the data file. Figure 7-6.a compares the total energy consumed when the spatial density of nodes is increased to 0.09 MRs/m, Figure 7-6.b when the speed is increased to 10 m/s (e.g. the MR is located inside a vehicle), and Figure 7-6.c when the file size is increased to 50 Mb. The average reduction in energy consumption achieved by AREA compared to traditional single-hop cellular communications is equal to 94.7% in Figure 7-6.a, 99% in Figure 7-6.b, and 95% in Figure 7-6.c. The average reduction in energy consumption achieved by DELAY compared to traditional single-hop cellular communications is equal to 93.4% in Figure 7-6.a, 98% in Figure 7-6.b, and 93.5% in Figure 7-6.c.

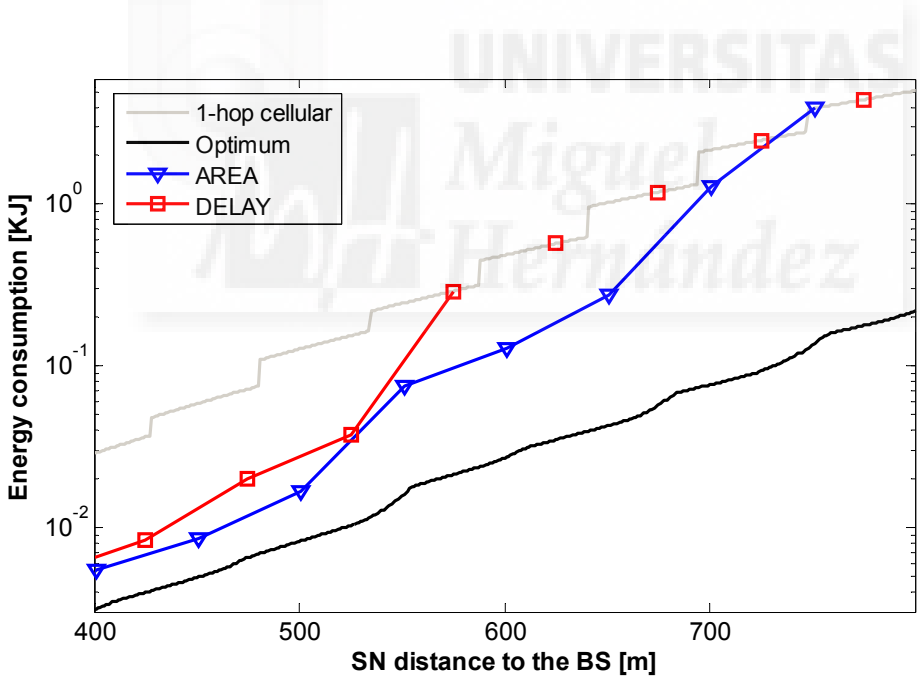

Figure 7-7. Total energy consumption (non-uniform distribution of nodes within the cell, v=2 m/s, T=60 s, F=10 Mb, μ/R=0.03 MRs/m).

Figure 7-7 compares the total energy consumed when MRs are not uniformly distributed within the cell[23]; μ/R is set equal to 0.03 MRs/m and the spatial distribution of users results in that approximately 68% of the nodes are located at distances to the BS smaller than 300 meters. A non-uniform distribution of users within the cell results in that *t* and *r* increase with the distance between SN and BS in order to compensate the smaller density of users when the distance to the BS increases. In this context, the AREA proposal considerably increases the energy consumed in the D2D transmission (and therefore the total energy consumption) with the SN distance to BS, and the DELAY proposal might exhaust the available deadline *T* without completely transmitting the file of size *F* because of the time it had to wait for an MR to arrive at the identified optimum location. It is important to remember that the current numerical evaluation considers a worst case scenario in which AREA selects the MR at the limit of the search area around the optimum MR location, and DELAY needs to wait for *t* to elapse before an MR reaches the optimum MR location. In any case, the results in Figure 7-7 clearly show that AREA and DELAY improve the energy consumption compared to traditional single-hop cellular communications. On average, AREA reduces the energy consumption compared to single-hop cellular communications by 40%, and DELAY by 26%. These results clearly highlight that opportunistic MCN communications still provide clear energy benefits (close to those achieved by the optimum configuration) compared to single-hop cellular communications under real deployments. The benefits of the AREA and DELAY proposals under worst case conditions reduce when SN is located at the cell edge. The reduction is influenced by the spatial density of users within the cell (it does not have an impact on the performance of the optimum configuration since it assumes an MR can be found when needed at the optimum location). Figure 7-7 shows that AREA is challenged to establish an efficient opportunistic MCN link for SN distances to the BS higher than 715 meters as a result of the large distances between SN and MR. DELAY experiences the same challenge for SN distances to the BS higher than 555 meters. If we increase *T* from 60 s to 100 s, 150 s or 200 s, the differences between AREA and DELAY decrease. For example, if we increase *T* from 60 s to 100 s, 150 s and 200 s, the SN distances to the BS from which DELAY cannot establish an efficient opportunistic MCN link (and needs to start a traditional single-hop cellular transmission) increase to 650 m, 715 m and 730 m respectively. These distances do not change for AREA when *T* is increased (remain equal to 715 meters) since AREA is challenged by the large distances between SN and MR. Under a non-uniform distribution of nodes within the cell, we can also observe that the

[23] The results are presented for SN distances to BS higher than 400 meters since the two schemes achieve very similar results for smaller distances.

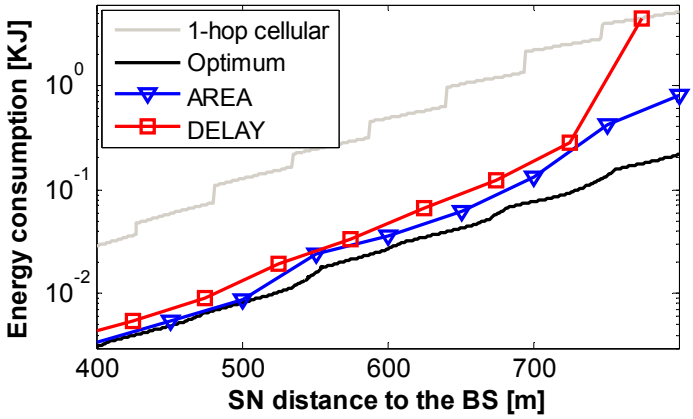

a) v=2 m/s, T=60 s, F=10 Mb, μ/R=0.09 MRs/m

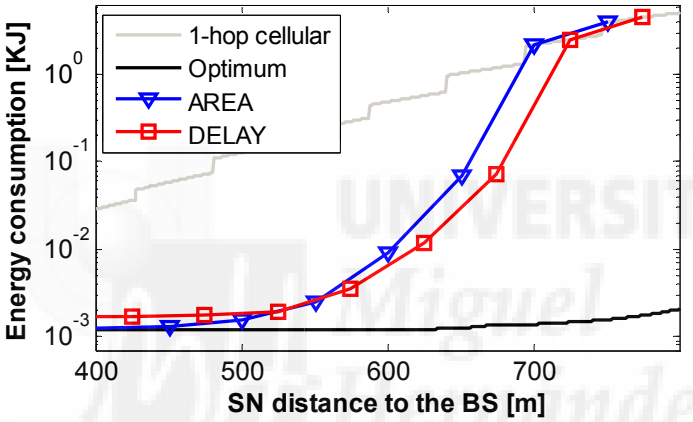

b) v=10 m/s, T=60 s, F=10 Mb, μ/R=0.03 MRs/m

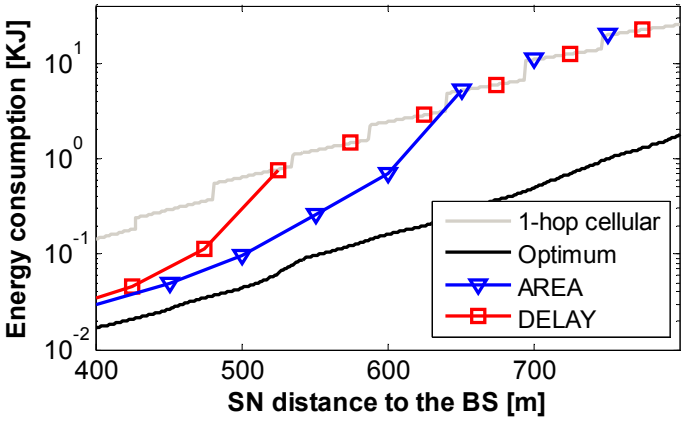

c) v=2 m/s, T=60 s, F=50 Mb, μ/R=0.03 MRs/m

Figure 7-8. Total energy consumption (non-uniform distribution of nodes within the cell).

differences between DELAY and AREA reduce if we increase the spatial density of nodes, the speed at which MR moves or the size of the file. Figure 7-8.a compares the total energy consumed when the spatial density of nodes is increased to 0.09 MRs/m, Figure 7-8.b when the speed is increased to 10 m/s (in this scenario AREA shows better energy performance than DELAY), and Figure 7-8.c when the file size is increased to 50 Mb. The average reduction in energy consumption achieved by AREA compared to traditional single-hop cellular communications is equal to 91.3% in Figure 7-8.a, 50% in Figure 7-8.b, and 32% in Figure 7-8.c. The average reduction in energy consumption achieved by DELAY compared to traditional single-hop cellular communications is equal to 53.8% in Figure 7-8.a, 52.3% in Figure 7-8.b, and 13.8% in Figure 7-8.c.

The conducted evaluation of the context-aware opportunistic forwarding proposals has shown that AREA and DELAY can notably reduce the energy consumption compared to traditional single-hop cellular communications even under worst case conditions. This is observed for all scenarios and conditions (Figure 7-5 to Figure 7-8). The two proposals better approximate the energy performance achieved with an optimum configuration of opportunistic MCN communications under a uniform distribution of users. The results have also shown that AREA can reduce the energy consumption compared to DELAY under a uniform distribution of users in the cell. This trend is also generally observed under a non-uniform distribution of users within the cell; DELAY only achieves better energy performance at larger distances to the BS under certain conditions (high deadline *T* and MR speed).

7.4.2 Energy Efficiency

The previous section numerically evaluated the energy performance of the proposed context-aware opportunistic forwarding schemes under defined worst-case conditions. The conducted evaluation allows identifying minimum energy performance bounds. This section seeks to complement the previous study with an evaluation that covers various and more general possible operating conditions. In other words, the AREA scheme is not bounded to select an MR at the border of the search area, and DELAY does not have to wait *t* seconds before an MR is found at the optimum location. The AREA and DELAY proposals are also configured so that if no MR can be found at the identified locations and within the estimated timeframe, then SN directly transmits the information to the BS using traditional single-hop cellular communications. The evaluation here reported also includes additional reference schemes for comparison, and introduces variants of the AREA and DELAY schemes.

The AREA and DELAY variants are defined based on how the cellular infrastructure provides the context information required to calculate *t* and *r*. The original DELAY and AREA proposals described in Section 7.2 and Section 7.3, respectively, consider that the context information (spatial density and distribution of users within the cell) is provided per cell. However, this context information could also be provided for each concentric ring that defines a cell[24]. In this study, we consider a total of 15 rings per cell with each ring characterized by the use of a different LTE transmission mode (see Section 6.4.1). When the context information is provided per ring rather than per cell, we denote the context-aware opportunistic forwarding schemes as AREA-Ring or DELAY-Ring. The original DELAY scheme and DELAY-Ring estimate *t* using the expression derived for a uniform distribution of nodes within the cell (equation (7-4)). When the context information is provided per ring, the spatial density of users (μ/R) in equation (7-4) is replaced by φ_i/l^i_r. φ_i represents the average number of nodes in the ring *i* where the optimum MR location is situated, and l^i_r the ring length. The average number of MRs within the cell can be then calculated as $\mu = \sum_{i=1}^{N} \varphi_i$ and the cell radius as $R = \sum_{i=1}^{N} l^i_r$, with *i* ϵ {1...N} and *N* representing the number of rings in the cell (*N*=15 in this study). The original AREA scheme and AREA-Ring estimate *r* using the expression derived for a uniform distribution of nodes within the cell (equation (7-12)). When the context information is provided per ring, the spatial density of users (μ/R) in equation (7-12) is also replaced by φ_i/l^i_r. It should be noted that the AREA and DELAY variants utilize the same expressions of *r* and *t* under uniform and non-uniform user distributions.

The AREA and DELAY performance is here compared against that obtained with traditional single-hop cellular communications ('1-hop cellular') and the optimum configuration of opportunistic MCN communications ('Optimum'). The performance is also compared against other reference schemes. The '1-hop Direct-contact' scheme refers to the case in which the SN is mobile and can store and carry the information to the BS without using a mobile relay [111]. 'MR closest to SN' and 'MR closest to BS' refer to two opportunistic MCN schemes in which SN selects the MR closer to its location [158] and the MR that provides the higher progress towards the BS [144], respectively. For a fair comparison with the proposed schemes, the configuration of the reference schemes is also derived following a similar optimization process to that reported in Chapter 6 (Section 6.3) that seeks minimizing the energy consumption. For example, the optimization process identifies for the 'MR closest to BS' scheme the MR location that

[24] Standards such as LTE or HSPA divide cells into concentric rings. Different transmission modes are used per ring based on parameters such as the signal strength or the CQI.

provides the highest progress towards BS and is able to upload the information before the deadline *T*. The location at which MR should start forwarding the information to the BS is also derived in the optimization problem.

The performance of all schemes is evaluated considering a single cell scenario that has been simulated using a discrete-event simulator implemented in Matlab. The implemented scenarios consider both uniform and non-uniform distribution of MRs in the cell. To create uniform distributions of nodes within the cell, MRs appear at the cell edge following a Poisson process with a rate equal to $\mu \cdot v/R$, and move towards the BS at a predefined constant speed. In the case of non-uniform distributions, MRs can be initially placed at intermediate locations between the BS and the cell edge. This process allows creating higher spatial densities of nodes close to BS by exploiting the additive property of Poisson processes. The results here presented have been obtained for a large number of experiments (minimum 80 experiments for each result) in order to ensure that the standard error of the mean (i.e. the standard deviation of the estimated mean with respect to the mean obtained in each experiment) is always below 0.01.

Table 7-2 reports the reduction (in percentage) of the average energy consumption achieved with the different schemes compared to traditional single-hop cellular communications. The depicted results clearly show that the use of opportunistic forwarding schemes helps reducing the energy consumption, with the benefits increasing when adequately combining opportunistic networking and MCN communications. Only the 'MR closest to BS' technique consumes more energy in some of the considered scenarios than single-hop cellular communications (negative values in Table 7-2). This is the case because of the high energy consumed during the D2D transmission as a result of selecting the MR as close as possible to the BS. The higher energy benefits would be achieved if the 'Optimum' reference configuration could be possible (Table 7-2). The results depicted in Table 7-2 for the 'Optimum' configuration correspond to the numerical results obtained in Section 6.4. These results assume that it is always possible to find an MR at the identified optimum location and time instant. This assumption is made to obtain a maximum performance bound with which to compare the energy benefits that can be obtained with the context-aware proposals. However, this assumption might not always be feasible. In fact, the probability that SN could find an MR at the required optimum location and time instant was less than 0.3 when the spatial density of users in the cell was 0.125 MRs/m. This probability decreased to 0.1 when μ/R was equal to 0.03 MRs/m.

Table 7-2. Reduction (in percentage) of the total average energy consumption compared to single-hop cellular communications.

a) Uniform spatial distribution of MRs within the cell

Technique	***μ/R*= 0.125 MRs/m**		***μ/R*= 0.03 MRs/m**	
	***F*=10 Mb, *v*=2m/s, *T*=30s**	***F*=10 Mb, *v*=10m/s, *T*=30s**	***F*=10 Mb, *v*=2m/s, *T*=30s**	***F*=10 Mb, *v*=2m/s, *T*=60s**
AREA	86.3	89.6	83.5	88.1
AREA – Ring	88.0	98.2	87.1	91.4
DELAY	84.5	94.6	66.1	85.1
DELAY – Ring	86.9	99.0	66.1	86.3
MR closest to BS	-129.1	45.3	-11.3	-8.0
MR closest to SN	23.8	96.1	28.2	75.2
1-hop Direct-contact	64.3	96.9	64.3	71.8
Optimum	91.7	99.0	91.7	95.6

b) Non-uniform spatial distribution of MRs within the cell

Technique	***μ/R*= 0.125 MRs/m**		***μ/R*= 0.03 MRs/m**	
	***F*=10 Mb, *v*=2m/s, *T*=30s**	***F*=10 Mb, *v*=10m/s, *T*=30s**	***F*=10 Mb, *v*=2m/s, *T*=30s**	***F*=10 Mb, *v*=2m/s, *T*=60s**
AREA	51.7	56.9	54.1	55.5
AREA – Ring	87.1	95.7	73.9	80.5
DELAY	52.0	68.1	38.3	50.9
DELAY – Ring	68.8	96.1	42.3	60.6
MR closest to BS	-117.9	47.0	-28.9	-21.9
MR closest to SN	39.4	96.8	53.0	76.1
1-hop Direct-contact	60.1	96.9	60.1	71.8
Optimum	91.7	99.0	91.7	95.6

Table 7-2 shows that the AREA and DELAY proposals can also achieve significant energy gains compared to traditional single-hop cellular communications. These gains can actually be very close to those that would be obtained with a potential optimum configuration under certain scenarios and conditions. In particular, AREA and DELAY increase their energy gains with the density of MRs within the cell and the MRs' speed[25].

[25] Increasing these two parameters helps reducing the time *t* SN needs to delay the D2D transmission (equation (7-4)) and the radius *r* around the optimum MR location (equation (7-12)).

This trend is observed independently of whether MRs are distributed uniformly or not within the cell. Higher *T* deadlines also tend to improve the performance of AREA and DELAY since the schemes have more time to exploit the benefits of opportunistic networking. A closer comparison of the AREA and DELAY schemes shows that AREA is particularly suitable under low density of users or a small *T* deadline. When the spatial density of users and *T* decrease, DELAY reduces its hit rate (Table 7-3) because the time SN needs to wait for an MR to reach the optimum MR location does not allow establishing the two-hop opportunistic MCN connection before *T* expires. The hit rate is defined as the average percentage of SN-BS links established using two-hop opportunistic MCN communications. The results in Table 7-3 show that AREA's hit rate is not that highly influenced by the *T* parameter, and explain why AREA outperforms DELAY for low values of *T*. When *T* increases to 60 seconds, DELAY and AREA achieve closer energy efficiency levels. This is due to the fact that higher *T* values allow DELAY to compensate the longer delays experienced for the D2D transmission as a result of the need to wait for an MR to reach the optimum MR location. For this scenario, the AREA and DELAY proposals show slightly lower energy performance than under worst case conditions (Section 7.3.1) where it was assumed that an MR was always found at the limit of the search area (AREA) or at the optimum MR location after *t* seconds elapse (DELAY). The simulation results here reported consider that if no MR can be found at the identified locations and within the estimated timeframe, then SN directly transmits the information to the BS using traditional single-hop cellular communications. This operational difference explains why the simulation results do not have to be equal or higher than those reported in Section 7.4.1 under worst case conditions. If in this scenario we only consider the SN-BS transmissions that took place using a two-hop opportunistic MCN link (Table 7-4), the average reduction in energy consumption achieved by AREA and DELAY compared to traditional single-hop cellular communications would be equal to 95% and 94%, respectively –i.e. higher energy performance levels than in worst-case conditions. Table 7-4 reports the energy performance achieved by the proposed context-aware proposals when only considering the SN-BS transmissions that took place using a two-hop opportunistic MCN link. The obtained results show that in this case the proposals achieve very similar energy performance levels to that obtained with the 'Optimum' configuration.

The results depicted in Table 7-2 show that a higher mobility of MRs improves the energy gains of AREA and DELAY, with the largest improvements obtained for DELAY. Increasing the MRs' speed results in that the cellular transmission from MR to the BS will start closer to the BS where higher cellular data rates are possible. However, it can also

Table 7-3. Hit rate: percentage of SN-BS links established using two-hop opportunistic MCN communications.

a) Uniform spatial distribution of MRs within the cell

Technique	***μ/R*=0.125 MRs/m**		***μ/R*= 0.03 MRs/m**	
	***F*=10 Mb, *v*=2m/s, *T*=30s**	***F*=10 Mb, *v*=10m/s, *T*=30s**	***F*=10 Mb, *v*=2m/s, *T*=30s**	***F*=10 Mb, *v*=2m/s, *T*=60s**
AREA	94.1	92.1	90.3	89.4
AREA – Ring	96.5	99.4	97.4	96.5
DELAY	93.0	96.7	79.1	89.0
DELAY – Ring	96.1	99.9	78.9	93.5

b) Non-uniform spatial distribution of MRs within the cell

Technique	***μ/R*=0.125 MRs/m**		***μ/R*= 0.03 MRs/m**	
	***F*=10 Mb, *v*=2m/s, *T*=30s**	***F*=10 Mb, *v*=10m/s, *T*=30s**	***F*=10 Mb, *v*=2m/s, *T*=30s**	***F*=10 Mb, *v*=2m/s, *T*=60s**
AREA	80.0	78.3	80.1	77.6
AREA – Ring	96.1	95.7	94.6	95.2
DELAY	80.9	85.9	67.0	76.5
DELAY – Ring	91.8	98.9	65.7	83.9

negatively impact AREA if the distance between SN and the selected MR exceeds the D2D communications range. This risk increases at higher speeds, which explains the slight negative impact of the MRs' speed on AREA's hit rate (Table 7-3). These trends are observed under uniform and non-uniform distribution of users in the cell. However, non-uniform distributions of users in the cell reduce the energy gains of both schemes. A non-uniform distribution of users in the cell results in a lower density of nodes with increasing distances to the BS. A varying user density across the cell influences the estimation of the *t* and *r* parameters. Providing the context information per cell in the case of a non-uniform distribution of MRs cannot take into account this variation, and can hence result in frequent incorrect estimations of *t* and *r*. The results depicted in Table 7-3 show that when the distribution of users per cell varies from a uniform one to a non-uniform one, the hit rate decreases. AREA and DELAY do not establish opportunistic MCN links to transmit the information from SN to BS when they cannot find an MR at the identified locations and within the estimated timeframe. A lower percentage of SN-BS links established using opportunistic MCN links[26] decreases the

[26] Especially those close to the cell edge where opportunistic networking shows higher energy efficiency.

energy gains of the AREA and DELAY proposals compared to traditional single-hop cellular communications (Table 7-2); the gains are still very significant and above 50% in most cases.

Table 7-3 shows that providing the context information per ring rather than per cell results in that AREA and DELAY increase their hit rate even under non-uniform user distributions per cell. In fact, the AREA-Ring and DELAY-Ring schemes can achieve hit rate levels with non-uniform distributions close to that obtained by AREA and DELAY under uniform user distributions per cell. Table 7-3 also shows that the impact of whether the context information is provided per cell or ring is higher for non-uniform user distributions than for uniform ones. As previously explained, this is the case because using context information per cell can result in incorrect estimations of the *t* and *r* parameters when users are non-uniformly distributed in the cell. Providing the context information per ring rather than per cell significantly improves the hit rate (Table 7-3) and the energy gains compared to traditional single-hop cellular communications (Table 7-2) independently of the user distribution. The results in Table 7-2 show that under a uniform distribution of users, the differences between AREA-Ring and DELAY-Ring appear only for a low density of users. In this case, AREA-Ring

Table 7-4. Reduction (in percentage) of the total average energy consumption compared to single-hop cellular communications (only two-hop opportunistic MCN transmissions).

a) Uniform spatial distribution of MRs within the cell

Technique	***μ/R*=0.125 MRs/m**		***μ/R*= 0.03 MRs/m**	
	***F*=10 Mb, *v*=2m/s, *T*=30s**	***F*=10 Mb, *v*=10m/s, *T*=30s**	***F*=10 Mb, *v*=2m/s, *T*=30s**	***F*=10 Mb, *v*=2m/s, *T*=60s**
AREA	91.5	99.0	90.6	94.9
AREA – Ring	91.5	99.0	89.8	94.5
DELAY	91.0	99.0	89.3	93.6
DELAY – Ring	91.0	99.0	89.3	93.4

b) Non-uniform spatial distribution of MRs within the cell

Technique	***μ/R*=0.125 MRs/m**		***μ/R*= 0.03 MRs/m**	
	***F*=10 Mb, *v*=2m/s, *T*=30s**	***F*=10 Mb, *v*=10m/s, *T*=30s**	***F*=10 Mb, *v*=2m/s, *T*=30s**	***F*=10 Mb, *v*=2m/s, *T*=60s**
AREA	90.8	98.9	88.8	94.0
AREA – Ring	90.5	98.9	80.6	86.8
DELAY	89.8	98.9	87.0	92.3
DELAY – Ring	89.3	98.8	87.1	91.3

outperforms DELAY-Ring, with higher differences observed for the lowest *T* value. This is due to the fact that DELAY needs to wait for an MR to reach the optimum MR location, with the D2D delay increasing with the lower density of users per cell. This delay, and decreasing the *T* deadline, results in the reduction of the hit-rate performance shown in Table 7-3. AREA-Ring also outperforms DELAY-Ring for non-uniform user distributions. In this case, the differences appear even for the higher density of users evaluated. The use of the context information per ring provides a better indication of how users are distributed within the cell, which allows better adjusting *t* and *r*.

7.4.3 Network Capacity

The previous sections have demonstrated that the use of opportunistic MCN communications can significantly improve the energy efficiency of MCNs compared to traditional single-hop cellular communications. The AREA and DELAY proposals have been shown to be able to provide energy gains close to that reached with an optimum energy configuration of opportunistic MCN communications if adequately configured, e.g. using context information per ring in the case of non-uniform user distributions. The observed energy gains result from a more efficient use of radio resources. Indeed, opportunistic MCN communications provide the means to decide when to establish a communications link based on its efficiency and quality. Table 7-5 demonstrates that the efficient use of radio resources that results from the combination of opportunistic networking and MCN for delay tolerant services can also provide very significant cellular capacity gains at the network level compared to traditional single-hop cellular communications. The capacity gain is measured in this study as the reduction of the time needed to complete the MR-BS cellular transmission in the case of two-hop opportunistic MCN communications compared to the time needed by traditional single-hop cellular communications to complete the SN-BS cellular transmission. The 'MR closest to BS' reference scheme is the one achieving higher capacity gains. This is the case because the MR is selected as close as possible to the BS, and therefore the scheme can minimize the time needed to upload the information to the BS. However, it is important to remember that this scheme actually consumed even more energy than traditional single hop cellular communications (Table 7-2). This is due to the fact that selecting an MR as close as possible to the BS significantly increases the energy consumption in the D2D transmission due to the lower quality/efficiency conditions for the D2D link. Table 7-5 also shows that the '1-hop Direct-contact' reference scheme can increase the capacity compared to traditional single-hop cellular communications. However, its capacity gains are in general below the ones obtained with opportunistic MCN as it does not take advantage of the D2D transmission to start the cellular

transmission closer to the BS. Similar trends are observed in terms of the impact of user density, MR speed, deadline *T* and context information (per cell or per ring) on the AREA and DELAY capacity performance and comparison (Table 7-5) as they were observed for the energy consumption (Table 7-2). The results reported in Table 7-6 also shows that when only considering the SN-BS transmissions that took place using a two-hop opportunistic MCN link, the context-aware proposals achieves very similar capacity gains levels to that obtained with the 'Optimum' configuration.

Table 7-5. Capacity gains with respect to single-hop cellular communications.

a) Uniform spatial distribution of MRs within the cell

Technique	***μ/R*= 0.125 MRs/m**		***μ/R*= 0.03 MRs/m**	
	***F*=10 Mb, *v*=2m/s, T=30s**	***F*=10 Mb, *v*=10m/s, T=30s**	***F*=10 Mb, *v*=2m/s, T=30s**	***F*=10 Mb, *v*=2m/s, T=60s**
AREA	63.1	72.6	61.1	66.3
AREA – Ring	64.2	78.5	63.5	68.6
DELAY	61.1	76.1	49.3	62.8
DELAY – Ring	62.6	78.9	49.3	63.5
MR closest to BS	74.7	81.8	72.4	76.6
MR closest to SN	18.5	72.4	20.5	48.3
1-hop Direct-contact	41.1	73.6	41.1	48.3
Optimum	66.9	79.1	66.9	72.1

b) Non-uniform spatial distribution of MRs within the cell

Technique	***μ/R*= 0.125 MRs/m**		***μ/R*= 0.03 MRs/m**	
	***F*=10 Mb, *v*=2m/s, T=30s**	***F*=10 Mb, *v*=10m/s, T=30s**	***F*=10 Mb, *v*=2m/s, T=30s**	***F*=10 Mb, *v*=2m/s, T=60s**
AREA	42.2	50.5	43.2	45.7
AREA – Ring	63.0	76.7	57.7	65.1
DELAY	41.7	58.4	31.0	40.8
DELAY – Ring	51.6	76.9	33.9	61.2
MR closest to BS	73.7	81.6	63.9	70.2
MR closest to SN	25.4	73.5	36.6	53.7
1-hop Direct-contact	41.4	73.6	41.4	48.3
Optimum	66.9	79.1	66.9	72.1

Table 7-6. Capacity gains with respect to single-hop cellular communications (only two-hop opportunistic MCN transmissions).

a) Uniform spatial distribution of MRs within the cell

Technique	***μ/R*=0.125 MRs/m**		***μ/R*= 0.03 MRs/m**	
	***F*=10 Mb, *v*=2m/s, *T*=30s**	***F*=10 Mb, *v*=10m/s, *T*=30s**	***F*=10 Mb, *v*=2m/s, *T*=30s**	***F*=10 Mb, *v*=2m/s, *T*=60s**
AREA	66.2	78.8	65.1	70.8
AREA – Ring	66.1	79.0	65.0	70.5
DELAY	64.9	78.8	61.1	67.7
DELAY – Ring	64.8	79.0	61.2	67.1

b) Non-uniform spatial distribution of MRs within the cell

Technique	***μ/R*=0.125 MRs/m**		***μ/R*= 0.03 MRs/m**	
	***F*=10 Mb, *v*=2m/s, *T*=30s**	***F*=10 Mb, *v*=10m/s, *T*=30s**	***F*=10 Mb, *v*=2m/s, *T*=30s**	***F*=10 Mb, *v*=2m/s, *T*=60s**
AREA	61.1	75.0	59.6	63.2
AREA – Ring	65.3	79.0	62.4	69.2
DELAY	59.3	76.1	52.8	61.1
DELAY – Ring	60.8	78.3	53.0	61.2

7.5 Summary and Discussion

This chapter has proposed a set of context-aware opportunistic forwarding schemes for MCN communications that exploit the store, carry and forward capabilities of mobile devices. The proposed schemes are based on the reference optimum configuration of opportunistic MCN communications analytically derived with the objective to minimize the energy consumption (Chapter 6). The set of derived schemes exploit context information available in cellular networks to identify adequate mobile relays taking into account the identified optimum configuration. If no MR can be found at the identified optimum location and time instant, the AREA proposal expands the MR search area around the optimum location using information about the spatial density and distribution of mobile nodes within the cell. The DELAY proposal uses the same context information to identify for how long the D2D transmissions from the source node can be delayed to find an MR at the identified optimum location. The conducted extended

numerical evaluations have shown that the integration of opportunistic networking principles into MCN yields significant energy savings and capacity gains compared to traditional single-hop cellular communications. The AREA proposal generally outperforms the DELAY scheme. Both schemes benefit from the provision of context information per ring rather than per cell. In this case, the proposals, and in particular the AREA scheme, can achieve energy and capacity performance levels close to those that could be obtained under an optimum configuration of opportunistic MCN communications. In this case, the context-aware schemes can reduce the energy consumption compared to traditional single-hop cellular communications by up to 98% for delay tolerant services, and increase the cellular capacity by up to 79%. These results demonstrate that opportunistic networking and MCN can significantly contribute towards achieving the capacity and energy efficiency gains sought for 5G networks.

UNIVERSITAS Miguel Hernández

UNIVERSITAS
Miguel
Hernández

8

Conclusions

Future 5G networks are being designed with the objective to efficiently handle the exponential growth in mobile data traffic. According to recent estimates, it is expected that mobile data traffic will increase nearly tenfold between 2014 and 2019. The objective of 5G networks is to support these growth levels while saving up to 90% of energy per provided service. To reach these goals, device-centric wireless solutions, including D2D and MCNs, are being considered as part of the 5G ecosystem as emerging alternatives to traditional cell-centric architectures. Device-centric MCNs utilize mobile relays and D2D communications. Device-centric MCNs can help address certain limitations of conventional cell-centric architectures. In particular, MCNs are capable to provide higher and more homogeneous QoS levels across the cell by substituting long-distance (NLOS) cellular links for multiple hops with better link budgets. Device-centric MCNs are aimed at exploiting the increasing intelligence, communications and computing resources of mobile devices. In device-centric MCNs, smart mobile devices become *prosumers* of wireless connectivity and act as a bridge between the cellular infrastructure and other devices. If efficiently coordinated, device-centric MCNs have demonstrated potential for significantly increasing the capacity, energy efficiency and QoS. In fact, several analytical and simulation-based studies proved the benefits of MCNs using mobile relays in terms of capacity improvement, cell coverage, network scalability and infrastructure deployment cost among others. However, to date, no study had previously experimentally evaluated the QoS benefits of MCNs using mobile relays

and D2D communications. In this context, this thesis has empirically contributed towards a better understanding of the real potential and performance benefits that device-centric MCNs can provide over traditional cellular systems. In particular, this thesis has designed a unique MCN hardware testbed that has been used to validate and quantify the QoS benefits of MCNs with respect to single-hop cellular communications, and the conditions under which such benefits can be obtained. This thesis has then used the data obtained from field measurements to derive a unique set of empirical models of the communications performance of MCNs.

A large portion of the traffic that is driving the mobile data growth can be deemed as delay tolerant. This is the case for example of mobile vide traffic, that is expected to represent 72% of mobile data traffic by 2019, and it also includes email, file sharing, social networking, software/firmware updates, cloud services, data metering and goods tracking. The integration of opportunistic networking and MCNs represents then an interesting option to provide QoS while improving energy-efficiency by taking advantage of the delay tolerance of these traffic services. Opportunistic schemes can exploit the mobile device's storing, carrying and forwarding capabilities, and the non real-time properties of delay tolerant services, to enhance the efficiency of wireless transmissions. In this context, this thesis has contributed towards the analysis of the capacity of opportunistic MCNs to improve the energy-efficiency of cellular networks. In particular, this thesis has proposed an analytical framework for two-hop opportunistic MCN communications designed to identify their optimum configuration in terms of energy efficiency. In addition, this thesis has proposed two context-aware opportunistic forwarding schemes. The proposed schemes exploit context information already available in the cellular networks to identify adequate mobile relays taking into account the identified optimum configuration. The proposed schemes increase the feasibility of integrating opportunistic networking mechanisms into MCNs, and contribute towards achieving the 5G capacity and energy-efficiency objectives.

The following sections provide a comprehensive summary of the main results and conclusions derived from the investigations carried out in this thesis. Finally, possible future research directions are discussed.

8.1 Experimental Evaluation of Multi-hop Cellular Networks

This thesis has introduced mHOP, the first research platform designed to investigate the performance benefits of MCNs using mobile relays over traditional cellular systems,

and to analyze the conditions under which such benefits can be obtained. To allow for their performance comparison, the platform includes a conventional single-hop cellular link and a MCN link that gains access to the cellular infrastructure through a hybrid mobile node capable of forwarding cellular data in real-time to (from) the destination mobile node. In addition, this thesis has also presented the first results obtained from an extensive field test campaign that validate the potential of MCNs using mobile relays and D2D communications, and demonstrate the important end-user QoS improvements that can be achieved with this emerging technology compared to traditional cellular systems. In particular, the conducted field tests have experimentally proved the capacity of MCN technologies to extend the cellular radius, and increase the QoS at large distances to the serving BS, in indoor environments, under NLOS propagation conditions, and in handover areas. The conducted measurements have also experimentally demonstrated the capability of MCNs using mobile relays to reduce the energy consumption compared to traditional single hop cellular systems.

8.2 Modeling the Performance of Multi-hop Cellular Networks

Using the experimental testbed and data previously discussed, this thesis has presented novel and unique empirical models for the communications performance of MCNs using mobile relays and D2D communications. The proposed models can be useful to support the design, test and optimization of novel communications and networking protocols tailored for MCNs. The models have been obtained following a large field testing campaign using an active cellular network in the city of Elche in Spain. The reported models represent the MCN throughput experienced at a mobile destination node as a function of the distance, propagation/visibility conditions, number of hops and communication settings. The MCN throughput performance has been modeled with a sigmoid function that is a function of the cellular throughput experienced at the hybrid or gateway mobile node. Models have been reported for MCN configurations of up to 5-hops. The models' fitting parameters have been shown to depend on key factors such as the propagation conditions and number of hops. Another relevant parameter is the critical distance or distance at which the MCN throughput operates below the cellular throughput. The models have been derived considering HSPA cellular transmissions (LTE was not deployed at the time of deriving the models) and IEEE 802.11g D2D communications. Extending the models to other cellular technologies could be feasible as long as the MCN performance is upper-bounded by the cellular link between the BS and the hybrid mobile node. Using the MCN measurements, this thesis has also derived

empirical models for the communications between mobile devices. In particular, the thesis provides models for the IEEE 802.11g data rate, PER and RSSI parameters as a function of the distance between the communicating devices.

8.3 Opportunistic Forwarding in Multi-hop Cellular Networks

A large portion of the cellular data traffic (present and future) can be deemed delay tolerant. In this context, this thesis has proposed to exploit this delay tolerance to further increases the MCN benefits through the integration of opportunistic networking policies. The study has focused on a two-hop MCN scenario, and has analytically formulated the energy optimization problem that allows identifying the optimum mobile relay location, and the location at which the relay needs to start forwarding the information to the cellular network, in order to minimize the energy consumption. The conducted study has analyzed the impact of traffic characteristics of delay tolerant services on the energy gains that can be reached with opportunistic MCN communications compared to traditional single-hop cellular communications. The study has also investigated how opportunistic MCN communications should be configured to exploit the traffic delay tolerance in order to reduce the total transmission energy consumption. The obtained results have shown that opportunistic MCN communications can significantly reduce the energy consumption compared to traditional single-hop cellular communications for delay tolerant services. The reduction can go beyond 95% under certain conditions. In particular, the reduction levels increase with increased traffic delay tolerance thresholds and increasing distances of the source node to the serving base station.

The derived optimum configurations have then been used as reference performance bounds for the design of realistic opportunistic forwarding schemes for MCN communications using mobile relays. In particular, a set of context-aware opportunistic forwarding schemes for MCN communications have been proposed. The schemes exploit context information available in cellular networks to identify adequate mobile relays taking into account the identified optimum configuration. If no MR can be found at the identified optimum location and time instant, the AREA proposal expands the MR search area around the optimum location using information about the spatial density and distribution of mobile nodes within the cell. The DELAY proposal uses the same context information to identify for how long the D2D transmissions from the source node can be delayed to find an MR at the identified optimum location. The conducted evaluations have shown that the integration of opportunistic networking principles into

MCN yields significant energy savings and capacity gains compared to traditional single-hop cellular communications. The AREA proposal generally outperforms the DELAY scheme. Both schemes benefit from the provision of context information per ring rather than per cell. In this case, the context-aware proposals can reduce the energy consumption (by up to 98%) and increase the cellular capacity (by up to 79%) compared to traditional single-hop cellular communications in the case of delay tolerant services. These results demonstrate that opportunistic networking and MCNs can significantly contribute towards achieving the capacity and energy efficiency gains sought for 5G networks.

8.4 Future Work

The mHOP testbed was implemented using Ubuntu laptops as mobile relays. This decision was taken due to the requirements of the platform in terms of monitoring capabilities, scalability and flexibility to investigate various communications settings. During the thesis, the author has closely followed the evolution of the Ubuntu for Devices project (also known as Ubuntu Touch or Ubuntu Phone) [160] since it would have been interesting to evolve the mHOP platform to integrate handheld devices. Given the fact that the mHOP implemented code is working on Ubuntu distributions, the migration to Ubuntu handheld devices should not require considerable efforts. However, a stable release of Ubuntu for Devices was not available at the time this thesis implemented mHOP (actually the first Ubuntu phone went on sale on February 2015 with BQ on the Aquaris E4.5). The releases available for developers (known as Developer Preview) lack yet of all the functionalities needed to implement a mHOP node. For example, the Developer Preview currently only supports limited voice and SMS services over GSM and UMTS. Some networking functionalities are supported such as IEEE 802.11 in ad-hoc mode, but limited access is yet provided to modify communication parameters at the PHY and MAC layers. Another issue is the fact that mHOP nodes are equipped with an external IEEE 802.11 wireless ExpressCard for the ad-hoc D2D communications since the built-in wireless interface is dedicated to monitor retransmitted packets. This ExpressCard can be plugged to the handheld devices using their mini USB port which needs to deliver power to the wireless ExpressCard. However, this USB On-The-Go (OTG) functionality is not yet supported.

Another interesting evolution for the mHOP platform would be the integration of alternative radio interfaces to support D2D communications. To this aim, Qualcomm's release of LTE-Direct certainly represents a progress towards the study of MCNs using

LTE-based D2D communications. The LTE-Direct software development kit is available from the manufacturer, and can be installed in handheld devices to develop proximal discovery solutions and proximity services. However, the software development kit provided by Qualcomm does not support yet D2D communications.

In parallel to this thesis, members of the UWICORE laboratory have been evolving the mHOP platform to implement link-aware opportunistic D2D communications by modifying the legacy IEEE 802.11 implementation in the Linux kernel, in particular its MAC layer [14]. The development is aimed at improving the efficiency and performance of D2D communications by avoiding unnecessary (and inefficient) transmissions when the link quality conditions are not good. In particular, the solution implemented pauses D2D transmissions between devices when the measured link quality conditions are below an RSSI threshold. The D2D transmission is then re-started when the link quality conditions improve. This opportunistic operation has shown to result in important energy, capacity and QoS benefits in D2D communications [14]. Efforts need now to be devoted to extend the platform to support multi-hop D2D opportunistic communications, but most importantly to support opportunistic MCN communications at the D2D and cellular levels considering the differences needed for uplink and downlink transmissions.

This thesis has demonstrated the energy efficiency and capacity benefits resulting from the integration of opportunistic networking mechanisms into MCNs for delay tolerant services. Following the results obtained, further work would be needed to design innovative wireless networking policies that exploit diverse service requirements and opportunistic networking principles to establish efficient connections. To this aim, it will be of paramount importance to increase the use of context information (e.g. user preferences, network state, spectrum availability and characteristics, link conditions, interference levels, operating conditions). Actually, context-awareness is clearly highlighted as a key characteristic for future 5G networks. However, acquiring and sharing such context could require significant signaling overhead that would need to be carefully controlled by evaluating the value and acquisition cost of the context information. In this context, lightweight schemes to extract and characterize context conditions considering the trade-offs between relevance and granularity of the context information and acquisition cost would be also needed to be analyzed.

Future 5G wireless networks will be characterized by the co-existence of different radio access technologies (adequate for the diverse 5G services requirements), spectrum bands (e.g. licensed and unlicensed), and communications modes (e.g. single-

hop cellular communications, D2D and MCNs). Future heterogeneous ecosystems will hence require advanced management techniques to exploit the envisioned heterogeneity. In this context, it would be interesting to extend the studies carried out in this thesis to heterogeneous, context-aware and spectrum agile multi-technology networks that allow D2D communications and MCNs to utilize heterogeneous technologies and spectrum bands for their transmissions. In this scenario, D2D and MCNs would be able to dynamically select the most appropriate configuration for each transmission, with the selection depending on the efficiency, reliability and latency requirements of the diverse 5G applications and services.

It would be also important to highlight the work to be done for progressing towards the envisioned 5G device-centric wireless networks. In order to ensure that nodes can take independent and local decisions, further work would need to be done in the evolution of current architectures to facilitate flexible device-centric architectures. To this aim, approaches could consider current proposals to decouple the control and user planes, which could operate under different technologies and/or spectrum bands. In addition, device-centric solutions would require the design of novel distributed and semi-centralized control algorithms that provide sufficient flexibility for local decisions at the device level while ensuring that such decisions, whether coordinated or not with the cellular network, can maximize network performance, capacity and efficiency with minimum signaling exchanges.

This thesis has demonstrated that the integration of opportunistic forwarding mechanisms into MCNs can help improve the capacity and energy-efficiency of future wireless networks. These networks will also need to reduce latency over the radio access network. Certainly, the proposals to decouple control and user planes in device-centric architectures are expected to have a significant impact on the reduction of the latency. A complementary solution that might benefit from the flexibility of device-centric wireless networks is the possibility to use the mobile devices as content distributors. Doing so, the information is stored at the pure edge of the network and the time to access the information is significantly reduced. However, important issues that need yet to be resolved are the decisions on which information should be stored, which node should store such information and how to distribute such information.

UNIVERSITAS
Miguel
Hernández

8

Conclusiones

Las futuras redes 5G están siendo diseñadas con el objetivo de hacer frente de una manera eficiente al tráfico de datos de las redes móviles que crece a tasas exponenciales. Estudios recientes han estimado que el tráfico de datos de las redes móviles se incrementará diez veces entre 2014 y 2019. El objetivo de las redes 5G es soportar estos niveles de crecimiento en el tráfico de datos a la vez que se reduce en un 90% el consumo energético por servicio ofrecido. Para alcanzar estos objetivos, las soluciones centradas en los dispositivos, incluyendo D2D y MCNs, están siendo consideradas como parte del ecosistema 5G como alternativas emergentes a las soluciones celulares tradiciones. Las redes MCNs centradas en los dispositivos utilizan retransmisores móviles y comunicaciones D2D. Las redes MCNs centradas en los dispositivos pueden ayudar a abordar ciertas limitaciones de las arquitecturas celulares tradicionales. En particular, las redes MCNs son capaces de proveer niveles de QoS más altos y más homogéneos en toda la celda mediante la sustitución de enlaces de larga distancia (y probablemente en condiciones NLOS) por múltiples enlaces de mejor calidad. Las redes MCNs centradas en los dispositivos persiguen explotar la inteligencia y los cada vez mayores recursos de comunicación y cómputo de los dispositivos móviles. En las redes MCNs centradas en los dispositivos, los dispositivos móviles se convierten en productores/consumidores de conectividad inalámbrica y actúan como puente entre la infraestructura celular y otros dispositivos. Las redes MCNs han demostrado tener el

potencial para ofrecer importantes beneficios de capacidad, eficiencia energética y QoS. De hecho, estudios analíticos y basados en simulación han demostrado los beneficios de las redes MCNs que utilizan retransmisores móviles en términos de mejora de la capacidad, extensión de la cobertura, escalabilidad de la red, y coste de despliegue. Sin embargo, hasta la fecha, ningún estudio había evaluado experimentalmente los beneficios de las redes MCNs que utilizan retransmisores móviles y comunicaciones D2D. En este contexto, esta tesis ha contribuido en el conocimiento del verdadero potencial y los beneficios de rendimiento que las redes MCNs centradas en los dispositivos pueden proporcionar con respecto a los sistemas celulares tradicionales. En particular, esta tesis ha diseñado una plataforma hardware MCN única que ha sido utilizada para validar y cuantificar los beneficios de QoS de las redes MCNs con respecto a las comunicaciones celulares basadas en un único salto, y las condiciones en las que estos beneficios pueden obtenerse. Esta tesis ha utilizado también los datos obtenidos de campañas de medidas para desarrollar un conjunto único de modelos empíricos del rendimiento de las comunicaciones en las redes MCNs.

Una gran porción del tráfico que está contribuyendo en el crecimiento de los datos en las redes móviles puede considerarse como tolerante a retardos. Este es el caso por ejemplo del tráfico de video móvil, que se espera que represente el 72% del tráfico de datos en las redes móviles en 2019, y también incluye tráfico de emails, compartición de ficheros, redes sociales, actualizaciones de software/firmware, servicios en la nube, datos medidos y seguimiento de productos/mercancías. La integración de mecanismos oportunistas en las redes MCNs representa una opción interesante para proveer QoS a la vez que se mejora la eficiencia energética aprovechando la tolerancia al retardo de estos servicios de tráfico. Los mecanismos oportunistas pueden sacar provecho de las capacidades de almacenamiento, transporte y reenvío de los dispositivos móviles, y de las propiedades de no tiempo real de los servicios tolerantes a retardos, para mejorar la eficiencia de las transmisiones inalámbricas. En este contexto, esta tesis ha contribuido en analizar la capacidad de las redes MCNs oportunistas de mejorar la eficiencia energética de las redes celulares. En particular, esta tesis ha propuesto un entorno analítico para las redes oportunistas MCN de dos saltos diseñado para identificar su configuración óptima en términos de eficiencia energética. Además, esta tesis ha propuesto dos técnicas oportunistas que hacen uso de la información de contexto que está disponible en las redes celulares para identificar a los retransmisores móviles adecuados y teniendo en cuenta la configuración óptima identificada. Los esquemas propuestos incrementan la viabilidad de integrar mecanismos oportunistas en las redes

MCNs, y contribuyen en alcanzar los objetivos de las redes 5G en cuanto a capacidad y eficiencia energética.

Las siguientes secciones proporcionan un completo resumen de los principales resultados y conclusiones obtenidos de las investigaciones llevadas a cabo en esta tesis. Finalmente, se discuten posibles líneas futuras de investigación.

8.1 Evaluación Experimental de las Redes MCN

Esta tesis ha desarrollado mHOP, la primera plataforma de investigación diseñada para investigar los beneficios de rendimiento de las redes MCNs con retransmisores móviles sobre los sistemas celulares tradicionales, y las condiciones en las que estos beneficios pueden obtenerse. Para permitir la comparativa de rendimiento, la plataforma incluye un enlace celular convencional y un enlace MCN que consigue el acceso a la infraestructura celular a través de un nodo móvil híbrido capaz de retransmitir los datos celulares en tiempo real hacia (desde) el nodo destino. Además, esta tesis ha presentado también los primeros resultados obtenidos de una extensa campaña de medidas que validan el potencial de las redes MCNs que utilizan retransmisores móviles y comunicaciones D2D, y demuestran las importantes mejoraras en la QoS que pueden conseguirse con esta tecnología emergente comparada con los sistemas celulares tradicionales. En particular, las pruebas de campo llevadas a cabo han demostrado experimentalmente la capacidad de las tecnologías MCN de extender el radio celular, y de incrementar la QoS a distancias alejadas de la BS, en entornos de interior, bajo condiciones de NLOS, y en zonas de traspaso de celda. Las medidas llevadas a cabo han demostrado también de modo experimental la capacidad de las redes MCNs que utilizan retransmisores móviles de reducir el consumo energético comparado con los sistemas celulares tradicionales.

8.2 Modelado del Rendimiento de Redes MCN

Utilizando la plataforma experimental mHOP y los datos obtenidos de la campaña de medidas comentada anteriormente, esta tesis ha obtenido unos novedosos y únicos modelos empíricos del rendimiento de las comunicaciones en redes MCNs que utilizan retransmisores móviles y comunicaciones D2D. Los modelos propuestos pueden ser útiles en el diseño, testeo y optimización de novedosos protocolos de comunicación y de red para redes MCNs. Los modelos han sido obtenidos tras una larga campaña de medidas en la red celular operativa de la ciudad de Elche en España. Los modelos

obtenidos representan el *throughput* experimentado en el nodo destino de la comunicación MCN en función a la distancia, las condiciones de visibilidad/propagación, número de saltos, y configuración de la comunicación. El *throughput* de la comunicación MCN ha sido modelado utilizando una función sigmoidea que depended del *throughput* celular experimentado en el nodo híbrido o pasarela. Se han obtenido modelos para configuraciones MCN de hasta 5 saltos. Los parámetros de ajuste de los modelos han demostrado depender de factores clave como las condiciones de propagación y el número de saltos. Otro parámetro relevante ha sido la distancia crítica o distancia a la que el *throughput* de la comunicación MCN opera por debajo del *throughput* de la conexión celular. Los modelos han sido obtenidos considerando transmisiones celulares HSPA (LTE no estaba desplegado cuando se estaban obteniendo los modelos) y IEEE 802.11g para las comunicaciones D2D. Extender estos modelos a otras tecnologías sería posible siempre y cuando el rendimiento de la comunicación MCN este limitado por el enlace celular entre la BS y el nodo híbrido. Utilizando los datos obtenidos en estas pruebas de campo, la tesis también ha obtenido modelos empíricos de la comunicación entre dispositivos. En particular, esta tesis proporciona modelos de la tasa de transmisión IEEE 802.11 (*data rate*), la tasa de paquetes erróneos (PER) y el nivel de la señal recibida (RSSI) en función a la distancia entre los nodos de comunicación.

8.3 Técnicas Oportunistas en Redes MCN

Una gran proporción del tráfico de datos (presente y futuro) pueden considerarse tolerante a retardos. En este contexto, esta tesis ha propuesto sacar provecho a esta tolerancia al retardo para mejorar aún más los beneficios de las redes MCNs a través de la integración de técnicas oportunistas. El estudio se ha centrado en un escenario con 2 saltos en la red MCN, y ha formulado analíticamente el problema de optimización de consumo energético que permite identificar la localización óptima del retransmisor móvil, y la localización en la que el retransmisor necesita iniciar la retransmisión de la información hacia la red celular, con el objetico de minimizar el consumo energético. El estudio llevado a cabo ha analizado el impacto de las características del tráfico tolerante a retardos en las ganancias de energía que pueden obtenerse con las comunicaciones oportunistas en redes MCNs utilizando como base de la comparación las comunicaciones celulares tradicionales. El estudio ha investigado también como las comunicaciones oportunistas en redes MCNs deben configurarse para sacar el máximo provecho a la tolerancia al retardo del tráfico con el objetivo de reducir el consumo energético total de las transmisiones. Los resultados obtenidos han demostrado que las

comunicaciones oportunistas en redes MCNs pueden reducir significativamente el consumo energético con respecto a las comunicaciones celulares tradicionales para tráfico tolerante a retardos. Los niveles de reducción pueden ir más allá del 95% en determinadas condiciones. En particular, los niveles de reducción del consumo energético se incrementan a medida que incrementa el tiempo límite que tolera el tráfico tolerante a retardos y se incrementa la distancia del nodo fuente a la estación base.

Las configuraciones óptimas obtenidas han sido utilizadas como referencia para el diseño de técnicas oportunistas realistas para redes MCNs que utilizan retransmisores móviles. En particular, un conjunto de técnicas oportunistas que hacen uso de información de contexto han sido propuestas. Las técnicas propuestas sacan provecho de la información de contexto que pueden obtener de las redes celulares para identificar a los retransmisores móviles más adecuados y teniendo en cuenta la configuración óptima identificada. Si no puede encontrarse un MR en la localización óptima identificada en el instante requerido, la propuesta AREA expande el área búsqueda alrededor de la localización óptima utilizando información acerca de la densidad de usuarios en la celda y su distribución. La propuesta DELAY utiliza la misma información de contexto para identificar cuánto tiempo puede retrasarse la transmisión D2D desde el nodo fuente para encontrar un MR en la localización óptima identificada. Las evaluaciones llevadas a cabo han demostrado que la integración de estas técnicas oportunistas realistas en las redes MCNs también permite obtener importantes ahorros energéticos y ganancias de capacidad en comparación con las redes celulares tradicionales. La propuesta AREA generalmente mejora el rendimiento de la propuesta DELAY. Ambas técnicas se benefician de la utilización de información de contexto por anillo en lugar de por celda. En este caso, las técnicas propuestas pueden reducir el consumo energético (hasta en un 98%) e incrementar la capacidad celular (hasta en un 79%) en comparación con las comunicaciones celulares tradicionales y para tráfico tolerante a retardos. Estos resultados demuestran que las técnicas oportunistas en las redes MCNs pueden contribuir significativamente a alcanzar las objetivos de las redes 5G en términos de capacidad y eficiencia energética.

8.4 Trabajos Futuros

La plataforma mHOP fue implementada utilizando portátiles Ubuntu como retransmisores móviles. Esta decisión fue tomada debido a los requisitos de la plataforma en términos de capacidades de monitorización, escalabilidad y flexibilidad

para investigar diferentes configuraciones de comunicación. Durante la tesis, el autor ha seguido muy de cerca la evolución del proyecto *Ubuntu for Devices* (también conocido como *Ubuntu Touch* o *Ubuntu Phone*) ya que hubiese sido interesante evolucionar la plataforma para integrar terminales móviles. Dado que el código de implementación de mHOP está desarrollado en Ubuntu, la migración a un terminal móvil Ubuntu no debería requerir muchos esfuerzos. Sin embargo, en el momento que se implementó mHOP no había una versión estable del proyecto *Ubuntu for Devices* (de hecho el primer terminal Ubuntu salió a la venta en Febrero de 2015 en el BQ Aquaris E4.5). Las versiones disponibles para desarrolladores (conocidas como *Developer Preview*) carecen todavía de todas las funcionalidades que se necesitan para implementar un nodo de la plataforma mHOP. Por ejemplo, en la versión disponible para desarrolladores sólo hay disponible servicios de SMS y voz sobre GSM y UMTS. Algunas funcionalidades de red están soportadas como la configuración en modo ad-hoc de IEEE 802.11, pero el acceso a modificar parámetros de comunicación de las capas PHY y MAC es todavía limitado. Otro tema es el hecho de que los nodos de la plataforma mHOP están equipados con una interfaz externa IEEE 802.11 para realizar las comunicaciones ad-hoc D2D ya que la interfaz interna se dedica a monitorizar los paquetes retransmitidos. Esta tarjeta externa puede conectarse al terminal móvil utilizando el puerto mini USB que necesita proveer de corriente a la tarjeta. Sin embargo, esta funcionalidad (USB OTG) no está todavía soportada.

Otra interesante evolución de la plataforma mHOP sería la integración de interfaces radio alternativas para soportar las comunicaciones D2D. La tecnología desarrollada por Qualcomm, LTE-Direct, representa un claro progreso para estudiar las comunicaciones MCN utilizando tecnologías basadas en LTE. El software de desarrollo de LTE-Direct está disponible y puede ser instalado en terminales para desarrollar soluciones de descubrimiento de proximidad y servicios de proximidad. Sin embargo, el software de desarrollo proporcionado por Qualcomm no soporta todavía comunicaciones D2D.

En paralelo al desarrollo de esta tesis, algunos miembros del laboratorio UWICORE han estado evolucionando la plataforma mHOP para implementar comunicaciones oportunistas D2D basadas en la calidad del enlace modificando la implementación por defecto de IEEE 802.11 que se encuentra en el Kernel de Linux, en particular su capa MAC. Este desarrollo persigue mejorar la eficiencia y rendimiento de las comunicaciones D2D evitando transmisiones innecesarias (e ineficientes) cuando la calidad de los enlaces no es lo suficientemente buena. En particular, la solución implementada pausa la comunicación D2D entre dos dispositivos cuando la calidad del enlace medida está

por debajo de un umbral de RSSI. La transmisión D2D se reinicia cuando la calidad del enlace mejora. Esta implementación ha demostrado resultar en importantes beneficios de para la comunicación D2D en términos de energía, capacidad y QoS. Los esfuerzos deben destinarse ahora a extender esta plataforma para soportar comunicaciones D2D oportunistas multi-salto, y aún más importante para soportar comunicaciones MCN en las que la pausa oportunista se efectúe tanto en los enlaces D2D como en el enlace celular.

Esta tesis ha demostrado los beneficios energéticos y de capacidad que pueden obtenerse de la integración de mecanismos oportunistas en redes MCNs para tráfico tolerante a retardos. A partir de los resultados obtenidos, se podría seguir trabajando en el diseño de novedosas políticas de red que tengan en cuenta los diferentes requisitos de los servicios y las particularidades de las técnicas oportunistas para establecer conexiones eficientes. Para este objetivo, disponer de mayor información de contexto será algo muy a tener en cuenta (por ejemplo, las preferencias de los usuarios, el estado de la red, la disponibilidad de espectro, las condiciones del enlace, niveles de interferencia, y condiciones de operación). De hecho, las comunicaciones basadas en el contexto están claramente marcadas como una característica clave de las futuras redes 5G. Sin embargo, adquirir y compartir esta información de contexto podría requerir mucha información de contexto, lo cual debe de ser controlado de manera muy cuidadosa evaluando el valor y el coste de adquisición de la información de contexto. En este contexto, deberán desarrollarse esquemas que requieran de poca señalización para extraer y caracterizar las condiciones de contexto considerando los compromisos entre relevancia y granuralidad de la información de contexto.

Las futuras redes 5G estarán formadas por la coexistencia de diferentes tecnologías de acceso radio (adecuadas para los diversos servicios 5G), bandas de espectro (con licencia y sin licencia), y modos de comunicación (tradicionales, D2D y MCNs). Los futuros ecosistemas heterogéneos requerirán por lo tanto técnicas de gestión avanzadas para utilizar de una manera adecuada la esperada heterogeneidad. En este contexto, sería interesante extender los estudios llevados a cabo en esta tesis a redes multitecnología heterogéneas y con una alta flexibilidad de espectro, en las que se permita que las comunicaciones D2D y las redes MCN utilicen tecnologías y bandas heterogéneas para sus transmisiones. En este escenario, las comunicaciones D2D y MCN serían capaces de seleccionar dinámicamente la configuración más adecuada para cada transmisión, dependiendo la selección de los diversos requisitos de eficiencia, fiabilidad y latencia de las aplicaciones y servicios de las redes 5G.

También sería importante mencionar el trabajo que queda por hacer para progresar hacia las redes inalámbricas centradas en los dispositivos. Para asegurar que los nodos pueden tomar decisiones independientes y locales, se necesita progresar en la evolución de las arquitecturas celulares actuales para facilitar arquitecturas más flexibles. Con este objetivo, las soluciones que se propongan podrían considerar las propuestas de separar los planos de control y de usuario, los cuales podrían operar en diferentes tecnologías y/o bandas de espectro. Además, las redes centradas en los dispositivos requieren del diseño de novedosos mecanismos de control distribuidos y semi-centralizados que ofrezcan la suficiente flexibilidad para tomar decisiones a nivel del dispositivo mientras que se asegura que esas decisiones, coordinadas o no por la red celular, ayudan a maximizar el rendimiento de la red, la capacidad y eficiencia con un mínimo intercambio de señalización.

Esta tesis ha demostrado que la integración de técnicas oportunistas en las redes MCNs puede ayudar a contribuir a conseguir los requisitos de capacidad y eficiencia energética de las futuras redes inalámbricas. Estas redes necesitarán también que reducir la latencia en la red de acceso. Las propuestas para separar los planos de control y de usuario en las arquitecturas centradas en los dispositivos pueden tener un efecto importante en la reducción de la latencia. Una solución complementaria que podría beneficiarse de la flexibilidad de las redes inalámbricas centradas en los dispositivos es la posibilidad de usar los terminales móviles como distribuidores de contenido. De este modo, la información está almacenada en el verdadero límite de la red y el tiempo para acceder a la información se reduce de manera significativa. Sin embargo, es necesario resolver todavía importantes asuntos como decidir qué información debe ser almacenada, quién debería almacenar esta información y cómo distribuir esta información.

Annex A.

Configuration of Opportunistic Forwarding using HSPA Technology

Chapter 6 has investigated the integration of opportunistic networking schemes into MCNs that utilize D2D communications for delay tolerant services. The study has focused on a two-hop MCN scenario in which a static Source Node (SN) uploads a message to the Base Station (BS) using a Mobile Relay (MR) with store, carry and forward capabilities (Figure 6-2). The scenario considers a delay tolerant service characterized by a message of size *F* that needs to be uploaded to the BS within a time *T*. The study has then proposed an analytical framework to manage the available time in order to reduce the energy consumption considering the processes involved in a two-hop opportunistic MCN transmission: selection of the mobile relay node, store and carry process, and the cellular communication with the base station. The analytical framework has allowed deriving an optimum configuration of opportunistic MCN communications that identifies the MR location at which the D2D transmission from SN to MR should start, and the MR location at which the cellular transmission starts. The study in Chapter 6 was carried out considering LTE at 2 GHz for the cellular transmission and IEEE 802.11g at 2.4 GHz for the D2D transmissions. This annex reproduces the study using High Speed

Packet Access (HSPA) at 2.1 GHz for the cellular transmissions to demonstrate that the conclusions reached in Chapter 6 are not dependent on the selected radio access technologies. To this aim, Annex A.b derives and analyzes the optimum configuration of opportunistic forwarding for the two-hop MCN scenario. Chapter 7 addressed the scenario in which the optimum configuration cannot be established, and presented suboptimum opportunistic forwarding approaches that use context-information provided by the cellular infrastructure. Annex A.c analyzes then the performance of the 'Space-dependent Opportunistic Forwarding' (AREA) context-aware opportunistic forwarding scheme[27] considering HSPA for the cellular radio access. See Chapter 7 for additional details on the definition of the AREA proposal (e.g. how to calculate the radius around the optimum MR search area for uniform and non-uniform distributions of users within the cell).

a. Evaluation Scenario

The numerical resolution of the multi-objective constrained optimization framework presented in Chapter 6 is done considering HSPA at 2.1 GHz for the cellular transmissions and IEEE 802.11g at 2.4 GHz for the ad-hoc D2D transmissions. The cellular transmission adapts the modulation and coding schemes based on the experienced channel conditions. Following the model reported in [159], the cellular transmission rate of the communication from MR to BS is modeled as follows:

$$R_{cell}(d) = k \cdot C \cdot log_2\left(M(d)\right) \cdot BW \qquad \text{(Annex A-1)}$$

where *BW, M* and *C* represent the system bandwidth, modulation constellation size and coding rate, respectively. *M* and *C* are selected according to the distance between the mobile device and the BS (the higher the distance, the lower the received signal strength, and more robust modulation and coding schemes are needed). This study considers seven possible combinations of modulation and coding schemes with a maximum transmission rate of 7 Mbps. *K* represents an attenuation factor that limits the cellular data rate, and includes, among others, the effect of transmission failures, retransmissions, and interference [159]. The SN needs to transmit to the BS a 10 Mb (*F*) file before a 60 seconds deadline *T*. The scenario considers that the MRs are in line with the SN, and moving towards the BS with a speed of 2 m/s. The rest of parameters are reported in Table A.1.

[27] AREA was selected since this proposal generally outperforms DELAY.

Table A.1. Evaluation parameters.

Parameter	Description	Value
Cell	Cell radius	1000 m
AMC	Adaptive modulation and coding	BPSK(r=1/3) QPSK(r=1/3, 1/2, 2/3) 16QAM(r=1/2, 2/3, 5/6)
BW	System bandwidth	10 MHz
G_{TX}, G_{RX}	Transmitter and receiver antenna gain	1
e_{tx}, e_{rx}	Energy consumed per bit by the transmitter/receiver	50 x 10-9 J/b
P_{RX}	Power reception threshold	-62 dBm
h_{SN}, h_{MR}, h_{BS}	Antenna height of SN, MR and BS	1.5 m, 1.5 m, 10 m
DRAM P_R, P_W, $P_{Idle\_self\text{-}refresh}$	DRAM power consumed for Reading, Writing and in Idle_self-refresh state	252 mW, 252 mW, 1.35 mW
NAND Eff_{Read}, Eff_{Write}, P_{Idle}	NAND efficiency for Reading and Writing, and Power consumed in Idle state	1.83 nJ/b, 11.92 nJ/b, 0.4 mW
Transf_DF, *Transf_EF*	Transfer speed from the DRAM to the NAND flash and vice versa	4.85 MiB/s, 927.1 KiB/s

b. Optimum Configuration

The resolution of the objective function presented in Chapter 6 results in the optimum MR location to start the D2D transmission depicted in Figure A.1.a. The MR location is represented by means of the distance between SN and MR, and is depicted in Figure A.1.a as a function of the distance between SN and BS. Figure A.1.a shows for example that if SN is located 400 meters away from the BS, the MR should be ideally located 65 meters away from the SN in the direction of the BS in order to minimize the total energy consumption. Figure A.1.a shows that the distance between SN and the optimum MR that minimizes the energy consumption increases with the distance between SN and BS. This is the case because as the distance between SN and MR increases, the MR is closer to the BS, and the cellular transmission energy decreases. On the other hand, the D2D transmission energy increases as MR is closer to the BS. As a result, the distance between SN and the optimum MR location only increases when the energy saving of the store and carry process can compensate the increase in the D2D transmission energy consumption. The energy consumption levels for the D2D transmission from SN to the optimum MR location are reported in Figure A.1.b in

logarithmic scale. The energy consumption levels are shown as a function of the distance between SN and BS, and are labeled 'Optimum'. The increasing distances between SN and the optimum MR (Figure A.1.a) result in that the D2D transmission energy consumption levels increase with the distance between SN and BS.

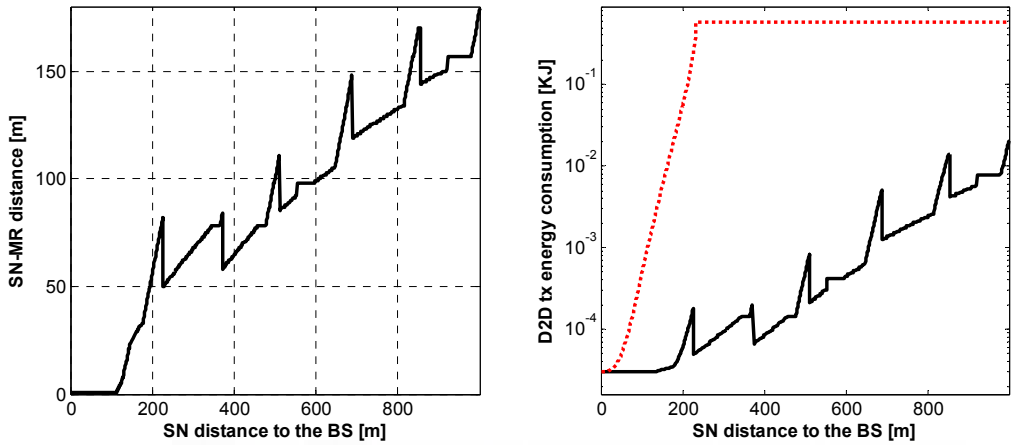

a) Optimum MR location

b) D2D transmission energy consumption

Figure A.1. Optimum configuration of two-hop opportunistic MCN communications using HSPA for the cellular transmission: D2D transmission.

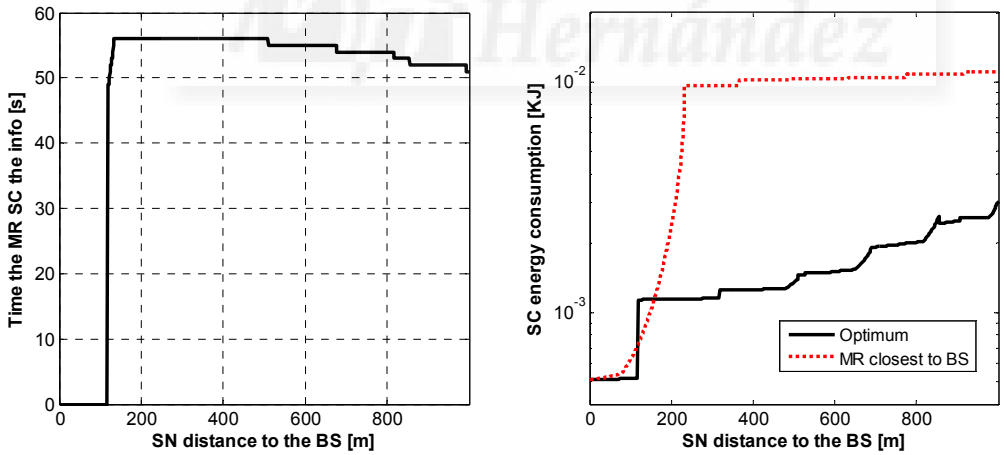

a) Time the MR stores and carries the information while moving towards the BS

b) Store and carry energy consumption

Figure A.2. Optimum configuration of two-hop opportunistic MCN communications using HSPA for the cellular transmission: Store and Carry (SC).

Figure A.2.a shows the time that the MR needs to store and carry the information towards the BS, from the location identified in Figure A.1.a, in order to minimize the total energy consumption. Figure A.1.a showed that if the distance between SN and BS is 400 meters, the optimum MR that minimizes the total energy consumption is located 65 meters away from SN. Figure A.2.a shows that this optimum MR needs then to store and carry the information for 56 seconds before transmitting it to the BS using its cellular interface. The obtained results indicate that when the SN is close to the BS, the optimum MR does not need to store and carry the information. The optimum MR should instead forward it to the BS as soon as received from the SN. This is the case because the store and carry energy consumption levels do not compensate the energy savings resulting from forwarding the information at distances closer to the BS. The results depicted in Figure A.2.b show that when the MS is close to the BS, the store and carry energy consumption level is minimum. Even if the MR does not need to store and carry the information when SN is close to the BS, the store and carry energy consumption levels are not null since they include the storage power consumption at SN and MR while transmitting and receiving the information (P_W and P_R, in Figure 6-3 –Chapter 6). As the distance from SN to the BS increases, the optimum MR should store and carry the information so that its cellular transmission starts closer to the BS where higher cellular data rates are possible. However, Figure A.2.a shows that for high distances between SN and BS, the time the MR stores and carries the information to minimize the total energy consumption decreases. On the other hand, the store and carry energy consumption levels increase with the distance between SN and BS ('Optimum' in Figure A.2.b). These

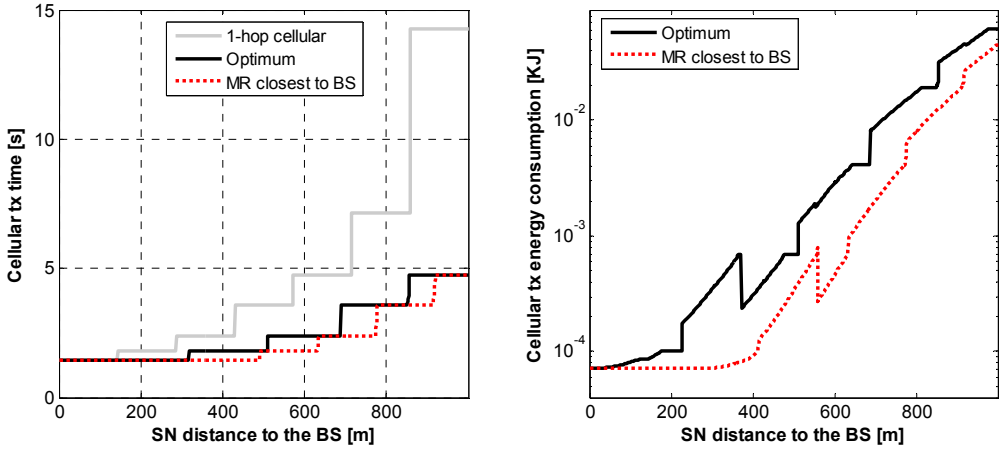

a) Time the to transmit the data to the BS b) Cellular transmission energy consumption

Figure A.3. Optimum configuration of 2-hop opportunistic MCN communications using HSPA for the cellular transmission: Cellular transmission.

two effects are due to the increase in the time needed to complete the D2D (Figure A.3.a) and cellular transmissions ('Optimum' in Figure A.3.a). Figure A.3.a shows the time the optimum MR needs to transmit the information to the BS using its cellular radio interface, while Figure A.3.b reports the resulting cellular transmission energy consumption levels. The results reported in Figure A.3.a demonstrate the capacity benefits of opportunistic MCN communications with regards to traditional single-hop cellular communications ('1-hop cellular'). The capacity benefits are depicted in terms of the reduction of the time needed to complete the cellular transmission.

The optimum configurations (i.e. MR location, time the MR should store and carry the information, and location at which the MR should start forwarding the information to the BS) illustrated in Figure A.1, Figure A.2 and Figure A.3, result in the total energy consumption levels shown in Figure A.4 ('Optimum' in Figure A.4). Figure A.4 also shows the total energy consumption level if the SN directly transmits the information to the BS through traditional single-hop cellular communications ('1-hop cellular' in Figure A.4). The obtained results show that when SN is very close to the BS, there are no energy benefits from using opportunistic MCN communications compared to traditional single-hop cellular communications. However, as the distance increases, opportunistic MCN communications can result in significant energy benefits compared to traditional single-hop cellular communications. For example, when the distance between SN and BS is 350 meters, opportunistic MCNs can reduce the energy consumption level by 50% compared to traditional single-hop cellular communications. This value increases to 90% at the

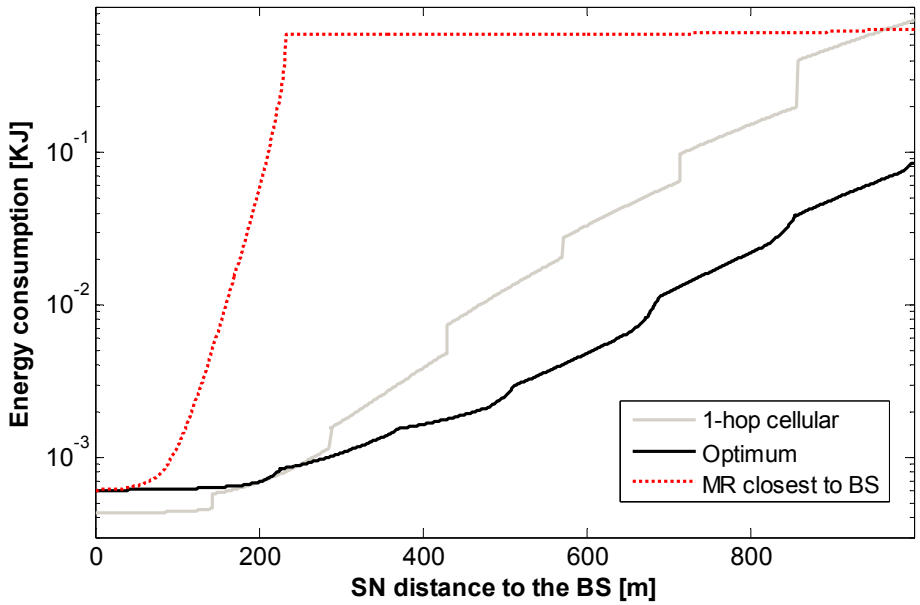

Figure A.4. Total energy consumption (the schemes use HSPA for the cellular transmission).

cell edge. On average, an optimum configuration of MCN schemes using opportunistic store, carry and forward can reduce energy consumption levels by over 85-90% compared to traditional single-hop cellular communications (Figure A.4).

The benefits that can be achieved when combining MCNs and opportunistic store, carry and forward schemes, depend on an adequate selection of the MR location and the location at which the MR should start forwarding the information to the BS. To demonstrate such dependency, Figure A.4 also reports the total energy consumption levels with a scheme in which the SN selects the MR that provides the higher progress towards the BS ('MR closest to BS' in Figure A.4) [144]. For a fair comparison, a similar optimization process to that reported in Chapter 6 is conducted for this scheme, but considering the new location of the MR (the closest to the BS). This configuration results in that the MR is able to minimize the time needed to upload the information to the BS (Figure A.3.a), and therefore the cellular transmission energy consumption (Figure A.3.b). However, this is obtained at the expense of a significant increase in the total energy consumption levels compared to an optimum configuration of opportunistic MCN communications (Figure A.4). Figure A.4 also shows that selecting the MR as close as possible to the BS can significantly increase the energy consumption levels when the SN is close to the BS. This effect is due to the high energy consumption levels experienced in the D2D transmission between SN and MR (Figure A.1.b), and the store and carry process (Figure A.2.b). The obtained results demonstrate that an optimum configuration of opportunistic MCN communications can reduce the energy consumption by up to 97% compared to selecting the MR that provides a higher progress towards BS.

The obtained results demonstrate that the benefits that opportunistic MCN communications can achieve with respect to single-hop cellular communications do not depend on the selected cellular radio access technology. This annex uses HSPA for the cellular link between the MR and the BS, while the study conducted in Chapter 6 used LTE. Similar trends in the energy consumption for opportunistic MCN communications are observed using both cellular radio access technologies. Considering all the scenarios analyzed (different traffic characteristics, etc.), only small differences are appreciated in the energy gains of opportunistic MCN communications with respect to single-hop cellular communications when using different radio access technologies. The energy gains are slightly smaller when using HSPA. This is due to the higher LTE transmission rates that benefit opportunistic MCN communications as the MR moves towards the BS and forwards the information to the cellular network.

c. Context-Aware Opportunistic Forwarding in MCN

This section evaluates the performance of the AREA proposal (see Chapter 7) in the scenario summarized by the parameters presented in Table A.1 and where cellular transmissions use HSPA. The scenario considers the SN needs to upload to the BS a file of size 10 Mb, and the time available to complete the transmission is set to 60 seconds. The scenario considers that the MRs are in line with the SN, and moving towards the BS with a speed of 2 m/s. The energy consumption of the proposed AREA context-aware opportunistic forwarding scheme is here compared against that obtained with traditional single-hop communications ('1-hop cellular'), the optimum configuration of opportunistic forwarding ('Optimum'), and 3 other reference schemes from the literature. In the reference scheme 'MR closest to BS', the SN selects the MR that provides a higher progress towards the BS [144]. On the other hand, the 'MR closest to SN' reference scheme selects the MR that is closer to SN [158]. Once the MR is selected (closest to the BS or SN), and for a fair comparison, a similar optimization process to that reported in Chapter 6 is then conducted for both techniques, but considering only the store and carry and the cellular transmission processes. This optimization process allows determining the location at which the selected MR should forward the information towards the BS in order to minimize the total energy consumption. Finally, the performance of the context-aware proposal is also compared to the '1-hop Direct-contact' [111]. In this scheme, the SN is mobile and can store, carry and forward the information to the BS without using a mobile relay. In this case, and for a fair comparison, the optimization process reported in Chapter 6 is used to define the optimum location at which the moving SN should start forwarding the information to the BS to minimize the energy consumption.

Table A.2 shows the average energy reduction that can be obtained with the different schemes compared to traditional single-hop cellular communications[28]. The depicted results correspond to average values obtained for all possible distances between SN and BS. Different tables are used for uniform and non-uniform spatial distributions of mobile devices within the cell. Results are shown for different spatial densities of MRs (μ/R={0.1, 0.05} MRs/m) within a cell. In the case of a non-uniform distribution of users within the cell, higher densities are considered for the rings closer

[28] The 'MR closest to BS' technique consumes more energy than single-hop cellular communications (negative values in Table A.2) due to the high energy being consumed during the D2D transmission as a result of selecting the MR as close as possible to the BS.

to the BS without loss of generality[29]. The context-aware AREA proposal requires information about the density of users. When such information is provided per cell, the proposal is referred to as AREA. When the information is provided per ring, the scheme is referred to as AREA-Ring. To provide the density information per ring, this study considers that a cell is divided into seven rings; a cellular transmission mode (Table A.1) is assigned to each ring.

The results depicted in Table A.2 show that the AREA proposal significantly reduces the energy consumption compared to single-hop cellular communications without sacrificing the end-user QoS (in this case, the transmission deadline). The reduction ranges from 50 to 80%, and is obtained independently on whether the density information is provided per cell or ring. The obtained results show that in terms of energy reduction levels compared to single-hop cellular communications, the AREA proposal is only outperformed by the optimum configuration of opportunistic forwarding ('Optimum'). As previously mentioned, it is possible that an MR cannot be found when needed at the identified optimum location. This reduces the feasibility to apply the optimum configuration in practical settings. Table A.2 shows that under a uniform distribution of users within the cell, there is not a significant performance difference between the AREA and AREA-Ring proposals. On the other hand, the AREA-Ring variant outperforms the AREA one when there is a non-uniform distribution of users within the cell. The context-aware proposal looks for potential MRs in a search area calculated using density information. When an MR cannot be found in the identified search area, the SN directly communicates with the BS using traditional single-hop cellular communications. The AREA variant looks for potential MRs in a search area calculated using density information per cell. When the distribution of users is non-uniform within a cell, the density information per cell can result in frequent incorrect estimations of the MR search area compared to the case in which the density information is provided per ring; the density information per ring can provide a better indication of the non-uniform distribution of users, and therefore better adjust the MR search area. This trend is observed when analyzing the hit rate of the context-aware proposal (Table A.3), or percentage of transmissions conducted using two-hop MCN communications. Table A.3 shows that in the case of non-uniform distribution of users within the cell, the AREA variant significantly decreases the hit rate

[29] For μ/R=0.1 MRs/m, the density (in MRs/m) in the seven rings is (values are shown from closer to more distant to the BS): {0.4, 0.085, 0.071, 0.057, 0.043, 0.029, 0.014}. For μ/R=0.05 MRs/m, these values are equal to: {0.2, 0.043, 0.036, 0.026, 0.021, 0.014, 0.007}.

Table A.2. Average energy reduction (in %) compared to single-hop cellular communications. The schemes use HSPA for the cellular transmission.

a) Uniform spatial distribution of MRs

Technique	***μ/R*=0.1 MRs/m**		***μ/R*=0.05 MRs/m**	
	***δ*=0.9**	***δ*=0.8**	***δ*=0.9**	***δ*=0.8**
AREA	78.9	74.6	77.8	75.2
AREA – Ring	82.5	77.8	82.8	77.5
MR closest to BS	-104.2		-49.1	
MR closest to SN	58.7		58.5	
1-hop Direct-contact	65.4			
Optimum	87.9			

b) Non-uniform spatial distribution of MRs

Technique	***μ/R*=0.1 MRs/m**		***μ/R*=0.05 MRs/m**	
	***δ*=0.9**	***δ*=0.8**	***δ*=0.9**	***δ*=0.8**
AREA	49.2	47.0	45.4	38.3
AREA – Ring	82.2	79.8	75.7	70.8
MR closest to BS	-90.7		-45.4	
MR closest to SN	62.8		62.7	
1-hop Direct-contact	65.4			
Optimum	87.9			

as a result of an incorrect definition of the MR search area. The lower percentage of two-hop MCN connections established with the AREA variant increases the energy consumption with respect to the AREA-Ring variant for non-uniform distributions (Table A.2.b). On the other hand, the AREA-Ring variant results in a better definition of the MR search area, and therefore a higher hit rate. This is illustrated in Figure A.5 that shows the hit rate as a function of the distance between SN and the BS[30]. Figure A.5.a shows that for a uniform distribution of users within the cell, the AREA and AREA-Ring variants achieve similar hit rate levels independently of the location of the SN. In the case of non-uniform distributions within the cell (in this study, higher MR densities close to the BS), the AREA variant underestimates the MR search area with increasing distances from SN to the BS, which results in a decrease of the hit rate (Figure A.5.b). On the other hand, the AREA-Ring variant adapts the MR search area to the density of users in the ring

[30] Similar trends are observed for δ=0.8 and μ/R=0.05 MRs/m.

around the MR optimum location. In particular, the AREA-Ring variant increases the radius of the MR search area as the distance between SN and BS increases in order to compensate the reduction of density of users. This capacity to adapt the MR search area explains the higher hit rate of AREA-Ring, and therefore its better energy performance (Table A.2). It is important to highlight that all the trends reported in this annex for the AREA and AREA-Ring proposals, under uniform and non-uniform distribution of nodes within the cell, are similar to those reported in Chapter 7 where the scenario considers LTE for the cellular transmissions.

Table A.3. Hit Rate: percentage of SN-BS transmissions established using two-hop MCN communications. The schemes use HSPA for the cellular transmission.

a) Uniform spatial distribution of MRs

Technique	***μ/R*=0.1 MRs/m**		***μ/R*=0.05 MRs/m**	
	***δ*=0.9**	***δ*=0.8**	***δ*=0.9**	***δ*=0.8**
AREA	91.7	85.3	90.9	84.0
AREA – Ring	95.0	87.9	95.0	88.0

b) Non-uniform spatial distribution of MRs

Technique	***μ/R*=0.1 MRs/m**		***μ/R*=0.05 MRs/m**	
	***δ*=0.9**	***δ*=0.8**	***δ*=0.9**	***δ*=0.8**
AREA	79.7	74.1	77.4	69.2
AREA – Ring	95.3	89.2	96.1	88.4

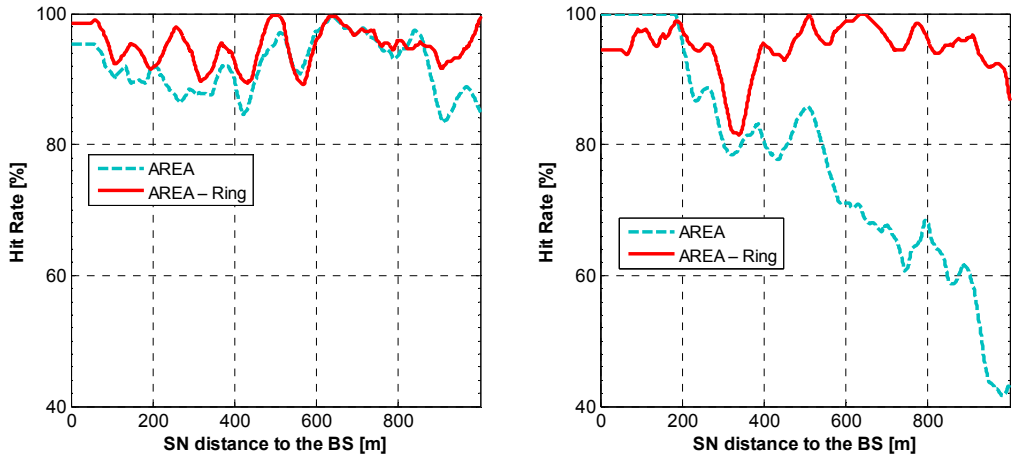

a) Uniform spatial distribution of MRs b) Non-uniform spatial distribution of MRs

Figure A.5. Percentage of transmissions established using two-hop MCN connections as a function of the distance from SN to the BS (*μ/R*=0.05 MRs/m, *δ*=0.9).

UNIVERSITAS
Miguel
Hernández

Annex B.

Configuration of Context-Aware Opportunistic MCN under Worst Case Conditions

This annex evaluates for the two proposed context-aware schemes (DELAY and AREA) how to configure the opportunistic forwarding process under worst case conditions. The two proposals are compared against the optimum configuration of opportunistic forwarding (Section 6.4) and hence are evaluated in the scenario presented in Section 6.4.1 that is characterized by the parameters summarized in Table 6-1. The study here presented considers uniform and non-uniform distributions of nodes and different spatial densities of nodes (μ/R={0.1, 0.05} MRs/m) within the cell. In the case of a non-uniform distribution of nodes within the cell, this study considers a standard deviation σ equal to 300 meters (this means that approximately 68% of the nodes are located at distances closer to 300 meters to the BS with cell radius equal to 1000 meters).

a. Configuration of DELAY

The worst case scenario for DELAY in case of opportunistic transmissions is experienced when SN needs to delay the D2D transmission for the full time t. In a real

operation, it might happen that SN does not need always to delay the D2D transmission by *t* seconds if an MR arrives earlier to the optimum MR location. Section 7.2 showed that the time *t* that guarantees with probability δ (set to 0.8 in this section) the arrival of an MR at the identified optimum location depends on the spatial density and distribution of nodes within the cell. Figure B.1 shows the time *t* the SN needs to delay the D2D transmission waiting for an MR to arrive at the identified optimum MR location in the worst case scenario[31]. *t* is depicted as a function of the distance between SN and BS, and is computed following equations (7-4) and (7-10) for uniform and non-uniform distributions of nodes within the cell, respectively. Figure B.1.a shows, for example, that when nodes are uniformly distributed within the cell, a SN located 400 meters away from the BS needs to delay the D2D transmission by 16.1 seconds waiting for an MR to arrive at the optimum MR location[32]. The results reported in Figure B.1 show that under uniform distribution of nodes *t* is constant for any location of the SN within the cell, but decreases as the spatial density of nodes within the cell increases (from 16.1 seconds to 8.05 seconds when the spatial density of MRs increases from 0.05 MRs/m –Figure B.1.a– to 0.1 MRs/m –Figure B.1.b).

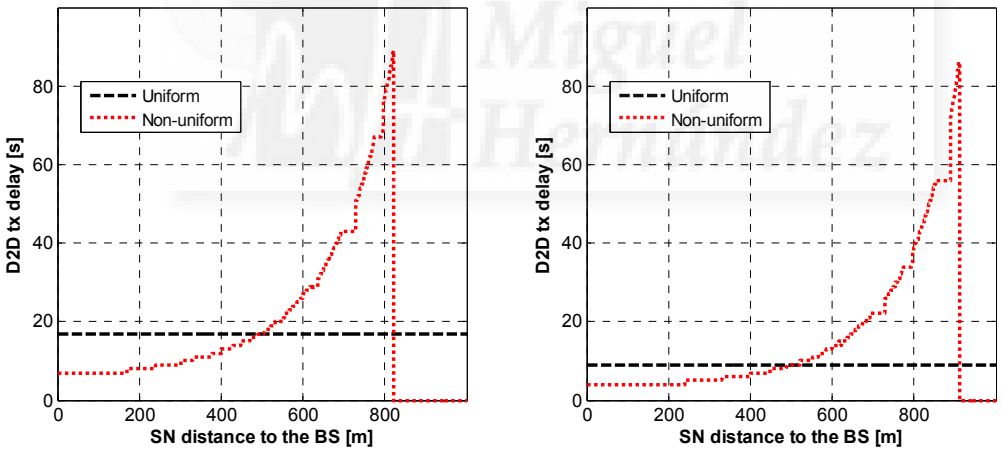

a) μ/R = 0.05 MRs/m b) μ/R = 0.1 MRs/m

Figure B.1. Delay time *t* in the D2D transmission to guarantee the arrival of at least one MR at the identified optimum MR location with δ equal to 0.8.

[31] The optimum MR location was reported in Chapter 6 (Section 6.4, Figure 6-4.a) as a function of the distance between SN and BS.

[32] The optimum MR location was at a 50 meters distance away from the SN in the direction of the BS according to Figure 6-4.a.

Figure B.1 also shows that under non-uniform distribution of nodes within the cell, *t* increases with the distance between SN and BS in order to compensate the smaller density of users as it is increased the distance to the BS. The considered non-uniform distribution scenario results in very low densities of nodes at the cell edge. At the cell edge, the delay *t* in the D2D transmission that would guarantee the arrival of an MR at the optimum location is therefore too high for opportunistic MCN transmissions to be completed before the service-dependent deadline *T*. In this case, SNs close to the cell edge (e.g. at distances higher than 912 meters when μ/R = 0.1 MRs/m, Figure B.1.b) should directly transmit the information to the cellular BS, which is represented by a *t* value equal to 0 in Figure B.1. It is important to recall that this situation corresponds to the worst case performance (i.e. SN needs to delay the D2D transmission for the full time *t*) since an MR might arrive earlier to the optimum MR location in a real operation.

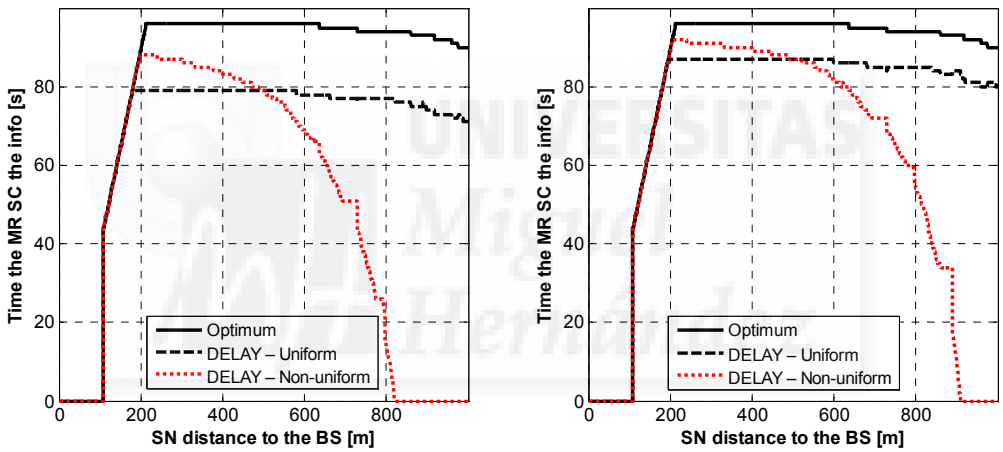

a) μ/R=0.05 MRs/m b) μ/R=0.1 MRs/m

Figure B.2. DELAY: Time the MR stores and carries the information towards the BS.

As a consequence of delaying the start of the D2D transmission at the SN, the selected MR at the identified optimum location needs to adjust its opportunistic operation compared with the optimum configuration derived in Chapter 6. Figure B.2 shows for the DELAY proposal the time the MR would store and carry the information from the optimum MR location until it starts its cellular transmission to the BS in order to minimize the total energy consumption. The reported time is shown in Figure B.2 for the uniform ('DELAY – Uniform') and non-uniform distribution ('DELAY – Non-uniform') of users within the cell. When compared with the optimum configuration ('Optimum' in Figure B.2), the context-aware opportunistic forwarding scheme reduces the time the

MR is allowed to store and carry the information towards the BS as a result of the need to delay the D2D transmission at the SN (Figure B.1). For example, when SN is located 400 meters away from the BS, the selected MR stored and carried the information for 96 seconds in the optimum configuration. When considering the DELAY proposal for real deployments, this time is reduced to 79 seconds (Figure B.2.a, uniform distribution of nodes within the cell and μ/R= 0.05 MRs/m). The results depicted in Figure B.2 also show that under non-uniform distribution of nodes within the cell, the time the MR stores and carries the information considerably reduces with the increasing distance between SN and BS. This is the case because of the increasing delay in the D2D transmission with the distance between SN and BS (Figure B.1).

The time the selected MR stores and carries the information reduces the cellular communications distance with the BS (which allows using higher cellular data rates). The reduction in the time the selected MR located at the optimum location can store and carry the information with the proposed context-aware scheme (Figure B.2) results in higher durations of the cellular transmission to the BS when compared with the optimum configuration (Figure B.3). However, the DELAY proposal reduces the time of the cellular transmission compared with traditional single-hop cellular communications from SN to BS ('1-hop cellular' in Figure B.3). In addition, it is important remembering that the context-aware proposal provides a solution to an unfeasible optimum configuration of opportunistic MCN communications in the case no MR can be found at the identified optimum location and requested time instant.

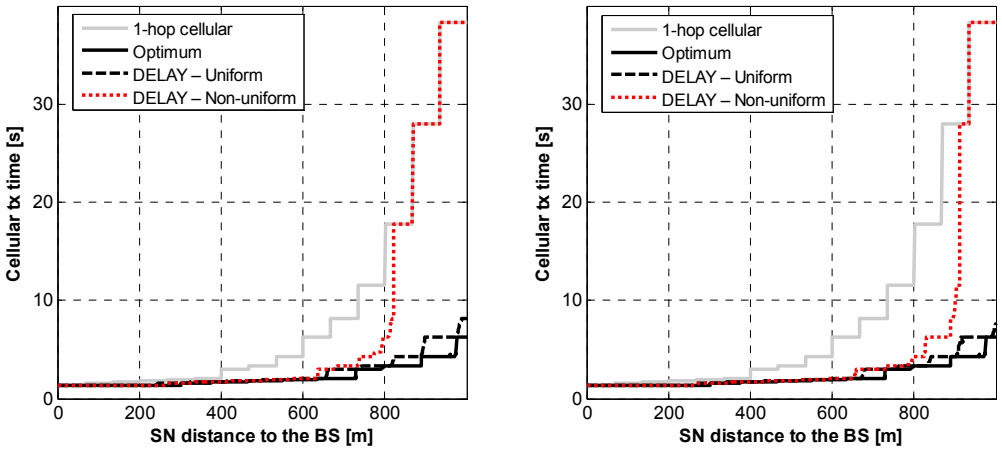

a) μ/R = 0.05 MRs/m b) μ/R = 0.1 MRs/m

Figure B.3. DELAY: Time the MR requires to transmit the data to the BS.

b. Configuration of AREA

The AREA proposal experiences the worst case scenario when the MR is found at the edge of the defined search area. The analysis conducted in Section 7.3 showed that the radius around the optimum MR location that guarantees with probability δ (set to 0.8 in this section) the presence of at least one MR within the search area depends on the spatial density and distribution of nodes within the cell. Figure B.4 shows the radius (r) around the optimum MR location[33] to guarantee the presence of at least one MR within the search area. r is depicted as a function of the distance between the SN and the BS and is computed following equations (7-12) and (7-15) for uniform and non-uniform distributions of nodes within the cell, respectively. Figure B.4.a shows, for example, that a SN located 400 meters away from the BS needs to search for potential MRs within a search area of radius 16 meters around the optimum location of the MR[34]. The results reported in Figure B.4 show that under uniform distribution of nodes, r is constant for any location of the SN within the cell, but decreases as the spatial density of nodes within the cell increases (from 16 meters to 8 meters when the spatial density of MRs increases from 0.05 MRs/m –Figure B.4.a– to 0.1 MRs/m –Figure B.4.b). The obtained results indicate that the worst-case performance occurs when the MR is selected at the edge of the search area closer to the BS (further away to the SN). This is the case because of the higher impact of an increase of the communication distance on the D2D transmission energy consumption compared with the cellular transmission energy consumption.

Figure B.4 also shows that under non-uniform distribution of nodes within the cell, r increases with the distance between SN and BS in order to compensate the smaller density of users as it is increased the distance to the BS. The considered non-uniform distribution scenario results in very low densities of nodes at the cell edge that hence require too high radius around the optimum MR location to guarantee the presence of an MR. It is important also remembering that the distance from the SN to the optimum MR location increases with the distance between the SN and the BS in order to reduce the distance at which the MR starts forwarding the information towards the BS (see Chapter 6, Section 6.4, Figure 6-4.a). As a consequence, when the SN is at the cell edge it

[33] The optimum MR location was reported in Chapter 6 (Section 6.4, Figure 6-4.a) as a function of the distance between SN and BS.

[34] The optimum MR location was at a 50 meters distance away from the SN in the direction of the BS according to Figure 6-4.a.

results unfeasible to complete the end-to-end opportunistic MCN transmissions before the deadline *T* for all the possible locations of an MR within the search area. This can be caused by the increase of the D2D transmission time (as the distance from the SN to the MR increases with respect to the distance from the SN to the optimum MR location), by the increase of the cellular transmission time (as it is increased the MR-BS distance at which the cellular transmission is conducted), or because the SN-MR distance exceeds the D2D transmission radio coverage limit. In these cases, the SN would directly transmit the information to the cellular BS, which is represented by an *r* value equal to 0 in Figure B.4.

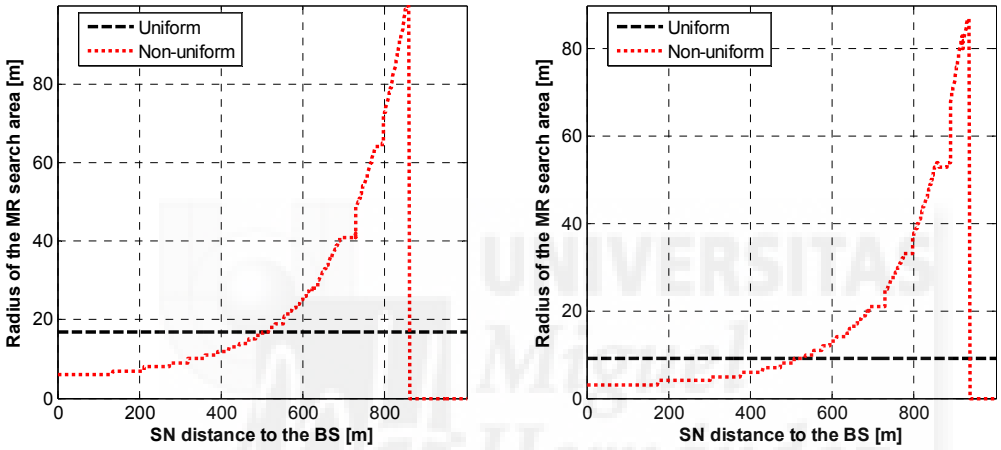

a) μ/R=0.05 MRs/m b) μ/R=0.1 MRs/m

Figure B.4. Radius around the optimum MR location to guarantee the presence of at least one MR within the search area with δ equal to 0.8.

As a consequence of varying the location at which the MR is selected, it is necessary to adjust the opportunistic operation compared with the optimum configuration derived in Chapter 6. Figure B.5 shows for the context-aware AREA opportunistic forwarding proposal the time the MR would store and carry the information from the identified location within the search area until it starts its cellular transmission to the BS in order to minimize the total energy consumption. The reported time is shown in Figure B.5 for the uniform ('AREA – Uniform') and non-uniform distribution ('AREA – Non-uniform') of users within the cell. Figure B.5 shows only slight differences between the optimum configuration and the performance of the context-aware opportunistic scheme in spite of the fact the study considers the worst-case scenario. This is the case because the AREA proposal does not delay the start of the D2D transmission and therefore the small

differences are only due to the variation in the location of the selected MR within the search area (which is different to the optimum MR location). The results depicted in Figure B.5 also show that the time the MR stores and carries the information only reduces when the SN is located at the cell edge and under non-uniform distribution of nodes within the cell. This is the case because of the increasing radius of the MR search area with the distance between SN and BS (Figure B.4).

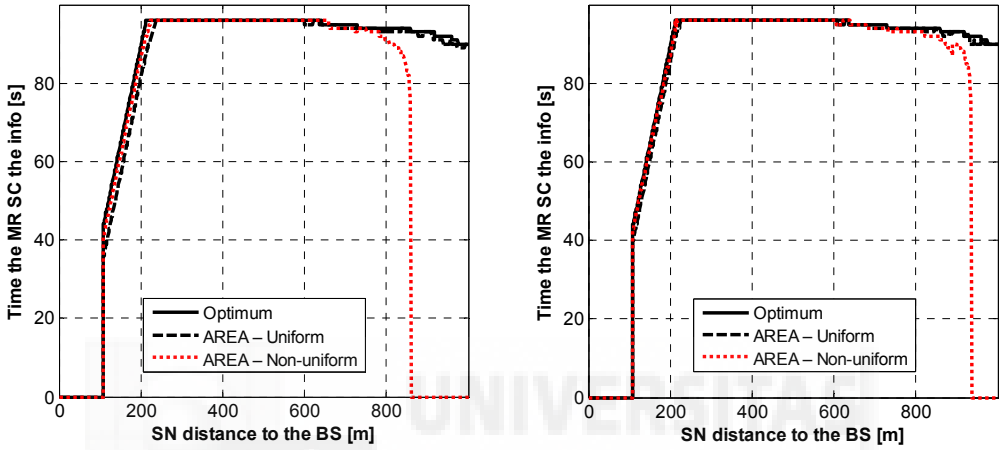

a) μ/R =0.05 MRs/m b) μ/R = 0.1 MRs/m

Figure B.5. AREA: Time the MR stores and carries the info towards the BS.

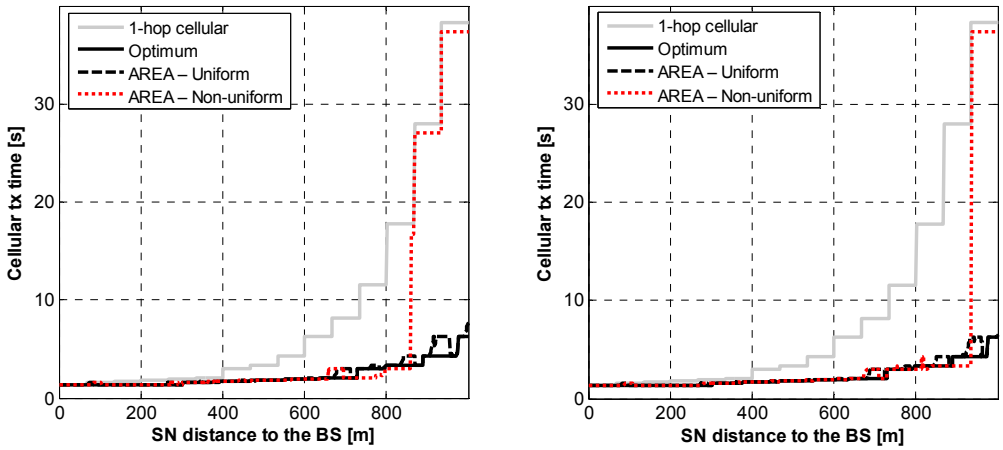

a) μ/R = 0.05 MRs/m b) μ/R = 0.1 MRs/m

Figure B.6. AREA: Time the MR requires to transmit the data to the BS.

The small changes of the AREA proposal in the time the selected MR stores and carries the information result also in minor variations in the duration of the cellular transmission to the BS when compared with the optimum configuration (Figure B.6). Actually, the differences are only appreciated when the SN is located at the cell edge and under non-uniform distribution of nodes within the cell; the transmissions at the cell edge that could not be conducted through a two-hop opportunistic MCN connection require the same duration as the single-hop cellular communications ('1-hop cellular in Figure B.6').

UNIVERSITAS Miguel Hernández

Bibliography

[1] A. Osseiran, V.Braun, H. Taoka, P. Marsch, H. Schotten, H. Tullberg, M. A. Uusitalo and M. Schellman, "The Foundation of the Mobile and Wireless Communications System for 2020 and Beyond: Challenges, Enablers and Technology Solutions", *Proceedings of the 77th IEEE Vehicular Technology Conference (VTC-Spring), pp. 1-5*, Dresden (Germany), 2-5 Jun. 2013. DOI: 10.1109/VTCSpring.2013.6692781.

[2] R. Baldemair, E. Dahlman, G. Fodor, G. Mildh, S. Parkvall, Y. Selen, H. Tullberg and K. Balachandran, "Evolving Wireless Communications: Addressing the Challenges and Expectations of the Future", *IEEE Vehicular Technology Magazine, vol. 8, no. 1, pp. 24-30*, Mar. 2013. DOI: 10.1109/MVT.2012.2234051.

[3] W. Roh, S. Ji-Yun, J. Park, B. Lee, J. Lee, Y. Kim, J. Cho, K. Cheun and F. Aryanfar, "Millimeter-wave Beamforming as an Enabling Technology for 5G Cellular Communications: Theoretical Feasibility and Prototype Results", *IEEE Communications Magazine, vol. 52, no. 2, pp. 106-113*, Feb. 2014. DOI: 10.1109/MCOM.2014.6736750.

[4] F. Boccardi, R.W. Heath, A. Lozano, T.L. Marzetta and P. Popovski, "Five Disruptive Technology Directions for 5G", *IEEE Communications Magazine, vol. 52, no. 2, pp. 74-80*, Feb. 2014. DOI: 10.1109/MCOM.2014.6736746.

[5] T. Jamal and P. Mendes, "Cooperative Relaying in User-centric Networking under Interference Conditions", *IEEE Communications Magazine, vol. 52, no. 12, pp. 18-24*, Dec. 2014. DOI: 10.1109/MCOM.2014.6979947.

[6] S. Mumtaz, H. Lundqvist, K.M. Saidul-Huq, J. Rodriguez and A. Radwan, "Smart Direct-LTE Communication: An Energy Saving Perspective", *Ad Hoc Networks, vol. 13, part B, pp. 296-311*, Feb. 2014. DOI:10.1016/j.adhoc.2013.08.008.

[7] M.J. Yang, S.Y. Lim, H.J. Park and N.H. Park, "Solving the Data Overload: Device-to-device Bearer Control Architecture for Cellular Data Offloading", *IEEE Vehicular Technology Magazine, vol. 8, no. 1, pp. 31-39*, Mar. 2013. DOI: 10.1109/MVT.2012.2234052.

[8] L. Keun-Woo, J. Woo-Sung and K. Young-Bae, "Energy Efficient Quality-of-Service for WLAN-based D2D communications", *Ad Hoc Networks, vol. 25, part A, pp. 102-116*, Feb. 2015. DOI: 10.1016/j.adhoc.2014.10.004.

[9] 3GPP TR 22.803 V12.1.0. Technical Specification Group Services and System Aspects; Feasibility study for Proximity Services (ProSe). Mar. 2013.

[10] Y. Lin and Y. Hsu, “Multihop Cellular: A New Architecture for Wireless Communications”, *Proceedings of the 19th IEEE Computer Communications Conference (INFOCOM), vol. 3, pp. 1273-1282*, Tel Aviv (Israel), 26-30 Mar. 2000,. DOI: 10.1109/INFCOM.2000.832516.

[11] D. Cavalcanti, D. Agrawal, C. Cordeiro, B. Xie and A. Kumar, "Issues in Integrating Cellular networks WLANs, AND MANETs: a Futuristic Heterogeneous Wireless Network", *IEEE Wireless Communications Magazine, vol. 12, no. 3, pp. 30-41*, Jun. 2005. DOI: 10.1109/MWC.2005.1452852.

[12] Y. Yang, H. Honglin, X. Jing and M. Guoqiang, "Relay Technologies for WiMax and LTE-advanced Mobile Systems", *IEEE Communications Magazine, vol. 47, no. 10, pp. 100-105*, Oct. 2009. DOI: 10.1109/MCOM.2009.5273815.

[13] L. Pelusi, A. Passarella and M. Conti, "Opportunistic Networking: Data forwarding in Disconnected Mobile Ad-hoc Networks", *IEEE Communications Magazine, vol. 44, no. 11, pp. 134-141*, Nov. 2006. DOI: 10.1109/MCOM.2006.248176.

[14] A. Moraleda-Soler, B. Coll-Perales and J. Gozalvez, "Link-aware Opportunistic D2D communications: Open Source Test-bed and Experimental Insights into their Energy, Capacity and QoS Benefits", *Proceedings of the 11th IEEE International Symposium on Wireless Communications Systems (ISWCS), pp. 606-610*, Barcelona (Spain), 26-29 Aug. 2014. DOI: 10.1109/ISWCS.2014.6933425.

[15] Cisco Visual Networking Index: Global Mobile Data Traffic Forecast Update, 2014–2019. *Cisco White Paper*, Feb. 2015.

[16] H. Nourizadeh, S. Nourizadeh and R. Tafazolli, "Performance Evaluation of Cellular Networks with Mobile and Fixed Relay Station", *Proceedings of the 64th IEEE Vehicular Technology Conference (VTC 2006-Fall), pp. 1-5*, Montreal (Canada), Sept. 2006. DOI: 10.1109/VTCF.2006.501.

[17] R. Pabst, B.H. Walke, D.C. Schultz, P. Herhold, H. Yanikomeroglu, S. Mukherjee, H. Viswanathan, M. Lott, W. Zirwas, M. Dohler, H. Aghvami, D.D. Falconer and G.P. Fettweis, "Relay-based Deployment Concepts for Wireless and Mobile Broadband Radio", *IEEE Communications Magazine, vol. 42, no. 9, pp. 80-89*, Sept. 2004. DOI: 10.1109/MCOM.2004.1336724.

[18] A. Radwan and H.S. Hassanein, "Does Multi-hop Communication Extend the Battery Life of Mobile Terminals?", Proceedings of the IEEE Global Telecommunications Conference (GLOBECOM '06), pp. 1-5, California (USA), 27 Nov.-1 Dec. 2006. DOI: 10.1109/GLOCOM.2006.337.

[19] A. Catovic and S. Tekinay, "Power Efficiency of User Cooperation in Multihop Wireless Networks", *IEEE Communications Letters, vol. 9, no. 12, pp. 1034-1036*, Dec. 2005. DOI: 10.1109/LCOMM.2005.1576579.

[20] H. Holma and A. Toskala, “WCDMA for UMTS: HSPA Evolution and LTE”, John Wiley & Sons, Ltd. Sept. 2007.

[21] Y. Sui, “On the Benefits of Moving Relay Nodes in Wireless Networks”, *Thesis for the Degreee of Engineering, Chalmers University of Technology*, Gothenburg (Sweden), 2012.

[22] 3GPP TR 36.814 V9.0.0. Technical Specification Group Radio Access Network; Further Advancements for E-UTRA Physical Layer Aspects. Mar. 2010.

[23] IEEE P802.16j/D9. Draft Amendment to IEEE Standard for Local and Metropolitan Area Networks Part 16: Air Interface for Fixed and Mobile Broadband Wireless Access Systems: Multihop Relay Specification. Feb. 2009.

[24] T. Wirth, V. Venkatkumar, T. Haustein, E. Schulz and R. Halfmann, "LTE-Advanced Relaying for Outdoor Range Extension", *Proceedings of the 70th IEEE Vehicular Technology Conference (VTC 2009-Fall), pp. 1-4*, Alaska (USA), Sept. 2009. DOI: 10.1109/VETECF.2009.5378969.

[25] G. Fettweis, J. Holfeld, V. Kotzsch, P. Marsch, E. Ohlmer, Z. Rong and P. Rost, "Field Trial Results for LTE-advanced Concepts", Proceedings of the IEEE International Conference on Acoustics Speech and Signal Processing (ICASSP), pp. 5606-5609, Texas (USA), Mar. 2010. DOI: 10.1109/ICASSP.2010.5495249.

[26] J.F. Monserrat, G. Mange, V. Braun, H. Tullberg, G. Zimmermann and Ö. Bulakci, “METIS Research Advances Towards the 5G Mobile and Wireless System Definition”, *EURASIP Journal on Wireless Communications and Networking 2015, vol. 2015, no. 53, pp. 1-16*, Mar. 2015. DOI: 10.1186/s13638-015-0302-9.

[27] The METIS project’s Official Web Site: https://www.metis2020.com/. Last accessed on Jan. 2015.

[28] The MOTO project’s Official Web Site: http://www.fp7-moto.eu/. Last accessed on Jan. 2015.

[29] 3GPP TR 23.703 V2.0.0. Technical Specification Group Services and System Aspects; Study on Architecture Enhancements to Support Proximity-based Services (ProSe). Feb. 2014.

[30] 3GPP TS 23.303 V12.3.0. Technical Specification Group Services and System Aspects; Proximity-based services (ProSe). Dec. 2014.

[31] 3GPP TR 33.833 V1.2.0. Technical Specification Group Services and System Aspects; Study on Security issues to support Proximity Services (ProSe). Nov. 2014.

[32] 3GPP TR 36.843 V12.0.1. Technical Specification Group Radio Access Network; Study on LTE Device to Device Proximity Services. Mar. 2014.

[33] 3GPP TS 24.333 V12.1.0. Technical Specification Group Core Network and Terminals; Proximity-services (ProSe) Management Objects (MO). Dec. 2014.

[34] 3GPP TS 24.334. Technical Specification Group Core Network and Terminals; Proximity-services (ProSe) User Equipment (UE) to ProSe Function Protocol Aspects. Dec. 2012.

[35] F. Daquan, L. Lu, Y. Yuan-Wu, G.Y. Li, F. Gang and L. Shaoqian Li, "Device-to-Device Communications Underlaying Cellular Networks", *IEEE Transactions on Communications, vol. 61, no. 8, pp. 3541-3551*, Aug. 2013. DOI: 10.1109/TCOMM.2013.071013.120787.

[36] P. Janis, V. Koivunen, C. Ribeiro, J. Korhonen, K. Doppler and K. Hugl, K., "Interference-Aware Resource Allocation for Device-to-Device Radio Underlaying Cellular Networks", *Proceedings of the IEEE 69th Vehicular Technology Conference (VTC Spring 2009), pp.1-5*, Barcelona (Spain), 26-29 Apr. 2009. DOI: 10.1109/VETECS.2009.5073611.

[37] K. Doppler, M. Rinne, C. Wijting, C. Ribeiro, and K. Hugl, "Device-to-device Communication as an Underlay to LTE-Advanced Networks", IEEE Communication Magazine, vol. 47, no. 12, pp. 42–49, Dec. 2009. DOI: 10.1109/MCOM.2009.5350367.

[38] Y. Pei and Y.C. Liang, "Resource Allocation for Device-to-Device Communication Overlaying Two-way Cellular Networks", *IEEE Transactions on Wireless Communications, vol. 12, no. 7, pp. 3611–3621*, Jul. 2013. DOI: 10.1109/TWC.2013.061713.121956.

[39] Deutsche Telekom AG, Orange Silicon Valley, Qualcomm Technologies Inc., Tagged Inc. and Samsung Electronics. LTE Direct Workshop White Paper. May 2013.

[40] Qualcomm Research White Paper. LTE Direct: The Case for Device-to-Device Proximate Discovery. Feb. 2013.

[41] Qualcomm Tech. LTE-Direct project's Official Web Site: https://ltedirect.qualcomm.com/ and https://www.qualcomm.com/invention/research/projects/lte-direct. Last accessed on Jan. 2015.

[42] W. Xinzhou, S. Tavildar, S. Shakkottai, T. Richardson, L. Junyi, R. Laroia and A. Jovicic, "FlashLinQ: A Synchronous Distributed Scheduler for Peer-to-Peer Ad Hoc Networks", IEEE/ACM Transactions on Networking, vol. 21, no. 4, pp. 1215-1228, Aug. 2013. DOI: 10.1109/TNET.2013.2264633.

[43] S. Dimatteo, P. Hui, B. Han and V.O.K Li, "Cellular Traffic Offloading through WiFi Networks", *Proceedings of the IEEE International Conference on Mobile Ad hoc and Sensor Systems (MASS), pp. 192-201*, Valencia (Spain), 17-22 Oct. 2011. DOI: 10.1109/MASS.2011.26.

[44] J. Kim, N.O. Song, B.H. Jung, H. Leem and D.K. Sung, "Placement of WiFi Access Points for Efficient WiFi Offloading in an Overlay Network", *Proceedings of the 24th IEEE International Symposium on Personal Indoor and Mobile Radio Communications (PIMRC), pp. 3066-3070*, London (UK), 8-11 Sept. 2013. DOI: 10.1109/PIMRC.2013.6666673.

[45] B. H. Walke, S. Mangold and L. Berlemann. IEEE 802 Wireless Systems: Protocols, Multi-hop Mesh/Relaying, Performance and Spectrum Coexistence. Chapter 5: IEEE 802.11 Wireless Local Area Networks. John Wiley and Sons, Ltd. Mar. 2008.

[46] S. Basagni, M. Conti, S. Giordano and I. Stojmenovic. Mobile Ad Hoc Networking. Chapter 3: IEEE 802.11 in Ad Hoc Networks: Protocols, Performance and Open Issues. John Wiley and Sons, Ltd. Sept. 2004.

[47] IEEE 802.11 Standard for Information Technology. Part 11: Wireless LAN Medium Access Control (MAC) and Physical Layer (PHY) Specifications. Dec. 2013.

[48] IEEE 802.11n Standard for Information Technology. Part 11: Wireless LAN Medium Access Control (MAC) and Physical Layer (PHY). Specifications Amendment 5: Enhancements for Higher Throughput. Oct. 2009.

[49] IEEE 802.11s Standard for Information Technology. Part 11: Wireless LAN Medium Access Control (MAC) and Physical Layer (PHY). Specifications Amendment 10: Mesh Networking. Feb. 2011.

[50] D. Camps-Mur, A. Garcia-Saavedra and P. Serrano, "Device-to-device communications with Wi-Fi Direct: overview and experimentation", *IEEE Wireless Communications, vol. 20, no. 3, pp. 96-104*, Jun. 2013. DOI: 10.1109/MWC.2013.6549288.

[51] IEEE 802.11ac Standard for Information Technology. Part 11: Wireless LAN Medium Access Control (MAC) and Physical Layer (PHY). Specifications Amendment 4: Enhancements for Very High Throughput for Operation in Bands below 6GHz. Dec. 2013.

[52] IEEE 802.11ad Standard for Information Technology. Part 11: Wireless LAN Medium Access Control (MAC) and Physical Layer (PHY). Specifications Amendment 3: Enhancements for Very High Throughput in the 60GHz band. Mar. 2014.

[53] IEEE 802.11af Standard for Information Technology. Part 11: Wireless LAN Medium Access Control (MAC) and Physical Layer (PHY). Specifications Amendment 5: Television White Spaces (TVWS) Operation. Mar. 2014.

[54] IEEE 802.11ah/D2.0 Draft Standard for Information Technology. Part 11: Wireless LAN Medium Access Control (MAC) and Physical Layer (PHY) Specifications: Amendment – Sub 1 GHz License-Exempt Operation. Jun. 2014.

[55] K.R. Jacobson and W.A. Krzymien, “Cell Dimensioning and Network Throughput in Cellular Multi-hop Relay Networks“, *Proceedings of the 64th IEEE Vehicular Technology Conference (VTC-Fall), pp. 1-5*, Montreal (Canada), 25-28 Sept. 2006. DOI: 10.1109/VTCF.2006.497.

[56] ETSI.TR 101 146 v3.0.0, “UMTS 30.06, Support for relaying ODMA“, December 1997.

[57] M. Hossain and A. Mammela, "Effect of User Density and Traffic Volume on Uplink Capacity of Multihop Cellular Network", *Proceedings of the 5th IEEE International Conference on Wireless and Mobile Communications (ICWMC)*, pp. 49-53, Cannes (France), 23-29 Aug. 2009. DOI: 10.1109/ICWMC.2009.79.

[58] M.C. Lucas-Estañ, J. Gozalvez and B. Coll-Perales, “Mode Selection for Mobile Opportunistic Multi-hop Cellular Networks", *Proceedings of the 79th IEEE Vehicular Technology Conference (VTC2014-Spring), pp. 1-5*, Seoul (Korea), 18-21 May 2014.

[59] A. Osseiran, K. Doppler, C. Ribeiro, M. Xiao, M. Skoglund and J. Manssour, "Advances in Device-to-Device Communications and Network Coding for IMT-Advanced", *Proceedings of the ICT Mobile and Wireless Communications Summit (ICT-Mobile Summit), pp. 1-8*, Santander (Spain), 10-12 Jun. 2009.

[60] R. Sisodia, B. Manoj and C. Murthy, "A Preferred Link Based Routing Protocol for Ad Hoc Wireless Networks", *Journal of Communications and Networks, vol. 4, no. 1, pp. 14-21*, Mar. 2002. DOI: 10.1109/JCN.2002.6596928.

[61] S. Itaya, J. Hasegawa, P. Davis, N. Kadowaki and S. Obana, "Achieving Stable Operation of Ad Hoc Wireless Networks with Neighbor Pre-selection and Synchronous Route Updates", *Proceedings of the 30th IEEE Local Computer Networks Conference (LCN), pp. 702-708*, Sydney (Australia), 15-17 Nov. 2005. DOI: 10.1109/LCN.2005.23.

[62] C. Cramer and T. Fuhrmann, "Proximity Neighbor Selection for a DHT in Wireless Multi-hop Networks", *Proceedings of the 5th IEEE Peer-to-Peer Computing Conference (P2P)*, pp. 3-10, Konstanz (Germany), 31 Aug.-2 Sept. 2005. DOI: 10.1109/P2P.2005.28.

[63] B. Coll-Perales and J. Gozalvez, "Neighbor Selection Techniques for Multi-hop Wireless Mesh Networks", *Proceedings of the 9th IEEE International Workshop on Wireless Local Networks (WLN), pp. 1020-1026*, Zürich (Switzerland), 20-23 Oct. 2009. DOI: 10.1109/LCN.2009.5355024.

[64] B. Coll-Perales and J. Gozalvez, "Energy Efficient Routing Protocols for Multi-hop Cellular Networks", *Proceedings of the 20th IEEE Personal, Indoor and Mobile Radio Communications Symposium (PIMRC), pp. 1457-1461*, Tokyo (Japan), 13-16 Sept. 2009. DOI: 10.1109/PIMRC.2009.5450170.

[65] C. Perkins and E. Royer, "Ad hoc On-Demand Distance Vector Routing", *Proceedings of the 2nd IEEE Workshop on Mobile Computing Systems and Applications (WMCSA), pp. 90-100*, Louisiana (USA), 25-26 Feb. 1999. DOI: 10.1109/MCSA.1999.749281.

[66] B. Coll-Perales and J. Gozalvez, "Contextual optimization of location-based routing protocols for multi-hop cellular networks using mobile relays", *Springer Telecommunication Systems*, in press, 2015. DOI: 10.1007/s11235-015-0036-3.

[67] 3G TR 25.924 V1.0.0. Technical Specification Group Radio Access Network; Opportunity Driven Multiple Access. Dec. 1999.

[68] C. Shin-Ming and L. Phone, "Power-efficient Routing Mechanism for ODMA Systems", *IEEE Transactions on Vehicular Technology, vol. 55, no. 4, pp. 1311-1319*, Jul. 2006. DOI: 10.1109/TVT.2006.877457.

[69] IWICS White Paper. ODMA Opportunity Driven Multiple Access. Available online at: http://www.iwics.com/. Last accessed on Dec. 2014.

[70] A. Papadogiannis, M. Farber, A. Saadani, M.D. Nisar, P. Weitkemper, T.M. de Moraes, J. Gora, N. Cassiau, D. Ktenas, J. Vihriala, M. Khanfouci and T. Svensson, "Pass It on: Advanced Relaying Concepts and Challenges for Networks Beyond 4G", *IEEE Vehicular*

Technology Magazine, vol. 9, no. 2, pp. 29-37, Jun. 2014. DOI: 10.1109/MVT.2014.2312268.

[71] Samsung' source, "Future 3GPP Radio Technologies for IMT-Advanced", 3GPP IMT-Advanced Workshop, Agenda item 3, REV-080037, Shenzhen (China), 7-8 Apr. 2008.

[72] L. Xingqin, J. Andrews, A. Ghosh and R. Ratasuk, "An Overview of 3GPP Device-to-Device Proximity Services", *IEEE Communications Magazine, vol. 52, no. 4, pp. 40-48*, Apr. 2014. DOI: 10.1109/MCOM.2014.6807945.

[73] J.G. Andrews, S. Buzzi, C. Wan Choi, S.V. Hanly, A. Lozano, A.C.K. Soong and J.C. Zhang, "What Will 5G Be?", *IEEE Journal on Selected Areas in Communications, vol. 32, no. 6, pp. 1065-1082*, Jun. 2014. DOI: 10.1109/JSAC.2014.2328098.

[74] Ericsson White Paper. 5G Radio Access: Research and Vision. Jun. 2013.

[75] DOCOMO 5G White Paper. 5G Radio Access: Requirements, Concept and Technologies. Jul. 2014.

[76] NetWorld2020 White Paper. 5G: Challenges, Research Priorities, and Recommendations. Aug. 2014.

[77] H.C. Woon, F. Zhong and R. Haines, "Emerging Technologies and Research Challenges for 5G Wireless Networks", *IEEE Wireless Communications, vol. 21, no. 2, pp. 106-112*, Apr. 2014. DOI: 10.1109/MWC.2014.6812298.

[78] T. Korakis, M. Knox, E. Erkip and S. Panwar, "Cooperative Network Implementation Using Open-Source Platforms", *IEEE Communication Magazine, vol. 47, no. 2, pp. 134-141*, Feb. 2009. DOI: 10.1109/MCOM.2009.4785391.

[79] P. Liu, T. Zhifeng, S. Narayanan, T. Korakis and S.S. Panwar, "CoopMAC: A Cooperative MAC for Wireless LANs", *IEEE Journal on Selected Areas in Communications, vol. 25, no. 2, pp. 340–354*, Feb. 2007. DOI: 10.1109/JSAC.2007.070210.

[80] A. Sharma, M. Tiwari and H. Zheng, "MadMAC: Building a Reconfiguration Radio Testbed using Commodity 802.11 Hardware", *Proceedings of the 1st IEEE Workshop on Networking Technologies for Software Defined Radio Networks (SDR '06), pp. 78-83*, Reston (USA), 25 Sept. 2006. DOI: 10.1109/SDR.2006.4286329.

[81] C. Cheng, P. Hsiao, H.T Kung and D. Vlah, "Adjacent Channel Interference in Dual-radio 802.11a Nodes and Its Impact on Multi-hop Networking", *Proceedings of the IEEE Global Telecommunications Conference (GLOBECOM '06), pp. 1-6*, San Francisco (USA), Nov. 27-Dec. 1 2006. DOI: 10.1109/GLOCOM.2006.500.

[82] A. Sharma, V. Navda, R. Ramjee, V.N, Padmanabhan and E. M. Belding, "Cool-Tether: Energy Efficient On-the-fly WiFi Hot-spots using Mobile Phones", *Proceedings of the 5th ACM Conference on emerging Networking EXperiments and Technologies (CoNEXT), pp. 109-120*, Rome (Italy), 1-4 Dec. 2009. DOI: 10.1145/1658939.1658952.

[83] Y. Hong, L. Shen and B. Xu, "Experimental System for Integration of Ad-Hoc and Cellular Network", *Proceedings of the 5th IEEE International Conference on Wireless*

Communications, Networking and Mobile Computing (WiCom '09), pp. 1-4, Beijing (China), 24-26 Sept. 2009. DOI: 10.1109/WICOM.2009.5301998.

[84] Anite's Official Web Site: http://www.anite.com. Last accessed on Jan. 2015.

[85] Wireshark's Official Web Site: https://www.wireshark.org/. Last accessed on Jan. 2015.

[86] Kismet's Official Web Site: https://www.kismetwireless.net/. Last accessed on Jan. 2015.

[87] P. Mahasukhon, M. Hempel, C. Song and H. Sharif, "Comparison of Throughput Performance for the IEEE 802.11a and 802.11g Networks", *Proceedings of the 21st IEEE International Conference on Advanced Information Networking and Applications (AINA), pp. 792-799*, Niagara Falls (Canada), 21-23 May 2007. DOI: 10.1109/AINA.2007.46.

[88] S. Mohan, R. Kapoor and B. Mohanty, "Enhanced HSDPA Mobility Performance: Quality and Robustness for Voice over HSPA Service", *Proceedings of the 71st IEEE Vehicular Technology Conference (VTC 2010-Spring), pp. 1-5*, Taipei (China), 16-19 May 2010. DOI: 10.1109/VETECS.2010.5493710.

[89] K. Pedersen, A. Toskala and P. Mogensen, "Mobility Management and Capacity Analysis for High Speed Downlink Packet Access in WCDMA", *Proceedings of the 60th IEEE Vehicular Technology Conference (VTC2004-Fall), pp. 3388-3392*, Los Angeles (USA), 26-29 Sept. 2004. DOI: DOI: 10.1109/VETECF.2004.1404692.

[90] L. Seunghyun, K. Daeeun, K. Younglak, K. Moonhong, K. Myungchan, S. Sungho, H. Seongho and I. Jongtae, "Optimization of the HSDPA Network in the Cell-Overlaid Area", *Proceedings of the 10th IEEE International Conference on Communication Systems (ICCS), pp. 1-5*, Singapore, 30 Oct.-2 Nov. 2006. DOI: 10.1109/ICCS.2006.301546.

[91] C. Sunghyun, E.W. Jang and J.M. Cioffi, "Handover in Multihop Cellular Networks", IEEE Communications Magazine, vol. 47, no. 7, pp. 64-73, Jul. 2009. DOI: 10.1109/MCOM.2009.5183474.

[92] K. Ronny, J. Inuk, Y. Xiangying and C. Chao-Chin, "Advanced Handover Schemes in IMT-Advanced Systems [WiMAX/LTE Update]", *IEEE Communications Magazine, vol. 48, no. 8, pp. 78-85*, Aug. 2010. DOI: 10.1109/MCOM.2010.5534590.

[93] M. Ghassemian, V. Friderikos and H. Aghvami, "Hybrid Handover in Multihop Radio Access Networks", *Proceedings of the 61st IEEE Vehicular Technology Conference (VTC 2005-Spring), pp. 22007-2211*, Stockholm (Sweden), 30 May-1 Jun. 2005. DOI: 10.1109/VETECS.2005.1543726.

[94] H. Nourizadeh, S. Nourizadeh and R. Tafazolli, "Impact of the Inter-Relay Handoff on the Relaying System Performance", *Proceedings of the 64th IEEE Vehicular Technology Conference (VTC-2006 Fall), pp. 1-5*, Montreal (Canada), Sept. 2006. DOI: 10.1109/VTCF.2006.521.

[95] Y.W. Blankenship, "Achieving High Capacity with Small Cells in LTE-A," *Proceedings of the 50th IEEE Annual Allerton Conference on Communication, Control, and Computing*

(Allerton), pp. 1680-1687, pp. 1-5, Monticello (USA), 1-5 Oct. 2012. DOI: 10.1109/Allerton.2012.6483424.

[96] H. Lei, X.F. Wang and P.H.J. Chong, "Opportunistic Relay Selection in Future Green Multihop Cellular Networks", *Proceedings of the 72nd IEEE Vehicular Technology Conference (VTC 2010-Fall), pp. 1-5*, Ottawa (Canada), 6-9 Sept. 2010. DOI: 10.1109/VETECF.2010.5594387.

[97] Microsoft Mobile's Official Store Site: http://store.ovi.com/. Last accessed on Jan. 2015.

[98] R. Ananthapadmanabha, B.S. Manoj and C.S.R. Murthy, "Multi-hop Cellular Networks: the Architecture and Routing Protocols", *Proceedings of the 12th IEEE International Symposium on Personal, Indoor and Mobile Radio Communications (PIMRC), pp. 78-82*, San Diego (USA), 29 Sept.-1 Oct. 2001. DOI: 10.1109/PIMRC.2001.965324.

[99] P. Kolios, V. Friderikos and K. Papadaki, "Future Wireless Mobile Networks", *IEEE Vehicular Technology Magazine, vol. 6, no. 1, pp. 24-30*, Mar. 2011. DOI: 10.1109/MVT.2010.939905.

[100] Q. Ayub, S. Rashid, M.S. Mohd-Zahid and A.H. Abdullah, "Contact Quality Based Forwarding Strategy for Delay Tolerant Network", *Journal of Network and Computer Applications, vol. 39, no. 3, pp. 302-309*, Mar. 2014. DOI: 10.1016/j.jnca.2013.07.011.

[101] iPerf's Web Site: http://iperf.sourceforge.net/. Last accessed on Jan. 2015.

[102] D. Krishnaswamy, "Game Theoretic Formulations for Network-Assisted Resource Management in Wireless Networks", *Proceedings of the 56th IEEE Vehicular Technology Conference (VTC 2002-Fall)*, pp. 1312-1316, Vancouver (Canada), 24-28 Sept. 2002. DOI: 10.1109/VETECF.2002.1040428.

[103] C. Moler. Numerical Computing with Matlab. Ed. SIAM, pp. 155-182, 2004.

[104] TradersPlace, "Moving Averages in Technical Analysis", WhitePaper. Available online at: http://www.tradersplace.in/moving_averages.html. Last accessed on Jan. 2015.

[105] D. Xia, J. Hart and Q. Fu, "Evaluation of the Minstrel Rate Adaptation Algorithm in IEEE 802.11g WLANs", *Proceedings of the IEEE International Conference on Communications (ICC), pp. 2223-2228*, Budapest (Hungary), 9-13 Jun. 2013. DOI: 10.1109/ICC.2013.6654858.

[106] S. Mare, D. Kotz and A. Kumar "Experimental Validation of Analytical Performance Models for IEEE 802.11 networks", *Proceedings of the 2nd IEEE International Conference on Communication Systems and Networks (COMSNETS), pp. 1-8*, Liverpool (UK), 5-9 Jan. 2010. DOI: 10.1109/COMSNETS.2010.5431957.

[107] F. Capulli, C. Monti, M. Vari and F. Mazzenga, "Path Loss Models for IEEE 802.11a Wireless Local Area Networks", *Proceedings of the 3rd IEEE International Symposium on Wireless Communication Systems (ISWCS'06), pp. 621-624*, Valencia (Spain), 6-8 Sept. 2006. DOI: 10.1109/ISWCS.2006.4362375.

[108] T. Rappaport. Wireless communications: principles and practices. Prentice Hall, 2001.

[109] C. Aydogdu and E. Karasan, "An Analysis of IEEE 802.11 DCF and Its Application to Energy-Efficient Relaying in Multihop Wireless Networks", *IEEE Transactions on Mobile Computing*, vol. 10, no. 10, pp. 1361-1373, Oct. 2011. DOI: 10.1109/TMC.2010.239.

[110] A. Duda, "Understanding the Performance of 802.11 Networks", *Proceedings of the 19th IEEE International Symposium on Personal, Indoor and Mobile Radio Communications (PIMRC), pp. 1-6*, Cannes (France), 15-18 Sept. 2008. DOI: 10.1109/PIMRC.2008.4699942.

[111] A. Chaintreau, P. Hui, J. Crowcroft, C. Diot, R. Gass and J. Scott, "Impact of Human Mobility on Opportunistic Forwarding Algorithms", *IEEE Transactions on Mobile Computing, vol. 6, no. 6, pp. 606-620*, Jun. 2007. DOI: 10.1109/TMC.2007.1060.

[112] Z. Ruifeng, J.M. Gorce and K. Jaffres-Runser, "Low Bound of Energy-Latency Trade-Off of Opportunistic Routing in Multi-hop Networks", *Proceedings of the IEEE International Conference on Communications (ICC), pp. 1-6*, Dresden (Germany), 14-18 Jun. 2009. DOI: 10.1109/ICC.2009.5199148.

[113] W. Moreira and P. Mendes, “Impact of Human Behavior on Social Opportunistic Forwarding”, *Ad Hoc Networks, vol. 25, part B, pp. 293-302*, Feb. 2015. DOI: 10.1016/j.adhoc.2014.07.001.

[114] L. Yong, J. Yurong, J. Depeng, S. Li, Z. Lieguang and D.O. Wu, "Energy-Efficient Optimal Opportunistic Forwarding for Delay-Tolerant Networks", *IEEE Transactions on Vehicular Technology, vol. 59, no. 9, pp. 4500-4512*, Nov. 2010. DOI: 10.1109/TVT.2010.2070521.

[115] T. Kimura, T. Matsuda and T. Takine, "Probabilistic Store-Carry-Forward Message Delivery Based on Node Density Estimation", *Proceedings of the 11th IEEE Consumer Communications and Networking Conference (CCNC), pp.432-437*, Las Vegas (USA), 10-13 Jan. 2014. DOI: 10.1109/CCNC.2014.6866606.

[116] M.J. Williams, R.M. Whitaker and S.M. Allen, “Decentralised Detection of Periodic Encounter Communities in Opportunistic Networks”, *Ad Hoc Networks, vol. 10, no. 8, pp. 1544-1556*, Nov. 2012. DOI: http://dx.doi.org/10.1016/j.adhoc.2011.07.008.

[117] J. Gebert, and R. Fuchs, "Probabilities for Opportunistic Networking in Different Scenarios", *Proceedings of the IEEE Future Network & Mobile Summit (FutureNetw), pp. 1-8*, Berlin (Germany), 4-6 Jul. 2012.

[118] G. Luo, J. Zhang, H. Huang, K. Qin, and H. Sun, “Exploiting Intercontact Time for Routing in Delay Tolerant Networks”, *Transactions on Emerging Telecommunications Technologies, vol. 24, no. 6, pp. 589-599*, Oct. 2013. DOI: 10.1002/ett.2553.

[119] Z. Huan Zhou, C. Jiming, Z. Hongyang, G. Wei Gao and C. Peng, "On Exploiting Contact Patterns for Data Forwarding in Duty-Cycle Opportunistic Mobile Networks", *IEEE Transactions on Vehicular Technology, vol. 62, no. 9, pp. 4629-4642*, Nov. 2013, DOI: 10.1109/TVT.2013.2267236.

[120] N. Nomikos, D. Vouyioukas, T. Charalambous, I. Krikidis, P. Makris, D.N. Skoutas, M. Johansson and C. Skianis, “Joint relay-pair selection for buffer-aided successive opportunistic relaying”, *Transactions on Emerging Telecommunications Technologies, vol. 25, no. 8, pp. 823–834*, Aug. 2014. DOI: 10.1002/ett.2718.

[121] N. Zlatanov, R. Schober and P. Popovski, "Buffer-Aided Relaying with Adaptive Link Selection", *IEEE Journal on Selected Areas in Communications, vol. 31, no. 8, pp. 1530-1542*, Aug. 2013. DOI: 10.1109/JSAC.2013.130816.

[122] W. Rui, V.K.N. Lau and H. Huang, "Opportunistic Buffered Decode-Wait-and-Forward (OBDWF) Protocol for Mobile Wireless Relay Networks", *IEEE Transactions on Wireless Communications, vol. 10, no. 4, pp. 1224-1231*, Apr. 2011. DOI: 10.1109/TWC.2011.020111.100466.

[123] B. Zhao and V. Friderikos, "Optimal stopping for energy efficiency with delay constraints in Cognitive Radio networks", *Proceedings of the IEEE Personal Indoor and Mobile Radio Communications (PIMRC), pp. 820-825*, Sydney (Australia), 9-12 Sept. 2012. DOI: 10.1109/PIMRC.2012.6362897.

[124] Ustream’s Official Web Site: http://www.ustream.tv/. Last accessed on Jan. 2015.

[125] Bambuser’s Official Web Site: http://bambuser.com/. Last accessed on Jan. 2015.

[126] Livestream’s Official Web Site: http://new.livestream.com/. Last accessed on Jan. 2015.

[127] P. Ameigeiras, J.J. Ramos-Muñoz, J. Navarro-Ortiz, and J.M. López-Soler, “Analysis and modelling of YouTube traffic”, *Transactions on Emerging Telecommunications Technologies, vol. 23, no. 4, pp. 360-377*, Jun. 2012. DOI: 10.1002/ett.2546.

[128] P. Kolios, V. Friderikos and K. Papadaki, “Energy-Aware Mobile Video Transmission Utilizing Mobility”, *IEEE Network, vol. 27, no. 2, pp. 34-40*, Mar. 2013. DOI: 10.1109/MNET.2013.6485094.

[129] A. Finamore, M. Mellia, M.M. Munafò, R. Torres and S.G. Rao, “YouTube Everywhere: Impact of Device and Infrastructure Synergies on User Experience”, *Proceedings of the ACM SIGCOMM conference on Internet Measurement Conference (IMC’11), pp. 345-360*, Berlin (Germany), 2-4 Nov. 2011. DOI: 10.1145/2068816.2068849.

[130] J.I. Moreno-Novella and F.J. Gonzalez-Castaño. Resource Management in Satellite Networks. Chapter 3: QoS Requirements for Multimedia Services. Ed. Springer, 2007.

[131] Facebook, Ericsson and Qualcomm WhitePaper, “A focus on Efficiency”, Sept. 2013.

[132] Line’s Official Web Site: http://line.me/en/. Last accessed on Jan. 2015.

[133] Viber’s Official Web Site: http://www.viber.com/en/. Last accessed on Jan. 2015.

[134] Heytell’s Official Web Site: http://www.heytell.com. Last accessed on Jan. 2015.

[135] B. Bing, "A fast and Secure Framework for Over-the-Air Wireless Software Download using Reconfigurable Mobile Devices", *IEEE Communications Magazine, vol. 44, no. 6, pp. 58-63*, Jun. 2006. DOI: 10.1109/MCOM.2006.1668420.

[136] C. Troncoso, G. Danezis, E. Kosta, J. Balasch and B. Preneel, "PriPAYD: Privacy-Friendly Pay-As-You-Drive Insurance", *IEEE Transactions on Dependable and Secure Computing, vol. 8, no. 5, pp. 742-755*, Sept.-Oct. 2011. DOI: 10.1109/TDSC.2010.71.

[137] WINNER consortium, "D1.1.2 V.1.1. WINNER II channel models", WINNER European Research project Public Deliverable, Nov. 2007.

[138] P. Bertrand, J. Jiang and A. Ekpenyong, "Link Adaptation Control in LTE Uplink", *Proceedings of the 72th IEEE Vehicular Technology Conference (VTC 2012-Fall), pp. 1-5*, Quebec (Canada), 3-6 Sept. 2012. DOI: 10.1109/VTCFall.2012.6399063.

[139] F.D. Calabrese, C. Rosa, M. Anas, P.H. Michaelsen, K.I. Pedersen and P.E. Mogensen, "Adaptive Transmission Bandwidth Based Packet Scheduling for LTE Uplink", *Proceedings of the 68th IEEE Vehicular Technology Conference (VTC 2008-Fall), pp. 1-5*, Calgary (Canada), 21-24 Sept. 2008. DOI: 10.1109/VETECF.2008.316.

[140] 3GPP TR 28.814. Technical Specification Group Radio Access Network; Physical Layer Aspects for Evolved UTRA. Sept. 2006.

[141] 3GPP TS 36.213. Technical Specification Group Radio Access Network; Physical layer procedures for Evolved UTRA. Sept. 2013.

[142] M. Greenberg, "How Much Power Will a Low-Power SDRAM Save you?", White Paper Denali Software, 2009.

[143] A. Carroll and G. Heiser, "An analysis of power consumption in a smartphone", *Proceedings of the USENIXATC*, pp. 21-25, Boston, USA, 23-25 Jun. 2010.

[144] B. Karp and H Kung, "Greedy Perimeter Stateless Routing for Wireless Networks", *Proceedings of the 6th ACM/IEEE Annual International Conference on Mobile Computing and Networking (MobiCom), pp. 243-254*, Boston (USA), 6-11 Aug. 2000. DOI: 10.1145/345910.345953.

[145] X. Cheng, J. Liu and C. Dale, "Understanding the Characteristics of Internet Short Video Sharing: A YouTube-Based Measurement Study", *IEEE Transactions on Multimedia, vol. 1, no. 5, pp. 1184-1194*, Aug. 2013. DOI: 10.1109/TMM.2013.2265531.

[146] H. Zhang, P. Hong and K. Xue, "Mobile-Based Relay Selection Schemes for Multi-hop Cellular Networks", *KICS/IEEE Journal of Communications and Networks, vol. 15, no. 1, pp. 45-53*, Feb. 2013. DOI: 10.1109/JCN.2013.000009.

[147] B. Lorenzo and S. Glisic, "Context-Aware Nanoscale Modeling of Multicast Multihop Cellular Networks", *IEEE/ACM Transactions on Networking*, vol. 21, no. 2, pp. 359-372, Apr. 2013. DOI: 10.1109/TNET.2012.2199129.ç

[148] L.M. Correia and R. Tafazolli, "A Strategy for Innovation in Future Networks in Europe", Net!works ETP: SRA v10, 10th ed. Strategy Research Agenda, Deliverable 1.4, Jul. 2012.

[149] H. A. Nguyen and S. Giordano, "Context Information Prediction for Social-based Routing in Opportunistic Networks", *Ad Hoc Networks, vol. 10, no. 8, pp. 1557-1569*, Nov. 2012. DOI: http://dx.doi.org/10.1016/j.adhoc.2011.05.007.

[150] E. Bastug, M. Bennis and M. Debbah, "Living on the Edge: The role of Proactive Caching in 5G Wireless Networks", *IEEE Communications Magazine, vol. 52, no. 8, pp. 82-89*, Aug. 2014. DOI: 10.1109/MCOM.2014.6871674.

[151] Lungaro, P.; Segall, Z.; Zander, J., "Predictive and Context-Aware Multimedia Content Delivery for Future Cellular Networks," *Proceedings of the 71st IEEE Vehicular Technology Conference (VTC 2010-Spring)*, pp. 1-5, Taipei (Taiwan), 16-19 May 2010. DOI: 10.1109/VETECS.2010.5493664.

[152] W. Xiaofei. C. Min, T. Kwon, L. Jin and V. Leung, "Mobile Traffic Offloading by Exploiting Social Network Services and Leveraging Opportunistic Device-to-Device Sharing", IEEE Wireless Communications, vol. 21, no. 3, pp. 28-36, Jun. 2014. DOI: 10.1109/MWC.2014.6845046.

[153] H. Bo, H. Pan, V.S.A. Kumar, M.V. Marathe, S. Jianhua and A. Srinivasan, "Mobile Data Offloading through Opportunistic Communications and Social Participation", *IEEE Transactions on Mobile Computing*, vol. 11, no. 5, pp. 821-834, May 2012. DOI: 10.1109/TMC.2011.101.

[154] D.C. Montgomery and G.C. Runger. Applied Statistics and Probability for Engineers. John Wiley and Sons, 2011.

[155] J. Tengviel, K.A. Dotche and K. Diawuo, "The Impact of Mobile Nodes Arrival Patterns in MANETS Using Poisson Models", *International Journal of Managing Information Technology, vol. 4, no. 3, pp. 55-71*, Aug. 2012. DOI : 10.5121/ijmit.2012.4305.

[156] M. Elalem and L. Zhao, "Realistic User Distribution and its Impact on Capacity and Coverage for a WCDMA Mobile Network", *Proceedings of the IEEE SARNOFF, pp. 1-5*, New Jersey (USA), Mar. 30-Apr. 1 2009. DOI: 10.1109/SARNOF.2009.4850342.

[157] C. Bettstetter, "Topology Properties of Ad hoc Networks with Random Waypoint Mobility", *ACM SIGMOBILE Mobile Computing and Communications Review, vol. 7, no. 3, pp. 50-52*, Jul. 2003. DOI: 10.1145/961268.961287.

[158] I. Stojmenovic and X. Lin, "Power-Aware Localized Routing in Wireless Networks", *IEEE Transaction on Parallel Distributed Systems, vol. 12, no. 11, pp. 1122-1133*, Nov. 2001. DOI: 10.1109/71.969123.

[159] R. Schoenen and B.H. Walke, "On PHY and MAC Performance of 3G-LTE in a Multi-hop Cellular Environment", *Proceedings of the IEEE International Conference on Wireless Communications, Networking and Mobile Computing (WiCom)*, pp. 926-929, Shangai (China), 21-25 Sept. 2007. DOI: 10.1109/WICOM.2007.238.

[160] Ubuntu for Devices's Official Web Site: https://developer.ubuntu.com/en/. Last accessed on Jan. 2015.